

Structure, flow, and inequality:

Analysing consumer outcomes in ecological and socio-ecological
resource distribution networks with spatially explicit modelling
approaches



Natalie Davis, MSc

This thesis is submitted for the degree of Doctor of Philosophy

June 2021

Lancaster Environment Centre

For my family

Declaration

This thesis has not been submitted in support of an application for another degree at this or any other university. It is the result of my own work and includes nothing that is the outcome of work done in collaboration except where specifically indicated. Many of the ideas in this thesis were the product of discussions with my supervisors: Andrew Jarvis, Gary Polhill, and Matt Aitkenhead.

Statement of authorship

This thesis has been prepared in the alternative format, as a set of three papers presented in Chapters 2 – 4, as submitted to or intended for submission to peer-reviewed journals. Please find below details of these publications with information regarding my contributions using the CRediT taxonomy, as certified by the signatures of all co-authors.

Chapter 2*

Davis, N., Jarvis, A., Aitkenhead, M. J., and Polhill, J. G. (2020) Trajectories toward maximum power and inequality in resource distribution networks. *PLoS ONE*.

doi: 10.1371/journal.pone.0229956

N Davis was responsible for Conceptualization, Methodology, Software, Formal analysis, Investigation, Data curation, Writing – original draft, Writing – review & editing, Visualization.

Chapter 3

Davis, N., Polhill, J. G., and Aitkenhead, M. J. (2021) Measuring heterogeneity in soil networks: a network analysis and simulation-based approach. *Ecological Modelling*, 439.

doi: 10.1016/j.ecolmodel.2020.109308

N Davis was responsible for Conceptualization, Methodology, Software, Formal analysis, Investigation, Data curation, Writing – original draft, Writing – review & editing, Visualization.

Chapter 4

Davis, N., Jarvis, A., and Polhill, J. G. The co-evolution of network structure and consumer inequality in a spatially explicit model of resource acquisition. *In preparation*.

N Davis was responsible for Conceptualization, Methodology, Software, Formal analysis, Investigation, Data curation, Writing – original draft, Writing – review & editing, Visualization.

Yours sincerely,

Andrew Jarvis

J. Gareth Polhill

M. J. Aitkenhead

* Chapter 2 was edited slightly from the published form during the process of thesis corrections.

Abstract

The energetic requirements of all physical systems are supplied by resource acquisition, distribution, and end-use (RADE) networks. While the characteristics of these networks vary considerably, they share similar outcomes, namely heterogeneity in natural systems, and inequality in social systems. Despite the criticality of resources for sustaining life, and impacts of their unequal distribution, little work has attempted to explicitly connect RADE network structure, resource flows, and consumer outcomes.

The overall aim of this thesis was to develop and use modelling approaches to identify relationships between network structure and consumer heterogeneity in stylised networks. After reviewing the current literature on RADE networks (Chapter 1), we develop a model of RADE networks using an electrical analogue and quantify consumer inequality as networks evolve toward maximum power (Chapter 2). In networks with heterogeneous architecture, such as commonly seen fractal structures, inequality between consumers increases as resource flows increase, even after maximum power has been reached.

We then develop a method to extract macropore networks from soil profile images and analyse them with metrics from network science and transport geography (Chapter 3). The networks are used as the environment in an agent-based model (ABM) of foraging soil organisms. The methodology captures known differences between soil types, and shows larger, more heterogeneous soil networks support larger, more diverse simulated consumer populations.

Finally, we develop an ABM of generic consumers building a network to move between resources in heterogeneous landscapes, attempting to maximise their time-discounted consumption (Chapter 4). The dynamics were similar across the landscapes, with the consumer inequality decreasing during initial network construction, then increasing as the network reached its stable state. The resource distribution in each landscape moderated the specific rates and timings of these dynamics.

Overall, the findings here linking known system development trajectories and network architectures to increased inequality provide insight into the emergence and persistence of heterogeneity among consumers in both ecological and socio-ecological systems, and alleviation of inequality in the latter.

Acknowledgements

This PhD was funded through a joint Lancaster Environment Centre and James Hutton Institute studentship. I am deeply grateful to both institutions for the support and welcome I received while working there. This thesis would not have been possible without the support of a wonderful team:

Thank you to my supervisors, Jarvis, Gary, and Matt, for your consistent guidance, support, and wisdom; for teaching me about everything from resource distribution networks to thermodynamics, from bicycle repair to agent-based modelling; and for encouraging me to take the research in directions I was passionate about. To my panellists, Kirsti and Alan, thank you for your attention to both my work and my wellbeing, and for your helpful, thoughtful feedback.

Thank you also to the many other lecturers and mentors that I taught and worked alongside at Lancaster, especially Jackie Pates, Sue Ward, and Ian Hartley. I learned so much from each of you about teaching and balancing the many roles of an academic. Thank you also to the brilliant and patient systems administrators who kept the servers running: Iain Milne, Mike Pacey, and especially Corran Musk, thank you for answering many, many questions, and putting up with my storage requirements. I promise I will let you clear off (some of) the data soon.

To my officemates in Lancaster and Aberdeen, and friends both here and back home – Becca, Emme, Erin, Mikaela, Hannah, Yuanlin, Rosanne, Helena, Kevin, Lol, Meghán, Jan, Ashley, Stephanie, Shane, Marcos, Miranda, Martin, Doug, Matt, Margaret, Bobby, and so many others – your kindness, encouragement, laughter, and honesty has meant the world to me. I couldn't have done it without you. Lastly, to my family: To my parents, for your wisdom and support, hiking with me in English downpours, stats advice, and always being just a call away – I cannot thank you enough. To Kathleen and Tristan, for always making time even with your own busy schedules, your excitement about my work, and still letting me cook with you even though I don't measure anything, you two are the best sister and brother-in-law. To Feather, for always. To Poppy, for (mostly) letting me get my work done but making sure I make time for play as well. And to Mounir, my partner in everything – I am so thankful to be on this journey with you.

Contents

1. Introduction	1
1.1. Heterogeneity and inequality	2
1.1.1. Natural systems.....	2
1.1.2. From heterogeneity to inequality	5
1.2. RADE networks	8
1.2.1. Nested networks.....	9
1.2.2. Active and passive transport.....	11
1.2.3. Energy, matter, and information.....	13
1.2.4. Spatial, temporal, and interactional dimensions	17
1.2.5. Summary.....	20
1.3. How do RADE networks work?.....	20
1.3.1. The thermodynamics of resource distribution.....	20
1.3.2. Energy allocation.....	21
1.3.3. Thermodynamic trajectories	23
1.4. Previous work	26
1.4.1. Allometric scaling.....	26
1.4.2. Optimality.....	28
1.4.3. Mass balance methods.....	30
1.4.4. Transport and movement networks	31
1.5. Next steps.....	33
1.6. Thesis overview	35
1.6.1. Thesis aims	35
1.6.2. Study approach and summary of findings	36
1.6.3. Thesis structure	40
1.7. References	41
2. Trajectories toward maximum power and inequality in resource distribution networks.....	58
2.1. Introduction	59
2.2. Inequality as a function of network architecture and resource flows.....	63
2.2.1. Modelling framework using an electrical analogue.....	63
2.2.2. Simulations to illustrate framework.....	67
2.3. Inequality in branching networks.....	72
2.3.1. Branching as a strategy to increase the maximum power of a system.....	72
2.3.2. Branching simulations	72
2.4. Conclusion.....	76
2.5. Materials and Methods.....	78

2.5.1.	Required simulation inputs	78
2.5.2.	Simulation code operation	80
2.5.3.	Simulation outputs	83
2.5.4.	Code availability statement and languages used.....	83
2.6.	References	84
2.7.	Supplementary Information.....	88
3.	Measuring heterogeneity in soil networks: A network analysis and simulation-based approach.....	94
3.1.	Introduction	94
3.2.	Methods	98
3.2.1.	Soil image collection	98
3.2.2.	Network extraction	99
3.2.3.	Network analysis	101
3.2.4.	Agent-based model overview	103
3.3.	Results	109
3.3.1.	Network metrics.....	109
3.3.2.	Agent-based model	114
3.4.	Discussion	119
3.4.1.	Network analysis	119
3.4.2.	ABM analysis	122
3.5.	Conclusion.....	126
3.6.	References	127
3.7.	Appendices.....	133
4.	The co-evolution of network structure and consumer inequality in a spatially explicit model of resource acquisition	150
4.1.	Introduction	151
4.2.	Model description.....	156
4.3.	Methods	162
4.3.1.	Overview, design concepts, and details (ODD)	162
4.3.2.	Generating the landscape.....	166
4.3.3.	Final experiments	167
4.3.4.	Analytical method	168
4.4.	Results	170
4.4.1.	Network structure and consumer inequality.....	171
4.4.2.	Co-evolution of network structure and inequality	179
4.5.	Discussion	183
4.5.1.	Effect of landscape heterogeneity on network structure and consumer inequality	183

4.5.2.	Co-evolution of network structure and consumer inequality	186
4.5.3.	Maximum power, entropy production, and inequality	188
4.5.4.	Limitations and future work	189
4.6.	Conclusion.....	191
4.7.	References	193
4.8.	Appendices	201
5.	Discussion.....	247
5.1.	Discussion of findings	248
5.1.1.	Chapter 2	248
5.1.2.	Chapter 3	251
5.1.3.	Chapter 4	254
5.2.	Common themes	258
5.2.1.	Agency	258
5.2.2.	Comparability of networks	260
5.2.3.	Heterogeneity and inequality	264
5.2.4.	Systems-level and individual-level analysis	267
5.3.	Future work.....	269
5.3.1.	Summary of future work from each chapter.....	270
5.3.2.	Programme of research	271
5.4.	References	274

Tables

Table 1.1 Some examples of resource acquisition, distribution, and end-use (RADE) networks.....	9
Table 1.2 The definition and location of energy, matter, and information in resource acquisition, distribution, and end-use networks (RADE networks).....	14
Table 2.1 Modified load flow methodology input parameters and description.....	78
Table 3.1 The name and description of the metrics used to analyse the soil networks.	102
Table 3.2 Final values for (a) consumer, (b) resource, and (c) general simulation parameters.	107
Table 3.3. The name and description of outcome variables calculated for the agent-based model (ABM)	108
Table 3.4. (a) Estimated marginal means, standard errors, and outcomes for mixed-effect nested ANOVAs comparing network metrics between Cambisol and Arenosol main soil networks, and (b) medians and 95 % confidence intervals and results of mixed-effect nested Aligned-Ranks Transformation (ART) ANOVAs comparing Cambisol and Arenosol subnetworks.....	110
Table 3.5. The medians, first and third quantiles for agent-based model (ABM) outcome variable values across the two soil types.	115
Table 3.6. Overview of Aligned Ranks Transformation ANOVA models of consumer population outcomes by consumer and resource parameterisation and soil type.....	118
Table 3.7. Results of Kruskal-Wallis tests and Dunn post-hoc analysis comparing entropy of consumer resource stocks and final population size by soil profile ID and soil type.	119
Table 4.1. Descriptions and diagrams of resource maps used in final experiments.	167
Table 4.2. The values for each parameter in the final experiments.	168
Table 4.3. Outcome variables calculated for each simulation run.	169
Table 4.4. The breakpoints and slopes identified by piecewise regression, showing the time points of major state changes in the simulations, and the rate of change of measured variables before and after these changes.	182
Table 5.1 Characteristics of environment, network, resources, and consumers in the models presented in Chapters 2-4.....	260

Figures

Figure 2.1 A sample of the networks used to simulate evolution toward maximum power. 68

Figure 2.2. For the six example networks, (a) the relationship between total final power (P) and the ratio of mean consumer potential to mean resource potential ($\overline{V_C}/\overline{V_R}$), (b) the relationship between the standard deviation of consumer final power (σ_{P_C}) and resource flow squared (I^2), and (c) the relationship between the slope of (b) and the standard deviation of effective resistance (σ_{R_E}) ... 70

Figure 2.3. Density plots of normalised consumer final power (P_C) for the six example networks, shown over decreasing ratios of mean consumer to mean resource potential, $\overline{V_C}/\overline{V_R}$ 71

Figure 2.4. (a) A ‘fully branched’ network, with consumers at each junction, and (b) ‘evolved branching’ networks illustrating the addition of branch points and links over the course of the simulations. 73

Figure 2.5. The total final power consumption (P) against the ratio of mean consumer potential to mean resource potential ($\overline{V_C}/\overline{V_R}$) for each level of the ‘evolved branching’ networks..... 74

Figure 2.6. The frequency distribution of consumer potentials (V_C) at maximum network final power for a hierarchically branched network, plotted on log-log axes. 75

Figure 2.7. The relative final power of consumers (P_C) at each level of the ‘fully branched’ network, as related to the relative resource flow to each consumer (I_C) 76

Figure 2.8. Code flow diagram for flow calculator program 81

Figure 3.1. The distribution of each network metric by soil type, for (a) main soil networks and (b) subnetworks..... 113

Figure 3.2. Distributions of (a) each agent-based model (ABM) outcome variable, grouped by resource parameterisation (columns, labelled at top) and consumer parameterisation (x axis within columns), across both soil types, and (b) ABM outcome variables that were significantly affected by soil type (represented by colour), grouped by resource parameterisation (columns) and consumer parameterisation (x axis within columns)..... 117

Figure 4.1. Images from the simulations. 158

Figure 4.2. Standard deviation (SD) of consumer energy reserves, total link length, mean node degree, and SD of link length over time, for Cities, Transition, and Villages landscapes 172

Figure 4.3. The overall network development and consumer energy reserves distributions, for Cities, Transition, and Villages networks, by timestep (T). 173

Figure 4.4. Standard deviation (SD) of consumer energy reserves, total link length, mean node degree, and SD of link length over time, for three example networks of each Cities, Transition, and Villages landscapes. 174

Figure 4.5. The network development and consumer energy reserves distributions, for three examples of each (a) Cities, (b) Transition, and (c) Villages networks, by timestep (T)..... 177

Figure 4.6. Time series showing evolution of total link length, mean and standard deviation of consumer energy reserves, and population size for Cities networks, with labels showing main simulation events..... 179

Figure 4.7. Time series showing evolution of total link length, mean and standard deviation (SD) of consumer energy reserves, and population size for (a) Cities, (b) Transition, and (c) Villages networks 181

1

Introduction

The requirement for energetic resources is ubiquitous across earth systems. Depending on the system, these resources are transported through a vast array of interconnected networks, such as foraging trails, vascular systems, electricity grids, roads, and railways. The heterogeneity of these resources in space and time, and the resulting heterogeneity of the networks distributing and providing access to them, has been linked with biodiversity, behavioural adaptations, and ecosystem functioning and stability in natural systems. In socio-ecological systems, however, this inequality in basic resources is linked with negative health, environmental, and economic outcomes for individuals and groups. This heterogeneity in natural systems and inequality in socio-ecological systems, as well as the resource distribution networks that supply them, have been studied from a variety of perspectives. However, the link between resource distribution network structure and heterogeneity of resource flow has rarely been studied, especially with explicit consideration of the spatial dimension of networks or the thermodynamic and physical laws governing earth systems.

This introduction provides an overview of the literature associated with heterogeneity and inequality in resource distribution networks. The first section outlines the causes and effects of heterogeneity and inequality in natural and socio-ecological systems. In the second and third sections, resource distribution networks are introduced, and their major shared characteristics are discussed, with a focus on how that affects heterogeneous distribution. Finally, a brief overview of previous analytical methods and conceptualisations, along with areas of future work, are highlighted, and the thesis aims and structure are outlined.

1.1. Heterogeneity and inequality

1.1.1. Natural systems

In natural systems, the concept of environmental heterogeneity is often divided into spatial or structural heterogeneity, and resource heterogeneity (Stevens and Tello, 2011). Structural heterogeneity refers to the different physical structures within the environment, such as rock formations, canopy layers, understory vegetation, soil pores, and other microhabitats. These provide a range of shelters, breeding and nesting grounds, and foraging and hunting territories. Resource heterogeneity refers to the unequal spatial and temporal distribution of energetic resources used by consumers. This distribution is caused by interactions of structural heterogeneity and local climatic and environmental factors, as well as disturbances and top-down forces such as predation, herbivory, parasites, and pathogens that prevent takeover by any single species (Eichhorn, 2016). These cause heterogeneity of primary producers, which is then propagated upward through trophic levels to create diversity of primary consumers and beyond, often involving dynamic ecological processes such as succession, predator-prey interactions, and dispersal (Eichhorn, 2016; Guichard, 2017).

Other processes which affect the resource heterogeneity of a system are anthropogenic impacts, such as fragmentation through habitat destruction. This limits the physical range of species, potentially cutting them off from key resources and causing extinction. While heterogeneity in the physical environment and resource ‘patchiness’ can lead to greater specialisation and biodiversity, as will be discussed, fragmentation often occurs at spatial scales to which local species are not adapted. This can interrupt larger ranges and territories, bar migration routes, cut off access to essential resources such as water sources, or trap species in effective ‘islands’ of habitat where such small populations are supported that stochastic disruption can quickly lead to extinction (Tews *et al.*, 2004; Seiferling, Proulx and Wirth, 2014).

Discussions of environmental or structural heterogeneity in natural systems often describe a relationship between a measure of heterogeneity and a measure of diversity. These so-called heterogeneity-diversity relationships (HDRs) have been investigated across a range of terrestrial and aquatic ecosystems (see reviews in Tews *et al.*, 2004; Stein, Gerstner and Kreft, 2014). In these systems, the relationship between heterogeneity and diversity is hypothesised to be positive, as an increase in the types of resources available creates more niches (in the sense of Grinnell, 1917; Hutchinson, 1978) for species. Depending on the size of the area in question, this relationship may also become unimodal, if increased heterogeneity beyond a threshold leads to areas that are too small to support populations of specialists that are large enough to avoid stochastic extinctions (Heidrich *et al.*, 2020). Efforts to prove this single rule relating heterogeneity to biodiversity have been hampered by the considerable situational differences that occur among natural systems (Naeem and Colwell, 2012), and different definitions of both heterogeneity and diversity (Tews *et al.*, 2004). However, several large meta-analyses suggest a generally positive or unimodal relationship between heterogeneity and the richness or abundance of species supported by an area (*e.g.* Tews *et al.*, 2004; Stein, Gerstner and Kreft, 2014). Furthermore, resource heterogeneity can lead to a range of behavioural and social adaptations within species (*e.g.* MacArthur and Pianka, 1966; Horn, 1968; Hopkins, 2011; Stevens and Tello, 2011; Croft, Hodge and Pitchford, 2012; Tanner and Jackson, 2012; Silva *et al.*, 2013; Wright and Rohde, 2013). It can also lead to population stability (*e.g.* Brown, 2007; Oliver *et al.*, 2010) and ecosystem functioning and stability (*e.g.* Tylianakis *et al.*, 2008; Godbold, Bulling and Solan, 2011; García-Palacios *et al.*, 2012; Wagg *et al.*, 2014; Wang *et al.*, 2019).

For example, the environmental heterogeneity of the soil matrix, and the range of habitats and resources this encompasses, creates niches for a diverse range of organisms. Soil involves a significant degree of both horizontal and vertical structural heterogeneity, which is caused by erosion and weathering processes, deposition, burrowing roots and organisms, and movements of

gas and water (Oades, 1993). This structural heterogeneity, coupled with nutrient build up from drainage and decomposition, creates a range of habitats and resource pools. This provides opportunities for resource and habitat specialisation, predator avoidance, and limitation of competitive exclusion (*e.g.* Ettema and Wardle, 2002; Bardgett, Yeates and Anderson, 2009; Young and Ritz, 2009), and results in significant biodiversity of microorganisms and fungi, and species that prey upon them (Bardgett, 2005). This includes both animals and fungi that live exclusively in the soil, as well as terrestrial plants and animals that burrow into the soil for shelter or to forage. For this reason, soil heterogeneity has also been linked to more productive and stable aboveground communities, again by limiting competitive exclusion, providing stable resource bases and refuge from predation, creating microhabitats with characteristics different to those of the surrounding soil matrix, and enabling signalling mechanisms and activities, such as the pathogenic fungi that promote tree spacing introduced above (Ettema and Wardle, 2002; Wardle *et al.*, 2004; Baer *et al.*, 2005).

While resource heterogeneity can lead to many positive outcomes, it can also lead to local and global extinction of species, especially if it is caused by anthropogenic fragmentation (Tews *et al.*, 2004; Seiferling, Proulx and Wirth, 2014). As discussed, the scales at which fragmentation occurs rarely correspond with the scales at which habitats and their inhabitants have co-evolved. For example, the natural structural and resource heterogeneity in the soil matrix is easily disrupted by ploughing and compacting activities of agriculture (Kravchenko *et al.*, 2011). Although ploughing arguably creates a certain type of heterogeneity, it is far more fractured and random than that which occurs through natural processes. Soil that has been ploughed repeatedly loses much of the structure and resources that allow it to support healthy ecosystems, such that this form of heterogeneity leads to decreased biodiversity and stability (Bardgett, Yeates and Anderson, 2009; Kravchenko *et al.*, 2011). The contrasting effects of heterogeneity have led some to argue that, in the face of anthropogenic modification of ecosystems, it would be better to conceptualise

naturally-occurring environmental heterogeneity as a form of complexity (Parrott, 2010; Seiferling, Proulx and Wirth, 2014). This term better captures the different effects of natural heterogeneity, which has co-evolved with the ecosystem in question, versus the randomising or fragmenting heterogeneity introduced by humans.

Regardless of terminology, however, identifying the cause of heterogeneity and the scale on which it occurs, compared to the scales on which the affected species operate, is necessary to predict its impacts. As many of these impacts have widespread ramifications for ecological and socio-ecological systems functioning and health, understanding the causes and effects of resource heterogeneity is crucial for guiding preservation, restoration, and management efforts.

1.1.2. From heterogeneity to inequality

The heterogeneous distribution of natural resources has profound impacts on human society as well. Many modern societies are physically distant from the natural resources that supply them, creating a sense that globalisation and international supply chains have severed the connection between heterogeneity of resources and of individuals and groups. In pre-modern societies, however, the spatial distribution and characteristics of resources, as well as the cultural dynamics that emerged around resource ownership and use, played a dominant role in determining social hierarchy and the origins of inequality. Here, 'inequality' is used to refer to differing levels of access that individuals of the same species have to the basic resources they require for survival and health, rather than higher-level resources within society. The focus of this work specifically is on energetic resources, such as food and fuel, which are typically classed in anthropological and sociological studies with material resources, including housing, livestock, and possessions. However, inequality in these energetic and other material resources is often linked to inequality in embodied wealth (physical health, abilities, and skills) or relational wealth (social status and connections) (Smith, Hill, *et al.*, 2010).

It is posited that historically, the ‘defensibility’ of certain types of resources, due to their reliable and dense but patchy occurrence, led to the development of territoriality and ownership behaviours in certain societies (Mattison *et al.*, 2016). For example, while undomesticated animal herds or nuts and seeds are widely distributed and difficult to predict or control, food-rich areas of streams or forests would have been more worth the energetic costs associated with defence, leading to territorial behaviour in groups with respect to these resources (Dyson-Hudson and Smith, 1978; Mattison *et al.*, 2016). As all these resources are geographically distributed, some individuals and groups had greater access, leading to inequality. The concentrated, predictable, and therefore defensible resources also allowed for the accrual of surplus (Gurven *et al.*, 2010), which increased inequality further, and encouraged some groups to remain more geographically fixed.

Similarly, the rise of agriculture during the Holocene epoch and the storage of surplus food that came with it effectively created a new type of patchy, defensible resource (Summers, 2005; Mattison *et al.*, 2016). As with the natural resources with similar characteristics, domesticated plants and livestock led to increased inequality between those who owned them and those who did not. This also brought an increased focus on material wealth, as groups became less nomadic and began accumulating possessions. Together, these changes led to the development of inheritance, or intergenerational wealth transmission, which cemented inequality in society (Smith, Hill, *et al.*, 2010; Shennan, 2011; Mattison *et al.*, 2016). Although inheritance took different forms depending on the society in question, it led to the children of wealthy parents becoming wealthier themselves, materially but also often physically, due to better nutrition, and relationally, due to good connections fostered by their parents (Smith, Bowles, *et al.*, 2010).

Over time, the development of modern society and its reliance on resource redistribution through elaborate, interconnected networks distanced most individuals from the original source of their energy resources, such as food and electricity. While the rise of distributed, renewable energy sources and local agricultural movements counteract this somewhat (*e.g.* Sattler, 2016), the overall

trend is still that resources are relocated considerable distances from their starting points. Therefore, it is now most relevant to discuss inequality from the perspective of access to re-distributed resources, rather than access to the resource's point of origin. This inequality can take the form of different quantity, cost, or quality of resources. Two particularly relevant examples are the food and energy insecurity faced by some, both of which can result in limited access to other goods and services that rely on these forms of energy, and significant health and educational disparities.

Food insecurity, or physical or financial inability to access enough quality food, is at its heart a problem of access. It often occurs in areas described as 'food deserts:' typically inner city or rural areas where there are few or no grocery stores providing reliable, inexpensive access to healthy food options (Hendrickson, Smith and Eikenberry, 2006). Residents of food deserts may be unable to afford a car or public transport to more distant grocery stores, or they may feel unsafe, be physically unable, or too busy to walk long distances to different shopping options (Walker, Keane and Burke, 2010). Cost also plays a role: while convenience stores and smaller grocery stores may charge more for what they sell than larger chain supermarkets, the combined cost of transport to distant stores, and higher prices of fresh fruit and vegetables may dissuade low-income customers from these options (see review in Walker, Keane and Burke, 2010). As a result, food deserts have been linked to higher rates of obesity, as well as health conditions such as diabetes, cancer, and cardiovascular disease where diet can play a significant role (Caspi *et al.*, 2012).

Energy insecurity is another redistribution problem facing a substantial percentage of the population. Currently, up to 770 million people, predominantly in sub-Saharan Africa, are without electricity, and more than 2.6 billion people worldwide still rely on traditional fuel sources such as biomass to cook and heat their homes (IEA, 2020). The use of this type of fuel is associated with many health hazards, including exposure to severe weather, wild animals, and assault during collection (Gaye, 2007; Sovacool, 2012), and a range of respiratory conditions during burning,

especially in the women, children, and elderly who spend the most time in the home (Gaye, 2007). Its use can also cause families to avoid or undercook protein-rich foods such as beans or meat, which take a long time to cook, or to not boil water to sanitise it before use (Murphy, 2001; Sovacool, 2012). Additionally, the time spent collecting and working with biomass energy sources prevents individuals, disproportionately women and girls, from attending school or engaging in income-generating activities to lift themselves and their families out of poverty (Sovacool, 2012).

As discussed, however, resource heterogeneity in natural systems, where species can adapt or disperse to take advantage of resource niches, results in biodiverse and stable ecosystems. These negative impacts of socio-ecological inequality and positive impacts of ecological heterogeneity are frequently the focus of mitigation or preservation efforts, respectively. To direct these efforts, it is crucial to understand what causes and maintains these phenomena as systems develop, and their effect on end consumers and overarching systems. The following sections will focus on resource distribution networks: what they are, how they function, and how they contribute to heterogeneity and inequality. This will establish a clearer understanding of the relationship between the structure and dynamics of these networks and resource distribution in ecological and socio-ecological systems, and present directions for future study.

1.2. RADE networks

Given the universal requirement of energetic resources for maintenance, growth, and development, and the heterogeneous distribution of these resources as discussed above, considerable energy must be spent relocating resources from points of acquisition to points of consumption and end use. The infrastructure enabling this relocation can be conceptualised as a series of nested, interconnected resource acquisition, distribution, and end-use networks ('RADE' networks, *e.g.* Jarvis, Jarvis and Hewitt, 2015). Examples of RADE networks include the vascular networks of plants and animals, food distribution systems, foraging trails, electricity and water grids, rivers, and soil macropore networks. In each of these examples, the overarching system is

comprised of resources, which move or are moved through the network of links from points of generation to consumption, and consumers, who are the end users and recipients of the resource flows (Table 1.1). While the specifics of resource and consumer mobility, link materials, and spatial scale differ among networks, the vocabulary of consumer, resource, and link remains useful to distinguish the parts within each system and make comparisons between them.

In the following sections, the main characteristics of RADE networks are introduced, and examples are presented to illustrate these characteristics in RADE networks across a range of earth systems. Also highlighted is the relationship between each of these characteristics and the heterogeneity that RADE networks encompass, and inequality that they can perpetuate.

Table 1.1 Some examples of resource acquisition, distribution, and end-use (RADE) networks.

System	Consumers	Resources	Links
Vascular network	Body tissues	Blood, photosynthates	Arteries and veins; xylem and phloem
Electricity grids	Houses, businesses, schools	Electricity	Power lines
Food distribution systems	Humans and domesticated animals	Raw and processed food products, feed	Freight networks (road, rail, aviation)
Soil matrix	Soil biota, plants	Minerals, water, lower trophic level producers and consumers	Macropores

1.2.1. Nested networks

While the vocabulary of resources, consumers, and links is useful for describing and comparing RADE networks, and all RADE networks can be conceptualised in this way, the networks are also inherently interconnected and nested. For example, a plant consuming nutrients and water is a consumer when viewed from the perspective of the soil matrix, but also contains a vascular network with xylem and phloem moving nutrients throughout the structure of the plant. To an herbivore, the plant may be the resource it seeks when it is following foraging routes. Similarly, food is grown with inputs from the energy grid and sourced through the freight network, and later

enters a human's digestive system, where it is transported throughout their body. Therefore, a caveat to this vocabulary is that it can quickly become complex to differentiate between consumers, resources, and links, when the relevant focus area includes nested systems of each.

To constrain analyses, much previous work has drawn boundaries to differentiate between 'internal' resource distribution networks, such as metabolic and vascular networks (West, Brown and Enquist, 1997; Banavar *et al.*, 2010), and 'external' networks, such as foraging (Charnov, 1976; Bianchi, Schellhorn and Van Der Werf, 2009), transport (Levinson and Yerra, 2006), or energy distribution networks (Dalgaard and Strulik, 2011). However, these boundaries are arguably imposed somewhat arbitrarily, and being 'internal' or 'external' is likely less relevant to the dynamics of resource flow than other topological and material aspects influencing network construction, evolution, and use. This has led others to focus more on the resource flowing through the network, and various transformations it undergoes along the way (Odum, 1988). When resource distribution networks are studied from the perspective of energy flows, it is easier to ensure physical consistency of the system, as will be discussed in later sections, and observe more systemic phenomena, such as inequality in resource flows and points of resource scarcity.

Originally, energy flow-based analyses focussed on the dynamics of energy and material flows through food webs. This led to Lindeman (1942) pioneering the concept of trophic levels to describe the hierarchical organisation of these flows in ecosystems. This structure has been linked to increased energy dispersal in natural systems, by showing that each trophic level acts as an energy gradient for the consumers of higher trophic levels to exploit (Annala and Kuismanen, 2009; Meysman and Bruers, 2010). Others have used similar methods on networks of species interactions to quantify system-wide properties that are difficult to measure from individual observations, such as modularity, homogenisation, synergism, and the impact of indirect effects (Fath, 2004; Fath *et al.*, 2007; Fath and Patten, 2013; Jørgensen, Nielsen and Fath, 2015; Dormann, Fründ and Schaefer, 2017; Tylianakis and Morris, 2017; Delmas *et al.*, 2019; Fath and Scharler, 2019).

Other examples of nested, energy-centric analyses are H.T. Odum's energy flow models (*e.g.* Odum, 1971), and other analyses based on similar concepts (see review in Brown and Ulgiati, 2004; also Yi *et al.*, 2017; Giannetti *et al.*, 2019). Odum used simple electrical analogues to model the flows of energy through macrosystems, such as entire ecosystems or socio-ecological systems. He pointed out that each transformation of energy, such as the uptake of a resource flow by a consumer or another state change in the resource prior to end use, resulted in the loss of some energy in the creation of a higher order of energy. He termed this energy consumed in creating higher forms of energy a 'transformity' (Odum, 1988). The concept of transformities allowed Odum to calculate the complexity and interconnectedness of natural and human-engineered systems, by tracking the number of transformations or interactions between a given resource and the primary solar energy input to the ecosystem.

Although more from a perspective of individuals, the Metabolic Theory of Ecology ('MTE', *e.g.* Brown *et al.*, 2004), also attempts to track energy flows throughout nested systems, starting from the perspective of organismal metabolism as determined by their internal metabolic network. This metabolic rate is considered the fundamental rate controlling individual life history, and therefore dynamics at scales from the individual, to population, and whole ecosystem (Brown *et al.*, 2004). An alternative metabolic theory called Dynamic Energy Budget theory ('DEB' *e.g.* Kooijman, 2009; Jusup *et al.*, 2017), attempts to make similar predictions of population- and ecosystem-level energy flows, but with different foundational assumptions: it focusses not on the internal metabolic networks of individuals, but how they allocate energy to different functions of maintenance and growth. Both MTE and DEB can provide insights into how the energy dynamics of an individual scale to higher levels of organisation, without imposing strict trophic levels.

1.2.2. Active and passive transport

Across all levels of organisation, resource distribution occurs via active transport and passive flows. Active transport applies reserves or external sources of energy to extract and redistribute resources.

It is therefore often conceptualised as an intentional choice on the part of the consumer (Haff, 2012), even when the resource distribution is necessary for survival. One example is foraging networks (*e.g.* Charnov, 1976; Menzel *et al.*, 2005; Silva *et al.*, 2013; Trapanese, Meunier and Masi, 2019), where organisms use energy stores to seek out resources in their environment, which they consume immediately, or bring back to a central point for storage and later consumption. Similarly, transportation networks in human society rely on fossil fuels, electricity, and other energy sources to transport stocks of primary energy such as oil and coal, as well as humans, food, and construction materials. As this type of resource distribution relies on reserves from previous resource flows, it can allow consumers who have more reserves to multiply these further, while consumers with fewer reserves are less able to engage in network development to increase resource flows to themselves. In this way, inequality that existed externally to the network can be perpetuated within the structure or flows of the network, and therefore increased, unless the external energy reserves are explicitly applied to equalise distribution. This will be discussed more in Section 1.3.

In contrast, passive flow networks are those which rely on gradients of gravitational energy, or forms of energy stored within the resource itself, to move the resource along the network. This consumes some of the potential energy of the resource but does not require external energy to be applied in transport. Two such examples are electricity and river networks. In these, the voltage and pressure respectively decrease as the flow moves through the network, such that the final energy, or energy at points of consumption and use, is lower than the primary energy at points of acquisition. As these networks rely on heterogeneously distributed resources, they are likely to perpetuate this heterogeneity through the network to create inequality among points of final consumption.

Although passive flow and active transport networks are typically studied separately, both forms of resource distribution require energy consumption, albeit from different sources. As will be

discussed, the total energy input into the network, either as primary energy in the passive flow networks, or primary energy plus energy used for distribution in the active transport networks, is always more than the final energy at the points of end use (Panda, 1981). Therefore, although the mechanisms of transport are different, these two types of RADE networks are energetically comparable, and analogies can be drawn between them for modelling and analysis (Odum, 1971, 2002).

Additionally, some networks facilitate both forms of resource transport, such as soil macropore networks where passive flows of water and nutrients occur alongside active foraging of organisms (Table 1.1). By accounting for the energy required for both forms of transport in a comparable manner, a clearer picture of the total energy used to create, expand, maintain, and use the network can emerge. This leads to a better understanding of the relationships between this energy consumption, network structure, and end consumer state.

1.2.3. Energy, matter, and information

Together, energy, matter, and information make up the three “joint pillars of living systems” (O’Connor *et al.*, 2019, p. 2), and comprise the building blocks of RADE networks. In the following, definitions for and examples of these three components in RADE networks will be presented. As the focus of the work here is on networks, and many consumers and resources are comprised of networks themselves, the following section will primarily reference where energy, matter, and information are located within the network architecture. However, much of the same could be said for the consumers these networks serve, and the resources they transport.

Table 1.2 The definition and location of energy, matter, and information in resource acquisition, distribution, and end-use networks (RADE networks).

Component	Definition	Location in RADE networks
Energy	The property required to change a substance	<ul style="list-style-type: none"> • Contained in potential form by the resources moving through the network • Used to grow or maintain the network or the end consumers
Matter	A substance with mass and volume	<ul style="list-style-type: none"> • The physical structure of the links of a network, such as asphalt; tissue; or permeated, packed, or smoothed soil • The physical structure containing the energy of the resources, such as chemical bonds
Information	The values of process outputs that determine the structure of the RADE network and differentiate it from its surrounding environment; or the difference between two system states	<ul style="list-style-type: none"> • Encoding used to determine network structure, <i>e.g.</i> genetic material • Signals transmitted that indicate the existence and location of a resource, <i>e.g.</i> scent trails

Energy is a fundamental component of all physical compounds, defined as the property required to change or heat the substance in some way. In the context of RADE networks, potential energy such as chemical bonds in food or charged ions in electricity are transported through the network to points of end use (Table 1.2). There, it is used for maintenance, such as the repair of tissues or other structures, and growth, through increases in size, organisation, or reserves of stored energy (Ulanowicz, 2011). This can occur at the level of end consumers, such as the energy used to grow or repair damaged tissues within a mammal's vascular system (Sousa, Domingos and Kooijman, 2008; Kearney and White, 2012). It can also occur as reinvestment at the level of the RADE network itself, such as the energy invested by humans in expanding and maintaining an electricity grid (*e.g.* Dalgaard and Strulik, 2011), or by foraging plants and animals in widening and connecting soil macropore networks (*e.g.* Hodge, 2004). The total of this energy consumption in maintenance and growth is defined as the embodied energy of the structure (Costanza, 1980).

The organisation of this energy into matter is a function of the information content of the structure (Table 1.2). In the context of RADE networks, information is the values of process outputs (Losee, 1997) that determine the structure of the RADE network and differentiate it from its surrounding environment. For this reason, information in biological and ecological systems is often defined as the difference between two possible system states (O'Connor *et al.*, 2019), and measured with Shannon entropy (a measurement of the complexity of a sequence, not to be confused with thermodynamic entropy, see Section 1.3.1) or similar metrics. For example, most studies of information within ecological systems have focussed on the genetic code of organisms, particularly with a view to the biodiversity of an area (Vallino, 2010; O'Connor *et al.*, 2019). This genetic information results from the process of the organisms' development, and determines, among other things, the structure and dynamics of the internal metabolic and circulatory networks of the organisms, with increasing information corresponding to increasing physical complexity (Vallino, 2010). Additionally, this information allows for system-level coordination, as evolutionary pressure and selection for different sequences allows organisms evolve to take advantage of different resources within their environment (Vallino, 2010) (see Section 1.3.3).

There are also RADE networks where the network structure is exclusively or predominantly comprised of information, rather than matter. For example, in the case of stigmergy (*e.g.* Klyubin, Polani and Nehaniv, 2004; Lecheval *et al.*, 2021), organisms overlay information trails via cues, such as scent trails, across physical routes. This serves to structure and differentiate their RADE network from the surrounding environment, and guide future foraging efforts undertaken by them or their kin. Resources can also leave informational cues in the environment, such as scent gradients or visual cues, that alert foragers to their presence. These are often followed using highly developed, but often quite simple search mechanisms, such as optimising time spent in local and global search strategies to maximise information about a target (Calhoun, Chalasani and Sharpee, 2014). Finally, some RADE networks are developed and maintained through direct transmission

of signals and information about the environment, without modifying the environment itself. Honeybee waggle dances (*e.g.* Seeley, 1995; Menzel *et al.*, 2005) are one such example.

In all these examples, information is used to structure and differentiate the RADE network from the surrounding environment, such that changes in the organisation or development of a network can also be conceptualised and measured as changes to its information content. As these changes also require energy, there is clearly a link between information and the energy invested in RADE network creation, development, and maintenance, suggesting parallels or equivalencies between embodied energy and embodied information. Although this has not yet been explored, work in this area could provide insight into the relationship between this energy investment, network structure, and end consumer or system outcomes.

Although not explicitly including information or discussion of RADE networks, a significant body of previous work has focussed on the flows of energy and matter in both ecosystems and socio-ecological systems. Alongside the work discussed in Section 1.2.2 is the meta-ecosystem theory, developed by Loreau *et al.* (2003) and later expanded (Guichard, 2017; Gounand *et al.*, 2018). Meta-ecosystem theory posits that ecosystems are connected through spatial flows of energy, matter, and organisms (Loreau, Mouquet and Holt, 2003). On smaller scales, local ecosystems take on roles as sources or sinks of given flows, and the properties of the encompassing meta-ecosystem emerge from these local dynamics. Similar ideas have been proposed by Polis *et al.* (1997) and Anderson *et al.* (2008) using the concept of spatially subsidised food webs, where dispersal of organisms, detritus, and nutrients from one habitat to another can create bottom-up or top-down effects that propagate through the food webs in both habitats. For example, inputs of nutrients and detritus can increase the secondary productivity of herbivores and decomposers, while dispersal of consumers can depress local resources, both of which affect the stability and functioning of the ecosystems (Polis, Anderson and Holt, 1997).

1.2.4. Spatial, temporal, and interactional dimensions

These components of energy, matter, and information in RADE networks are expressed across three dimensions: spatial, temporal, and interactional. The spatial dimension describes the existence of the network across physical distances, even for networks comprised solely of information, such as some of those described above. The temporal dimension describes how the network emerges, is developed, and is maintained or eventually decays over time. The interactional dimension describes the relationships among consumers and resources connected via the network. While these are rarely studied simultaneously, understanding each dimension and its relationship with the others is crucial for an accurate and comprehensive description of resource distribution. In this section, these three dimensions will be described in more detail, and the role of each in the dynamics of the network will be discussed.

Typically, the spatial dimension of RADE networks has been the focus of disciplines such as transport geography (*e.g.* Yerra and Levinson, 2005; Levinson and Yerra, 2006), electrical and hydrological engineering (*e.g.* Carradore and Turri, 2009; Dalgaard and Strulik, 2011; Yang *et al.*, 2017; Ma, Chen and Wang, 2018), and some subsets of metabolic biology and ecology (West, Brown and Enquist, 1997; Brown *et al.*, 2004). It is often measured by some length metric describing the total, mean, or maximum link length; the area of the irregular polygon encompassing all points in the network; or the mean or maximum path length between any two given points (Rodrigue, 2017). As will be discussed, the energetic costs of moving resource flows increase with distance, which determine the financial or metabolic costs of constructing, maintaining, and using the network. Therefore, in disciplines such as transport geography or metabolic biology, where these costs are a key focus and networks tend to operate at a consistent state or predictable pattern, analyses have focussed predominantly on measuring the spatial extent of the network.

In addition to the spatial size of RADE networks, another factor that affects resource flows is the spatial heterogeneity of the network structure, or the evenness of the spatial distribution and size

of links. For example, a highly branched or fractal network structure is much more spatially heterogeneous than a random or uniform network structure. While the branched architecture is a more efficient space-filling structure (West, Brown and Enquist, 1997), flows across a hierarchical structure are necessarily hierarchical themselves, leading to inequality in the resource distribution (Bejan and Errera, 2017). This connection between spatial heterogeneity and resource flows has also been illustrated empirically in soil networks, where the heterogeneity, connectivity, and tortuosity of the pore space is linked to soil functions, such as diffusion of water, gasses, and nutrients, and movement of organisms (Crawford, Ritz and Young, 1993; Young, Crawford and Rappoldt, 2001). Spatial heterogeneity should be able to be measured and compared between networks using measures of the network's information content (see Section 1.2.3), such as the Shannon entropy (O'Connor *et al.*, 2019). However, the relationship between spatial network heterogeneity and inequality of resource distribution has not yet been explored in this way.

In other disciplines, such as economics and ecology, the focus of most RADE network analysis is the interactional component. In economics, this often takes the form of analysing the exchanges of money and resources that occur across RADE networks, while focussing less on the physical structure of the network itself (*e.g.* King, 2016, 2020). The financial or energetic costs of transport may also be considered part of the economic output of an area or sector, as opposed to necessary thermodynamic costs (see discussion in Jarvis, 2018). In ecology, due to the difficulty of establishing the exact foraging routes taken by organisms, the focus is similarly on quantifying who eats whom or what, perhaps with an acknowledgement of the temporal dimension in discussion of how often or how much they consume (*e.g.* Odum, 1968; Fath *et al.*, 2007; Fath, 2012; Jørgensen and Nielsen, 2015). Although limited, there has been discussion of the importance of incorporating a spatial dimension into these analyses (*e.g.* Loreau and Holt, 2004), and the unrealistic results that nonspatial analyses can produce (McCann, Rasmussen and Umbanhowar, 2005). The increased use of GPS tracking, remote sensing, and isotopic analysis (*e.g.* Choy *et al.*, 2010; de Lecea, Smit

and Fennessy, 2016; Fauchald *et al.*, 2017) could lend a clearer spatial dimension to ecological network analysis, and wider availability of infrastructure data could do the same for human-engineered networks.

Similarly, the network analyses that are performed on social networks (see review in Borgatti, Everett and Johnson, 2018), focus less on physical distances between interactors. Instead, these are analysed with measures of connectivity to quantify who interacts with whom, and potentially how much or how often. For example, inequality in the connectivity of a network, measured by the node degree distribution, has been shown to dramatically impact the survival of nodes when they each rely on a certain amount of resource flow (Ingale and Shekatkar, 2020). Therefore, the interactional dimension of RADE networks is important for understanding the emergence of networks as links between end consumers and their resource bases, and the quantity of flows through the network to different consumers. These interactions are necessarily mediated over space and time, though, making the latter two dimensions equally critical for a clear picture of the impact of RADE network size, structure, and dynamics on consumer and system outcomes.

In some disciplines, the temporal dimension of RADE networks is encompassed in the treatment of the spatial or interactional effects, as measurements of resource flow are often in units of mass per time. The rate at which resources are transferred across space or between entities can significantly impact the resulting state of end consumers, whose own metabolic rates, energy budgets, and lifecycles depend on the resources available to them (Brown *et al.*, 2004; Kooijman, 2009). For example, in foraging networks, the speed with which the forager navigates a patch affects the energy expended and the quantity of potential resources that are encountered (Charnov, 1976; McNair, 1982). Similarly, the current of water or electricity, measured in metres or amps per second, determines the resulting power at end points and transformers along the network. The variance in availability of resources over time, such as pulsing or seasonality, can also affect the growth or activity rates of consumers: migration, nomadism, and hibernation are common

responses to seasonal changes in resource availability (Humphries, Thomas and Kramer, 2003; Mueller *et al.*, 2011; Teitelbaum *et al.*, 2015), and adaptation to pulsing resources has been shown to increase the total productivity of an ecosystem (Lee, 2014).

1.2.5. Summary

Although RADE networks are typically studied within specific disciplines, such that only one or a few of the characteristics highlighted here are discussed explicitly, each of these characteristics and the interactions among them can have considerable impact on the state of end consumers or the overarching system. For example, the heterogeneous spatial configuration of the network can lead to unequal resource flows to end consumers, who then have less energy to reinvest in developing the network, resulting in a feedback on inequality of resource distribution. Without due consideration of the spatial, energetic, and informational characteristics of the network, this feedback could easily be missed. Additionally, considering both active and passive transport occurring within a network, or the nested levels on which resource flows operate, can provide a clearer picture of the overall energy balance and flows through the system. In the following section, the dynamics of these energy flows will be discussed in more detail, further clarifying the importance of each of the different RADE network characteristics described here.

1.3. How do RADE networks work?

1.3.1. The thermodynamics of resource distribution

The dynamics of resource flows across these dimensions are constrained by the same physical and thermodynamic laws that govern all physical substances on Earth. Here, these laws will be introduced as they relate to RADE networks, and in the following sections, their role in determining RADE network dynamics and development trajectories will be discussed.

Briefly, the first law of thermodynamics states that energy is conserved, such that all energetic inputs to a system must be accounted for as outputs. This constrains the total energetic throughput

of a system. Similarly, the conservation of mass requires matter to be conserved throughout transformations and relocations in the system. Hereon, this conservation of energy and matter will be referred to as ‘flow consistency.’ Within the context of RADE networks, flow consistency constrains that the total output of the network must be equal to the inputs. Depending on the network, these outputs may take the form of energy lost as waste, such as through leakage or system by-products, and energy output to end consumers for useful work (Odum, 1988).

In all systems, energy transformations also consume energy that is released from the system as an unusable form of energy called entropy, which often takes the form of heat. This is described by the second law of thermodynamics, which states that the entropy of a closed system cannot decrease, and it increases during energy transformations. In the context of RADE networks, energy transformations include any state change in the energetic resource, such as consumption and digestion by a higher-level consumer, or applying stored energy to move more resources.

When coupled with the first law, the second law indicates that the proportion of potential energy available to the end consumers to do useful work is less than the original energetic inputs to a network. This can be stated in terms of all resource flows being ‘downgradient’ with respect to total energetic inputs: the final energy contained in the resource flow at points of consumption and end use is lower than the initial primary energy input to the network. As discussed previously, this is somewhat more complex in networks where the energetic inputs include both primary energy of the resource and additional energetic inputs for its extraction and transportation, sourced from reserves of previous flows. In these networks, the final energy is still less than the combination of all primary energy and inputs, but several networks and timescales may have to be included to fully establish the energy balance (Panda, 1981; Odum, 1988).

1.3.2. Energy allocation

The energy requirement for moving resources across a RADE network from points of supply to points of consumption and end-use consumes a sizeable quantity of this input or stored energy.

The energy required to move these resources is due to the friction experienced when moving matter over distance, which generates heat. This heat is a form of entropy, which is lost from the proportion of potential energy for useful work as discussed above. The friction can also be described as resistance, impedance, or drag, depending on the system in question. Frictional losses are proportional to the distance that the resources are transported and are also related to inherent roughness of the network surface or terrain over which the resource flow is moving. Therefore, accurate measures of both distance and roughness are crucial for calculations of the energy balance and understanding the state of the network and its end consumers.

To minimise these frictional losses, networks have evolved toward theoretically optimal transport architectures. For example, the self-similar or fractal hierarchical branching structures, seen across a diverse range of both natural and human-engineered RADE networks, are hypothesised to be an adaptation to minimise the frictional losses of a space-filling network (West, Brown and Enquist, 1997). The ubiquity of the architecture suggests that the frictional losses it minimises are a dominant effect across different networks. As will be discussed, however, the spatial heterogeneity of this architecture may also increase the heterogeneity of resource flows through it, and therefore the inequality experienced by end consumers.

After the energy consumption in moving the resources and maintaining both the network and the end consumers is considered, the net excess resource flow can be used for growth and development. As detailed earlier, this can take the form of expansion and improvement of the RADE network. These can increase the efficiency of future resource flows by minimising frictional losses incurred during transportation. For example, adding lanes to a congested road, increasing the strength of scent markers along a foraging route, or progressive widening and deepening of river channels are all ‘improvements’ to the network that can increase total and net future resource flows. These improvements can also be conceptualised as increasing the information content of the network, through using energy to increase the structuring of the network architecture itself.

Notably, any expansion or growth in the physical size of the network must necessarily be accompanied by these efficiency-increasing improvements as well, to offset the increased energy requirement for transporting resources across longer distances (Jarvis, 2018). Even then, larger networks can suffer from decreasing returns to scale, when the efficiency improvements cannot fully compensate for the increased size (Jarvis, 2018). This is perhaps most acutely felt by consumers who are less well-positioned in the network, especially as any improvements can only be implemented by consumers with already enough net energy to do so or will occur along preferential flow paths in passive flow networks. The next section will relate this back to the thermodynamics of resource flows introduced previously and describe how this feedback can effectively lock in the inequality of a network.

1.3.3. Thermodynamic trajectories

This coupling of increases in efficiency, resource flows, and physical size creates a growth-oriented positive feedback, inevitably evolving to some boundary or constraint, which can be considered a thermodynamic limit on efficiency (Kleidon, 2016). This trajectory of systems to grow toward a thermodynamic limit has been formalised in the theories of maximum power production (MPP), and its corollary, the maximum entropy production principle (MEPP). MPP states that systems self-organise to maximise the rate of free energy that they consume and apply to useful work, or their power production (Odum and Pinkerton, 1955). As the necessary result of this useful work is entropy production, maximising power production can be equivalent to maximising entropy production, depending on how the system is conceptualised. This is formalised in MEPP, which states that systems self-organise to maximise their rate of entropy production (see review in Kleidon, Malhi and Cox, 2010). Both MPP and MEPP describe an emergent property of the system, resulting from evolutionary pressure at points of end consumption. A restatement of the same concept, instead viewing the system from the perspective of the resource flows and networks, highlights the opposite: by minimising the energy used for extracting, transporting, and consuming

resources, more energy can be applied to the growth and development of the end consumers. This drives systems to evolve increasingly efficient network structures for resource transport (Prigogine, 1955, 1978). Therefore, RADE networks would evolve toward *minimum* entropy production, such that the energy consumption and energy production of the end consumers is *maximised*.

The nested and interconnected nature of RADE networks (see Section 1.2.1) can complicate identifying the levels of selection within a system, and at which points power and entropy production are maximised. For example, the networks within an organism's body evolve to minimise energy consumption in distributing nutrients and performing other basal functions, and to maximise energy for growth, development, and reproduction, such that the whole-organism power and entropy are maximised. Similarly, organisms compete for resources in the environment, evolving to take advantage of different niches through changes to their genetic material (see Section 1.2.3). This increase of information, represented by changing genetic material and the resulting increased physical complexity of organisms and their RADE networks, coordinates the system so that all available resources can be consumed (Vallino, 2010). MPP and MEPP should therefore be considered emergent properties at the higher, system-level of organisation, due to the coordination of system components under evolutionary pressure to maximise individual productivity (Vallino, 2010).

This trajectory toward maximisation of power and entropy, and minimisation of energy required in the associated transport network, has been proven theoretically (Ziegler and Wehrli, 1987; Dewar, 2006) and demonstrated empirically in a diverse range of biological, ecological, and environmental systems (see reviews in Martyushev and Seleznev, 2006; Kleidon, Malhi and Cox, 2010; as well as Meysman and Bruers, 2010; Salthe, 2010; Vallino, 2010; Unrean and Srienc, 2011). It is intuitively applicable to human-engineered and social systems as well, despite the lack of explicit research in this area. Although criticisms of these thermodynamic extremization principles have been raised (*e.g.* Ross, Corlan and Müller, 2012), these have mostly been resolved with

clarification of the theories (Martyushev, 2013; Martyushev and Seleznev, 2014). For example, to evolve toward maximum entropy, systems must have sufficient degrees of freedom, as well as feedbacks or other signalling mechanisms, to explore distinct states corresponding to a range of entropy production (Martyushev and Seleznev, 2014). This entails that MPP and MEPP are rarely applicable to highly linear or deterministic systems, which cannot explore different states. Additionally, MPP and MEPP should not be confused with measurements that describe the optimality of the system by any other criterion, such as efficiency. Outstanding research questions remain, especially in predicting the outcome of systems where the same amount of power and entropy can be produced through different means (Martyushev and Seleznev, 2014), but the theories remain useful for understanding overall system trajectories and guiding model parameterisation (*e.g.* Lorenz, 1960; Kleidon *et al.*, 2003, 2006, 2013).

While MPP and MEPP have been widely applied in understanding and predicting overall systems development, there has been less explicit discussion of how this trajectory affects RADE networks, and vice versa, outside of specific systems (*e.g.* metabolic systems in Unrean and Sreenc, 2011; and rivers in Kleidon *et al.*, 2013). For example, modelling of channel network evolution has been demonstrated to drive the system toward maximum entropy production, in a cycle that involves rainfall, sediment movement, and crust uplift (Kleidon *et al.*, 2013). However, similar links between network evolution and thermodynamic limits have not been explored in socio-ecological or ecological systems, nor has the intersection between this development trajectory and the inequality or heterogeneity of end consumers or groups relying on those resource networks. If networks evolve toward flows occurring primarily down preferentially developed channels and often in a hierarchical branching pattern, to maximise power and entropy production, this will lead to resource saturation in some areas and deprivation in others. This suggests there could be a linkage between networks developing toward maximum power and entropy production and increasing inequality among end consumers. While co-evolution of network structure and state has been

discussed for non-spatial networks (*e.g.* Gross and Blasius, 2008), there has not yet been work that relates the development of systems along these known thermodynamic trajectories, the architecture or flows of the network, and the state of end consumers across that network.

1.4. Previous work

The ubiquity and importance of RADE networks has led to a significant amount of published work analysing them, but much of it has focussed on narrow, discipline-specific studies. While some studies have taken a somewhat broader approach to understanding optimal resource distribution and network structure from a more physics-based perspective, most have focussed on RADE networks within a specific discipline, such as biology, transport geography, ecology, or engineering. The similarity of the structures, purpose, and costs of RADE networks across diverse systems means that many of the conceptualisations and analytical methods are quite similar. Combining insights from different disciplines and methods, along with ensuring that all analyses explicitly consider the interacting dimensions of RADE networks (Section 1.2.5), could improve understanding of resource distribution, especially the effect of heterogeneity in networks and flows on end consumers and systems. In this section, different analytical methods focussing on allometric scaling, optimality, mass balance, and transport and movement networks will be presented and compared, and areas where future work could combine, improve, or apply these methods will be highlighted.

1.4.1. Allometric scaling

As introduced in Sections 1.3.2 – 1.3.3, the energetic costs of moving resources across space are theorised to drive RADE networks toward optimal forms, which minimise the costs associated with transport and maximise the energy that can be used by the system or end consumers for useful work. As these forms can often be classified as fractals, the study of the allometry of the network, underlying scaling exponent, and its effect on resource flows and system outcomes, has received considerable attention.

The study of allometric scaling in RADE networks began with the work of West *et al.* (1997), who hypothesised that the seemingly universal quarter-power scaling between mass and metabolic rate observed by Kleiber (1932) was due to the ubiquity of self-similar – or fractal – vascular network structures. Key assumptions of this ‘WBE model’ have been debated and revised (Savage, Deeds and Fontana, 2008; Banavar *et al.*, 2010; Brummer, Savage and Enquist, 2017), and other causal mechanisms relating flow rates to structure have also been proposed (Banavar *et al.*, 2010). While the WBE model focusses more on the spatial aspect of the RADE network, and the Banavar *et al.* (2010) model focusses more on the temporal aspect, both models clearly indicate the importance of RADE network structure and flows, in this case vascular network and blood or phloem flow, to the overall functioning of the system.

The allometric scaling theories have since been picked up by other researchers and applied further to human-engineered systems. Dalgaard and Strulik (2011) used it to study scaling in electrical distribution networks, and Jarvis *et al.* (2015) applied it to the global energy network, showing that primary and final energy use scale equivalently to the $\frac{3}{4}$ power exponent observed by West *et al.* (1997). Jarvis *et al.* (2015) further emphasise that this is an artefact of the structure of the resource distribution networks used to transport energy, but do not extend their analysis to discussion of the inequality of energy distribution. Although inequality in energy distribution has been discussed in depth elsewhere (*e.g.* Sovacool, 2012), this is mostly outside of the context of network architecture.

Together, these analyses highlight the importance of network structure and flows on resource distribution dynamics in both naturally-occurring and human-engineered systems. Notably, however, the tree-like structure identified by West *et al.* (1997) and Jarvis *et al.* (2015) leads to unequal flows to more peripheral areas. In the context of a body this is adaptive, as it causes lower blood pressure in areas of the body that are more likely to be damaged or lost, and higher blood flow to essential organs. In human-engineered systems, however, unequal distribution can lead to

problems such as the food deserts and energy insecurity introduced in Section 1.2. This has not been discussed within the context of this previous work, however.

1.4.2. Optimality

The theorised and observed optimality of naturally-occurring and human-engineered RADE networks has also led to many analyses from a more physics-based perspective, focussing on the conditions under which different structures are optimal. Typically, the cost functions under optimisation are related to the energy consumption of moving resource flows through the network, such that these analyses have broad interdisciplinary applications.

For example, Banavar *et al.* (2000) analysed the concavity of the cost function describing moving materials through a transportation network. They showed that concave cost functions were optimised by using all pathways, as the cost for transporting additional materials increases as the amount of material increases. Convex cost functions, however, had an economy of scale for transport, such that it was more economical to send all flows from one location to another directly. A similar model was developed by Han *et al.* (2019), who explored the interaction between economies of scale and transport distance in determining which nodes become dominant in a model of a socioeconomic supply network. Both Banavar *et al.* and Han *et al.* rely on a nonspatial definition for distance, involving number of connections, which may limit how fully their work can be applied to spatial networks.

Other work focussed on optimality included Bottinelli *et al.* (2017), who showed that distinct strategies are required for optimising building and maintenance costs, when the location of new nodes is not known in advance. The former involves minimum spanning trees that optimise total link length, while dynamic minimum spanning trees that maximise transport efficiency emerge in the latter.

Similarly, Hu and Cai (2013) studied the role of local adaptation in giving rise to optimal biological transport networks, in systems where there is fluctuation in sinks and sources. They showed that loops are adaptive in systems with sufficiently strong flow fluctuations, and that networks can approach an optimal structure and minimum energy consumption with only local adaptation to changes in flow rate. The effect of flow fluctuations and how that relates to network topology was also analysed by Gavrilenko and Katifori (2019) who showed that the topology of a network affects the ability of a given link to contain displacement of flow due to local perturbations.

Finally, Ronellfisch and Katifori (2016) focussed on how positive feedbacks driving growth in high-flow areas, combined with pruning of less-used areas, could identify globally optimal networks in terms of energy efficiency. They highlighted two phases of network dynamics: a dense and homogenous initial phase, and a more efficient phase after feedbacks preferentially strengthen and eliminate parts of the network based on flow.

While it would be difficult to prove that any of the causal processes that these authors suggest is the true cause of observable network structures, an interesting picture begins to emerge relating local adaptation, growth, and optimal network architecture. As introduced, however, the relationship between this optimal structure and flows toward which networks evolve, and the heterogeneity of flows and how that affects end consumers, is a crucial area of future work.

In more applied studies, human-engineered networks such as water and electrical grids have also been analysed extensively using equation-based modelling and simulations, mostly for the purposes of optimising criteria of efficiency and resilience (*e.g.* Miranda *et al.*, 1994; Montesinos, Garcia-Guzman and Ayuso, 1999; Jebaraj and Iniyar, 2006; Mahmood and Kubba, 2009; Shrawane and Diagavane, 2013; Zischg, Rauch and Sitzenfrei, 2018; Bernstein and Dall’Anese, 2019; Karimianfard and Haghghat, 2019; Huang *et al.*, 2020). As these networks have specific criteria around locations of substations and generators, pipe thicknesses, and flow rates, among others, multi-objective optimisation provides a useful way to create the most efficient design that

also meets physical constraints. Rarely does the algorithm consider the equality of distribution, however, apart from meeting any constraints on flow rates, pressure, or voltage.

1.4.3. Mass balance methods

Mass balance or mass flow methods, such as input-output analysis, material flow analysis, and ‘energy’ analysis were also developed to analyse systems from a resource distribution perspective. One of the earliest examples of this was the energy analysis of Odum (*e.g.* Odum, 1971). The concept of energy was first introduced to describe the amount of available energy used up in transformations to create products or services (Brown and Ulgiati, 2004). Alongside this definition, Odum developed a method for analysing ecosystems and socio-ecological systems that attempted to quantify and balance the energy and matter inputs and outputs of a system, often illustrated with Sankey diagrams and his own energy flow analysis symbols (*e.g.* Odum, 1957, 1971, 2002). While his work did not take explicit account of spatial location of the sources and sinks, or energy required for consumers to move through the system, it highlighted the importance of energy and mass conservation and whole-systems analysis in ecological and socio-ecological systems.

This theme of energy flows in socio-ecological systems was continued in the fields of industrial ecology and social metabolism. Both describe industrial or socio-ecological systems in ecological and metabolic terms, by balancing flows and conversions of energy and matter and noting interactions between and impacts of human systems on the environment, and vice versa (Bullard and Herendeen, 1975; Moffatt and Kohler, 2008; Liao, Heijungs and Huppes, 2012; Pauliuk and Hertwich, 2015; Bourg, Erkman and Chirac, 2017; Haberl *et al.*, 2019). These fields use methods such as input-output (I/O), lifecycle assessment (LCA), and material flow analysis (MFA) to account for energy and matter inputs, storage, outputs, and wastes produced by a system. As with energy analysis, however, not all work in these fields explicitly included the spatial and temporal dimensions of flows (Moffatt and Kohler, 2008), or cross-level analysis, such as including cycling of resources in both natural systems and anthropogenic processes. This view of the built

environment as embedded within resource flows, rather than isolated from the natural environment, still marks a considerable shift from traditional macroeconomic conceptualisations of human systems (Georgescu-Roegen, 1986). By highlighting the non-substitutability of natural resources with labour and capital, and the essential loss of some primary energy flows in conversions due to the second law of thermodynamics, it provides many useful insights to understand and potentially improve the sustainability of industries and economies. As with energy analysis, these techniques have rarely, if ever, been used to study the inequality of resource distribution, but their application in this area could provide considerable insight.

1.4.4. Transport and movement networks

Another type of RADE network common to many species is movement or transport networks, including foraging networks in ecosystems, and road and rail networks in human society. Foraging has been studied extensively from an optimisation perspective, assuming that evolutionary pressures would drive many of the routes to be optimal. In this case, optimality is typically defined with respect to energy returned on energy invested, or energy returned on time invested, if the energy used while foraging is assumed to be constant or averaged over time. This energy optimality may be balanced by other goals of the species in question, such as territory surveillance, predator avoidance, finding a mate, or prey density management, which all affect the structure of the resulting RADE network (Hopkins, 2011; Schlägel, Merrill and Lewis, 2017).

As the foraging network structure emerges from the decisions the animals make in responding to the signals available to them, theories around info- and chemotaxis and search strategies have been proposed and empirically validated to explain the network structure in some species (*e.g.* Klyubin, Polani and Nehaniv, 2004; Menzel *et al.*, 2005; Calhoun, Chalasani and Sharpee, 2014). More recent work in animal cognition has attempted to separate the effects of memory and perception on foraging decisions in different species, showing the importance of memory to foragers such as primates and large herbivores (Trapanese, Meunier and Masi, 2019; Ranc *et al.*, 2021). Other

theories, such as marginal value theorem (Charnov, 1976) and optimal giving-up time (McNair, 1982), have focussed on discounting and temporal strategies, using equations to model organism behaviour in such a way that maximises energy consumption for each unit of energy or time expended. This has been expanded by the more recent energy landscapes theory (Wilson, Quintana and Hobson, 2012; Shepard *et al.*, 2013; Halsey, 2016; Masello *et al.*, 2017; Green, Boruff and Grueter, 2020), which describes animal foraging behaviour and routes as resulting from a combination of landscape features, such as slope, terrain, and speed and direction of wind and water currents; individual characteristics and state; and competing goals such as predator avoidance and mate attraction. While it would be difficult, if not impossible, to fully determine the cause of a given foraging network structure, these theories provide possible explanations for why a network might take the form that it does, and how that compares to the causal process or structure of another species' network.

Although some previous modelling work on foraging networks has explicitly accounted for the spatial dimension of the network (*e.g.* Baveco *et al.*, 2016), many others rely on averaged energy consumption over time spent foraging (*e.g.* Ward, Austin and Macdonald, 2000), which may or may not be realistic, depending on the species in question and the terrain over which they forage. Increasingly, spatially explicit agent-based models (ABMs, also known as individual-based models in ecology), underpinned with theories such as energy landscapes, have been used to simulate and analyse foraging behaviour in a range of species (*e.g.* Epstein and Axtell, 1996; Nonaka and Holme, 2007; Anderson, 2008; Beltran, Testa and Burns, 2017; Lihoreau *et al.*, 2017; Liu *et al.*, 2017; Miller *et al.*, 2017; Sikk and Caruso, 2020; Chudzinska *et al.*, 2021). These models can provide more insights into how distance and terrain affect energy intake and use in foragers, and how heterogeneity in spatial and temporal resource distribution can lead to the behavioural adaptations, specialisation, speciation, and possible extinction described in Section 1.1.

Beyond foraging networks, the emergent structure of other movement and transportation networks has been studied extensively in both naturally-occurring and human-engineered systems (*e.g.* Yerra and Levinson, 2005; Xie and Levinson, 2007, 2009; Roshier, Doerr and Doerr, 2008; Marleau, Guichard and Loreau, 2014; Perna and Latty, 2014; Strano *et al.*, 2017). These networks have been shown to emerge from both positive reinforcement, resulting in least-cost paths being selected through the collective action of many individuals, which may be triggered by a single individual leaving a trail or signal of some kind to indicate the path that should be chosen (Xie and Levinson, 2007; Perna and Latty, 2014; Lecheval *et al.*, 2021). Decentralised decision-making can also lead to a hierarchy emerging, nesting paths with less flow or slower speed within larger networks (Yerra and Levinson, 2005; Levinson and Yerra, 2006). Overall, these networks emerge through a combination of behavioural strategies and the spatial and temporal distribution of the resources to which they connect their users (Roshier, Doerr and Doerr, 2008).

While the research on transport networks has provided insight into how their structure might emerge, less attention has been paid to the feedbacks between that structure and the end state of the users, and how inequality between users may play a role in shaping the evolution of network structure. Furthermore, the insights gained from any one discipline, such as behavioural ecology or transport geography, are rarely compared with those from other disciplines, creating a silo for both the methods and findings. These networks are likely emerging in similar structures due to analogous requirements of those constructing and using them, or because similar structures are optimal for a range of situations and requirements. Using comparable methods, and comparing results across disciplines, could therefore uncover new insights into the generality or uniqueness of the situations in which these networks emerge.

1.5. Next steps

Given the significant impacts of resource heterogeneity on both biodiversity and ecosystem functioning in natural systems, and inequality in socio-ecological systems, it is crucial to develop a

clear understanding of the relationship between the structure and flows of RADE networks, especially as systems develop along known thermodynamic trajectories; the heterogeneity of resource distribution; and the state of the overarching system or end consumers within it.

Specifically, maximum power and entropy production are empirically verified theories for systems development, and clearly resource distribution plays a determining role in the power and entropy production of a system. However, no work to date has focussed on the intersection of maximum power and entropy, and resource distribution network development, especially regarding how that affects the inequality of resource flows to end consumers. As introduced in Section 1.3.3, the evolution of resource distribution networks toward more efficient structures maximises energy throughput, but the form of these structures is inherently heterogenous, such as fractal branching networks. To gain insight into the causes of heterogeneity and biodiversity in natural systems, and the inequality present in socio-ecological systems, there must be more focus on the impact of thermodynamic trajectories and network development on the heterogeneity of resource flows, and the inequality experienced by end consumers.

In ecological systems, while the heterogeneity of resource spatial and temporal distribution has been shown to affect the biodiversity and dynamics of populations in an area (see Section 1.1), the impact of RADE network structure, in the form of foraging networks or passive flows and diffusion of nutrients, has not been widely studied. Specifically, there is limited understanding of the impacts of resource characteristics, consumer characteristics, and distribution network structure, and the relationships between them, on the size and heterogeneity of consumer populations. While the complexity of natural systems makes the impact of these factors and their relationship difficult to assess, a combination of empirical analyses and simulation modelling holds promise for generating more insight into this area.

Finally, while there has been a substantial body of research focussing on networks that are optimal in some sense, there has been less emphasis on the relationship between network development

over time, structural heterogeneity, and inequality among end consumers. As described in Section 1.2.5, consumption allows end consumers in some RADE networks to expand and improve the network further. A feedback may emerge between higher consumption levels of well-positioned agents within the network, and their ability to further increase resource flows to themselves. The effect of different resource and consumer characteristics on the emergent network architecture, consumer inequality, and feedbacks therein can provide a deeper understanding of how networks form, and how the emergent network structure impacts the state of agents operating within it, both as individuals and a collective.

1.6. Thesis overview

1.6.1. Thesis aims

In response to these areas of future work, this thesis will take steps toward increasing understanding of RADE network structure, development, and dynamics. It will include explicit consideration of thermodynamic principles and known systems development trajectories, and a focus on the relationship between resource and network heterogeneity, and inequality among end consumers. This will be done primarily through equation-based and simulation modelling, along with analysis of empirical networks. The insights generated will provide a foundation for future work to increase the equality, sustainability, and resilience of these networks.

To this end, included are three chapters that address the following objectives:

Chapter 2: Trajectories toward maximum power and inequality in resource distribution networks

Explore the relationship between the evolution toward maximum power production, network structure and characteristics at maximum power, and inequality in consumption among nodes, using mathematical modelling and simulations.

Chapter 3: Measuring heterogeneity in soil networks: a network analysis and simulation-based approach

Analyse soil networks as an example of ecological networks, using metrics adapted from network science and simulations to quantify the heterogeneity of soil networks and how that interacts with

resource and consumer characteristics to affect the heterogeneity of energy consumption across the simulated populations.

Chapter 4: The co-evolution of network structure and consumer inequality in a spatially explicit model of resource acquisition

Model the emergence of a network from agents making choices to attempt to maximise their time-discounted utility of energy consumption, explicitly including laws of energy conservation and entropy production, and relate the landscape heterogeneity and network structure to the inequality in resource consumption among agents.

1.6.2. Study approach and summary of findings

Chapter 2

The second chapter focusses on resource distribution networks developing toward maximum power, through increasing resource flows and changing state, re-configuring network architecture, or both. Equations were derived to determine the relationships between force, flow, friction, and power in the network as it increased toward and reached maximum power. The effects of this trajectory on the variance in power consumption across end consumers was highlighted, with additional equations derived to determine the relationship between this variance, and the resource flow through the network. A simple electrical analogue model was used to represent generalised energy resource distribution networks and illustrate the dynamics of power consumption at consumers as the resource flow through the network increased.

The equations and simulation model demonstrated that increasing flows across structurally unequal networks exponentially increases power inequality. Specifically, it showed that the standard deviation in power consumption of the consumers was equal to the resource flow squared, times the standard deviation of the ‘effective resistance’ experienced by consumers, a derived measure that incorporated both spatial and interactional components of energetic losses in transport. This inequality in power consumption was most notable in the hierarchical branched networks, an optimal distribution architecture common to both natural and human-engineered

systems. This raises significant questions about the relationship between heterogeneity in natural systems and inequity in human systems, as well as how best to alleviate the latter.

Key findings:

- Increasing resource flow through networks with heterogeneous link length, connectivity, or both, increases inequality in resource consumption between end consumers.
- Inequality is highest, and increases the most quickly, in hierarchical branching networks similar to those seen in a range of biological, environmental, and socio-ecological systems.

Chapter 3

The third chapter focusses on resource distribution networks in empirical ecological systems, and how heterogeneity in the network structure affects the outcomes of a consumer population. The work presents a novel method for extracting a soil macropore network from images of a soil profile, which is then analysed and used as the environment of a generic consumer species in simulations with an agent-based model (ABM). Two locations in Aberdeenshire, United Kingdom, with Cambisol and Arenosol soils, respectively, are used as test cases.

The network extraction method uses an image of a soil profile, taken by a smartphone camera, and processes it with image morphology techniques to identify and retain the underlying pore network. The network structure is quantified with metrics from network science and transport geography, chosen to measure size, structure, and connectivity. A simple ABM of generic agents navigating the pore network, consuming food resources, and reproducing is also presented, and simulation experiments are run across a range of consumer and resource parameters combinations, and networks from both soil types.

Overall, the network analysis showed that networks extracted from the Cambisol soil profiles were larger, more connected, and more structured as compared to those from Arenosols. This is to be

expected, given the known characteristics and development of these soils. In the simulation experiments, the larger Cambisol soil networks also supported higher populations of the simulated consumers. Although the model did not allow the consumers to be exposed to the full range of the network heterogeneity, the findings suggest an important effect of soil network structure on consumer population outcomes. Future work would be necessary to further validate the network extraction and analysis presented here with comparisons to measurements from more established methods, and the model could be extended with additional consumer behaviour and more species-specific parameterisation.

Key findings:

- Network extraction from soil profile images and subsequent analysis can highlight differences in soil structure and suggest differences in ecological viability, helping to guide management practices and improve understanding of ecological changes.
- Larger, more heterogeneous networks supported a larger, slightly more heterogeneous population of generic consumers, but the effect of environmental heterogeneity on consumer heterogeneity was limited by the network heterogeneity occurring at a larger spatial scale than consumers could access.

Chapter 4

The fourth chapter explores the co-evolution of network structure and consumer inequality, by developing and analysing a spatially-explicit, energetically consistent ABM of resource acquisition. In the model, agents (called ‘consumers’) built links between generic energy sources (‘resources’) by investing energy in the environment patches to reduce the patches’ roughness. The consumers chose target resources that maximised their time-discounted energy consumption. Once a consumer reached a threshold energy level, based on its initial energy reserves, it could reproduce and transfer some of this energy to an offspring. The network structure, measured by the total,

mean, and standard deviation (SD) of link lengths, and the consumer inequality, measured by the SD of energy reserves, were calculated, and their co-evolution was analysed over the course of the simulation. This was further compared across three different landscapes, or resource arrangements, to determine the effect of landscape heterogeneity on consumer and network outcomes.

Over the course of the simulations, a negative feedback emerged between network pruning and inequality, constrained by the population size: networks with smaller populations, due to more consumers not surviving the initial construction phases, had fewer consumers to maintain links. As more links decayed, inequality increased; some consumers were effectively trapped in less connected areas, while other consumers could use previously-constructed links to move between optimal nearby resources. This inequality further limited the number of consumers who could construct or maintain links, or produce offspring, so the network structure, inequality, and population size reached a dynamic equilibrium state. While these dynamics were quite similar across the three landscapes, the spatial distribution of the resources constrained the networks that could emerge. As this constrained the rates and times of network structure dynamics, it also indirectly affected consumer inequality. In this way, the network mediated the landscape heterogeneity-consumer inequality relationship.

Similar phenomena have been observed in empirical systems, such as adaptation and speciation of disconnected sub-populations, and relationships between poverty and heterogeneous connectivity and accessibility in cities. This work demonstrates a possible means by which network structure and consumer inequality can co-evolve, and how this is constrained by the spatial distribution of resources in the landscape.

Key findings:

- Network structure and consumer inequality co-evolve in a landscape, with the rates of dynamics and system transitions also affected by the spatial distribution of resources and the life history and biology of consumers.
- The rate of network growth and decay, as affected by population size, current levels of consumer inequality, and the spatial distribution of resources, also determines the extent to which inequality can emerge in a population over time.

1.6.3. Thesis structure

The rest of this thesis is structured as a series of three manuscripts written for publication, followed by a final discussion chapter that synthesises key findings and highlights areas for future research. References and supplementary information for each manuscript are included with it. For published manuscripts, a citation for the published version is included on the first page.

1.7. References

- Anderson, J. J. (2008) ‘An agent-based event-driven foraging model’, *Natural Resource Modeling*, 15(1), pp. 55–82. doi: 10.1111/j.1939-7445.2002.tb00080.x.
- Anderson, W. B., Wait, D. A. and Stapp, P. (2008) ‘Resources from another place and time: Responses to pulses in a spatially subsidized system’, *Ecology*, 89(3), pp. 660–670. doi: 10.1890/07-0234.1.
- Annala, A. and Kuusmanen, E. (2009) ‘Natural hierarchy emerges from energy dispersal’, *BioSystems*, 95(3), pp. 227–233. doi: 10.1016/j.biosystems.2008.10.008.
- Baer, S. G. *et al.* (2005) ‘Soil Heterogeneity Effects on Tallgrass Prairie Community Heterogeneity: An Application of Ecological Theory to Restoration Ecology’, *Restoration Ecology*, 13(2), pp. 413–424. doi: 10.1111/j.1526-100x.2005.00051.x.
- Banavar, J. R. *et al.* (2000) ‘Topology of the fittest transportation networks’, *Physical Review Letters*, 84(20), pp. 4745–4748. doi: 10.1103/PhysRevLett.84.4745.
- Banavar, J. R. *et al.* (2010) ‘A general basis for quarter-power scaling in animals’, *Proceedings of the National Academy of Sciences*, 107(36), pp. 15816–15820. doi: 10.1073/pnas.1009974107.
- Bardgett, R. D. (2005) *The Biology of Soil: A community and ecosystem approach*. Oxford: Oxford University Press.
- Bardgett, R. D., Yeates, G. W. and Anderson, J. M. (2009) ‘Patterns and determinants of soil biological diversity’, in *Biological Diversity and Function in Soils*, pp. 100–119.
- Baveco, J. M. *et al.* (2016) ‘An energetics-based honeybee nectar-foraging model used to assess the potential for landscape-level pesticide exposure dilution’, *PeerJ*, 4, p. e2293. doi: 10.7717/peerj.2293.
- Bejan, A. and Errera, M. R. R. (2017) ‘Wealth inequality: The physics basis’, *Journal of Applied Physics*, 121(12), p. 124903. doi: 10.1063/1.4977962.
- Beltran, R. S., Testa, J. W. and Burns, J. M. (2017) ‘An agent-based bioenergetics model for predicting impacts of environmental change on a top marine predator, the Weddell seal’, *Ecological Modelling*, 351, pp. 36–50. doi: 10.1016/j.ecolmodel.2017.02.002.

- Bernstein, A. and Dall'Anese, E. (2019) 'Real-Time Feedback-Based Optimization of Distribution Grids: A Unified Approach', *IEEE Transactions on Control of Network Systems*, 6(3), pp. 1197–1209. doi: 10.1109/TCNS.2019.2929648.
- Bianchi, F. J. J. A., Schellhorn, N. A. and Van Der Werf, W. (2009) 'Foraging behaviour of predators in heterogeneous landscapes: The role of perceptual ability and diet breadth', *Oikos*, 118(9), pp. 1363–1372. doi: 10.1111/j.1600-0706.2009.17319.x.
- Borgatti, S. P., Everett, M. C. and Johnson, J. C. (2018) *Analyzing Social Networks*. 2nd edn. London: SAGE Publications.
- Bottinelli, A., Louf, R. and Gherardi, M. (2017) 'Balancing building and maintenance costs in growing transport networks', *Physical Review E*, 96(3). doi: 10.1103/PhysRevE.96.032316.
- Bourg, D., Erkman, S. and Chirac, P. J. (eds) (2017) *Perspectives on Industrial Ecology*. London: Routledge. doi: 10.4324/9781351282086.
- Brown, B. L. (2007) 'Habitat heterogeneity and disturbance influence patterns of community temporal variability in a small temperate stream', *Hydrobiologia*, 586(1), pp. 93–106. doi: 10.1007/s10750-006-0531-3.
- Brown, J. H. *et al.* (2004) 'Toward a metabolic theory of ecology', *Ecology*, 85(7), pp. 1771–1789. doi: 10.1890/03-9000.
- Brown, M. T. and Ulgiati, S. (2004) 'Energy quality, emergy, and transformity: H.T. Odum's contributions to quantifying and understanding systems', *Ecological Modelling*, 178, pp. 201–213. doi: 10.1016/j.ecolmodel.2004.03.002.
- Brummer, A. B., Savage, V. M. and Enquist, B. J. (2017) 'A general model for metabolic scaling in self-similar asymmetric networks', *PLOS Computational Biology*, 13(3), p. e1005394. doi: 10.1371/journal.pcbi.1005394.
- Bullard, C. W. and Herendeen, R. A. (1975) 'The energy cost of goods and services', *Energy Policy*, 3(4), pp. 268–278. doi: 10.1016/0301-4215(75)90035-X.
- Calhoun, A. J., Chalasani, S. H. and Sharpee, T. O. (2014) 'Maximally informative foraging by *Caenorhabditis elegans*', *eLife*, 3(3), pp. 1–13. doi: 10.7554/eLife.04220.001.

- Carradore, L. and Turri, R. (2009) 'Modeling and Simulation of Smart Energy Systems', *PowerTech*, pp. 1–7. doi: 10.1109/PTC.2009.5281933.
- Caspi, C. E. *et al.* (2012) 'The relationship between diet and perceived and objective access to supermarkets among low-income housing residents', *Social Science and Medicine*, 75(7), pp. 1254–1262. doi: 10.1016/j.socscimed.2012.05.014.
- Charnov, E. L. (1976) 'Optimal foraging, the marginal value theorem', *Theoretical Population Biology*, 9, pp. 129–136.
- Choy, E. S. *et al.* (2010) 'An isotopic investigation of mercury accumulation in terrestrial food webs adjacent to an Arctic seabird colony', *Science of The Total Environment*, 408(8), pp. 1858–1867. doi: 10.1016/j.scitotenv.2010.01.014.
- Chudzinska, M. *et al.* (2021) 'AgentSeal: Agent-based model describing movement of marine central-place foragers', *Ecological Modelling*, 440, p. 109397. doi: <https://doi.org/10.1016/j.ecolmodel.2020.109397>.
- Costanza, R. (1980) 'Embodied energy and economic valuation', *Science*, 210(4475), pp. 1219–1224. doi: 10.1126/science.210.4475.1219.
- Crawford, J. W., Ritz, K. and Young, I. M. (1993) 'Quantification of fungal morphology, gaseous transport and microbial dynamics in soil: an integrated framework utilising fractal geometry', *Geoderma*, 56, pp. 157–172. doi: 10.1016/0016-7061(93)90107-V.
- Croft, S. A., Hodge, A. and Pitchford, J. W. (2012) 'Optimal root proliferation strategies: The roles of nutrient heterogeneity, competition and mycorrhizal networks', *Plant and Soil*, 351, pp. 191–206. doi: 10.1007/s11104-011-0943-3.
- Dalgaard, C.-J. J. and Strulik, H. (2011) 'Energy distribution and economic growth', *Resource and Energy Economics*, 33(4), pp. 782–797. doi: 10.1016/j.reseneeco.2011.04.004.
- Delmas, E. *et al.* (2019) 'Analysing ecological networks of species interactions', *Biological Reviews*, 94(1), pp. 16–36. doi: 10.1111/brv.12433.
- Dewar, R. C. (2006) 'Maximum Entropy Production and Non-equilibrium Statistical Mechanics', in Kleidon, A. and Lorenz, R. (eds) *Non-equilibrium Thermodynamics and the Production of Entropy: Life, Earth, and Beyond*. Berlin: Springer Science & Business Media, pp. 41–55. doi: 10.1007/11672906.

- Dormann, C. F., Fründ, J. and Schaefer, H. M. (2017) 'Identifying Causes of Patterns in Ecological Networks: Opportunities and Limitations', *Annual Review of Ecology, Evolution, and Systematics*, 48(1), pp. 559–584. doi: 10.1146/annurev-ecolsys-110316-022928.
- Dyson-Hudson, R. and Smith, E. A. (1978) 'Human Territoriality: An Ecological Reassessment', *American Anthropologist*, 80(1), pp. 21–41. doi: 10.1525/aa.1978.80.1.02a00020.
- Eichhorn, M. P. (2016) 'Drivers of diversity', in *Natural Systems: The Organization of Life*. John Wiley and Sons, pp. 95–112. doi: 10.1002/9781118905982.ch8.
- Epstein, J. M. and Axtell, R. (1996) *Growing artificial societies: Social science from the bottom up*. Washington, D.C.: Brookings Institution Press.
- Ettema, C. H. and Wardle, D. A. (2002) 'Spatial soil ecology', *Trends in Ecology & Evolution*, 17(4), pp. 177–183. doi: 10.1016/S0169-5347(02)02496-5.
- Fath, B. D. (2004) 'Distributed control in ecological networks', *Ecological Modelling*, 179(2), pp. 235–245. doi: 10.1016/j.ecolmodel.2004.06.007.
- Fath, B. D. *et al.* (2007) 'Ecological network analysis: network construction', *Ecological Modelling*, 208(1), pp. 49–55. doi: 10.1016/j.ecolmodel.2007.04.029.
- Fath, B. D. (2012) 'Analyzing Ecological Systems Using Network Analysis', *Ecological Questions*, 16(1), p. 77. doi: 10.2478/v10090-012-0008-0.
- Fath, B. D. and Patten, B. C. (2013) 'Review of Network the Foundations of Environ Analysis', *Ecosystems*, 2(2), pp. 167–179.
- Fath, B. D. and Scharler, U. M. (2019) 'Systems Ecology: Ecological Network Analysis', in Fath, B. (ed.) *Encyclopedia of Ecology*. 2nd edn. Oxford: Elsevier, pp. 643–652. doi: 10.1016/B978-0-12-409548-9.11171-6.
- Fauchald, P. *et al.* (2017) 'Spring phenology shapes the spatial foraging behavior of Antarctic petrels', *Marine Ecology Progress Series*, 568, pp. 203–215. doi: 10.3354/meps12082.
- García-Palacios, P. *et al.* (2012) 'Plant responses to soil heterogeneity and global environmental change', *Journal of Ecology*, 100(6), pp. 1303–1314. doi: 10.1111/j.1365-2745.2012.02014.x.

- Gavrilenko, T. and Katifori, E. (2019) 'Resilience in hierarchical fluid flow networks', *Physical Review E*, 99(1). doi: 10.1103/PhysRevE.99.012321.
- Gaye, A. (2007) 'Access to Energy and Human Development', *United Nations Development Programme*, (25), p. 21.
- Georgescu-Roegen, N. (1986) 'The Entropy Law and the Economic Process in Retrospect', *Eastern Economic Journal*, 12(1), pp. 3–25.
- Giannetti, B. F. *et al.* (2019) 'Howard Odum's "Self-organization, transformity and information": Three decades of empirical evidence', *Ecological Modelling*, 407. doi: 10.1016/j.ecolmodel.2019.06.005.
- Godbold, J. A., Bulling, M. T. and Solan, M. (2011) 'Habitat structure mediates biodiversity effects on ecosystem properties', *Proceedings of the Royal Society B: Biological Sciences*, 278(1717), pp. 2510–2518. doi: 10.1098/rspb.2010.2414.
- Gounand, I. *et al.* (2018) 'Meta-Ecosystems 2.0: Rooting the Theory into the Field', *Trends in Ecology and Evolution*, 33(1), pp. 36–46. doi: 10.1016/j.tree.2017.10.006.
- Green, S. J., Boruff, B. J. and Grueter, C. C. (2020) 'From ridge tops to ravines: landscape drivers of chimpanzee ranging patterns', *Animal Behaviour*, 163, pp. 51–60. doi: 10.1016/j.anbehav.2020.02.016.
- Grinnell, J. (1917) 'The Niche-Relationships of the California Thrasher', *The Auk*, 34(4), pp. 427–433. doi: 10.2307/4072271.
- Gross, T. and Blasius, B. (2008) 'Adaptive coevolutionary networks: a review', *Journal of The Royal Society Interface*, 5(20), pp. 259–271. doi: 10.1098/rsif.2007.1229.
- Guichard, F. (2017) 'Recent advances in metacommunities and meta-ecosystem theories', *F1000Research*, 6, p. 610. doi: 10.12688/f1000research.10758.1.
- Gurven, M. *et al.* (2010) 'Domestication alone does not lead to inequality: Intergenerational wealth transmission among horticulturalists', *Current Anthropology*, 51(1), pp. 49–64. doi: 10.1086/648587.
- Haberl, H. *et al.* (2019) 'Contributions of sociometabolic research to sustainability science', *Nature Sustainability*, 2(3), pp. 173–184. doi: 10.1038/s41893-019-0225-2.

Haff, P. K. (2012) 'Technology and human purpose: The problem of solids transport on the Earth's surface', *Earth System Dynamics*, 3(2), pp. 149–156. doi: 10.5194/esd-3-149-2012.

Halsey, L. G. (2016) 'Terrestrial movement energetics: current knowledge and its application to the optimising animal', *Journal of Experimental Biology*, 219(10), pp. 1424–1431. doi: 10.1242/jeb.133256.

Han, C. *et al.* (2019) 'The winner takes it all—Competitiveness of single nodes in globalized supply networks', *PLOS ONE*, 14(11), p. e0225346. doi: 10.1371/journal.pone.0225346.

Heidrich, L. *et al.* (2020) 'Heterogeneity–diversity relationships differ between and within trophic levels in temperate forests', *Nature Ecology and Evolution*. doi: 10.1038/s41559-020-1245-z.

Hendrickson, D., Smith, C. and Eikenberry, N. (2006) 'Fruit and vegetable access in four low-income food deserts communities in Minnesota', *Agriculture and Human Values*, 23(3), pp. 371–383.

Hodge, A. (2004) 'The plastic plant: Root responses to heterogeneous supplies of nutrients', *New Phytologist*, 162(1), pp. 9–24. doi: 10.1111/j.1469-8137.2004.01015.x.

Hopkins, M. E. (2011) 'Mantled Howler (*Alouatta palliata*) Arboreal Pathway Networks: Relative Impacts of Resource Availability and Forest Structure', *International Journal of Primatology*, 32(1), pp. 238–258. doi: 10.1007/s10764-010-9464-9.

Horn, H. S. (1968) 'The Adaptive Significance of Colonial Nesting in the Brewer's Blackbird (*Euphagus cyanocephalus*)', *Ecology*, 49(4), pp. 682–694.

Hu, D. and Cai, D. (2013) 'Adaptation and optimization of biological transport networks', *Physical Review Letters*, 111(13), pp. 1–5. doi: 10.1103/PhysRevLett.111.138701.

Huang, Y. *et al.* (2020) 'Multi-Objective Optimal Design of Water Distribution Networks Accounting for Transient Impacts', *Water Resources Management*, 34(4), pp. 1517–1534. doi: 10.1007/s11269-020-02517-4.

Humphries, M. M., Thomas, D. W. and Kramer, D. L. (2003) 'The Role of Energy Availability in Mammalian Hibernation: A Cost-Benefit Approach', *Physiological and Biochemical Zoology*, 76(2), pp. 165–179. doi: 10.1086/367950.

Hutchinson, G. E. (1978) *An introduction to population ecology*. New Haven, Connecticut: Yale University Press.

- IEA (2020) *SDG7: Data and Projections*. Paris. Available at: <https://www.iea.org/reports/sdg7-data-and-projections>.
- Ingale, M. and Shekatkar, S. M. (2020) ‘Resource dependency and survivability in complex networks’. Available at: <http://arxiv.org/abs/2006.07082>.
- Jarvis, A. (2018) ‘Energy Returns and The Long-run Growth of Global Industrial Society’, *Ecological Economics*, 146, pp. 722–729. doi: 10.1016/j.ecolecon.2017.11.005.
- Jarvis, A. J., Jarvis, S. J. and Hewitt, C. N. (2015) ‘Resource acquisition, distribution and end-use efficiencies and the growth of industrial society’, *Earth System Dynamics*, 6(2), pp. 689–702. doi: 10.5194/esd-6-689-2015.
- Jebaraj, S. and Iniyar, S. (2006) ‘A review of energy models’, *Renewable and Sustainable Energy Reviews*, 10(4), pp. 281–311. doi: 10.1016/j.rser.2004.09.004.
- Jørgensen, S. E. and Nielsen, S. N. (2015) ‘Hierarchical networks’, *Ecological Modelling*, 295(January), pp. 59–65. doi: 10.1016/j.ecolmodel.2014.06.012.
- Jørgensen, S. E., Nielsen, S. N. and Fath, B. D. (2015) ‘Recent progress in systems ecology’, *Ecological Modelling*, 319(September), pp. 112–118. doi: 10.1016/j.ecolmodel.2015.08.007.
- Jusup, M. *et al.* (2017) ‘Physics of metabolic organization’, *Physics of Life Reviews*, 20, pp. 1–39. doi: 10.1016/j.plrev.2016.09.001.
- Karimianfard, H. and Haghghat, H. (2019) ‘Generic Resource Allocation in Distribution Grid’, *IEEE Transactions on Power Systems*, 34(1), pp. 810–813. doi: 10.1109/TPWRS.2018.2867170.
- Kearney, M. R. and White, C. R. (2012) ‘Testing metabolic theories’, *American Naturalist*, 180(5), pp. 546–565. doi: 10.1086/667860.
- King, C. W. (2016) ‘Information Theory to Assess Relations Between Energy and Structure of the U.S. Economy Over Time’, *BioPhysical Economics and Resource Quality*, 1(2), p. 10. doi: 10.1007/s41247-016-0011-y.
- King, C. W. (2020) ‘An integrated biophysical and economic modeling framework for long-term sustainability analysis: the HARMONEY model’, *Ecological Economics*, 169. doi: 10.1016/j.ecolecon.2019.106464.

- Kleiber, M. (1932) 'Body size and metabolism', *Hilgardia*, 6(11), pp. 315–353. doi: 10.3733/hilg.v06n11p315.
- Kleidon, A. *et al.* (2003) 'The atmospheric circulation and states of maximum entropy production', *Geophysical Research Letters*, 30(23), pp. 1–4. doi: 10.1029/2003GL018363.
- Kleidon, A. *et al.* (2006) 'Maximum entropy production and the strength of boundary layer exchange in an atmospheric general circulation model', *Geophysical Research Letters*, 33(6), pp. 2–5. doi: 10.1029/2005GL025373.
- Kleidon, A. *et al.* (2013) 'Thermodynamics, maximum power, and the dynamics of preferential river flow structures at the continental scale', *Hydrology and Earth System Sciences*, 17(1), pp. 225–251. doi: 10.5194/hess-17-225-2013.
- Kleidon, A. (2016) *Thermodynamic Foundations of the Earth System*. First. Cambridge, UK: Cambridge University Press.
- Kleidon, A., Malhi, Y. and Cox, P. M. (2010) 'Maximum entropy production in environmental and ecological systems', *Philosophical Transactions of the Royal Society B: Biological Sciences*, 365(1545), pp. 1297–1302. doi: 10.1098/rstb.2010.0018.
- Klyubin, A. S., Polani, D. and Nehaniv, C. L. (2004) 'Tracking information flow through the environment: Simple cases of stigmergy', *Proceedings of the Ninth International Conference on the Simulation and Synthesis of Living Systems (ALIFE '04)*, pp. 563–568.
- Kooijman, S. A. L. M. (2009) *Dynamic Energy Budget Theory for Metabolic Organisation*. 3rd edn. Cambridge, UK: Cambridge University Press.
- Kravchenko, A. N. *et al.* (2011) 'Long-term Differences in Tillage and Land Use Affect Intra-aggregate Pore Heterogeneity', *Soil Science Society of America Journal*, 75(5), pp. 1658–1666. doi: 10.2136/sssaj2011.0096.
- de Lecea, A. M., Smit, A. J. and Fennessy, S. T. (2016) 'Riverine dominance of a nearshore marine demersal food web: evidence from stable isotope and C/N ratio analysis', *African Journal of Marine Science*, 38. doi: 10.2989/1814232X.2016.1142898.

- Lecheval, V. *et al.* (2021) 'From foraging trails to transport networks: how the quality-distance trade-off shapes network structure', *Proceedings. Biological sciences.* 2021/04/21 edn, 288(1949), pp. 20210430–20210430. doi: 10.1098/rspb.2021.0430.
- Lee, S. (2014) 'Resource pulses can increase power acquisition of an ecosystem', *Ecological Modelling*, 271, pp. 21–31. doi: 10.1016/j.ecolmodel.2012.11.028.
- Levinson, D. and Yerra, B. (2006) 'Self-Organization of Surface Transportation Networks', *Transportation Science*, 40(2), pp. 179–188. doi: 10.1287/trsc.1050.0132.
- Liao, W., Heijungs, R. and Huppes, G. (2012) 'Thermodynamic analysis of human-environment systems: A review focused on industrial ecology', *Ecological Modelling*, 228, pp. 76–88. doi: 10.1016/j.ecolmodel.2012.01.004.
- Lihoreau, M. *et al.* (2017) 'Collective foraging in spatially complex nutritional environments', *Philosophical Transactions of the Royal Society B: Biological Sciences*, 372(1727), p. 20160238. doi: 10.1098/rstb.2016.0238.
- Lindeman, R. L. (1942) 'The Trophic-Dynamic Aspect of Ecology', *Ecology*, 23(4), pp. 399–417.
- Liu, Y. *et al.* (2017) 'A new multi-agent system to simulate the foraging behaviors of Physarum', *Natural Computing*, 16(1), pp. 15–29. doi: 10.1007/s11047-015-9530-5.
- Loreau, M. and Holt, R. D. (2004) 'Spatial Flows and the Regulation of Ecosystems', *The American Naturalist*, 163(4), pp. 606–615. doi: 10.1086/382600.
- Loreau, M., Mouquet, N. and Holt, R. D. (2003) 'Meta-ecosystems: A theoretical framework for a spatial ecosystem ecology', *Ecology Letters*, 6(8), pp. 673–679. doi: 10.1046/j.1461-0248.2003.00483.x.
- Lorenz, E. N. (1960) *Generation of available potential energy and the intensity of the general circulation*, *Climate Dynamics*. Oxford: Pergamon Press. doi: 10.1016/b978-1-4831-9890-3.50021-9.
- Losee, R. M. (1997) 'A discipline independent definition of information', *Journal of the American Society for Information Science*, 68789(48), pp. 154–269.
- Ma, J., Chen, Y. and Wang, Y. (2018) 'Multi-Objective Optimal Energy Management for the Combined Cooling, Heat and Power Plants', *Energies*. doi: 10.3390/en11040734.

- MacArthur, R. H. and Pianka, E. R. (1966) 'On Optimal Use of a Patchy Environment', *The American Naturalist*, 100(916), pp. 603–609.
- Mahmood, S. S. and Kubba, H. A. (2009) 'Genetic algorithm based load flow solution problem in electrical power systems', *Journal of Engineering*, 15(4), pp. 4142–4162.
- Marleau, J. N., Guichard, F. and Loreau, M. (2014) 'Meta-ecosystem dynamics and functioning on finite spatial networks', *Proceedings of the Royal Society B: Biological Sciences*, 281(1777). doi: 10.1098/rspb.2013.2094.
- Martyushev, L. (2013) 'Entropy and Entropy Production: Old Misconceptions and New Breakthroughs', *Entropy*, 15(4), pp. 1152–1170. doi: 10.3390/e15041152.
- Martyushev, L. M. and Seleznev, V. D. (2006) 'Maximum entropy production principle in physics, chemistry and biology', *Physics Reports*, 426(1), pp. 1–45. doi: 10.1016/j.physrep.2005.12.001.
- Martyushev, L. M. and Seleznev, V. D. (2014) 'The restrictions of the maximum entropy production principle', *Physica A: Statistical Mechanics and its Applications*, 410, pp. 17–21. doi: 10.1007/978-3-642-40154-1.
- Masello, J. F. *et al.* (2017) 'How animals distribute themselves in space: variable energy landscapes', *Frontiers in Zoology*, 14(1), p. 33. doi: 10.1186/s12983-017-0219-8.
- Mattison, S. M. *et al.* (2016) 'The evolution of inequality', *Evolutionary Anthropology: Issues, News, and Reviews*, 25(4), pp. 184–199. doi: 10.1002/evan.21491.
- McCann, K. S., Rasmussen, J. B. and Umbanhowar, J. (2005) 'The dynamics of spatially coupled food webs', *Ecology letters*, 8(5), pp. 513–523. doi: 10.1111/j.1461-0248.2005.00742.x.
- McNair, J. N. (1982) 'Optimal giving-up times and the Marginal Value Theorem.', *American Naturalist*, 119(4), pp. 511–529. doi: 10.1086/283929.
- Menzel, R. *et al.* (2005) 'Honey bees navigate according to a map-like spatial memory', *Proceedings of the National Academy of Sciences*, 102(8), pp. 3040–3045. doi: 10.1073/pnas.0408550102.
- Meysman, F. J. R. and Bruers, S. (2010) 'Ecosystem functioning and maximum entropy production: A quantitative test of hypotheses', *Philosophical Transactions of the Royal Society B: Biological Sciences*, 365, pp. 1405–1416. doi: 10.1098/rstb.2009.0300.

- Miller, M. L. *et al.* (2017) ‘Time to fly: A comparison of marginal value theorem approximations in an agent-based model of foraging waterfowl’, *Ecological Modelling*, 351, pp. 77–86. doi: 10.1016/j.ecolmodel.2017.02.013.
- Miranda, V. *et al.* (1994) ‘Genetic algorithms in optimal multistage distribution network planning’, *IEEE Transactions on Power Systems*, 9(4), pp. 1927–1933. doi: 10.1109/59.331452.
- Moffatt, S. and Kohler, N. (2008) ‘Conceptualizing the built environment as a social-ecological system’, *Building Research and Information*, 36(3), pp. 248–268. doi: 10.1080/09613210801928131.
- Montesinos, P., Garcia-Guzman, A. and Ayuso, J. L. (1999) ‘Water distribution network optimization using a modified genetic algorithm’, *Water Resources Research*, 35(11), pp. 3467–3473. doi: 10.1029/1999WR900167.
- Mueller, T. *et al.* (2011) ‘How landscape dynamics link individual- to population-level movement patterns: a multispecies comparison of ungulate relocation data’, *Global Ecology and Biogeography*, 20(5), pp. 683–694. doi: 10.1111/j.1466-8238.2010.00638.x.
- Murphy, J. T. (2001) ‘Making the energy transition in rural East Africa: Is leapfrogging an alternative?’, *Technological Forecasting and Social Change*, 68(2), pp. 173–193.
- Naeem, S. and Colwell, R. K. (2012) ‘Ecological Consequences of Heterogeneity of Consumable Resources’, in Kolasa, J. and Pickett, S. T. A. (eds) *Ecological Heterogeneity*. Springer Science & Business Media (Ecological Studies).
- Nonaka, E. and Holme, P. (2007) ‘Agent-based model approach to optimal foraging in heterogeneous landscapes: Effects of patch clumpiness’, *Ecography*, 30(6), pp. 777–788. doi: 10.1111/j.2007.0906-7590.05148.x.
- Oades, J. M. (1993) ‘The role of biology in the formation, stabilization and degradation of soil structure’, *Geoderma*, 56, pp. 377–400. doi: 10.1016/0016-7061(93)90123-3.
- O’Connor, M. I. *et al.* (2019) ‘Principles of ecology revisited: Integrating information and ecological theories for a more unified science’, *Frontiers in Ecology and Evolution*, 7, pp. 1–20. doi: 10.3389/fevo.2019.00219.
- Odum, E. P. (1968) ‘Energy flow: A historical review’, *American Zoologist*, 8, pp. 11–18.

- Odum, H. T. (1957) 'Trophic Structure and Productivity of Silver Springs, Florida', *Ecological Monographs*, 27(1), pp. 55–112.
- Odum, H. T. (1971) *Environment, Power and Society*. New York: Wiley.
- Odum, H. T. (1988) 'Self-Organization, Transformity, and Information', *Science*, 242. doi: 10.1126/science.242.4882.1132.
- Odum, H. T. (2002) 'Explanations of ecological relationships with energy systems concepts', *Ecological Modelling*, 158(3), pp. 201–211. doi: 10.1016/S0304-3800(02)00232-6.
- Odum, H. T. and Pinkerton, R. C. (1955) 'Time's speed regulator: The optimum efficiency for maximum power output in physical and biological systems', *American Scientist*, 43(2), pp. 331–343.
- Oliver, T. *et al.* (2010) 'Heterogeneous landscapes promote population stability', *Ecology Letters*, 13(4), pp. 473–484. doi: 10.1111/j.1461-0248.2010.01441.x.
- Panda, B. C. (1981) 'Active transport in the light of thermodynamics of open systems', *International Journal of Quantum Chemistry*, 20(2), pp. 567–571. doi: 10.1002/qua.560200228.
- Parrott, L. (2010) 'Measuring ecological complexity', *Ecological Indicators*, 10(6), pp. 1069–1076. doi: 10.1016/j.ecolind.2010.03.014.
- Pauliuk, S. and Hertwich, E. G. (2015) 'Socioeconomic metabolism as paradigm for studying the biophysical basis of human societies', *Ecological Economics*, 119, pp. 83–93. doi: 10.1016/j.ecolecon.2015.08.012.
- Perna, A. and Latty, T. (2014) 'Animal transportation networks', *Journal of The Royal Society Interface*, 11(100), p. 20140334. doi: 10.1098/rsif.2014.0334.
- Polis, G. A., Anderson, W. B. and Holt, R. D. (1997) 'Toward an integration of landscape and food web ecology: The dynamics of spatially subsidized food webs', *Annual Review of Ecology and Systematics*, 28, pp. 289–316. doi: 10.1146/annurev.ecolsys.28.1.289.
- Prigogine, I. (1955) *Introduction to Thermodynamics of Irreversible Processes*. Chicago, Illinois: Thournes.
- Prigogine, I. (1978) 'Time, Structure, and Fluctuations (Nobel Lecture)', *Science (New York, N.Y.)*, 201(4358), pp. 777–785. doi: 10.1126/science.201.4358.777.

- Ranc, N. *et al.* (2021) 'Experimental evidence of memory-based foraging decisions in a large wild mammal', *Proceedings of the National Academy of Sciences*, 118(15), p. e2014856118. doi: 10.1073/pnas.2014856118.
- Rodrigue, J. P. (2017) *The Geography of Transport Systems*. Hofstra University, Department of Global Studies & Geography. Available at: <https://transportgeography.org>.
- Ronellenfitch, H. and Katifori, E. (2016) 'Global Optimization, Local Adaptation, and the Role of Growth in Distribution Networks', *Physical Review Letters*, 117(13), pp. 1–5. doi: 10.1103/PhysRevLett.117.138301.
- Roshier, D. A., Doerr, V. A. J. and Doerr, E. D. (2008) 'Animal movement in dynamic landscapes: Interaction between behavioural strategies and resource distributions', *Oecologia*, 156(2), pp. 465–477. doi: 10.1007/s00442-008-0987-0.
- Ross, J., Corlan, A. D. and Müller, S. C. (2012) 'Proposed Principles of Maximum Local Entropy Production', *The Journal of Physical Chemistry B*, 116(27), pp. 7858–7865. doi: 10.1021/jp302088y.
- Salthe, S. N. N. (2010) 'Maximum power and maximum entropy production: Finalities in nature', *Cosmos and History*, 6(1), pp. 114–121.
- Sattler, M. L. (2016) 'Energy for Sustainable Development: The Energy–Poverty–Climate Nexus', in. InTech. doi: 10.5772/62254.
- Savage, V. M., Deeds, E. J. and Fontana, W. (2008) 'Sizing Up Allometric Scaling Theory', *Energy*, 4, pp. 1–18. doi: 10.1371/journal.pcbi.1000171.
- Schlägel, U. E., Merrill, E. H. and Lewis, M. A. (2017) 'Territory surveillance and prey management: Wolves keep track of space and time', *Ecology and Evolution*, 7(20), pp. 8388–8405. doi: 10.1002/ece3.3176.
- Seeley, T. D. (1995) *The Wisdom of the Hive*. Cambridge, Massachusetts: Harvard University Press. Available at: <https://www.journals.uchicago.edu/doi/10.1086/285726>.
- Seiferling, I., Proulx, R. and Wirth, C. (2014) 'Disentangling the environmental-heterogeneity–species-diversity relationship along a gradient of human footprint', *Ecology*, 95(8), pp. 2084–2095. doi: 10.1890/13-1344.1.

- Shennan, S. (2011) 'Property and wealth inequality as cultural niche construction', *Philosophical Transactions of the Royal Society B: Biological Sciences*, 366, pp. 918–926. doi: 10.1098/rstb.2010.0309.
- Shepard, E. L. C. *et al.* (2013) 'Energy Landscapes Shape Animal Movement Ecology.', *The American Naturalist*, 182(3), pp. 298–312. doi: 10.1086/671257.
- Shrawane, S. S. and Diagavane, M. (2013) 'Application of Genetic Algorithm for Power Flow Analysis', *International Journal of Engineering Research & Technology*, 2(9), pp. 453–456.
- Sikk, K. and Caruso, G. (2020) 'A spatially explicit agent-based model of central place foraging theory and its explanatory power for hunter-gatherers settlement patterns formation processes', *Adaptive Behavior*, 28(5), pp. 377–397. doi: 10.1177/1059712320922915.
- Silva, P. S. D. *et al.* (2013) 'Foraging in highly dynamic environments: Leaf-cutting ants adjust foraging trail networks to pioneer plant availability', *Entomologia Experimentalis et Applicata*, 147(2), pp. 110–119. doi: 10.1111/eea.12050.
- Smith, E. A., Bowles, S., *et al.* (2010) 'Intergenerational wealth transmission and inequality in premodern societies: Reply', *Current Anthropology*, 51(1), pp. 119–126. doi: 10.1086/650152.
- Smith, E. A., Hill, K., *et al.* (2010) 'Wealth transmission and inequality among hunter-gatherers', *Current Anthropology*, 51(1), pp. 19–34. doi: 10.1086/648530.
- Sousa, T., Domingos, T. and Kooijman, S. A. L. M. (2008) 'From empirical patterns to theory: A formal metabolic theory of life', *Philosophical Transactions of the Royal Society B: Biological Sciences*, 363, pp. 2453–2464. doi: 10.1098/rstb.2007.2230.
- Sovacool, B. K. (2012) 'The political economy of energy poverty: A review of key challenges', *Energy for Sustainable Development*, 16(3), pp. 272–282. doi: 10.1016/j.esd.2012.05.006.
- Stein, A., Gerstner, K. and Kreft, H. (2014) 'Environmental heterogeneity as a universal driver of species richness across taxa, biomes and spatial scales', *Ecology Letters*, 17(7), pp. 866–880. doi: 10.1111/ele.12277.
- Stevens, R. D. and Tello, J. S. (2011) 'Diversity begets diversity: relative roles of structural and resource heterogeneity in determining rodent community structure', *Journal of Mammalogy*, 92(2), pp. 387–395. doi: 10.1644/10-mamm-a-117.1.

Strano, E. *et al.* (2017) ‘The scaling structure of the global road network’, *Royal Society Open Science*, 4(10). doi: 10.1098/rsos.170590.

Summers, K. (2005) ‘The evolutionary ecology of despotism’, *Evolution and Human Behavior*, 26(1), pp. 106–135. doi: 10.1016/j.evolhumbehav.2004.09.001.

Tanner, C. J. and Jackson, A. L. (2012) ‘Social structure emerges via the interaction between local ecology and individual behaviour’, *Journal of Animal Ecology*, 81(1), pp. 260–267. doi: 10.1111/j.1365-2656.2011.01879.x.

Teitelbaum, C. S. *et al.* (2015) ‘How far to go? Determinants of migration distance in land mammals’, *Ecology Letters*. Edited by M. Festa-Bianchet, 18(6), pp. 545–552. doi: 10.1111/ele.12435.

Tews, J. *et al.* (2004) ‘Animal species diversity driven by habitat heterogeneity/diversity: The importance of keystone structures’, *Journal of Biogeography*, 31(1), pp. 79–92. doi: 10.1046/j.0305-0270.2003.00994.x.

Trapanese, C., Meunier, H. and Masi, S. (2019) ‘What, where and when: spatial foraging decisions in primates’, *Biological Reviews*, 94(2), pp. 483–502. doi: 10.1111/brv.12462.

Tylianakis, J. M. *et al.* (2008) ‘Resource heterogeneity moderates the biodiversity-function relationship in real world ecosystems’, *PLoS Biology*, 6(5), pp. 0947–0956. doi: 10.1371/journal.pbio.0060122.

Tylianakis, J. M. and Morris, R. J. (2017) ‘Ecological Networks Across Environmental Gradients’, *Annual Review of Ecology, Evolution, and Systematics*, 48(1), pp. 25–48. doi: 10.1146/annurev-ecolsys-110316-022821.

Ulanowicz, R. E. (2011) ‘Some steps toward a central theory of ecosystem dynamics’, *Computational Biology and Chemistry*, 27, pp. 523–530. doi: 10.1007/978-0-8176-4904-3.

Unrean, P. and Sreenc, F. (2011) ‘Metabolic networks evolve towards states of maximum entropy production’, *Metabolic Engineering*, 13(6), pp. 666–673. doi: 10.1016/j.ymben.2011.08.003.

Vallino, J. J. (2010) ‘Ecosystem biogeochemistry considered as a distributed metabolic network ordered by maximum entropy production’, *Philosophical Transactions of the Royal Society B: Biological Sciences*, 365, pp. 1417–1427. doi: 10.1098/rstb.2009.0272.

- Wagg, C. *et al.* (2014) ‘Soil biodiversity and soil community composition determine ecosystem multifunctionality’, *Proceedings of the National Academy of Sciences of the United States of America*, 111(14), pp. 5266–5270. doi: 10.1073/pnas.1320054111.
- Walker, R. E., Keane, C. R. and Burke, J. G. (2010) ‘Disparities and access to healthy food in the United States: A review of food deserts literature’, *Health and Place*, 16(5), pp. 876–884. doi: 10.1016/j.healthplace.2010.04.013.
- Wang, Y. *et al.* (2019) ‘Global evidence of positive biodiversity effects on spatial ecosystem stability in natural grasslands’, *Nature Communications*, 10(1), pp. 1–9. doi: 10.1038/s41467-019-11191-z.
- Ward, J. F., Austin, R. M. and Macdonald, D. W. (2000) ‘A simulation model of foraging behaviour and the effect of predation risk’, *Journal of Animal Ecology*, 69(1), pp. 16–30. doi: 10.1046/j.1365-2656.2000.00371.x.
- Wardle, D. A. *et al.* (2004) ‘Ecological linkages between aboveground and belowground biota’, *Science*, 304, pp. 1629–1633. doi: 10.1126/science.1094875.
- West, G. B., Brown, J. H. and Enquist, B. J. (1997) ‘A General Model for the Origin of Allometric Scaling Laws in Biology’, *Science*, 276(April), pp. 122–126. doi: 10.1126/science.276.5309.122.
- Wilson, R. P., Quintana, F. and Hobson, V. J. (2012) ‘Construction of energy landscapes can clarify the movement and distribution of foraging animals’, *Proceedings of the Royal Society B: Biological Sciences*, 279(1730), pp. 975–980. doi: 10.1098/rspb.2011.1544.
- Wright, S. D. and Rohde, K. (2013) ‘Energy and spatial order in niche and community’, *Biological Journal of the Linnean Society*, 110(3), pp. 696–714. doi: 10.1111/bij.12141.
- Xie, F. and Levinson, D. (2007) ‘Measuring the structure of road networks’, *Geographical Analysis*, 39(3), pp. 336–356. doi: 10.1111/j.1538-4632.2007.00707.x.
- Xie, F. and Levinson, D. (2009) ‘Modeling the growth of transportation networks: A comprehensive review’, *Networks and Spatial Economics*, 9(3), pp. 291–307. doi: 10.1007/s11067-007-9037-4.
- Yang, Z. *et al.* (2017) ‘A novel network model for optimal power flow with reactive power and network losses’, *Electric Power Systems Research*, 144, pp. 63–71. doi: 10.1016/j.epsr.2016.11.009.

- Yerra, B. M. and Levinson, D. M. (2005) 'The emergence of hierarchy in transportation networks', *Annals of Regional Science*, 39(3), pp. 541–553. doi: 10.1007/s00168-005-0230-4.
- Yi, H. *et al.* (2017) 'Measuring ecological characteristics of environmental building performance: Suggestion of an information-network model and indices to quantify complexity, power, and sustainability of energetic organization', *Ecological Indicators*, 83, pp. 201–217. doi: 10.1016/j.ecolind.2017.07.056.
- Young, I. M., Crawford, J. W. and Rappoldt, C. (2001) 'New methods and models for characterising structural heterogeneity of soil', *Soil and Tillage Research*, 61, pp. 33–45. doi: 10.1016/S0167-1987(01)00188-X.
- Young, I. M. and Ritz, K. (2009) 'The habitat of soil microbes', in *Biological Diversity and Function in Soils*. (1994), pp. 31–43.
- Ziegler, H. and Wehrli, C. (1987) 'On a Principle of Maximal Rate of Entropy Production', *Journal of Non-Equilibrium Thermodynamics*, 12(3). doi: 10.1515/jnet.1987.12.3.229.
- Zischg, J., Rauch, W. and Sitzenfrei, R. (2018) 'Morphogenesis of Urban Water Distribution Networks: A Spatiotemporal Planning Approach for Cost-Efficient and Reliable Supply', *Entropy*, 20(9). doi: 10.3390/e20090708.

2

Trajectories toward maximum power and inequality in resource distribution networks

Abstract

Resource distribution networks are the infrastructure facilitating the flow of resources in both biotic and abiotic systems. Both theoretical and empirical arguments have proposed that physical systems self-organise to maximise power production, but how this trajectory is related to network development, especially regarding the heterogeneity of resource distribution in explicitly spatial networks, is less understood. Quantifying the heterogeneity of resource distribution is necessary for understanding how phenomena such as economic inequality or energetic niches emerge across socio-ecological and environmental systems. Although qualitative discussions have been put forward on this topic, to date there has not been a quantitative analysis of the relationship between network development, maximum power, and inequality. This paper introduces a theoretical framework and applies it to simulate the power consumption and inequality in generalised, spatially explicit resource distribution networks. The networks illustrate how increasing resource flows amplify inequality in power consumption at network end points, due to the spatial heterogeneity of the distribution architecture. As increasing resource flows and the development of hierarchical branching can both be strategies for increasing power consumption, this raises important questions about the different outcomes of heterogeneous distribution in natural versus human-engineered networks, and how to prioritise equity of distribution in the latter.

2.1. Introduction

Both biotic and abiotic systems require energy for maintenance and growth, necessitating the relocation of energetic resources from points of supply to points of consumption and end use. This need for energy drives the development of resource acquisition, distribution, and end-use (RADE) networks (Jarvis, Jarvis and Hewitt, 2015) in all earth systems. RADE networks are by definition spatial structures, constructed with both physical materials, such as asphalt, wire, or connective tissue, and informational cues, such as scent trails or memories. Additionally, all RADE networks can be conceptualised as a collection of resources, where the energy flow is generated and supplied; end-use consumers, where the energy flow is required; and the links between them. The construction, maintenance, and use of these networks inevitably requires a considerable proportion of the resources available to consumers. As it is evolutionarily advantageous to maximise the net resources available for further growth and development (Boltzmann, 1905; Lotka, 1922), there is significant adaptive pressure to drive RADE network development toward increasing efficiency. Additionally, these networks often share common forms such as hierarchical branching, and serve end consumers operating in highly heterogeneous states. Rarely, if ever, are these two observations explicitly associated, but given the role of RADE networks in determining the states of the consumers they support, correlation between network topology and variance in supply to these points of end use should be expected. Establishing this connection is crucial, not only in natural systems as a means of accounting for variability, but especially in social systems where inequality is of such profound importance.

Inequality in access to basic resources in human society is typically conceived as an outcome of combined social, political, psychological, and economic influences. Although many theories about the origins of inequality include discussion of resources, such as their economic defensibility, most theories still invoke cultural or technological arguments as well (Mattison *et al.*, 2016). Additionally, even arguments based on instincts and social behaviour rarely connect these to resource

distribution explicitly (Charlton, 1997), despite the essential role of resource movement in giving rise to any cultural, technological, and social forces. This gives the appearance of resource distribution and emergent inequality in social systems as having fundamentally different causes than hierarchies in environmental and biological systems, or energetic niches in ecosystems. Moreover, while energy consumption is not typically the named objective of economic management, the drive toward ever-increasing economic growth still requires energetic resources to build and maintain the infrastructure that generates returns (Georgescu-Roegen, 1986), paralleling the energy used for growth and maintenance within natural systems. As both natural and human-engineered systems rely on resource distribution networks to relocate energetic resources, it seems logical to consider heterogeneity within the networks and resources themselves as potentially foundational causes of inequality (Bejan and Errera, 2017). However, a formal, quantitative linkage between RADE network architecture, inequality in resource distribution, and the rate of increase of that inequality during network development, has not yet been elucidated.

RADE networks are theorised to develop in a way that maximises the availability of resources to points of end use, such that these end consumers capture the maximum free energy for their own purposes in doing ‘useful work’ (Lotka, 1922), such as increases in growth, development, or storage (Ulanowicz, 2011). This is formalised in the Maximum Power Principle (MPP), which states that, given adequate degrees of freedom, a system will self-organise to maximise its power output, or capture and use of free energy per unit time (Odum and Pinkerton, 1955). An explanation for why such behaviour would emerge is that increasing the availability of useful energy currently within a system allows the system to capture more free energy in the future, such that MPP is simply the expression of a growth-orientated positive feedback, which inevitably evolves to some boundary or constraint. Often these constraints can be considered thermodynamic limits on efficiency (Kleidon, 2016). Hereon, this maximisation of energy consumption and power production will be referred to as ‘maximum power,’ to include the transfer or capture of free energy, and its

consumption in performing useful work. MPP is closely related or equivalent in many systems to the Maximum Entropy Production Principle (MEPP) and related thermodynamic extremisation principles (see *e.g.* Kleidon, Malhi and Cox, 2010; Kleidon *et al.*, 2013). While criticisms of both MPP and MEPP (Mansson and McGlade, 1993; Ross, Corlan and Müller, 2012; Poletini, 2013) have been put forward, these have mostly been resolved through clarification and restrictions to the theories (Odum, 1983; Martyushev and Seleznev, 2014). As such, these extremisation principles provide a framework and directionality for evolution and systems progression, and can be used to help understand broader trajectories for systems development, and network development within that (Kleidon, Malhi and Cox, 2010).

Specifically, systems often maximise power via changing state with respect to available energy inputs and constraints; changing network architecture to take advantage of untapped resources or minimise energy consumption in transporting resources; or both. Some theorise that the development of self-similar hierarchical branched networks, seen in a diverse array of naturally-occurring and human-engineered systems, including vascular networks in plants and animals, power grids, and river basins, is an example of the latter strategy (West, Brown and Enquist, 1997; Banavar, Maritan and Rinaldo, 1999). Resource flows transmit energy using a mass carrier, such as food or electrons; and during transmission these carriers experience frictional dissipation when moving over distances. This creates the evolutionary pressure to minimise transmission distance to maximise the energy transferred, hence the development of optimal space-filling structures such as hierarchical branching. Despite the theoretical universal drive toward increasing levels of energy consumption, there has been limited study on the relationship between this increasing trajectory, the architectures favourable to it, and the impact that has on the inequality of energy distribution in ecological and socio-ecological systems, as introduced above.

Since frictional dissipation derives from distance, spatially explicit modelling of RADE networks is crucial to understanding their development and dynamics, and the impacts these have on

inequality. The dynamics of energy-mass flows over distances are described by a group of phenomenological linear flow laws, including Ohm's law for electrical current, Darcy's law for fluid flow, Fick's law for diffusion, and Fourier's law for heat transport. These flow laws state how force and flux are closely related to one another (Kirkham, 2014), making them useful for modelling a diverse range of energy-mass flow systems. It is hypothesised that, when viewed from the appropriate perspective, physical systems such as ecosystems and socio-ecological systems should all follow these force-flux relationships (Odum, 1971). Odum in particular made extensive use of electrical analogue modelling, which calculated the flows through a system using Ohm's law, by identifying the analogous concepts to voltage, current, and resistance or conductance in a system (see *e.g.* Odum, 1967, 2002). While his focus was on interactional models such as food webs, less work has been done applying this type of modelling to spatially-explicit networks, where the friction or resistance term, or equivalently the latter's inverse, conductance, is related to the physical distance the flows must cover (although see specific case studies in Collier, 2010; Wang *et al.*, 2012).

Drawing analogies between resource flows in complex coupled socio-ecological systems and electrical circuits can be criticized because the formulas underlying analysis of electrical systems are linear, while those of the former are nonlinear. However, Wang *et al.* (2012) argue that many systems show linear behaviour at macroscales or microscales, and these can be modelled individually and recombined. While degrees of freedom to explore different system states and feedbacks and signalling between system components are required for systems to evolve toward maximum power or entropy production (Martyushev and Seleznev, 2014), these can be represented more simply within a model, as will be shown, for the purposes of exploring the minimal case. Such linear models thus remain useful analogies for exploring generalized realistic systems (Levins, 1966), and may still result in the emergence of complex properties. Exploration of the effects on our observations of nonlinear formulas is the potential subject of future work.

Given the theoretical argument and empirical evidence for systems to evolve toward a state of maximum power, this paper will explore the potential relationships between the trajectory towards maximum power, RADE network structure, and inequality. It will thereby generate further insight into the characteristics of complex spatially explicit RADE networks as they develop toward and operate at maximum power. Specifically, systems will be modelled with representative electrical circuits to elucidate the dynamics and characteristics of generalised RADE networks evolving toward maximum power transfer, explore characteristics of those networks and the evolutionary levers employed in their development, and discuss how these relate to the existence and development of inequality between end consumers in those networks.

2.2. Inequality as a function of network architecture and resource flows

2.2.1. Modelling framework using an electrical analogue

In mass-flow networks, the flow through the network is generally conceptualised as a function of the driving potential gradient, and the characteristics of the material through which it flows. As introduced above, this relationship can be represented in a given system using an analogue of one of the phenomenological flow laws, such as Ohm's law,

$$I = \frac{\Delta V}{R} . \quad (1)$$

In the framework here, ΔV is the potential gradient driving the flow between two points in the network, I is the resource flow, and R is the resistance of the associated link, a measure of the friction encountered by the flow, given by the ratio of link length to link strength or capacity, $R = \frac{L}{S}$. The power output P delivered to a given end-point consumer c_i in the network, or final power, is defined as

$$P_{C_i} = I_{C_i} V_{C_i} . \quad (2)$$

Alternatively, ΔV can be conceptualised as the energy consumed in transport, whether active or passive, as the power consumed in transport between two points, P_L , is given by combining Eq. 1 and 2 as

$$P_L = I\Delta V = I^2R. \quad (3)$$

The relationship between this power consumption in transport and the spatially-related resistance term clarifies the evolutionary pressure for a system to minimise resistance, such as through the development of increasingly efficient structures that are hypothesised to minimise frictional losses (West, Brown and Enquist, 1997). Specifically, minimising the frictional losses maximises the rate of energy transfer, or power, at the spatially disparate points of final dissipation or consumption.

Along with reorganisation of network architecture to minimise resistance, systems can evolve toward higher final power by adapting network state with respect to the quantity and potential of available resources. For example, the increased availability of resources in summer months allows mammals to operate at a higher metabolism and in a greater geographic range, whereas hibernation is an adaptation to decreased resource availability in the same range during winter months (Humphries, Thomas and Kramer, 2003). In the framework here, adaptation of network state can be represented by changing I , or by changing the potentials that comprise V_C . In the former case, increasing I causes P_{C_i} to increase (Eq. 2), until the increased frictional losses from higher resource flow (Eq. 3) causes a large enough increase in ΔV , such that P_{C_i} decreases. In this way, the trade-off between I and ΔV is mediated by R , again providing evolutionary pressure for a system to develop lower resistance, as it increases resource flows.

Due to this trade-off between I and ΔV , maximum final power occurs in this framework when the potential at the consumer is half the potential at the resource (see S1 for derivation). This is consistent with the Maximum Power Transfer theorem for electrical circuits (Paul, 2001), empirical findings of maximum power in natural systems such as streamflow (Bejan, 1996), muscle

contraction (Santillán and Angulo-Brown, 1997), sediment transport (Kleidon *et al.*, 2013), and the Maximum Power Principle as extended to generalised interacting components (Odum and Pinkerton, 1955). In electrical circuits, simplification algorithms such as Thévenin's theorem (Paul, 2001) allow for complex circuits to be represented by simpler equivalents. Similarly, in the framework presented here, the relationship between consumer and resource potential can be extended over the entire network using the network mean values for power consumption, resource flow, resistance, and potentials. Specifically, the network-wide maximum final power state is then

$$\overline{V}_C = \frac{\overline{V}_R}{2}, \quad (4)$$

where \overline{V}_C and \overline{V}_R are the network mean values for consumer and resource potential, respectively.

In order to extend this framework to explore the heterogeneity among consumers within the network, and how this is affected by increasing consumption and changing network organisation, the relationship between consumer potential, resource flow, and resistance can also be expressed in terms of the respective standard deviations. Although it is more common to use the Gini coefficient or other relative measures to quantify inequality in economic and similar analyses, these can obfuscate increases in absolute inequality when the relationship between variables stays constant (Sutcliffe, 2005; Niño-Zarazúa, Roope and Tarp, 2017). For example, if each number in a distribution is increased by 50 %, the standard deviation of the distribution increases by 50 % and the range by 50 %, but the Gini coefficient remains the same as the relative relationships are unchanged. Moreover, the Gini coefficient and similar metrics are unitless measures, whereas the standard deviation has the same units as the mean. Any relationships elucidated involving standard deviation will therefore be more consistent with those identified above using means.

The distributions of consumer potentials and final power consumption in a network are the result of the spatial distribution of consumer and resource nodes and links, and the magnitude of resource flow. In networks where there is a single direct connection from each consumer to a

resource point, equal resource flow to all consumers, and no interconnections between consumers, the standard deviation of the consumer potentials is $\sigma_{V_C} = \sigma_R I$, derived from Eq. 1, and the standard deviation of consumer final power is $\sigma_{P_C} = \sigma_R I^2$. Therefore, in networks with equal resistances along all links, such as an idealised radial burst network, the standard deviations of consumer potentials and final power consumption would be zero. In contrast, increasing resource flows along links with unequal resistance would cause an increase in the standard deviations of potential and final power consumption, due to unequal decreases in consumer potentials.

In more interconnected networks, however, the standard deviations of consumer potential and final power consumption are complex properties, as changes in potential at one node would propagate to interconnected nodes throughout the entire network. As such, determining the baseline structural heterogeneity of the network helps isolate the effects of spatial distribution and connectivity from those of resource flow in increasing the distributions of consumer potential and final power consumption. Here, the ‘effective resistance’ R_{E_i} is the resource flow-normalised drops in potential from a resource to a given consumer i ,

$$R_{E_i} = \frac{V_R - V_{C_i}}{I_i}. \quad (5)$$

As opposed to the traditional measure of resistance, which is calculated for a given link, the effective resistance is calculated along the whole path between a given consumer and resource, even if the two nodes are connected indirectly via multiple links. The effective resistance therefore considers the interaction effects along the links, as well as the real resistances of the link or links between a consumer and resource: its standard deviation relates the heterogeneity in physical distances around the network that the flows cross, network connectivity, and the quantity of flow, to the disparities in consumer potential or power.

In the special case of direct connections between consumers and a resource, the effective resistance simplifies to the link resistance. In all networks, therefore, the standard deviation of effective resistance is the constant of proportionality between the standard deviation of consumer potential or power, and resource flow, such that $\sigma_{V_C} = \sigma_{R_E} I$, and $\sigma_{P_C} = \sigma_{R_E} I^2$. As with the traditional measure of resistance, effective resistance and its standard deviation are stationary for any quantity of resource flow through a given link in the network architecture. It is clearly influenced by the connectivity and symmetry of the network, as asymmetry in path length, Euclidean distance, or number of intermediary or downstream nodes all increase the inequality in consumer potential and final power consumption. Notably, since effective resistance includes the effects of both physical structure and connectivity, it could potentially be a useful mapping between spatial and relational dimensions of networks, which have typically been analysed separately.

2.2.2. Simulations to illustrate framework

To illustrate these described dynamics of resource flow in networks, generalised RADE networks were modelled using the relationships presented above. Initially, the networks comprised only two types of nodes distributed in space: resource supply nodes and consumer nodes. Consumer nodes could be connected to one another, such that the consumers who were more directly connected to resource nodes passed resource flow along the network to more distant consumers. However, this was limited to the excess resource flow remaining after the initial consumers had met their requirement: consumer nodes could not act as resources to generate additional flow. The resistance was held constant across all links, and was modelled as the ratio of link length to strength, as described previously. The networks were evolved toward maximum power by increasing the resource flows through them and determining the distribution of power consumption across the network using a matrix inversion. Assuming that the system would reach an equilibrium state around the level of maximum power, this incremental addition of resource flow and resulting adjustment of potential at the consumers replicated the ability of a more complex system to explore

different states, and self-organise to inhabit the state of maximum network power consumption. The full details are provided in Section 2.5. This approach, modified from load flow analysis in electrical grids (von Meier, 2006), ensured that the resource flows calculated for each node were consistent with the constraints of the first and second laws of thermodynamics, as resource flow was conserved, and power losses around the network were proportional to the size of the network. A sample of the networks simulated is shown in Figure 2.1, and complete results are in S2.

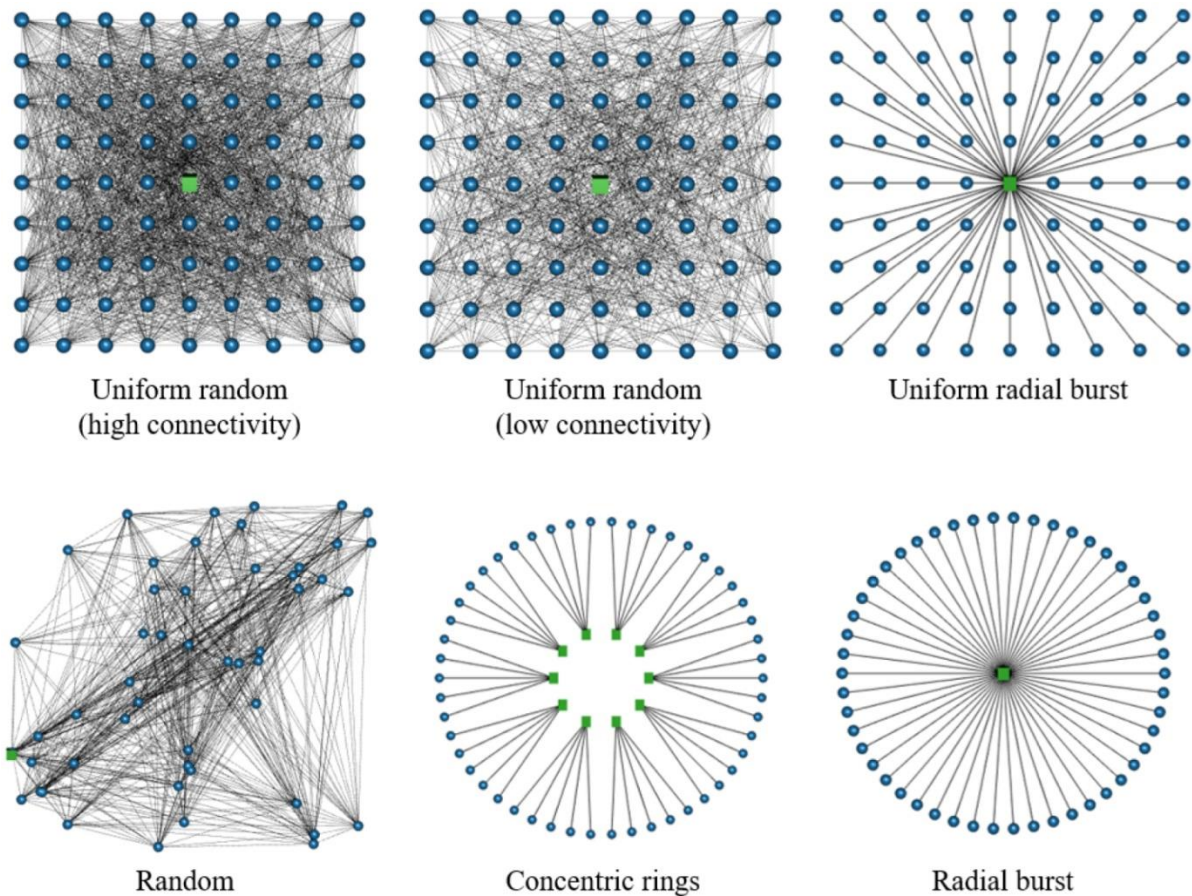


Figure 2.1 A sample of the networks used to simulate evolution toward maximum power. The green squares are resource nodes, and the blue circles are consumer nodes. The grey lines are links between them. Maximum power was calculated by varying the resource flow through the network and calculating the total final power across all consumer nodes.

The outcomes of a representative sample of the simulations are shown in Figure 2.2. As consistent with Eq. 4 above, in all simulations maximum power occurs when the mean consumer operates at 50 % of the potential of the mean resource (Figure 2.2a). Moreover, the relationship between resource flow per consumer squared, I_C^2 , and the standard deviation of consumer power, σ_{P_C} , is

linear (Figure 2.2b), with slope σ_{RE} , as calculated by least-squares regression and plotted against the estimate using Eq. 5 (Figure 2.2c). This heterogeneity of distances and connections between the consumers and resource causes a distribution of consumer potentials, reflected in σ_{P_C} . The relationship between consumer potential and power heterogeneity for the different networks, and the resource flow per consumer, is also shown in Figure 2.3, where increasing I_C over the course of the simulation, and hence decreasing $\overline{V_C}/\overline{V_R}$, causes σ_{P_C} to increase.

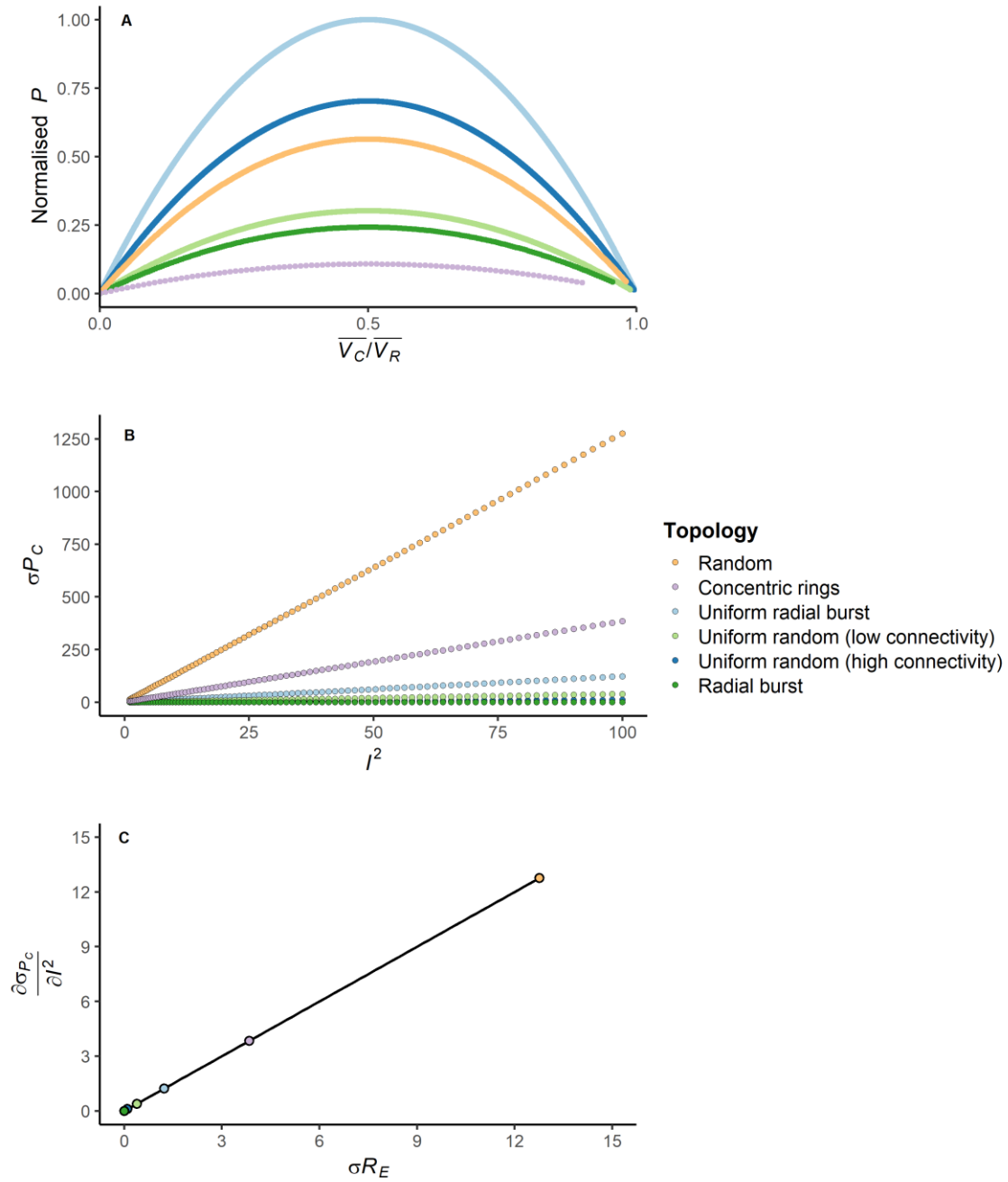


Figure 2.2. For the six example networks, (a) the relationship between total final power (P) and the ratio of mean consumer potential to mean resource potential ($\overline{V_C}/\overline{V_R}$), (b) the relationship between the standard deviation of consumer final power (σ_{P_C}) and resource flow squared (I^2), and (c) the relationship between the slope of (b) and the standard deviation of effective resistance (σR_E). These illustrate the main equations derived in the presentation of the modelling framework. Here, each coloured point range represents a different network topology over which the simulations were run. The slope of (c) is exactly 1. Units are generalised units of power, potential, and resource flow. A copy of (a) with raw data is included in S3.

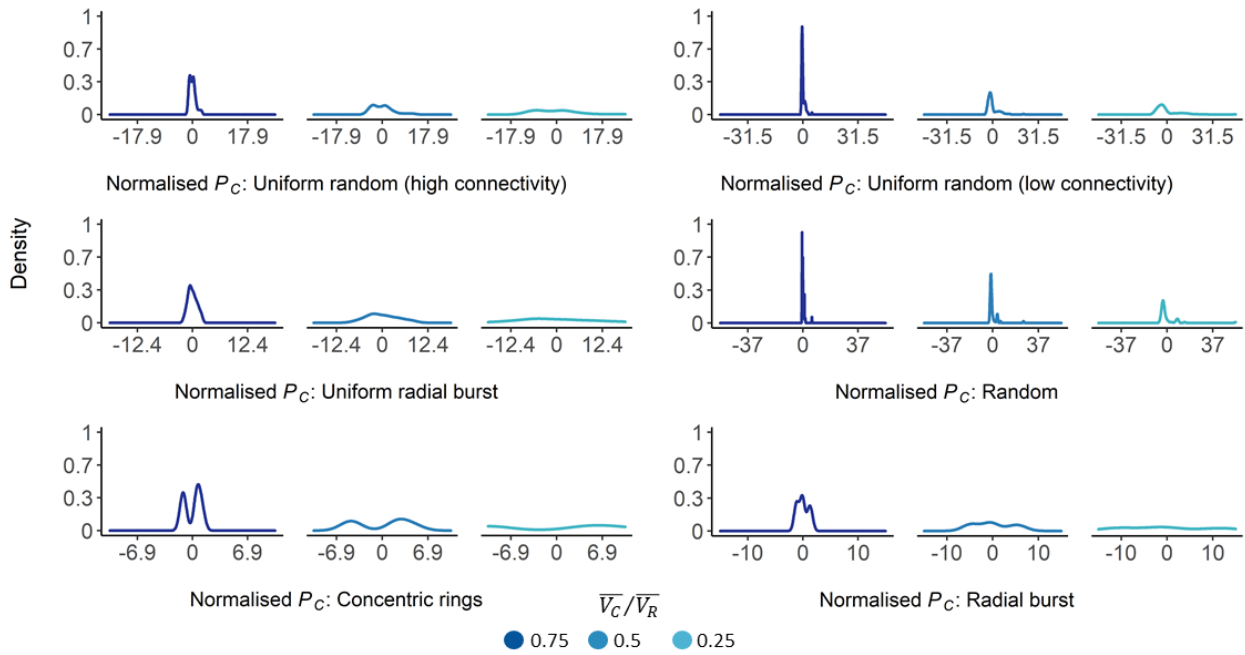


Figure 2.3. Density plots of normalised consumer final power (P_C) for the six example networks, shown over decreasing ratios of mean consumer to mean resource potential, $\overline{V}_C/\overline{V}_R$. Each plot shows the density for the normalised consumer final power at $\overline{V}_C/\overline{V}_R = 0.75, 0.5$, and 0.25 , from left to right, as the ratio decreases due to increased resource flow during the simulation. The data were normalised by subtracting the mean consumer power at each ratio level, and dividing by the standard deviation of consumer power at $\overline{V}_C/\overline{V}_R = 0.75$, such that the width of the first subplot for each network is one standard deviation.

The networks that show more heterogeneity in the Euclidean distance, path distance, or both, and less connectivity between consumers, have higher inequality as measured by σ_{RE} (Figures 2.1 and 2.2c). This suggests that connectivity among consumers can also play a role in limiting the inequality in frictional losses and the resultant consumer potential heterogeneity. This mechanism is perhaps similar to the translocation of nutrients through fungi, where symbiotic connections between the mycelium and plant root systems allow for the redistribution of heterogeneously-located nutrients, providing more remote portions of the mycelial network greater access to resources (Boswell *et al.*, 2002).

While the resource nodes in these simulations operated at a constant potential, similarly to time-averaged behaviour of renewable resources, or a system observed over a short timeframe, these results suggest that inequality would increase even more quickly in systems with diminishing

resources. This would be because the less optimally located and connected consumers would experience larger decreases in power, due to the decreasing resource potential amplifying the effects of their higher effective resistance. This is a current line of investigation for an extension of this work.

2.3. Inequality in branching networks

2.3.1. Branching as a strategy to increase the maximum power of a system

Although changes in state variables, such as potential, allow any given network architecture to achieve its maximum power, this maximum can be increased further through the evolution of the network architecture itself, as discussed. In the framework presented here, this would be illustrated by network reorganisation or otherwise reducing R , such that higher resource flows do not cause as much frictional loss (Eq. 3). This does not necessarily require decreasing σ_{R_E} however, as theoretically the distribution of effective resistances could remain the same for a different configuration of actual resistances.

One means by which systems evolve toward increased consumption through network change is through self-organisation into hierarchical branching structures, which are prevalent in both naturally-occurring and human-engineered systems (West, Brown and Enquist, 1997; Banavar, Maritan and Rinaldo, 1999). In these networks, multiple downstream consumers may draw resource flow from the same resource, although this causes increased frictional losses by increasing the I term in Eq. 3. This is offset in many systems by the development of higher-capacity links along shared pathways, such as preferential flow paths (Zehe *et al.*, 2012; Kleidon *et al.*, 2013). This is equivalent to varying the link strength in the equation for R (see Methods).

2.3.2. Branching simulations

To illustrate the dynamics of branching networks more clearly, another set of simulations was performed, featuring idealised self-similar hierarchical branching networks. In these simulations,

two networks were constructed. In the first, the network had consumers arranged in a branching pattern around a single resource ('fully branched' network, Figure 2.4a). In the second, a branching network was artificially evolved from a nearly radial burst pattern, by adding in consecutive levels of non-demand junctions or 'branch points,' and re-calculating the consumption ('evolved branching' networks, Figure 2.4b). In the 'evolved branching' networks, at each iteration of the evolution, the average link length became shorter, and the network became more similar to a fractal branching structure. This was done to observe how power consumption was affected by changing the architecture to reflect known optimal distribution patterns, without increasing the number of consumers in the network.

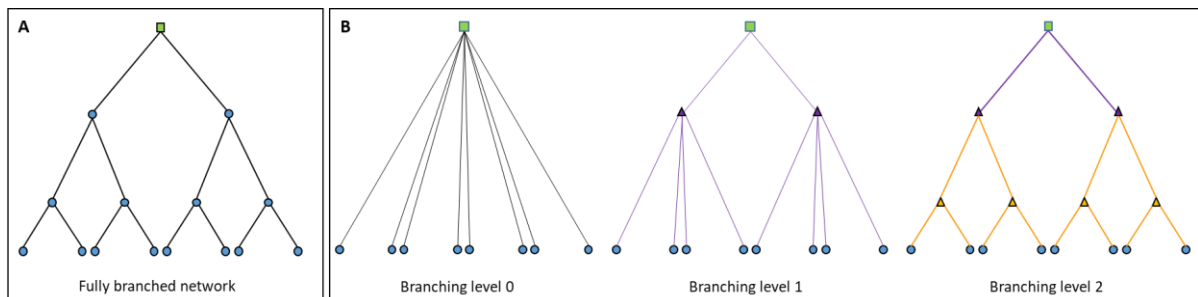


Figure 2.4. (a) A 'fully branched' network, with consumers at each junction, and (b) 'evolved branching' networks illustrating the addition of branch points and links over the course of the simulations. In each network, the green square is the resource, and the blue circles are consumers. In the 'evolved branching' networks, the branch points, represented by triangles, and links of the same colour denote when they were added during the evolution of branching: black links are the original network with no branch points, purple links and branch points are the first level of branching, and gold links and branch points are the second level, which also includes some branch points from previous levels. The network shown here is simplified for illustration purposes: the simulated 'evolved branching' networks contained seven levels of branch points at the final stage of development, and 512 consumers.

In the 'fully branched' network, both the total quantity of power consumption, and inequality of consumer potential and power, were considerably higher than in the other architectures illustrated in Figure 2.1 (see S2). In contrast, the 'evolved branching' simulations showed lower total power consumption and no inequality present in the final stage of network evolution, as the consumers were all placed equal path distances from the resource, despite being at slightly differing Euclidean distances. This demonstrates that the self-similar branching architecture itself does not lead to inequality, but rather the hierarchical or otherwise heterogeneous distribution of consumers.

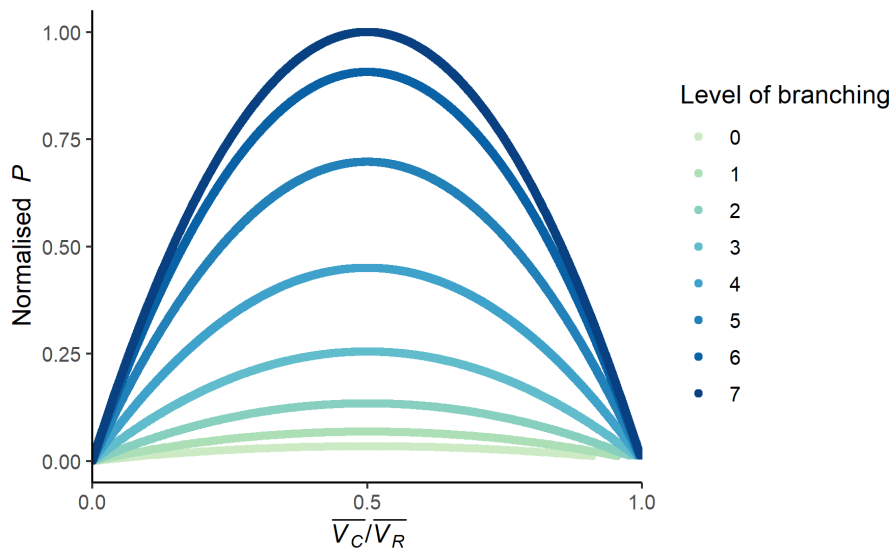


Figure 2.5. The total final power consumption (P) against the ratio of mean consumer potential to mean resource potential ($\overline{V}_C/\overline{V}_R$) for each level of the ‘evolved branching’ networks. With additional levels of branching, the network became more similar to a fractal branching structure: average link length shortened, and resource flow was concentrated onto fewer, more shared links. Here, each coloured point series represents the trajectory of final power consumption as the network became more branched: Level 0 had no branch points, and Level 7 was a fully self-similar fractal. Relative total final power is the sum of final power consumption at all consumer nodes, normalised by the maximum power achieved by the network, which preserves relative differences. A copy of the figure with raw data is included in S4.

In the fully branched network, the underlying hierarchical spatial distribution of consumer nodes and links led to a highly skewed distribution of consumer potentials and final power at network maximum final power, which appears to show power-law properties (Figure 2.6). While the focus of the work here is on spatial networks, hierarchies can also emerge in relational ‘scale-free’ networks. These are often represented as hub-and-spoke topologies, with power law distributions of node degrees. Power law or similarly heavy-tailed distributions in physical systems are typically described as resulting from interactions between interdependent components (Parunak, Brueckner and Savit, 2004), but the simulations here demonstrate how this distribution can also occur as a result of the spatial organisation of interacting components. It is therefore possible that similar processes give rise to scale-free characteristics both spatially, as in self-similar hierarchical branching, and relationally, as in a power-law distribution of node degrees.

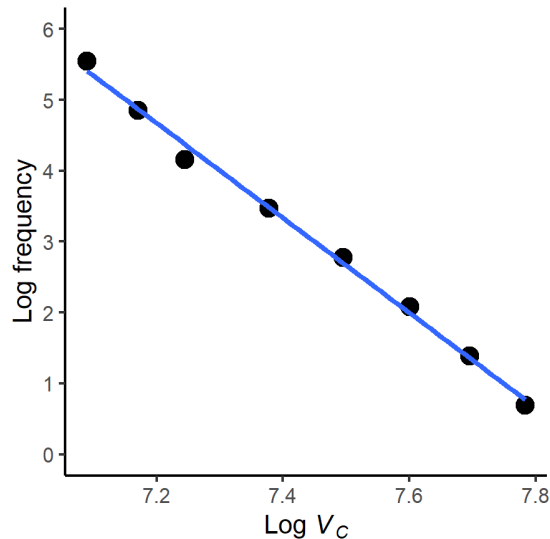


Figure 2.6. The frequency distribution of consumer potentials (V_C) at maximum network final power for a hierarchically branched network, plotted on log-log axes. The highly heterogeneous consumer potentials are due to the hierarchical network structure shown in Figure 2.4a.

Notably, although self-similar hierarchical branching networks such as the ‘fully branched’ network can achieve a higher maximum power at the network level, most individual consumers would have higher power if they had direct links to the resource, such as in the radial burst networks. Therefore, branching is still only energetically advantageous to the overall system, and those positioned close to the resource within the network architecture. This corresponds to maximum power and entropy production being emergent, system-level properties, resulting from system components each attempting to maximise their own consumption (Vallino, 2010). In addition, these optimally located and connected consumers experience increased final power even after the total network final power begins to decrease (Figure 2.7), due to the larger frictional losses experienced by the more distant consumers along the bottom level of the network, who have higher effective resistance (Figure 2.4a). This suggests that hierarchical organisation is only beneficial to the system if the consumers located further from the resource benefit from the overall system operating at a higher maximum power: the more peripheral elements need to gain some of the system-level returns. One example of hierarchical branching as a system-optimal configuration in this way is in the circulatory system of some organisms, where more distant organs and limbs may benefit from the hierarchical organisation of the whole system, even if their individual blood

pressure and oxygen levels are lower. Alternatively, if the consumers in more energetically privileged locations exerted enough dominance over the system, the hierarchy could be enforced despite being sub-optimal for more distant consumers, and potentially the network as a whole (Figure 2.7).

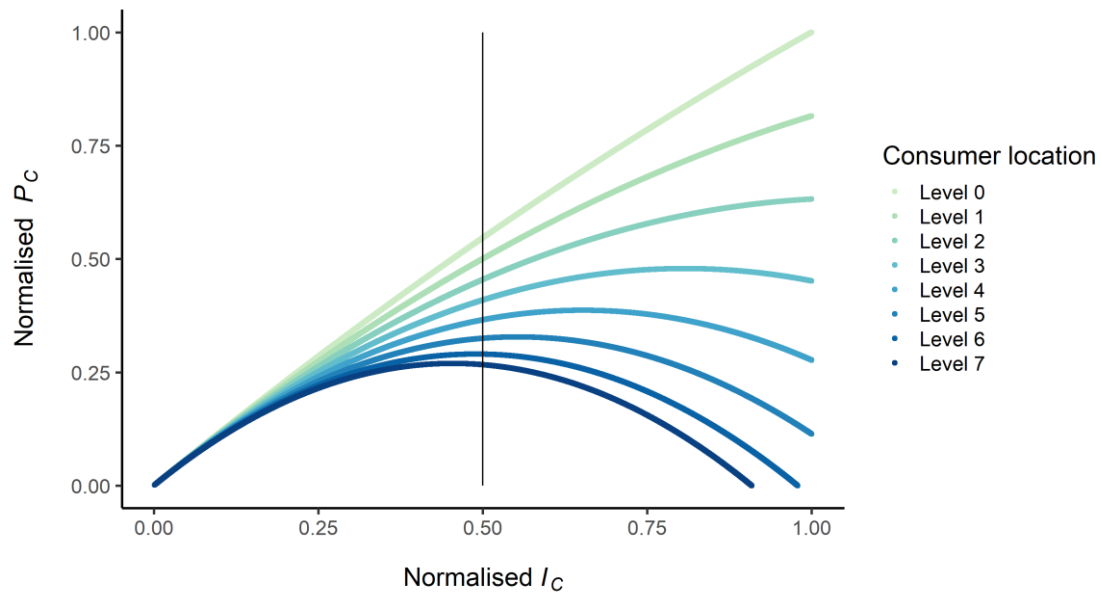


Figure 2.7. The relative final power of consumers (P_C) at each level of the ‘fully branched’ network, as related to the relative resource flow to each consumer (I_C). The vertical black line denotes the relative resource flow associated with network-wide maximum final power. Each series represents the relative final power consumption of consumers at that level in the network, where Level 0 is the consumers closest to the resource, and Level 7 are the consumers furthest from the resource in the network. As the resource flow increases across the network, the more distant consumers experience disproportionately greater frictional losses and therefore power losses, while consumers closer to the resource continue to increase in power. Values have been normalised by the maximum consumer final power and maximum consumer resource flow, which preserves relative differences. A copy of the figure with raw data is included in S5.

2.4. Conclusion

This work has explored the characteristics of complex networks evolving toward maximum power production, and the relationship between the development and dynamics of these networks and the inequality of resource distribution through them. The derived equations and illustrative simulations related the potential, resource flow, power, and resistance across a network of resources and consumers, and illustrated how those relationships changed as the network evolved toward maximum power, through adaptation in network state, architecture, or both. Specifically,

it was shown that if the network structure consists of unequal link resistances, resulting from heterogeneity in path distance or connectivity in the network, the inequality of resource distribution will increase as the quantity of resource flow across the network increases. The potential for this architecturally-driven inequality is seen most prominently in hierarchical structures, such as the branching architectures common across in biological, environmental, and human-engineered systems (see *e.g.* Banavar, Maritan and Rinaldo, 1999; West, Brown and Enquist, 1999; Tero, Kobayashi and Nakagaki, 2007; Hines *et al.*, 2010).

Additionally, this hierarchical branching was shown to only increase the energy transferred through the network at maximum power at the scale of the entire network, and for the consumers located and connected closely to the resources. In contrast, more distant consumers in these architectures experienced rapid decreases in energy consumption as the resource flow through the network increased, due to higher frictional losses of energy in transport. While prescription is not a focus of the current work, it has illustrated how RADE networks, and specifically hierarchical branching architectures, can be fundamentally linked to the deep inequality experienced by those served by these networks. Explicitly structuring these networks in an attempt to equalise distribution could take the form of co-locating resources and end-users to the greatest extent possible, such as locating solar panels or other forms of renewable energy on homes and businesses (Alstone, Gershenson and Kammen, 2015), or increasing the integration of locally-sourced products into a community's food system (Martinez, 2010). Additional efforts, such as intentionally improving RADE network infrastructure to currently underserved populations of end users (Brelsford *et al.*, 2018), could also be a significant step in the right direction. The question remains, however, as to whether even the best efforts at improving equality of distribution can offset the argued thermodynamic trajectory for systems to develop increasing patterns of consumption and dissipation (Kleidon, Malhi and Cox, 2010), which appears to be most effectively facilitated by inherently unequal distribution networks.

2.5. Materials and Methods

2.5.1. Required simulation inputs

The simulation code required a Comma-Separated Values (CSV) file to specify parameterisation, including the number of nodes of each type, the size and shape of the spatial topology where they were distributed, whether links were all unit strength or potentially heterogeneous, and the file paths of the CSV files storing the locations of the nodes, or specifying random consumer placement. A complete list of the parameters required, and a description of each, is listed in Table 2.1.

Table 2.1 Modified load flow methodology input parameters and description.

Parameter name	Description
topology	The name of the shape in or on which the nodes are distributed. Values: SPHERE (nodes located within a sphere of a given radius), SPHERE_SURFACE (nodes located on the surface of a sphere a given radius), PLANE (nodes located on the surface of a plane).
pNoConnection	The probability of two nodes not connecting, in a network with random links.
noConnection	The placeholder value in the connections matrix for non-connected nodes.
resourcesFile	The file path of the CSV file storing the coordinate locations and potentials of the resources.
planeMaxCoords	The maximum coordinates of the plane, stored as a pair of values separated with a semi-colon (e.g. 100;100).
sphereR	The radius of the sphere, or sphere surface.
nBranchPoints	The number of branch points.
nConsumers	The number of consumers.
useStrength	Whether or not to use link strength in calculating the resistance between nodes. Values: TRUE/FALSE.
strengthExponent	The exponent to which the link strength, if used, should be raised.
manualNetwork	Whether to read in a pre-specified connections matrix or generate the links randomly. Values: TRUE/FALSE.
randomConsumers	Whether to distribute the consumers randomly in the topology or use specified locations. Values: TRUE/FALSE.
consumersFile	The file path of the CSV file storing the coordinate locations of the consumers (if not random).
matrixFile	The file path of the CSV file storing the connections matrix, if a pre-specified one is used.
branchPointsFile	The file path of the CSV file storing the coordinate locations of the branch points (if used).
outputCSV	The file path to the CSV file where the output of the code run is stored. Includes the resource flow specification per consumer, the power and potential at each resource and consumer, and the total link length of the network.

The topologies simulated here included planes, spheres, and sphere surfaces. Planes and spheres can be classed as two- and three-dimensional spaces, respectively, while sphere surfaces are of a more ambiguous dimension (Jarvis, Jarvis and Hewitt, 2015). The exploration of these three relevant topologies, commonly used to represent idealised spaces in physical systems, allowed identification of any effect on power consumption or resource distribution due to dimensionality. In these networks, the size of the topology, measured in generalised units as the radius of the sphere or sphere surface, or one side of the square plane, was determined by the number of nodes of each type,

$$Size = \sqrt{10nC * 100nR} , \quad (6)$$

where nC is the number of consumers, and nR is the number of resources. This was chosen as it allowed for meaningfully large distances between nodes in networks with multiple consumer and resource nodes. The branched networks had set lengths for each link, such that topology size was not a factor.

The relationship between spatial size and power distribution and consumption was not directly explored, such as by spreading the same network architecture across a larger area, but the linearity of the equation for resistance with unit-strength links suggests that inequality in consumer potential would increase linearly, and power consumption would decrease linearly, with increases in topological size. Similarly, the resource potentials were chosen to provide a clear visualisation of the maximum power ‘curve’ (Figure 2.2a), but a range was not explored, as increasing or decreasing the resource potential(s) would simply linearly increase or decrease the consumer potentials (see Eq. 1).

In all simulations with random and radial burst topologies, link strength was set to 1. In the branching simulations, it was set to be proportional to the resource flow, squared, to offset the increased frictional losses from higher resource flow along shared links. Specifically, by re-

arranging Eq. 1, the potential gradient along a link can be calculated as a product of resource flow I and link resistance R . Recall that power loss along a link P_L is a product of this potential gradient and resource flow along it (Eq. 3), which when combined with Eq. 1 gives

$$P_L = \frac{I^2 L}{S} . \quad (7)$$

Since losses are proportional to the resource flow squared, it rapidly dominates the energy losses. Therefore, as branching networks combine resource flows onto shared branches, they experience higher flow-driven losses on those shared links, despite having lower total network resistance, due to the shared links shortening the total path length around the network. It follows that, for the branching to be energetically advantageous, the link strength must be a function of resource flow, $S = f\{I\}$. If $P_L \propto I^2$, then $S \propto I^2$, resulting in the power loss becoming a function exclusively of link length (Eq. 7). This allows the advantages of shorter total link length in a branching network to be realised.

2.5.2. Simulation code operation

An overview of the simulation code is shown in Figure 2.8. After the program read in the specified parameters above, it created a customised data structure to store the node locations, resource potentials, and connections matrix. If the consumer locations were random, the program placed each consumer in space by drawing each coordinate from a uniform distribution bounded by the maximum topology coordinates supplied. If the links were random, the program put a link between each node, except for resources, with the probability of $1 - \text{pNoConnection}$ parameter described above (Table 2.1).

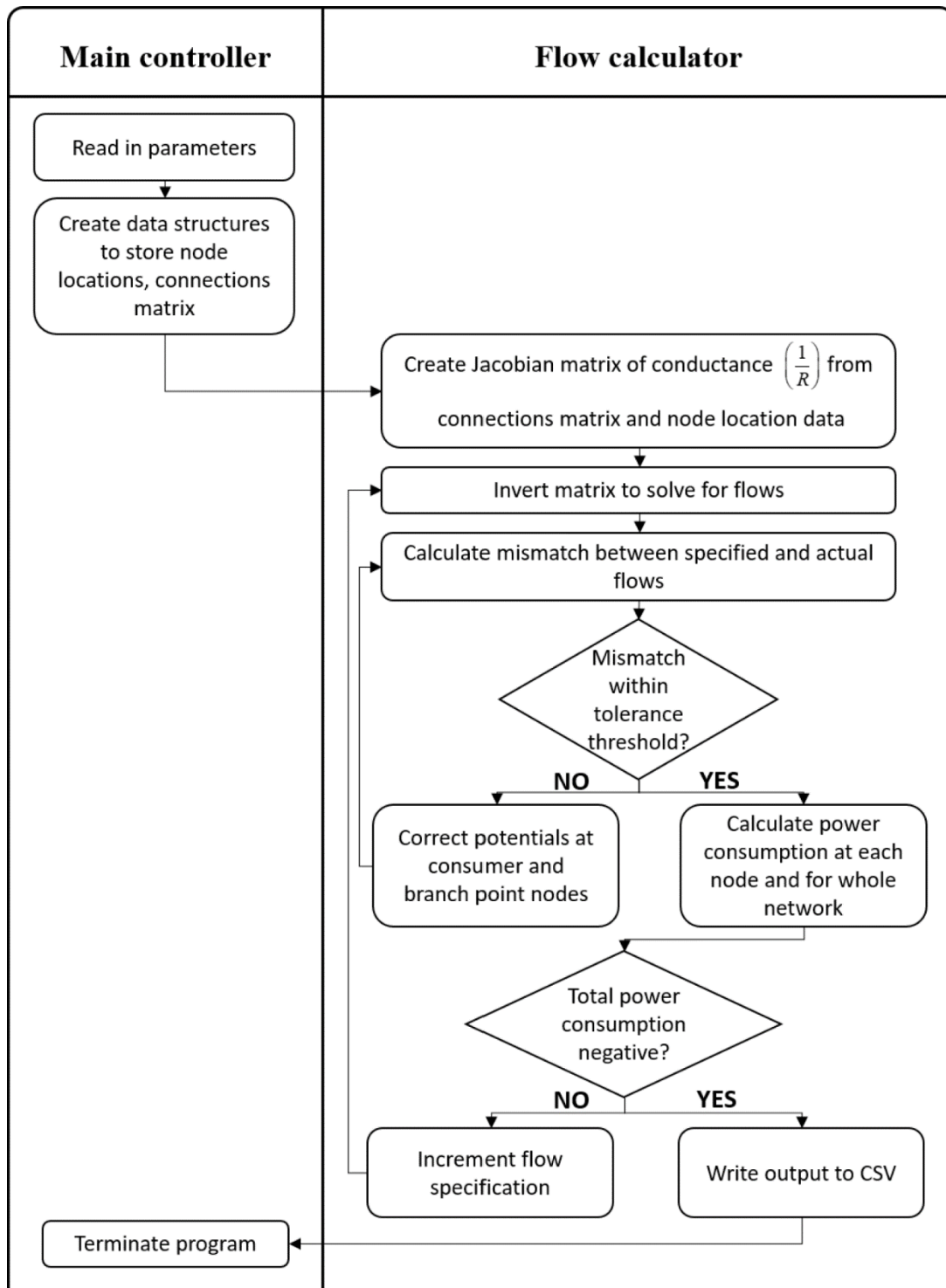


Figure 2.8. Code flow diagram for flow calculator program. The main controller of the program reads in the parameters and creates the network, and eventually terminates the program when complete, while the main calculations of the program are based on an iterative matrix inversion process in the flow calculator class.

To calculate the resource flows and power consumption of the network, the program constructed a Jacobian matrix representing the conductance of the network, or the inverse of the resistance, using the connections matrix. This was inverted to solve for the mismatch between specified and received resource flow at each consumer node, based on the consumer potentials. These were determined by the load flow equations using a matrix form of Eq. 1.

The potentials at the consumers, and branch points if used, were then adjusted to counter the mismatch. The matrix inversion and mismatch calculations were repeated until the mismatches were within the specified error threshold of 0.001. After convergence, the total power consumption of the network $P_{Network}$ was calculated as the sum of the power consumption at each consumer P_{C_i} , which was the product of potential V_{C_i} and resource flow I_{C_i} (Eq. 2):

$$P_{Network} = \sum_{i=1}^{nConsumers} P_C . \quad (8)$$

Initially, the total power consumption was calculated for 1 unit of resource flow arriving at each consumer. With each iteration, the specification was incremented by 0.1 unit, and the resource flows were re-calculated. This was repeated until either 1000 units of resource flow was arriving at each consumer, or the power consumption of the network was negative, due to the inverse relationship between consumer potential and resource flow (Eq. 1). In the evolving branching simulations, an additional level of branch points was added, and the links between nodes re-arranged, after the iterations had completed for a given network, until there were 7 levels of branch points between the resource and consumers (Figure 2.4b).

For a simple network with direct connections between the resource and consumer nodes, such as the radial burst networks (Figure 2.1), the power consumption can be solved analytically with Ohm's law, rather than using the Jacobian matrix inversion method. An example of this, used to validate the model, is shown in Davis (2018).

2.5.3. Simulation outputs

The program output was a single CSV file, with the potential at each resource and consumer, and the power production and consumption of each resource and consumer, respectively, at each resource flow specification tested. It also included the total link length of the network, which does not change over the duration of the simulations.

2.5.4. Code availability statement and languages used

A complete copy of the code, along with usage instructions, a sample parameter file, and sample resource, consumer, branch point, and matrix CSVs, is available upon request. The code is written in Java Version 8. All figures and analyses were generated using R, including the base R package version 3.6.1 (R Core Team, 2018), ggplot2 (Wickham, 2009), and the rgl package (Adler and Murdoch, 2019).

2.6. References

- Adler, D. and Murdoch, D. (2019) ‘rgl: 3D Visualization using OpenGL’. <http://cran.r-project.org/web/packages/rgl/index.html>.
- Alstone, P., Gershenson, D. and Kammen, D. M. (2015) ‘Decentralized energy systems for clean electricity access’, *Nature Climate Change*, 5(4), pp. 305–314. doi: 10.1038/nclimate2512.
- Banavar, J. R., Maritan, A. and Rinaldo, A. (1999) ‘Size and form in efficient transportation networks’, *Nature*, 399(6732), pp. 130–132. doi: 10.1038/20144.
- Bejan, A. (1996) ‘Maximum power from fluid flow’, *International Journal of Heat Mass Transfer*, 39(6), pp. 1175–1181. doi: 10.1016/0017-9310(95)00209-X.
- Bejan, A. and Errera, M. R. R. (2017) ‘Wealth inequality: The physics basis’, *Journal of Applied Physics*, 121(12), p. 124903. doi: 10.1063/1.4977962.
- Boltzmann, L. V. (1905) *Populäre Schriften*. Leipzig: J.A. Barth.
- Boswell, G. P. *et al.* (2002) ‘Functional consequences of nutrient translocation in mycelial fungi.’, *Journal of Theoretical Biology*, 217(4), pp. 459–77. doi: 10.1006/jtbi.3048.
- Brelsford, C. *et al.* (2018) ‘Toward cities without slums: Topology and the spatial evolution of neighborhoods’, *Science Advances*, 4(8), pp. 1–9. doi: 10.1126/sciadv.aar4644.
- Charlton, B. G. (1997) ‘The Inequity of Inequality’, *Journal of Health Psychology*, 2(3), pp. 413–425. doi: 10.1177/135910539700200309.
- Collier, C. G. (2010) ‘Modelling a river catchment using an electrical circuit analogue’, *Hydrology and Earth System Sciences*, 2(1), pp. 9–18. doi: 10.5194/hess-2-9-1998.
- Davis, N. (2018) ‘Spatial energetics: A thermodynamically-consistent methodology for modelling resource acquisition, distribution, and end-use networks in nature and society’, Masters thesis, Lancaster University, Lancaster, UK.
- Georgescu-Roegen, N. (1986) ‘The Entropy Law and the Economic Process in Retrospect’, *Eastern Economic Journal*, 12(1), pp. 3–25.
- Hines, P. *et al.* (2010) ‘The topological and electrical structure of power grids’, *Proceedings of the Annual Hawaii International Conference on System Sciences*. doi: 10.1109/HICSS.2010.398.

Humphries, M. M., Thomas, D. W. and Kramer, D. L. (2003) 'The Role of Energy Availability in Mammalian Hibernation: A Cost-Benefit Approach', *Physiological and Biochemical Zoology*, 76(2), pp. 165–179. doi: 10.1086/367950.

Jarvis, A. J., Jarvis, S. J. and Hewitt, C. N. (2015) 'Resource acquisition, distribution and end-use efficiencies and the growth of industrial society', *Earth System Dynamics*, 6(2), pp. 689–702. doi: 10.5194/esd-6-689-2015.

Kirkham, M. B. (2014) *Principles of Soil and Plant Water Relations*. 2nd edn. Cambridge, Massachusetts: Elsevier. doi: 10.1016/C2013-0-12871-1.

Kleidon, A. *et al.* (2013) 'Thermodynamics, maximum power, and the dynamics of preferential river flow structures at the continental scale', *Hydrology and Earth System Sciences*, 17(1), pp. 225–251. doi: 10.5194/hess-17-225-2013.

Kleidon, A. (2016) *Thermodynamic Foundations of the Earth System*. First. Cambridge, UK: Cambridge University Press.

Kleidon, A., Malhi, Y. and Cox, P. M. (2010) 'Maximum entropy production in environmental and ecological systems', *Philosophical Transactions of the Royal Society B: Biological Sciences*, 365(1545), pp. 1297–1302. doi: 10.1098/rstb.2010.0018.

Levins, R. (1966) 'The strategy of model building in population biology', *American Scientist*, 54(4), pp. 421–431. doi: 10.1086/521118.

Lotka, A. J. (1922) 'Contribution to the Energetics of Evolution', *Proceedings of the National Academy of Sciences*, 8(6), pp. 147–151. doi: 10.1073/pnas.8.6.147.

Mansson, B. A. and McGlade, J. M. (1993) 'Ecology, thermodynamics and H.T. Odum's conjectures', *Oecologia*, 93(4), pp. 582–596. doi: 10.1007/BF00328969.

Martinez, S. (2010) *Local Food Systems: Concepts, Impacts, and Issues*. Darby, Pennsylvania: DIANE Publishing.

Martyushev, L. M. and Seleznev, V. D. (2014) 'The restrictions of the maximum entropy production principle', *Physica A: Statistical Mechanics and its Applications*, 410, pp. 17–21. doi: 10.1007/978-3-642-40154-1.

- Mattison, S. M. *et al.* (2016) 'The evolution of inequality', *Evolutionary Anthropology: Issues, News, and Reviews*, 25(4), pp. 184–199. doi: 10.1002/evan.21491.
- von Meier, A. (2006) 'Power Flow Analysis', in *Electric Power Systems: A Conceptual Introduction*, pp. 195–228.
- Niño-Zarazúa, M., Roope, L. and Tarp, F. (2017) 'Global Inequality: Relatively Lower, Absolutely Higher', *Review of Income and Wealth*, 63(4), pp. 661–684. doi: 10.1111/roiw.12240.
- Odum, H. T. (1967) 'Biological circuits and the marine systems of Texas', in Olson, T. A. and Burgess, F. J. (eds) *Pollution and Marine Ecology*. New York: Wiley Interscience, pp. 99–157.
- Odum, H. T. (1971) *Environment, Power and Society*. New York: Wiley.
- Odum, H. T. (1983) 'Maximum power and efficiency: A rebuttal', *Ecological Modelling*, 20(1), pp. 71–82. doi: 10.1002/etc.2226.
- Odum, H. T. (2002) 'Explanations of ecological relationships with energy systems concepts', *Ecological Modelling*, 158(3), pp. 201–211. doi: 10.1016/S0304-3800(02)00232-6.
- Odum, H. T. and Pinkerton, R. C. (1955) 'Time's speed regulator: The optimum efficiency for maximum power output in physical and biological systems', *American Scientist*, 43(2), pp. 331–343.
- Parunak, H. V. D., Brueckner, S. and Savit, R. (2004) 'Universality in multi-agent systems', in *Proceedings of the Third International Joint Conference on Autonomous Agents and Multi-Agent Systems*. New York. doi: 10.1109/AAMAS.2004.290.
- Paul, C. R. (2001) *Fundamentals of Circuit Analysis*. Hoboken, New Jersey: John Wiley and Sons.
- Polettini, M. (2013) 'Fact-checking Ziegler's maximum entropy production principle beyond the linear regime and towards Steady States', *Entropy*, 15(7), pp. 2570–2584. doi: 10.3390/e15072570.
- R Core Team (2018) 'R: A Language and Environment for Statistical Computing'. Vienna, Austria.
- Ross, J., Corlan, A. D. and Müller, S. C. (2012) 'Proposed Principles of Maximum Local Entropy Production', *The Journal of Physical Chemistry B*, 116(27), pp. 7858–7865. doi: 10.1021/jp302088y.
- Santillán, M. and Angulo-Brown, F. (1997) 'A thermodynamic approach to the compromise between power and efficiency in muscle contraction', *Journal of Theoretical Biology*, 189(4), pp. 391–398. doi: 10.1006/jtbi.1997.0526.

- Sutcliffe, B. (2005) *A Converging or Diverging World?*, *DESA Working Paper*.
- Tero, A., Kobayashi, R. and Nakagaki, T. (2007) 'A mathematical model for adaptive transport network in path finding by true slime mold', *Journal of Theoretical Biology*, 244(4), pp. 553–564. doi: 10.1016/j.jtbi.2006.07.015.
- Ulanowicz, R. E. (2011) 'Some steps toward a central theory of ecosystem dynamics', *Computational Biology and Chemistry*, 27, pp. 523–530. doi: 10.1007/978-0-8176-4904-3.
- Vallino, J. J. (2010) 'Ecosystem biogeochemistry considered as a distributed metabolic network ordered by maximum entropy production', *Philosophical Transactions of the Royal Society B: Biological Sciences*, 365, pp. 1417–1427. doi: 10.1098/rstb.2009.0272.
- Wang, L. *et al.* (2012) 'Characterizing ecohydrological and biogeochemical connectivity across multiple scales: a new conceptual framework', *Ecohydrology*, 5, pp. 221–233. doi: 10.1002/eco.
- West, G. B., Brown, J. H. and Enquist, B. J. (1997) 'A General Model for the Origin of Allometric Scaling Laws in Biology', *Science*, 276, pp. 122–126. doi: 10.1126/science.276.5309.122.
- West, G. B., Brown, J. H. and Enquist, B. J. (1999) 'The Fourth Dimension of Life: Fractal Geometry and Allometric Scaling of Organisms', *Science*, 284(5420), pp. 1677–1679. doi: 10.1126/science.284.5420.1677.
- Wickham, H. (2009) *ggplot2: Elegant Graphics for Data Analysis*. New York: Springer-Verlag.
- Zehe, E. *et al.* (2012) 'Connected flow paths as first order control on critical zone water flows: coincidence or self-organized optimality?', *Hydrology and Earth System Sciences Discussions*, 9(9), pp. 10595–10655. doi: 10.5194/hessd-9-10595-2012.

2.7. Supplementary Information

S1 Text. Maximum power derivation

Recall from Eq. 2, assuming that the network is flow-preserving, such that the sum of all resource flows into the system is equal to the sum of the resource flows across all consumers, the equation for power consumption at the consumer nodes P_C is:

$$P_C = I_C V_C = \left(\frac{V_R - V_C}{R} \right) V_C = \left(\frac{V_R V_C - V_C^2}{R} \right). \quad (9)$$

To find the maximum power, the first derivative of power with respect to potential is taken and set to zero, and the equation is solved to find the critical points:

$$\frac{\partial P_C}{\partial V_C} = (-RV_R) + 2RV_C = 0, \quad (10a)$$

$$V_C = \frac{V_R}{2}, \quad (10b)$$

While this is most simply illustrated in the case of power transfer between two nodes on a single link, complex networks such as the ones in view here can be simplified using an algorithm such as Thévenin's theorem. Although an explicit Thévenin equivalent was not computed for the networks here, their dynamics could be mapped to one, such that at maximum power,

$$\bar{V}_C = \frac{\bar{V}_R}{2}, \quad (11)$$

This also implies that R in these equations is a mean term for the characteristics of all links across the network, or \bar{R} , which is discussed further in the text as R_E .

S2 Table. Parameterisation and power consumption details of networks simulated: a) branched networks, and b) random and radial burst networks. The slope of the linear relationship between σ_{P_C} and I^2 shown in Fig. 1 was calculated for each plot using least-squares regression, and compared to the value of σ_{R_E} calculated using Eq. 5 and the consumer and resource potentials for each network, shown in the table here. The least-squares regression estimate of σ_{R_E} is shown in brackets below the original estimate using consumer and resource potentials, for the networks plotted.

A.

Topology	Link strength	No. of consumers	Branch points	Avg. consumer potential at maximum power	Avg. resource potential at maximum power	Maximum power	σ_{R_E}
Plane	Proportional	510	0	1267.963	2560	3362638.240	10.117
Plane	Proportional	256	0	1280.465	2560	1802894.140	10.380
Plane	Proportional	256	2	1291.671	2560	1719472.636	5.208
Plane	Proportional	256	6	1287.332	2560	1680741.209	2.621
Plane	Proportional	256	14	1272.968	2560	1661986.846	1.327
Plane	Proportional	256	30	1291.163	2560	1652688.496	0.678
Plane	Proportional	256	62	1287.644	2560	1648183.681	0.350
Plane	Proportional	256	126	1285.886	2560	1645933.596	0.177
Plane	Proportional	256	254	1285.000	2560	1644800.000	0.000
Plane	Proportional squared	510	0	1280.114	2560	262514277.899	0.506
Plane	Proportional squared	256	0	1280.465	2560	1802894.140	10.380
Plane	Proportional squared	256	2	1285.688	2560	3587582.693	5.208
Plane	Proportional squared	256	6	1279.833	2560	7044199.485	2.621
Plane	Proportional squared	256	14	1280.543	2560	13375014.776	1.327
Plane	Proportional squared	256	30	1280.746	2560	23606702.551	0.678
Plane	Proportional squared	256	62	1279.803	2560	36563458.045	0.350
Plane	Proportional squared	256	126	1279.801	2560	47538966.426	0.177
Plane	Proportional squared	256	254	1280.000	2560	52428799.937	0.000

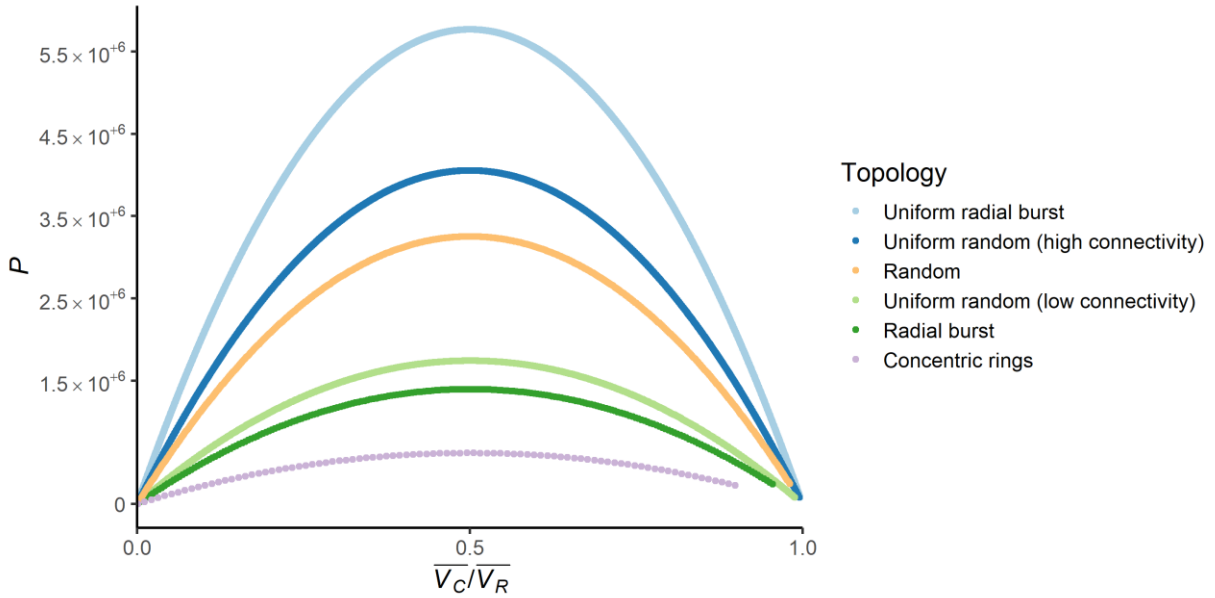
Chapter 2: Trajectories toward maximum power and inequality

B.

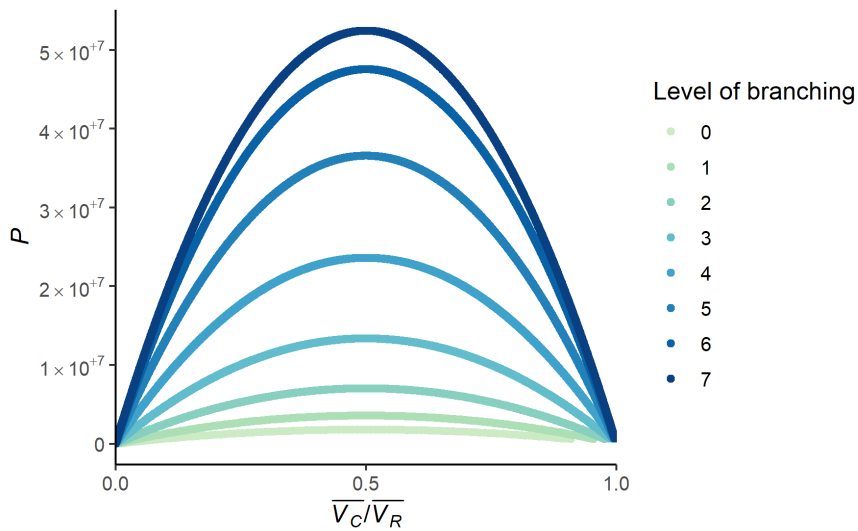
Topology	Total network length	Node distribution	Resource potentials	No. of consumers	No. of resources	Mean consumer potential at maximum power	Mean resource potential at maximum power	Maximum power	σ_{R_E}
Plane	74877.080	Random	Equal	50	1	2501.289	5000.000	3251676.144	12.758 (12.760)
Plane	415061.500	Random	Equal	100	1	4989.508	10000.000	11376078.579	3.249
Plane	1510034.000	Random	Equal	50	50	51.000	100.000	5864.995	4.974
Plane	3531541.000	Random	Equal	50	100	24.880	50.000	2114.770	2.898
Plane	1487595.000	Random	Varied	50	50	49.408	99.207	5681.931	4.602
Plane	3422254.000	Random	Varied	50	100	25.622	50.917	2177.879	2.941
Plane	11200.000	Ring of consumers	Equal	50	1	2491.200	5000.000	1395072.000	0.000 (0.000)
Plane	31600.000	Ring of consumers	Equal	100	1	5007.200	10000.000	7911376.000	0.000
Plane	25228.310	Ring of consumers	Equal	50	10	2477.169	5000.000	619292.343	3.845 (3.845)
Plane	25228.310	Ring of consumers	Varied	50	10	2508.767	5031.598	627191.844	70.955
Plane	25228.310	Ring of resources	Equal	10	50	99.093	200.000	990.925	0.000
Plane	25228.310	Ring of resources	Varied	10	50	98.335	199.261	983.353	5.802
Plane	4099.363	Uniform random (low connectivity)	Equal	81	1	500.452	1000.000	1741572.000	0.387 (0.387)
Plane	7680.167	Uniform random (med. connectivity)	Equal	81	1	499.762	1000.000	4054065.000	0.102 (0.102)
Plane	277.362	Uniform radial	Equal	81	1	500.056	1000.000	5768642.000	1.224 (1.224)
Sphere	119384.300	Random	Equal	50	1	2517.610	5000.000	742694.886	6.084
Sphere	970045.300	Random	Equal	100	1	50006.146	100000.000	454555862.837	5.187
Sphere	2345486.000	Random	Equal	50	50	500.440	1000.000	357814.260	5.913
Sphere	5728683.000	Random	Equal	50	100	250.839	500.000	112877.518	4.952
Sphere	2321974.000	Random	Varied	50	50	501.006	1003.963	355714.309	7.556
Sphere	5766936.000	Random	Varied	50	100	249.526	501.682	121019.957	5.854
Sphere surface	214750.300	Random	Equal	50	1	24989.678	50000.000	40608226.348	16.033
Sphere surface	1216917.000	Random	Equal	100	1	49978.937	100000.000	525278626.787	13.582
Sphere surface	4600103.000	Random	Equal	50	50	497.706	998.014	194105.429	9.849

Structure, flow, and inequality

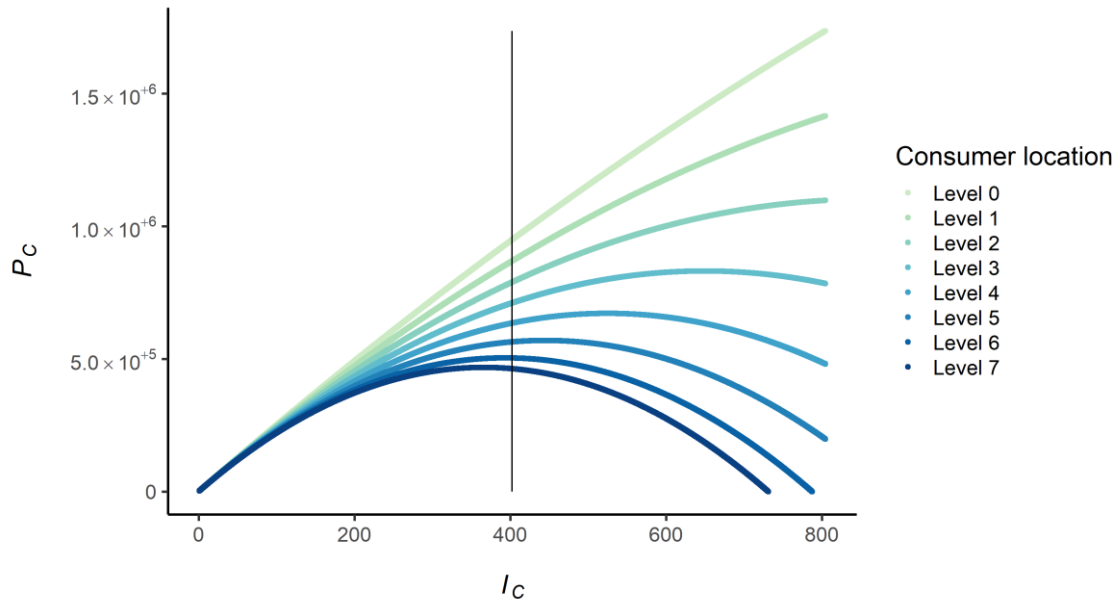
Sphere surface	10934860.000	Random	Equal	50	100	250.887	500.000	63976.129	5.982
Sphere surface	4607672.000	Random	Varied	50	50	498.283	1000.000	176890.508	13.087
Sphere surface	11111457.000	Random	Varied	50	100	253.070	501.161	62002.112	6.912
Sphere surface	8796.595	Ring of consumers	Equal	50	1	25000.077	50000.000	177625544.692	0.000
Sphere surface	24818.580	Ring of consumers	Equal	100	1	49990.557	100000.000	1007309730.737	0.000
Sphere surface	22606.750	Ring of consumers	Equal	50	10	2513.257	5000.000	691145.733	12.537
Sphere surface	22606.750	Ring of consumers	Varied	50	10	2493.034	5024.990	698049.528	58.146
Sphere surface	22606.750	Ring of resources	Equal	10	50	997.010	2000.000	110668.165	0.000
Sphere surface	22606.750	Ring of resources	Varied	10	50	996.453	1999.405	110606.287	16.571



S3 Figure. Non-normalised version of Figure 2.2a, showing the relationship between total final power (P) and the ratio of mean consumer potential to mean resource potential ($\overline{V_C}/\overline{V_R}$) for six example networks. Each coloured point range represents a different network topology over which the simulations were run. The units are generalised units of power, rather than units only applicable to a specific type or types of resource distribution network.



S4 Figure. Non-normalised version of Figure 2.5, showing total final power consumption (P) against the ratio of mean consumer potential to mean resource potential ($\overline{V_C}/\overline{V_R}$), for the ‘evolved branching’ networks. The units are generalised units of power, rather than units only applicable to a specific type or types of resource distribution network.



S5 Figure. Non-normalised version of Figure 2.7, showing final power of consumers (P_C) at each level of the ‘fully branched’ network, as related to the resource flow to each consumer (I_C). The units are generalised units of power and resource flow, rather than units only applicable to a specific type or types of resource distribution network.

3

Measuring heterogeneity in soil networks: A network analysis and simulation-based approach

Abstract

Quantifying soil structural and ecological heterogeneity is crucial for understanding their interactions and their relationships to the resilience and health of the wider ecosystem. However, a clear understanding of how structural heterogeneity affects soil biodiversity is still emerging. Previous work has primarily used expensive, often laboratory-based methods to quantify soil pore network structure, and typically separated study of structural and biological dimensions. Here, we test whether standard network metrics can be used to quantify structural heterogeneity in soil pore networks, and how this network structure, along with characteristics of the consumer and resource populations, affects the heterogeneity of a population of consumers. Specifically, we extract simplified soil pore networks from digital photographs of soil profiles and apply established metrics from network science and transport geography to quantify and compare the networks. The networks are also used as the medium for an agent-based model of generalised consumers, to analyse the effects of consumer and resource parameterisations and network structure. Combining network analysis and simulation modelling in this way can provide insights on the structure, function, and diversity possible in the soil, as well as avenues for exploring the impact of future structural or environmental changes.

3.1. Introduction

The distribution of energetic resources in an ecosystem plays a key role in determining the complexity, quantity, and behaviour of organisms that it can support (e.g. Giller, 1996; Tews *et al.*,

2004; Roshier, Doerr and Doerr, 2008; Stevens & Tello, 2011). To understand these systems more fully, and inform actions to protect those relying on them, we must understand how resource distribution networks develop and function. For example, resource location and movement can create heterogeneity that allows species to specialise and differentiate (e.g. Bardgett, Yeates and Anderson, 2009; Tews *et al.*, 2004; Stevens & Tello, 2011), as well as cause inequality among individuals of the same species, topics that are relevant for both biologists and ecologists.

The soil provides a unique and diverse ecosystem in which to study resource distribution, and its effect on organisms. Soil structure can be defined as the collection of soil particles and pore space among them (Oades, 1993). This pore space provides access to nutrients stored on the surface of soil particles, allows for preferential flow of water through the soil matrix, and serves as the resource distribution network through which micro-, meso-, and macrofauna (soil biota) forage. As this structure determines how air, water, and soil biota move through the soil, it allows or impedes the foraging of organisms, regulates the air and water balance in the soil matrix, and affects chemical signals used in foraging, such as those of bacterial decomposition (Young and Ritz, 2009). Furthermore, crevices and niches along soil pores provide habitats for smaller microbes to avoid predation, and the overall spatial and temporal heterogeneity of the soil environment allows for resource partitioning and habitat specialisation that limits the effect of competitive exclusion (Bardgett, Yeates and Anderson, 2009). This is similar to the hypothesised effect of heterogeneity in aboveground habitats (e.g. Tews *et al.*, 2004; Stevens and Tello, 2011).

Soil biota in turn can increase the porosity of soil, through burrowing and consuming organic matter, and releasing gases during decomposition, which create or expand soil pores (Kravchenko and Guber, 2017). Additionally, there is evidence of feedbacks between the soil biota and aboveground plant communities (e.g. Baer *et al.*, 2005; Wijesinghe, John and Hutchings, 2005; García-Palacios *et al.*, 2012), which alter soil structure as their roots burrow in pore networks, and roots and hyphae bind and stabilise soil particles (Vezzani *et al.*, 2018). Through regulating

movement and diffusion of water and energy resources, gases, and fauna in the soil matrix; providing habitat; and mediating biological feedbacks; soil structure is the foundation of all earth systems.

Past efforts to quantify and model soil structure have primarily focussed on measuring the stability of soil, by utilising soil aggregate size distribution as a measure of structure. While this does represent the spatial distribution in the soil, it is not a complete representation of physical properties (see e.g. Young, Crawford and Rappoldt, 2001). Several frequently used methods for visualising the pore network within a soil sample include CT scans and X-ray tomography, NMR, and SPECT scanning, mostly for the purposes of measuring solute flow and transport processes (see review in Young, Crawford and Rappoldt, 2001). Gas diffusion and solute flow have also been examined with modelling approaches, including neural networks, Boolean models, and cellular automata. Additionally, fractal modelling has also been used successfully to quantify the degree of connectivity, tortuosity, and heterogeneity of the soil pore network (Crawford, Ritz and Young, 1993), three characteristics that have also been associated with a higher level of heterogeneity of resource distribution in generalised networks (Davis *et al.*, 2020).

Overall, past work has highlighted the important connections between soil function and structure, especially of the pore network. Much of this work has been done from a geometric or hydrological perspective, however, rather than an energetic one, leading to criticisms of unrealistic separation of soil physics and biology, and emphasis on the importance of integrating these spatially explicit approaches in future soil ecology research (Bardgett, Yeates and Anderson, 2009). Additionally, much of the imaging equipment required for the techniques above is large and expensive, requiring soil samples to be brought back to the laboratory. Even if disruption to the soil structure during extraction and transport is minimised, these methods are more suitable for intensive analyses of individual samples and smaller areas.

In contrast, some previous work has focussed on quantifying the structure of soil networks through image morphology techniques applied to a photograph of a sample, in order to extract the relevant network (e.g. Velde, Moreau and Terribile, 1996; Gargiulo, Mele and Terribile, 2013; Hartemink and Minasny, 2014). This method will not reveal the network at the same level of detail as CT scans or X-ray tomography, and may require use of resins and dyes to highlight the underlying structure (Hartemink and Minasny, 2014). Good arguments have also been raised regarding the importance of analysing soil structure from a three-dimensional perspective, as it reveals considerably more about the habitat of the soil (Young and Ritz, 2009). However, if rotational invariance is assumed, connectivity and structure of a two-dimensional sample can be assumed representative of any random two-dimensional plane taken through the system. This inference does not consider lateral flow, which would undoubtedly play an important influence in sloping areas by transporting nutrients laterally through the soil. In areas where the surface is flat and lateral flow effects are negligible, standard network metrics could usefully approximate soil structure and provide insights into its effect on biotic and abiotic processes within an environment. Moreover, the two-dimensional techniques are considerably more portable and feasible than the three-dimensional techniques, and processing time can be significantly faster. Image analysis methods, particularly those that can be performed entirely in the field, could potentially be incorporated into software for use by farmers and researchers who may otherwise not have access to the equipment necessary for the more costly and lab-intensive methods of quantifying structure (e.g. Aitkenhead *et al.*, 2016). These methods could also act as preliminary investigations to highlight potential areas of future exploration using more intensive analyses.

In this paper, we test whether standard network metrics can be used to quantify structural heterogeneity in soil pore networks, and how this network structure, along with characteristics of the consumer and resource populations, affects the heterogeneity of a population of consumers. Specifically, we develop a method for extracting approximate soil networks from digital

photographs using image morphology techniques, then apply metrics from network science and transport geography to quantify and compare the networks. The networks are also used as the medium for an agent-based model (ABM, which in ecology is more typically known as an individual-based model, e.g. Grimm *et al.*, 2006), where the agents represent generalised consumers who explore the network and consume food resources. The variation in population size and resource consumption is compared across simulations, to evaluate how both the network structure and simulation parameters affect outcomes of the biotic community. This methodology is applied to a case study using soil images from two test sites in Aberdeenshire, United Kingdom.

3.2. Methods

3.2.1. Soil image collection

Images were taken at two field sites in Aberdeenshire, United Kingdom. The first site had a brown forest soil, or Cambisol (Figure A1a); photographs were taken from seven locations in both forested and converted agricultural areas. The second site had a sandy beach soil, or Arenosol (Figure A1b); photographs were taken at five locations across a dune area, with sparse grass and shrub cover. Neither Cambisols nor Arenosols are highly developed, but Cambisols have some diagnostic features, while Arenosols are lacking diagnostic features and are defined only on the basis of being coarse (sandy) textured (FAO, 2015). The known difference between the two soils therefore provides a basis for preliminarily evaluating the methodology. Additionally, both soil types can be assumed to show limited profile variation with depth on the scale of the observed soil profile sections under study (FAO, 2015), such that a uniform network extraction method and analysis can be applied across the image. The specific sampling sites were also chosen as they provided easy access to multiple sampling locations for both soil types. As this work is an exploratory proof-of-concept, an exhaustive sampling regime across different soil, land use, and geographic regions was not undertaken.

The methodology for taking pictures was replicated from Aitkenhead *et al.* (2016). In summary, the photographs were taken of the soil profile of shallow (30 cm) pits in flat areas, using an angle that provided maximum natural light and minimum shadow (Figure A1a, b). No artificial lighting was required during photography. Additionally, each photograph included a 10 cm x 6 cm colour correction card within the frame. Colour correction has been used in past work (e.g. Aitkenhead *et al.*, 2016) to correct colour variation in ambient lighting. However, in this work we were only interested in overall intensity, rather than light balance, so the cards were inserted into the image to provide a spatial scale reference for future work.

In Figure A1a and A1b, the white area is an excised section of the image that is larger than the correction card. The imaging was taken with the card viewed straight on, without distortion, so the image distortion and impact on length of edges is not an issue. Extracting an area larger than the correction card also attempted to eliminate shading effects around the card. This may not have been done sufficiently to eliminate all the shading, possibly introducing some additional dark pixels and error into the network metric calculations. However, taking multiple pictures within the same profile can provide some robustness against this. Future work should attempt to remove this effect from near the correction card.

In total, seven Cambisol profiles and five Arenosol pits were used for each soil type, with several images taken of the profile of each pit. In taking multiple images from each soil pit, we moved the camera slightly to present different viewing angles and thus generate different images. This was done to compare the robustness of extracted networks from each pit (see Section 2.2), and replication within pit was considered in all statistical analyses.

3.2.2. Network extraction

To extract the approximate soil network structure from the photographs, the photographs were converted to text files containing the red, green, and blue (RGB) triplet values for each pixel. All non-soil pixels were then identified as those whose triplet values exceeded the ranges expected for

soil particles, based on the average of the rest of the image. Using the average to determine this threshold customised it slightly for each image, so that outliers such as roots and rocks specific to that sample were captured, but samples having an overall more reddish tone were not stripped completely. The identified non-soil particles were removed, and variations in brightness across the remaining pixels were standardised using the mean pixel intensity.

As soil structure and porosity are only loosely related, soils of the same porosity can have different structural properties. A common assumption made is that soils, unless compressed/compacted, have up to 50 % pore space. As the pixel resolution of the images here is between 0.3 – 0.5 mm, and therefore much higher than the smallest pore space possible (sub-micron scale), it follows that the pore space actually visible is less than this 50 %. An evaluation of the distribution of pixel values showed that for soil profile images used in this study, the greatest change in the distribution occurred around a pixel intensity where 30 – 40 % of the pixels were below this value (Figure A2). We have therefore assumed that 30 % of the soil is ‘void’ (i.e. dark pixels). Therefore, the darkest 30 % of the soil pixels were retained as pores, and the image was inverted to convert these darker pixels to white, and vice versa (Figure A1e, f). The images from the same profile were visually compared after thresholding and showed a high degree of agreement in the pores identified (e.g. Figure A3). Network outlines were then drawn through a process known in image morphology as ‘skeletonization,’ where lines of white pixels were iteratively stripped down until they were all one pixel in width (Figure. A1g, h). We then mapped the networks to a list of links, which were series of pixels that were more than one pixel long, and nodes, defined as junction points between two or more links. Redundant links between nodes were removed.

For simplicity, all links in the final networks were represented with straight lines along the shortest distance between two nodes. This lost some of the details of the topology, such as pore size and shape. However, this work intended to create an abstraction of the network taken from the soil, rather than replicate and analyse the exact soil structure itself. This emphasised overall soil

structural characteristics and heterogeneity, rather than modelling how specific transport processes and biological activities would occur. Replicating the exact soil network would also have markedly increased the computational burden, as link lengths would have had to be calculated through pixel-counting rather than the Euclidean geometry measuring shortest distances. As many of the links as represented were quite short (see Section 3.3.1), the difference between the true link length and the shortest distance between nodes was assumed to be negligible. Currently, we assume that the method requires further validation and improvement to provide a measure of soil structure that can be used in soil science or pedological characterisation of the soil. We also assume however, that the method, while not perfect in its current form, provides sufficient quality of network data to allow simplified networks to be extracted and analysed, and used as the basis for simulations.

The process of rendering the network also identified which sections of the network were fully connected, and which nodes were part of disconnected subnetworks (Figure. A1i, j). An outline of the image morphology process, and images of each step, are available in Appendix 1.

3.2.3. Network analysis

Two types of analysis were used to quantify the heterogeneity present in the soil network images. The first involved applying metrics adapted from network science and transport geography to measure structural characteristics of the abstracted networks, which allows for easy comparison among soil types. These were calculated using R v4.0.2 (R Core Team, 2020), including the packages *igraph*, *qgraph*, and *sp* (Pebesma and Bivand, 2005; Csardi and Nepusz, 2006; Epskamp *et al.*, 2012; Bivand, Pebesma and Gomez-Rubio, 2013). All additional data analysis and visualisations were also done in R, using the packages *ARTool* v0.10.7 (Kay and Wobbrock, 2020; Wobbrock *et al.*, 2011), *emmeans* v1.5.0 (Lenth, 2020), *lmerTest* v3.1.2 (Kuznetsova, Brockhoff, and Christensen, 2017), *dunn.test* v1.3.5 (Dinno, 2017), *rcompanion* v2.3.25 (Mangiafico, 2020), *dplyr* v1.0.0 and *ggplot2* v3.3.2 packages (Wickham, 2016; Wickham *et al.*, 2019). The scripts for calculating network metrics are available at (Davis, 2020).

A brief description of each of the metrics chosen is given in Table 3.1. These were chosen to measure the size, connectivity, and structural heterogeneity of the networks from a range of node-centric, link-centric, and global perspectives, to obtain a broad picture how the networks may differ. The metrics chosen also minimised assumptions about inaccessibility of the soil matrix between pores: for example, the convex hull area was chosen over the concave hull area as the former is a more generous estimate of the spatial area.

Table 3.1 The name and description of the metrics used to analyse the soil networks.

Metric name	Description	Type of measure	Reference
Mean and standard deviation (SD) of link length	Quantifies the typical length and variability of lengths included within the network.	Size	N/A
Beta index	The ratio of links to nodes.	Connectivity	Rodrigue, 2017
Gamma index	Number of observed vs. possible links: $nLinks / (nNodes * (nNodes - 1))$	Connectivity	Rodrigue, 2017
Diameter	The length of the longest geodesic (shortest path between two nodes) in the network – the shortest path between the two most distant nodes.	Size	Rodrigue, 2017
Node count	The number of nodes in the network.	Size	Barabási, 2016
Edge count	The number of edges (links) in the network.	Size	Barabási, 2016
Mean node degree	Mean number of links per node.	Connectivity	Barabási, 2016
Cost	The total length of the network measured in real transport distances.	Size	Rodrigue, 2017
Global reach centrality (GRC)	The difference between the maximum and average local reach centrality (LRC), where the LRC is the nodes that a given node can connect to, weighted by distance (here, spatial distance).	Structure, connectivity	Adapted from Mones, Vicsek and Vicsek (2012)
Mean convex hull area	The area of a polygon that minimally encompasses every node in the network.	Size, connectivity	Rockafellar, 1970
Network density	The ratio of the number of nodes to the convex hull area.	Structure	N/A

As introduced, the imaging method and metrics used here are two-dimensional (2D), and we have been unable to find literature describing characterisations of three-dimensional (3D) soil structure metrics based on two-dimensional imaging. Aitkenhead *et al.* (1999) derived 3D models of soil pore systems based on 2D metrics but did not compare the two sets of structural metrics. Future work would be necessary to determine the extent to which 3D variation in soil structural metrics correlates to the variation seen in 2D. Here, we are assuming that it does correlate, and that this allows 2D imaging to provide structural metrics representative of different soil types.

We calculated each metric for each of the networks, which contained all nodes and links in the image, hereon called ‘main networks.’ We also calculated each metric for each of the disconnected subnetworks within the main networks, hereon called ‘subnetworks.’ As the distributions of metrics in the main soil networks had similar variance across soil types and relatively normal distributions, these were compared with nested ANOVA, using profile ID as a random effect to account for replication. The distribution of metrics across the subnetworks did not meet the assumptions for classical ANOVA, so non-parametric Aligned-Ranks Transformation (ART) ANOVAs were used instead, also with profile ID as a random effect.

3.2.4. Agent-based model overview

The second analytical method used a simulated population of consumers to explore each network, using the resulting heterogeneity in consumer resource stocks to further elucidate the heterogeneity of the network. This provided a more functional perspective, alongside the structural quantification of the network metrics. The purpose was to investigate the structure’s generalised impact, rather than test the precision of this model in predicting outcomes for real species. Therefore, rather than using parameterisations that reflected specific species or groups, five generic model species with different sets of values for each trait were used, similarly to e.g. Polhill and Gimona (2014).

The same approach was taken for resources, with three sets of resource bases of different combinations of maximum capacity and maximum growth rates. Resources were assumed to be located at nodes within the network, as identified during the extraction process (see Section 2.2). Food resources in real soil networks are located throughout the soil matrix, but are often concentrated in ‘hotspots’ such as those created by plant roots and decomposition processes (Ettema and Wardle, 2002), which would be represented in the networks here as nodes. As exploring the effect of size of the generic species was not in scope for the work here, only the most accessible areas of the network were treated as potential resources.

A brief description of the model purpose, variables, and processes is presented below, following the Overview, Design concepts, and Details (ODD) protocol (Grimm *et al.*, 2006, 2010). The full ODD document, including description of design concepts, initialisation, input data, and sub-models, is available in Appendix 2. The model source code, written in NetLogo 6.1, is available in the Modelling Commons repository as “Soil network simulation” (see also Davis and Polhill, 2021).

3.2.4.1 *Overview section of Overview, Design Concepts, and Details (ODD)*

I. Model purpose

The model is designed to be an analytical tool to explore the heterogeneity in resource supply potential of a network by populating it with idealised energy-consuming agents, and to quantify the effects of consumer, resource, and network characteristics on resulting consumer population outcomes.

II. Entities, state variables, and scales

i. Consumer entities

State variables

Property	Description
Location	The resource on which the consumer is located
Target location	The resource to which the consumer will move next
Active?	Whether a consumer is active (or dead)

Parameters

Property	Description
Basal metabolism	How much resource an agent needs per day to stay alive
Active metabolism	How much resource an agent uses with each step
Resource stock	How much resource an agent has consumed but not metabolised
Consumption rate	Maximum number of resource units that an agent takes from a resource it visits, per timestep
Spawn energy	How much energy an agent requires to spawn (depletes this quantity from stocks and passed to offspring as starting quota)

ii. Resource entities

State variables

Property	Description
Current supply	The current quantity of resource at this point

Parameters

Property	Description
Resource capacity	How much energy is stored in a resource when it is full
Regrow rate	The amount the resource regrows each timestep

iii. Link entities

State variables

Property	Description
Length	The length of the link - determines energy and time required to traverse it

Scales

Property	Description
Timestep	A single unit of time in the model, defined as that which is required for consumers to move 1 pixel (approximately 0.3 – 0.5 mm), and for which they require basal-metabolism units of energy.
World size	400 x 500, determined by the size of the soil networks used as the environment.

III. Sequence of events

1. Consumers start on random nodes around a pre-specified network, where nodes are resource patches.
2. Consumers move around the network randomly following links. If they find a resource patch, they consume as much as they can from it, and the patch depletes.
 - Consumers require basal-metabolism units of resource per timestep. If they do not consume this resource, they die.
 - Consumers can stay put on a resource and consume it (consumption-rate units consumed per timestep), but it depletes, and if there is no more resource there then they move on.
 - Consumers metabolise active-metabolism units of resource per patch of link that they cross.
 - If there is more than one agent on a resource patch, they each take consumption-rate units per timestep, or split the remainder if there is not enough resource remaining for them to each get consumption-rate units.
3. If consumers have twice as much energy as the set spawn-energy, they can spawn new consumers (who take the same amount of resource-stock from their parent that the parent started with, so now parent and offspring both have the same resource-stock).
4. Resources regrow at a constant rate (regrow-rate) per timestep, up to their maximum capacity (resource-capacity).

3.2.4.2 *Sensitivity analysis*

To determine the sensitivity of the ABM to input parameters, and the robustness of any emergent patterns of heterogeneity, we performed an extensive sensitivity analysis following

recommendations in the agent-based modelling literature. This is detailed in Appendix 3. Table 3.2 shows the final parameter values used for the consumer populations, resource populations, and general model. In the actual simulation runs, each combination of the five consumer parameter sets, and three resource parameter sets, was tested against each network architecture, resulting in 8700 total runs including replicates.

Table 3.2 Final values for (a) consumer, (b) resource, and (c) general simulation parameters.

Consumer parameters

Parameter	Consumer type					
	High metabolism, high consumption, high spawn energy (HHH)	Low metabolism, low consumption, low spawn energy (LLL)	Low metabolism, moderate consumption, low spawn energy (LML)	Low metabolism, moderate consumption, moderate spawn energy (LMM)	Moderate metabolism, moderate consumption, moderate spawn energy (MMM)	
Basal metabolism	3	1	1	1	1	2
Active metabolism	3	1	1	1	1	2
Consumption rate	10	5	7	7	7	7
Spawn energy	100	50	50	50	75	75
Initial resource stock	30	30	30	30	30	30

Resource parameters

Parameter	Resource type		
	High capacity, low growth (HL)	Moderate capacity, moderate growth (MM)	Low capacity, high growth (LH)
Maximum resource capacity	50	35	20
Maximum regrow rate	10	15	20

General parameters

Parameter	Value
Initial population size	500 consumers
Length of simulation	2000 timesteps

3.2.4.3 *Analytical method*

At each time step, the ABM calculated five metrics (Table 3.3), including measures of centre and spread of consumer resource stocks, the final population size, and two additional inequality metrics: the Gini coefficient and a modified form of the Shannon entropy. The latter estimates the

differential entropy of a continuous variable, by discretising the distribution into bins (Appendix 4). These metrics were chosen to include measures of absolute and relative inequality, and a measure of evenness common to ecology. As the distributions of each metric across the soil types did not meet assumptions of most parametric tests, mixed-effects ART ANOVAs with profile ID as a random effect were again used to quantify how the outcome metrics differed, for each combination of resource and consumer population parameters and soil type. As the final population size and the entropy of consumer resource stocks both showed variance not fully explainable by consumer or resource population parameters, these were also tested with Kruskal-Wallis tests comparing them across profile IDs and soil types. The significantly different pairs of profiles were identified with Dunn post-hoc analysis. All data processing, analysis, and visualisation was done in R, using the packages listed previously, as well as the entropy v1.2.1 (Hausser and Strimmer, 2014) and ineq v0.2.13 packages (Zeileis, 2014).

Table 3.3. The name and description of outcome variables calculated for the agent-based model (ABM).

Variable name	Description
Mean consumer resource stock	The mean of the resource stocks held by all active consumers. Units are the same as those of the quantity measured.
Standard deviation consumer resource stock	The square root of the sum of squared absolute differences between each observation and the mean, normalised by the number of observations (minus one, to allow for sample estimation). Units are the same as those of the quantity measured.

$$s = \sqrt{\frac{\sum |x_i - \bar{x}|^2}{n - 1}}$$

Gini coefficient consumer resource stock	Measures the deviation of a population from perfect equality. Mathematically, it can be calculated as half the relative mean absolute difference, or half the average absolute difference between all pairs of the population, divided by the average of the population to normalise. Unitless.
--	---

$$G = \frac{\sum_{i=1}^n \sum_{j=1}^n |x_i - x_j|}{2n^2 \bar{x}}$$

Entropy consumer resource stock (Shannon index) Measures the amount of information that would be needed to represent the state of the system. Specifically, it is the negative sum of the probability of a consumer's resource stock occurring within a given range, and the log of that probability, normalised by the maximum value ($\log n$). This is the discretised formula for entropy. The units depend on the base of the log: here we use base 2 (units: bits).

$$H(X) = \frac{-\sum f(x_i) \log_2 \frac{f(x_i)}{w(x_i)}}{H_{max}}$$

Final population size Count of currently active ('alive') consumers.

3.3. Results

3.3.1. Network metrics

The network metrics showed several significant differences between the Cambisols and Arenosols, with the Cambisols having higher values for most metrics measuring size and structure. These are summarised in Table 3.4 and Figure 3.1.

Table 3.4. (a) Estimated marginal means, standard errors, and outcomes for mixed-effect nested ANOVAs comparing network metrics between Cambisol and Arenosol main soil networks, and (b) medians and 95 % confidence intervals and results of mixed-effect nested Aligned-Ranks Transformation (ART) ANOVAs comparing Cambisol and Arenosol subnetworks. Shown in (a) are the Type II Wald Chi-square statistic and p-values for models comparing each network metric across soil types. Profile ID was included as a mixed effect; its log-likelihood ratio test (LRT) statistic and p-value are also shown. Both the Chi-square and LRT used one degree of freedom to compare soil types. Estimated marginal means and standard errors were calculated from ANOVAs. In (b) ART ANOVAs were used as the data were non-normal; profile ID was also included as a mixed effect. Shown are Type III Wald F tests with Kenward-Roger degrees of freedom. The asterisks designate level of significance: p < 0.1: ·, p < 0.05: *, p < 0.01: **, p < 0.001: ***. Descriptions of the metrics are in Table 3.1.

Main networks

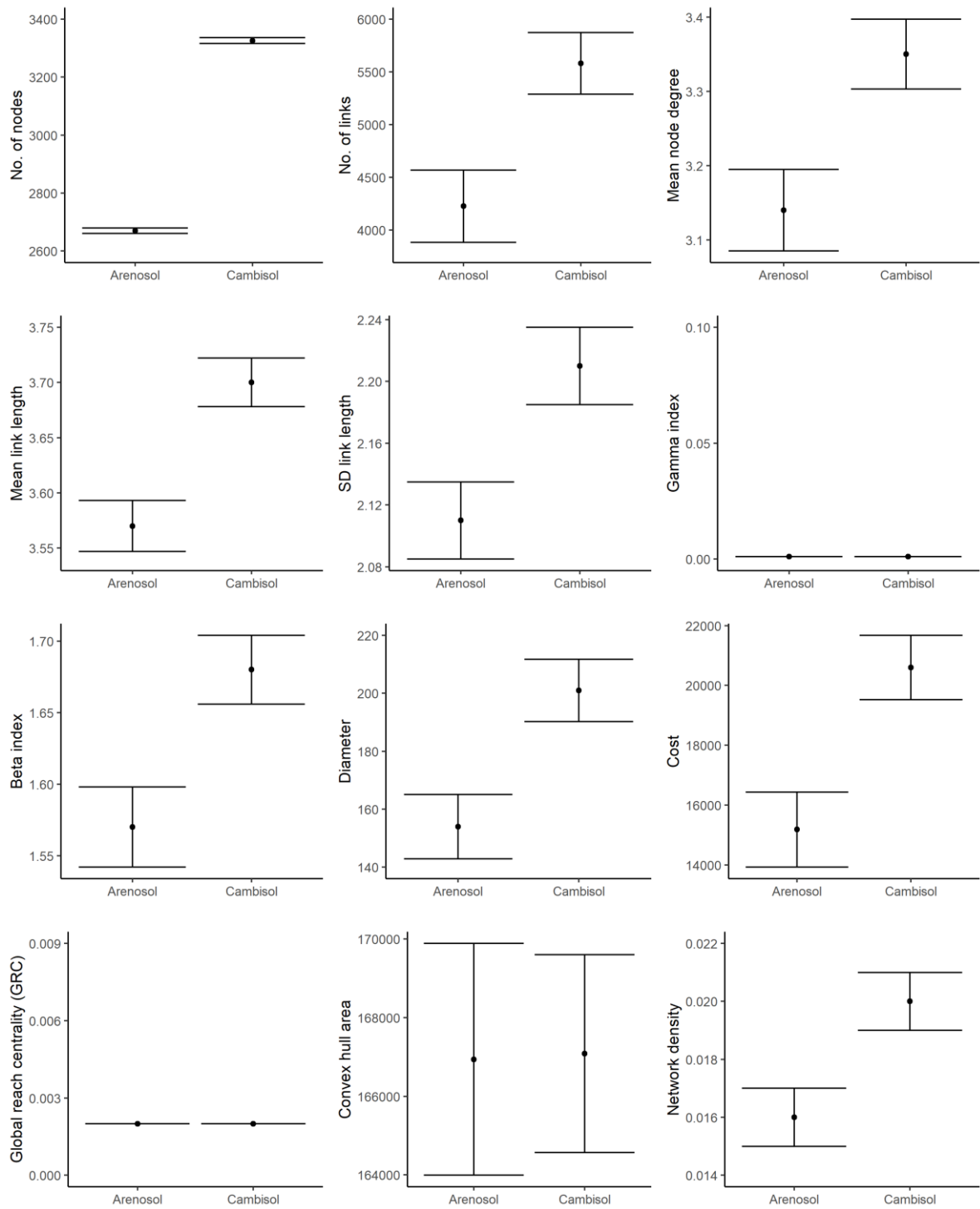
	Arenosols (n = 25)		Cambisols (n = 25)		Soil type		Profile ID (random effect)	
	Est. marginal mean	SE	Est. marginal mean	SE	χ^2	p	LRT	p
No. of nodes	2670.000	9.570	3326.000	10.070	7.809	0.005 **	21.384	< 0.001 ***
No. of links	4225.000	344.000	5581.000	293.000	9.058	0.003 **	19.280	< 0.001 ***
Mean node degree	3.140	0.055	3.350	0.047	9.098	0.003 **	9.005	0.003 **
Mean link length	3.570	0.023	3.700	0.022	17.667	0.000 ***	0.414	0.520
SD link length	2.110	0.025	2.210	0.025	9.815	0.002 **	0.000	1.000
Gamma index	0.001	0.000	0.001	0.000	4.838	0.028 *	20.231	< 0.001 ***
Beta index	1.570	0.028	1.680	0.024	9.098	0.003 **	9.005	0.003 **
Diameter	154.000	11.100	201.000	10.700	10.017	0.002 **	0.141	0.708
Cost	15180.000	1257.000	20600.000	1072.000	10.840	0.001 ***	16.153	< 0.001 ***
Global reach								
centrality	0.002	0.000	0.002	0.000	0.049	0.825	10.923	< 0.001 ***
Convex hull area	166940.000	2949.000	167086.000	2514.000	0.001	0.970	11.730	< 0.001 ***
Network density	0.016	0.001	0.020	0.001	8.037	0.005 **	16.547	< 0.001 ***
No. of subnetworks	163.000	3.382	158.000	3.236	0.009	0.924	6.302	0.012 *

Structure, flow, and inequality

Subnetworks

	Arenosols (n = 3906)			Cambisols (n = 3834)			ANOVA	
	Median	Lower CI	Upper CI	Median	Lower CI	Upper CI	<i>F</i>	<i>p</i>
Number of nodes	11.000	11.000	11.000	11.000	11.000	11.000	F(1, 8.614) = 1.542	0.247
Number of links	15.000	14.000	15.000	15.000	15.000	16.000	F(1, 8.443) = 3.793	0.085 ·
Mean node degree	2.670	2.640	2.670	2.710	2.670	2.750	F(1, 7.971) = 9.239	0.016 *
Mean link length	3.190	3.170	3.220	3.250	3.230	3.280	F(1, 7.011) = 11.322	0.012 *
SD link length	1.620	1.600	1.640	1.670	1.640	1.690	F(1, 8.334) = 3.648	0.091 ·
Gamma index	0.132	0.127	0.136	0.133	0.128	0.136	F(1, 8.720) = 0.355	0.567
Beta index	0.133	0.132	0.133	0.136	0.133	0.138	F(1, 7.971) = 9.239	0.016 *
Diameter	19.000	18.600	19.500	19.300	18.800	19.700	F(1, 7.957) = 1.664	0.233
Cost	46.700	45.200	48.700	49.200	47.500	51.600	F(1, 8.161) = 4.717	0.061 ·
Global reach centrality	0.058	0.057	0.059	0.058	0.057	0.059	F(1, 7.645) = 0.554	0.479
Convex hull area	63.500	59.800	67.000	62.500	58.500	66.000	F(1, 8.132) = 0.385	0.552
Network density	0.171	0.167	0.176	0.172	0.168	0.179	F(1, 8.117) = 0.013	0.913

A



B

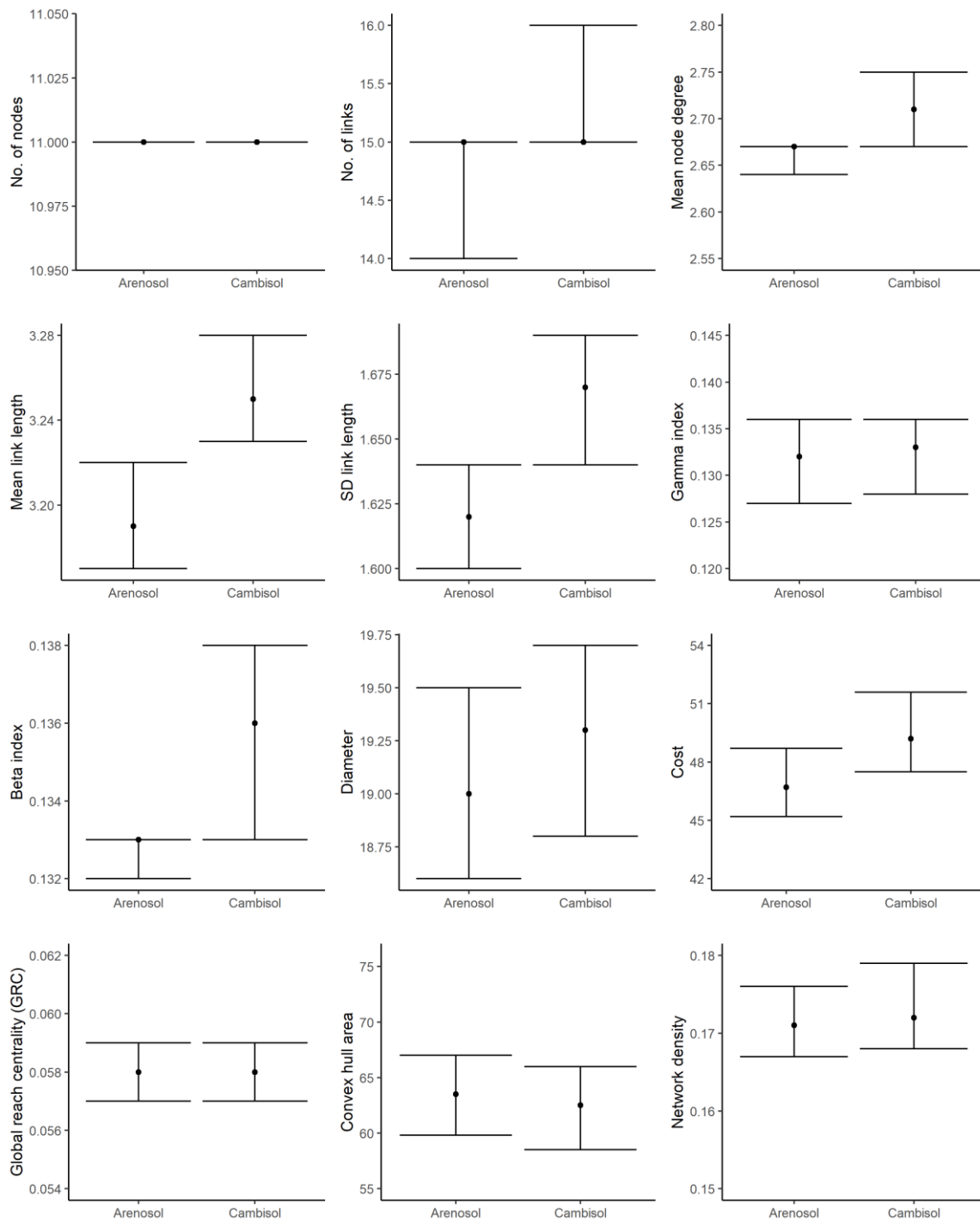


Figure 3.1. The distribution of each network metric by soil type, for (a) main soil networks and (b) subnetworks. The point and error bars in (a) represent the estimated marginal mean and standard error for that network type and soil type, as determined by the ANOVAs (Table 3.4a), and the point and error bars in (b) represent the median and upper and lower 95 % confidence intervals, respectively. Descriptions of the network metrics are in Table 3.1.

At the main network level, the networks extracted from the Cambisols had significantly more nodes and links, a larger mean node degree and standard deviation of link length, and longer mean link length (Table 3.4a). These networks also had a higher beta index, higher cost, and higher density. While the main networks of the two soil types had significantly different gamma indexes, the absolute difference in the estimated marginal means between the two soil types was negligible ($< 10^{-3}$) (Table 3.4a, Figure 3.1a). At the subnetwork level, Cambisol networks had longer mean link length, and higher mean node degree and beta index (Table 3.4b). While not significant, Cambisol subnetworks also had noticeably larger number of links and standard deviation of link length, and higher cost (Figure 3.1b).

To control for the effect of replication on the significance, the profile ID was included in the ANOVAs as a mixed effect. This was significant for all metrics except mean and standard deviation of link length and diameter. Most profiles within each soil type at the main network level showed low absolute variation across the networks extracted from each however, and noticeably higher metric values for Cambisols than Arenosols (Figure A7a). At the subnetwork level, the distributions were quite similar across all profiles, but the Cambisol profiles showed more frequent and higher outliers.

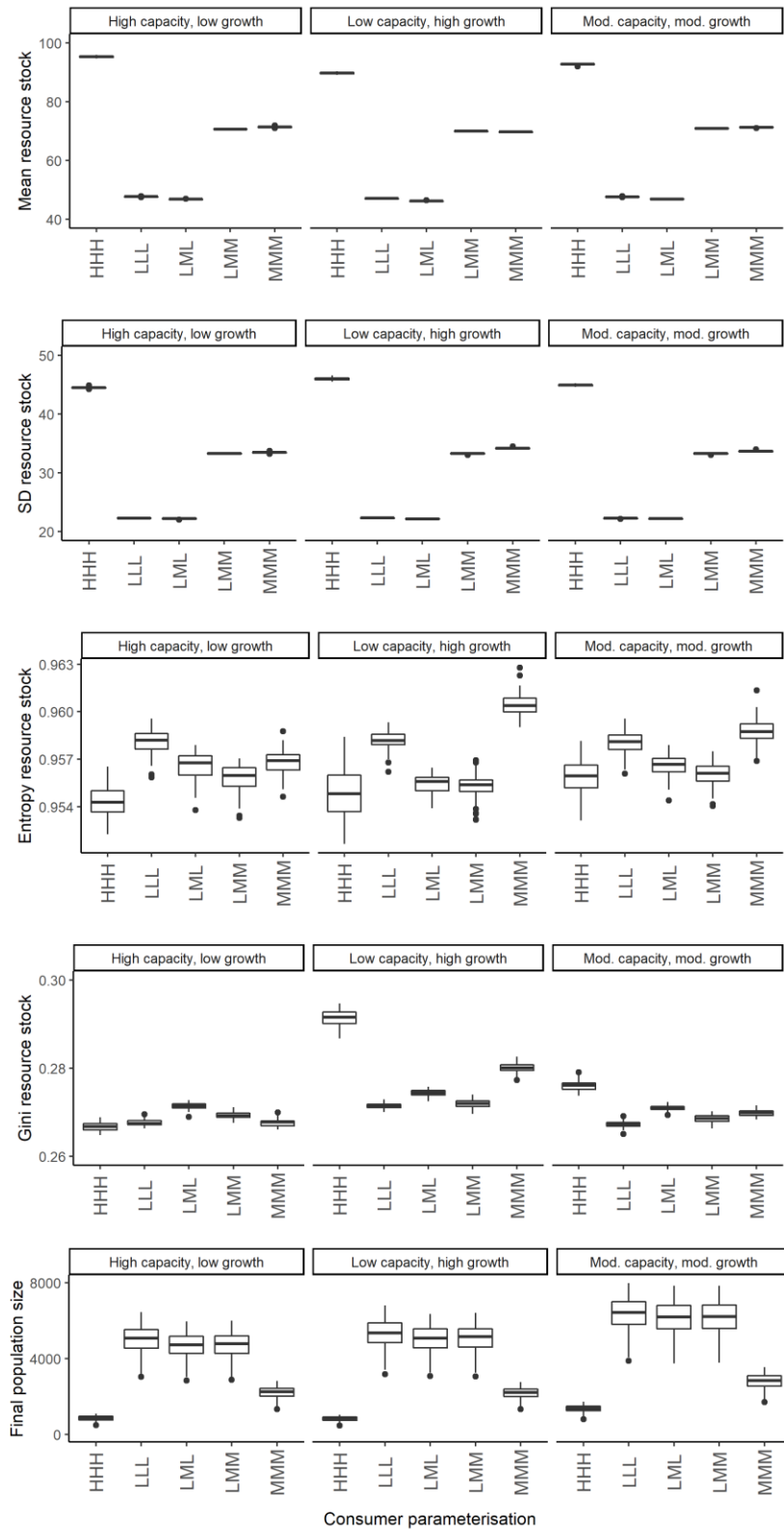
3.3.2. Agent-based model

The ABM results showed significant differences across the different combinations of parameterisations and soil types, summarised in Tables 3.5 and 3.6 and Figure 3.2. The simulations run on the Cambisol networks had significantly higher final population sizes (Tables 3.5 and 3.6, Figure 3.2b), and interactions between soil type and consumer and resource parameterisation were significant for several outcome variables (Table 3.6).

Table 3.5. The medians, first and third quantiles for agent-based model (ABM) outcome variable values across the two soil types. These values represent the overall results across all consumer and resource parameterisations. Descriptions of the variables are in Table 3.3.

	Arenosols (n = 375)			Cambisols (n = 375)		
	Median	1 st Quantile	3 rd Quantile	Median	1 st Quantile	3 rd Quantile
Mean resource stock	69.970	47.086	71.391	69.940	47.077	71.397
SD resource stock	33.266	22.262	34.123	33.300	22.276	34.112
Entropy resource stock	0.956	0.955	0.958	0.957	0.956	0.958
Gini resource stock	0.271	0.268	0.273	0.271	0.268	0.274
Final population size	4049.728	1967.921	5102.043	4890.158	2279.1560	5842.834

A



B

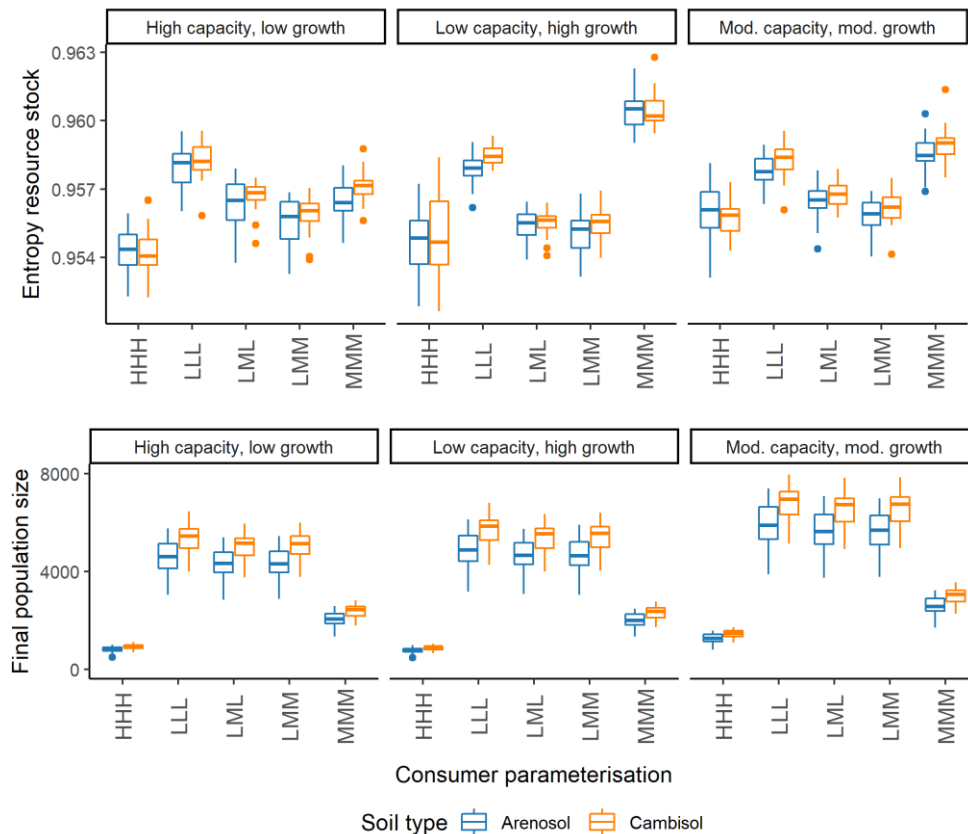


Figure 3.2. Distributions of (a) each agent-based model (ABM) outcome variable, grouped by resource parameterisation (columns, labelled at top) and consumer parameterisation (x axis within columns), across both soil types, and (b) ABM outcome variables that were significantly affected by soil type (represented by colour), grouped by resource parameterisation (columns) and consumer parameterisation (x axis within columns). The three-letter consumer parameterisation codes refer to the metabolism, consumption rate, and spawning threshold, respectively, where H is high, M is medium, and L is low. Descriptions of the resource and consumer parameterisations are in Table 3.2, and descriptions of the outcome variables are in Table 3.3.

The ART ANOVAs showed that measured outcomes all differed significantly across consumer parameterisation, resource parameterisation, and consumer-resource parameterisation interactions. Final population size differed significantly by soil type, soil type-resource parameterisation interaction, and soil type-consumer parameterisation interaction. Mean resource stock also differed significantly by soil type-resource parameterisation interaction.

Table 3.6. Overview of Aligned Ranks Transformation ANOVA models of consumer population outcomes by consumer and resource parameterisation and soil type. The tests were Type III Wald F tests with Kenward-Roger degrees of freedom. Profile ID was included as a random effect. The asterisks designate level of significance: $p < 0.1$: ·, $p < 0.05$: *, $p < 0.01$: **, $p < 0.001$: ***. Descriptions of consumer and resource parameterisations are in Table 3.2 and descriptions of response variables are in Table 3.3.

Response	Predictors	F	Significance
Mean consumer resource stock	Consumer population	F(4, 710.063) = 3585.924	< 0.001 ***
	Resource population	F(2, 710.063) = 2585.400	< 0.001 ***
	Soil type	F(1, 9.692) = 0.328	0.560
	Consumer pop. x resource pop.	F(8, 710.094) = 998.152	< 0.001 ***
	Consumer pop. x soil type	F(4, 710.106) = 1.460	0.213
	Resource pop. x soil type	F(2, 710.103) = 3.513	0.030 *
	Consumer pop. x resource pop. x soil type	F(8, 710.102) = 1.020	0.419
	Consumer population	F(4, 710.185) = 3629.337	< 0.001 ***
	Resource population	F(2, 710.292) = 1137.215	< 0.001 ***
	Soil type	F(1, 9.212) = 0.555	0.475
SD consumer resource stock	Consumer pop. x resource pop.	F(8, 710.233) = 677.837	< 0.001 ***
	Consumer pop. x soil type	F(4, 710.315) = 2.164	0.071 ·
	Resource pop. x soil type	F(2, 710.32) = 0.538	0.584
	Consumer pop. x resource pop. x soil type	F(8, 710.306) = 1.123	0.345
	Consumer population	F(4, 710.030) = 586.700	< 0.001 ***
Entropy consumer resource stock	Resource population	F(2, 710.036) = 59.661	< 0.001 ***
	Soil type	F(1, 9.861) = 3.105	0.109
	Consumer pop. x resource pop.	F(8, 710.025) = 67.989	< 0.001 ***
	Consumer pop. x soil type	F(4, 710.037) = 2.364	0.052 ·
	Resource pop. x soil type	F(2, 710.037) = 0.241	0.786
	Consumer pop. x resource pop. x soil type	F(8, 710.037) = 0.949	0.475
Gini consumer resource stock	Consumer population	F(4, 710.677) = 1296.640	< 0.001 ***
	Resource population	F(2, 711.086) = 2004.095	< 0.001 ***
	Soil type	F(1, 7.791) = 2.445	0.158
	Consumer pop. x resource pop.	F(8, 710.847) = 1005.251	< 0.001 ***
	Consumer pop. x soil type	F(4, 711.364) = 0.470	0.758
	Resource pop. x soil type	F(2, 711.281) = 2.502	0.083 ·
Final population size	Consumer pop. x resource pop. x soil type	F(8, 711.287) = 0.614	0.766
	Consumer population	F(4, 710.001) = 1361.66	< 0.001 ***
	Resource population	F(2, 710.001) = 604.376	< 0.001 ***
	Soil type	F(1, 9.998) = 9.239	0.012 *
	Consumer pop. x resource pop.	F(8, 710.001) = 33.651	< 0.001 ***
	Consumer pop. x soil type	F(4, 710.001) = 41.516	< 0.001 ***
Final population size	Resource pop. x soil type	F(2, 710.001) = 5.039	0.007 **
	Consumer pop. x resource pop. x soil type	F(8, 710.001) = 0.282	0.972

The entropy of consumer resource stocks and the final population size both showed considerable variation in the initial boxplots that was not explained by the consumer and resource parameterisation (Figure 3.2a), and the ANOVA results suggested that soil type was influential on final population size. Therefore, these were further explored with Kruskal-Wallis tests, first with profile ID as the grouping variable, then soil type (Table 3.7, also Figure 3.2b). Significant differences in profile ID were explored with Dunn post-hoc analysis. This showed that entropy differed significantly between profiles D and H, which were Cambisol and Arenosol, respectively, while final population size differed significantly between several pairs of profiles, including both intra- and inter-type profile pairings.

Table 3.7. Results of Kruskal-Wallis tests and Dunn post-hoc analysis comparing entropy of consumer resource stocks and final population size by soil profile ID and soil type. The degrees of freedom for the Chi-square statistics were 11 and 1 for profile ID and soil type, respectively. Profile IDs A – G correspond to Cambisols, while profile IDs H – K correspond to Arenosols. Significant pairs of profiles were identified at the level of $\alpha/2$, where $\alpha = 0.05$. Profile pairings in italics denote inter-type pairs.

Response variable	Grouping variable	Significance		Significantly different pairs ($p < 0.025$)
		χ^2	p	
Entropy consumer resource stock	Profile ID	25.824	$p = 0.007^{**}$	<i>D : H</i>
	Soil type	4.965	$p = 0.026^*$	Cambisol : Arenosol
Final population size	Profile ID	65.167	$p < 0.001^{***}$	<i>A : C, A : H, A : I, A : K, A : L, B : H, B : I, B : K, D : H, D : I, D : K, G : H, G : I, G : K, H : J, I : J, J : K</i>
	Soil type	21.974	$p < 0.001^{***}$	Cambisol : Arenosol

3.4. Discussion

3.4.1. Network analysis

Given the known characteristics of the two soil types, the results of the network analysis suggest that the methodology developed here captures overall trends of soil structural development. Cambisols typically have more soil structure, higher porosity, higher levels of biotic activity, and greater stability than Arenosols (FAO, 2015). Correspondingly, the abstracted Cambisol soil

networks analysed here showed higher values for the metrics measuring size, structure, and connectivity than the abstracted Arenosol soil networks did.

Specifically, the Cambisol soil networks had significantly more nodes and links, longer mean and standard deviation of link lengths, and higher total cost, density, and diameter (Table 3.4). This suggests more pore-creating activities modifying the soil, and a soil structural matrix that can support longer pores. This would also lead to higher water holding capacity, and increased internal drainage, both of which are commonly associated with Cambisols (FAO, 2015). In contrast, the smaller and less connected Arenosol networks have a low water-holding capacity, and the weaker coherence of their matrix material prevents longer pores from being stable, making them prone to erosion (FAO, 2015). Cambisols are also classified as more structurally developed than Arenosols, and contain more organic matter (FAO, 2015), both of which further validate the increased structure seen in the Cambisol networks here.

The global reach centrality, gamma index, and convex hull area were not as clearly differentiated between the Cambisol and Arenosol soil networks, however. The global reach centrality values were small and functionally identical, with an estimated marginal mean of 0.001 and 0.058 for both soil types at the main and subnetwork level, respectively (Table 3.4). Similarly, the estimated marginal mean gamma index for main networks of both soil types was 0.001. This is likely due to the presence of a similar number of disconnected subnetworks within each soil network, limiting the total number of nodes that any given node can reach. The Cambisol main networks also had a slightly smaller range of convex hull areas, although the opposite trend emerges at the subnetwork level (Figure 3.1, Table 3.4). When this is decomposed by profile, the Cambisols show more variation and outliers across and within profiles for several metrics, including convex hull area (Figure A7), suggesting that soil type includes a greater heterogeneity of network sizes and structures. As with the other metrics, further work is required to establish ranges across different soil types and geographical regions, and to compare these metrics with those more commonly used

in soil analysis. Overall, however, the differences between the Cambisols and Arenosols as captured in this analysis broadly reflects those expected, given the known differences in their properties.

The improved profile development and heterogeneity of Cambisols highlights their potential for agriculture and forestry, and in underpinning the diversity of a range of ecosystems. It is vital to manage them in a way that preserves and enhances their soil structure, however, to maintain their porosity and biodiversity, and resulting stability, drainage, and aeration. Similarly, Arenosols should be managed in a way that minimises their propensity for erosion and soil loss. In both cases, this can be accomplished through limiting or eliminating tillage (e.g. Young and Ritz, 2000; Helgason, Walley and Germida, 2010; Kravchenko *et al.*, 2011), and increasing cover crops and native species (e.g. Fernández *et al.*, 2019; Kravchenko *et al.*, 2011). These provide additional organic inputs to the soil to promote an active and diverse soil biota, and therefore the positive feedback between biota, and structural development and stability (e.g. Oades, 1993; Young and Ritz, 2009; Crawford *et al.*, 2012). The feasibility of the measurement and analysis methods presented here could provide a basis for estimating changes in structure over time and under different management strategies or environmental changes. This would help inform actions taken to preserve or improve the soil structure. However, further work is required to standardise the approach and demonstrate its application over multiple soil types.

As introduced in the Methods, the networks analysed here represent abstractions of the true soil structure present in the samples. This simplification is reasonable for analysing overall structural characteristics and heterogeneity and made the computation of the network metrics feasible. Although the short link lengths (Table 3.4) suggest that using Euclidean distance is likely negligibly different than measuring the path through the pixels, it does limit the interpretation of the findings we present. Specifically, the absolute values of the metrics cannot be taken to characterise the precise soil structure, but rather suggest general trends in structural development. As the exact size

and shape of the pores was not preserved, many of the finer distinctions between networks may also be lost. This could cause the magnitudes of differences found between soil samples here to appear lower than they are. As discussed above, the relatively rapid, low-cost, and lightweight approach used here for estimating soil structure should be compared against more established approaches and metrics to determine its effectiveness. This methodology provides simplified and potentially inaccurate measurements of soil structure, but with further improvement it could be a suitable approach for rapid assessment of soil structure in the field. The results presented suggest that the methodology can still capture general known trends of heterogeneity within soil networks, meriting further refinements and application.

3.4.2. ABM analysis

The ABM evaluated the effects of and interactions between consumer and resource characteristics, and the structure of the abstracted soil networks, on the measured consumer outcomes. Overall, the results showed that the size and energetic heterogeneity of the consumer population was heavily influenced by the parameterisation of the consumer population and resource base, and their interactions. Moreover, while outcome variables were less directly affected by soil network structure, they were more influenced by the interactions between this network structure and consumer or resource parameterisations.

Across all simulations, measured outcomes varied most strongly across consumer and resource characteristics, and their combinations as overall consumer and resource parameterisations or types (Figure 3.2a, Table 3.6). Specifically, the mean, standard deviation, and entropy of consumer resource stocks, as well as the final population size, were most different across consumer types. These differences in outcome variables resulted from how each consumer population responded to the provided resource base. For example, the consumer populations with low metabolisms, low consumption rate, and a low energy requirement for spawning had a lower mean resource stock, and a higher final population size, for any given resource base. The consumers with high

metabolisms, high consumption rate, and a high energy requirement for spawning had a lower final population size, but higher mean resource stock. This is similar to the distinction between r-strategists and K-strategists. In these simulations, the threshold for spawning and the active and basal metabolic rates appeared to have the largest impact on the measured outcome variables (Figure 3.2a). This is likely due to these parameters balancing one another in determining energy allocation between maintenance and reproduction (e.g. Brown *et al.*, 2004; Kooijman, 2009).

In addition to consumer and resource characteristics, the soil type, and therefore soil network structure, also affected population size and diversity (Table 3.6). Specifically, the mean consumer resource stock and final population size showed significant differences across resource and soil type interactions, and final population size also showed significant differences between soil types (Table 3.5). While the final population size and entropy also differed significantly across profiles (Table 3.6), post-hoc analysis revealed that for entropy this was only significant for inter-type profile pairings, and a slight difference was visible between groups when plotted (Figure 3.2b). This entropy is also known as the Shannon Index or Shannon-Wiener Index, and here measures the diversity or ‘evenness’ of the distribution of consumer resource stocks (Hill, 1973; Spellerberg and Fedor, 2003). Higher entropy therefore meant that given quantities of resource stock were represented in equal proportional abundance across the population. This is typically caused by groups of consumers emerging, where group members each have the same quantity of resource stock, but these quantities differ among groups. Over time, adaptations in this context could drive the system toward speciation. In these simulations, the larger populations supported by the larger Cambisol soil networks were more likely to have higher entropy, through different quantities of consumer resource stocks represented with equal proportional abundance.

The relatively low Gini coefficients (Table 3.5, Figure 3.2a) can also suggest the emergence of distinct groups of consumers with equal resource stocks, with similar numbers of consumers across the groups. As the Gini coefficient measures relative inequality, both inequality in resource

stocks across groups, and more groups, cause it to increase. Equal group sizes can somewhat counter this. In both soil types however, as the consumers in a given simulation had identical characteristics, it is reasonable that they would have similar outcomes, slightly differing based on the subnetwork in which they found themselves, and the resource base available to them there. The similarity among subnetworks of the two soil types (Table 3.4b) suggests that the heterogeneity between soil types is more apparent at the main network level. As the consumers in these simulations were unable to move between subnetworks, they likely did not experience the full range of environmental heterogeneity between the soil types, which would have limited its effect on the measured outcomes.

Overall, the simulations highlight the differences in population size and diversity across consumer and resource parameterisations and interactions, soil and resource type interactions, and to a lesser extent, soil type on its own. Spatial heterogeneity, through both resource and network structural heterogeneity, can increase the microhabitat diversity (Anderson, 1978; Giller, 1996; Ettema and Wardle, 2002; Nielson *et al.*, 2010), which was shown here through the increased evenness of consumer groups with different resource stocks. Similarly, the heterogeneous habitat of soils can limit competitive exclusion by providing structural and resource niches for different species (Bardgett, Yeates and Anderson, 2009), such that more structurally heterogeneous Cambisols have larger and more diverse populations (FAO, 2015). This was reproduced by the larger populations that emerged in the Cambisol simulations here, although speciation was not explicitly modelled. As with the findings of the network analysis, this emphasises the importance of preserving soil structure and providing adequate substrate for maintaining an active soil biota (e.g. Young and Ritz, 2009; Crawford *et al.*, 2012; Fernández *et al.*, 2019).

While the parameterisations presented here were limited, they revealed interesting effects of consumer and resource characteristics and interactions. The programming of the model itself, however, may also have had an impact on the outcome of consumer populations. For example,

consumers moved randomly among resources rather than following any sort of search strategy, and there was no energetic penalty imposed for turning, which are simplifying assumptions based on the limited sensory and processing capabilities of most soil biota. This eliminated free parameters that would have to be tuned and analysed or sourced from limited data about specific soil biota metabolism and cognition. It also eliminated any effect that tortuosity of the network would have on consumer resource stocks, though. This may not be a correct assumption if turning has a higher burden physically, cognitively, or both. Furthermore, as consumers were not able to extend the network or move between subnetworks, they were unlikely to experience the full difference between soil networks, as discussed above. This may have led to a smaller effect of soil type on measured consumer outcomes.

Additionally, the extraction and simplification process used to create the soil networks may have affected the outcomes of the ABM. As the details of pore size and shape were not maintained, the consumers' ability to forage or hide in crevices was not intended to mimic the true range of consumer sizes and behaviours. Since predation was not included in the model, however, we did not intend to explore the hypothesised effect of physical niches on populations by limiting competitive exclusion and predation. While this would be an interesting future extension, and these changes could increase the observed effect of the soil network structure on consumer population outcomes, it would require refining the network extraction process as discussed above, as well as estimating ranges of consumer sizes and predation dynamics. The model presented here instead focussed on exploring the overall trends that might emerge in a population of consumers, rather than attempting to predict how specific populations might evolve. While its design limits the precision of the implications, it maintains the level of realism and generality assumed within the overall methodology (Levins, 1966).

3.5. Conclusion

This work has explored how analysing abstracted soil networks using standard network metrics, combined with simulations, can quantify the underlying structural and functional differences between soil types. We showed that networks derived from a brown forest soil, or Cambisol, were significantly larger, more connected, and more spatially heterogeneous than the networks derived from a less developed sandy beach soil, or Arenosol. These larger and more structured networks were in turn able to support larger populations of simulated consumers in an agent-based model (ABM). The ABM also demonstrated how the size and heterogeneity of the simulated population were significantly different across consumer and resource parameterisations, and interactions between these parameterisations and soil type.

In conclusion, standard network metrics applied to images can be a useful way to quickly assess the structure of networks within a soil profile, by capturing the broad structural differences between distinct soil types, in a way that can suggest functional differences as well. These initial estimates can be used on their own to survey an area more extensively or affordably, or coupled with more intensive analyses, such as three-dimensional imaging techniques. Agent-based modelling can also be used, when seeded with networks obtained from images or scans, to evaluate interactions between consumer and resource characteristics and network structure, and to quantify the impact these and other environmental factors have on the outcomes of simulated populations. Overall, combining network analysis and simulation modelling can provide unique insights on the structure, function, and diversity of an area of soil, and provide avenues for exploring the impact of future management, structural, or environmental changes.

3.6. References

- Aitkenhead, M. J. *et al.* (1999) 'Modelling water release and absorption in soils using cellular automata', *Journal of Hydrology* 220(1-2), pp. 104-112. doi: 10.1016/S0022-1694(99)00067-0.
- Aitkenhead, M. *et al.* (2016) 'Automated soil physical parameter assessment using smartphone and digital camera imagery', *Journal of Imaging*, 2(4). doi: 10.3390/jimaging2040035.
- Anderson, J. M. (1978) 'Inter- and intra-habitat relationships between woodland cryptostigmata species diversity and the diversity of soil and litter microhabitats', *Oecologia*, 32, pp. 341-348. doi: <https://doi.org/10.1007/BF00345112>.
- Baer, S. G. *et al.* (2005) 'Soil Heterogeneity Effects on Tallgrass Prairie Community Heterogeneity: An Application of Ecological Theory to Restoration Ecology', *Restoration Ecology*, 13(2), pp. 413–424. doi: 10.1111/j.1526-100x.2005.00051.x.
- Barabási, A.-L. (2016) *Network Science*. Cambridge, UK: Cambridge University Press.
- Bardgett, R. D., Yeates, G. W. and Anderson, J. M. (2009) 'Patterns and determinants of soil biological diversity', in *Biological Diversity and Function in Soils*, pp. 100–119.
- Bivand, R. S., Pebesma, E. and Gomez-Rubio, V. (2013) *Applied spatial data analysis with R*. 2nd edn. New York, New York, USA: Springer. Available at: <http://www.asdar-book.org>.
- ten Broeke, G., van Voorn, G. and Ligtenberg, A. (2016) 'Which Sensitivity Analysis Method Should I Use for My Agent-Based Model?', *Journal of Artificial Societies and Social Simulation*, 19(1), pp. 1–35. doi: 10.18564/jasss.2857.
- Brown, J. H. *et al.* (2004) 'Toward a metabolic theory of ecology', *Ecology*, 85(7), pp. 1771–1789. doi: 10.1890/03-9000.
- Crawford, J. W. *et al.* (2012) 'Microbial diversity affects self-organization of the soil - Microbe system with consequences for function', *Journal of the Royal Society Interface*, 9(71), pp. 1302–1310. doi: 10.1098/rsif.2011.0679.
- Crawford, J. W., Ritz, K. and Young, I. M. (1993) 'Quantification of fungal morphology, gaseous transport and microbial dynamics in soil: an integrated framework utilising fractal geometry', *Geoderma*, 56(1–4), pp. 157–172. doi: 10.1016/0016-7061(93)90107-V.

Csardi, G. and Nepusz, T. (2006) 'The igraph software package for complex network research', *InterJournal, Complex Sy*, p. 1695.

Davis, N. *et al.* (2020). 'Trajectories toward maximum power and inequality in resource distribution networks', *PLoS ONE*, 15(3), e0229956. doi: <https://doi.org/10.1371/journal.pone.0229956>.

Davis, N. and Polhill, J. G. (2021). 'Soil network simulation (Version 1.0.1)', *Zenodo*. <http://doi.org/10.5281/zenodo.4001621>

Davis, N. (2020) 'Soil network analysis functions (Version 1.0.0)!' *Zenodo*. <http://doi.org/10.5281/zenodo.4001702>

Dinno, A. (2017) 'dunn.test: Dunn's Test of Multiple Comparisons Using Rank Sums.' R package version 1.3.5. <https://CRAN.R-project.org/package=dunn.test>

Epskamp, S. *et al.* (2012) 'qgraph: Network Visualizations of Relationships in Psychometric Data', *Journal of Statistical Software*, 48(4), pp. 1–18.

Ettema, C. H. and Wardle, D. A. (2002) 'Spatial soil ecology', *Trends in Ecology and Evolution*, 17(4), pp. 177–183. doi: 10.1016/S0169-5347(02)02496-5.

FAO (2015) *World reference base for soil resources 2014: International soil classification system for naming soils and creating legends for soil maps, World Soil Resources Reports No. 106*. Rome, Italy: Food and Agriculture Organization of the United Nations. doi: 10.1017/S0014479706394902.

Fernández, R. *et al.* (2019) 'Pore morphology reveals interaction of biological and physical processes for structure formation in soils of the semiarid Argentinean Pampa', *Soil and Tillage Research*. Elsevier, 191, pp. 256–265. doi: 10.1016/j.still.2019.04.011.

García-Palacios, P. *et al.* (2012) 'Plant responses to soil heterogeneity and global environmental change', *Journal of Ecology*, 100(6), pp. 1303–1314. doi: 10.1111/j.1365-2745.2012.02014.x.

Gargiulo, L., Mele, G. and Terribile, F. (2013) 'Image analysis and soil micromorphology applied to study physical mechanisms of soil pore development: An experiment using iron oxides and calcium carbonate', *Geoderma*. Elsevier B.V., 197–198, pp. 151–160. doi: 10.1016/j.geoderma.2013.01.008.

Giller, Paul S. (1996) 'The diversity of soil communities, the 'poor man's tropical rainforest'', *Biodiversity and Conservation*, 5, pp. 135-168. doi: <https://doi.org/10.1007/BF00055827>.

- Grimm, V. *et al.* (2006) 'A standard protocol for describing individual-based and agent-based models', *Ecological Modelling*, 198(1–2), pp. 115–126. doi: 10.1016/j.ecolmodel.2006.04.023.
- Grimm, V. *et al.* (2010) 'The ODD protocol: A review and first update', *Ecological Modelling*, 221(23), pp. 2760–2768.
- Hartemink, A. E. and Minasny, B. (2014) 'Towards digital soil morphometrics', *Geoderma*. Elsevier B.V., 230–231, pp. 305–317. doi: 10.1016/j.geoderma.2014.03.008.
- Hausser, J. and Strimmer, K. (2014) 'entropy: Estimation of Entropy, Mutual Information and Related Quantities.' R package version 1.2.1. <https://CRAN.R-project.org/package=entropy>
- Helgason, B. L., Walley, F. L. and Germida, J. J. (2010) 'No-till soil management increases microbial biomass and alters community profiles in soil aggregates', *Applied Soil Ecology*. Elsevier B.V., 46(3), pp. 390–397. doi: 10.1016/j.apsoil.2010.10.002.
- Hill, M. O. (1973) 'Diversity and evenness: A unifying notation and its consequences', *Ecology*, 54(2), pp. 427–432.
- Kay M., Wobbrock J. (2020) 'ARTool: Aligned Rank Transform for Nonparametric Factorial ANOVAs.' doi: 10.5281/zenodo.594511
- Kooijman, S. A. L. M. (2009) *Dynamic Energy Budget Theory for Metabolic Organisation*. 3rd edn. Cambridge, UK: Cambridge University Press.
- Kravchenko, A. N. *et al.* (2011) 'Long-term Differences in Tillage and Land Use Affect Intra-aggregate Pore Heterogeneity', *Soil Science Society of America Journal*, 75(5), pp. 1658–1666. doi: 10.2136/sssaj2011.0096.
- Kravchenko, A. N. and Guber, A. K. (2017) 'Soil pores and their contributions to soil carbon processes', *Geoderma*. Elsevier B.V., 287, pp. 31–39. doi: 10.1016/j.geoderma.2016.06.027.
- Kuznetsova, A., Brockhoff, P. B., Christensen, R. H. B. (2017) 'lmerTest Package: Tests in Linear Mixed Effects Models', *Journal of Statistical Software*, 82(13), pp. 1–26. doi: 10.18637/jss.v082.i13
- Lenth, R. (2020). 'emmeans: Estimated Marginal Means, aka Least-Squares Means', R package version 1.5.0. <https://CRAN.R-project.org/package=emmeans>

Levins, R. (1966) 'The strategy of model-building in population biology', *American Scientist*. Sigma Xi, 54(4), pp. 421-431. www.jstor.org/stable/27836590.

Lorscheid, I., Heine, B.-O. and Meyer, M. (2012) 'Opening the "black box" of simulations: increased transparency and effective communication through the systematic design of experiments"', *Computational and Mathematical Organization Theory*. Springer US, 18(1), pp. 22–62. doi: 10.1007/s10588-011-9097-3.

Mangiafico, S. (2020) 'rcompanion: Functions to Support Extension Education Program Evaluation.' R package version 2.3.25. <https://CRAN.R-project.org/package=rcompanion>

Mones, E., Vicsek, L. and Vicsek, T. (2012) 'Hierarchy measure for complex networks', *PLoS ONE*, 7(3), pp. 1–10. doi: 10.1371/journal.pone.0033799.

Nielson, U. N. *et al.* (2010) 'The enigma of soil animal species diversity revisited: The role of small-scale heterogeneity', *PLoS ONE*, 5(7), e11567. doi: 10.1371/journal.pone.0011567.

Oades, J. M. (1993) 'The role of biology in the formation, stabilization and degradation of soil structure', *Geoderma*, 56(1–4), pp. 377–400. doi: 10.1016/0016-7061(93)90123-3.

Pebesma, E. J. and Bivand, R. S. (2005) 'Classes and methods for spatial data in R', *R News*, 5(2). Available at: <https://cran.r-project.org/doc/Rnews/>.

Polhill, G. and Gimona, A. (2014) 'Using genetic algorithms to fit species and habitat parameters for modelling the effect of climate change on species distributions with stochastic patch occupancy models', *Proceedings - 7th International Congress on Environmental Modelling and Software: Bold Visions for Environmental Modeling, iEMSs 2014*, 3.

R Core Team (2020) 'R: A Language and Environment for Statistical Computing', *R Foundation for Statistical Computing*. Vienna, Austria, p. <https://www.R-project.org>. Available at: <http://www.r-project.org>.

Rockafellar, R. T. (1970) *Convex Analysis*. Princeton, NJ: Princeton University Press.

Rodrigue, J. P. (2017) *The Geography of Transport Systems*. Hofstra University, Department of Global Studies & Geography. Available at: <https://transportgeography.org>.

- Roshier, D.A., Doerr, V. A. J. and Doerr, E. D. D. (2008) 'Animal movement in dynamic landscapes: interaction between behavioural strategies and resource distributions', *Oecologia*, 156, pp. 465-477. doi: 10.1007/s00442-008-0987-0.
- Spellerberg, I. F. and Fedor, P. J. (2003) 'A tribute to Claude Shannon (1916–2001) and a plea for more rigorous use of species richness, species diversity and the “Shannon–Wiener” Index', *Global Ecology and Biogeography*, 12, pp. 177–179. doi: 10.1046/j.1466-822X.2003.00015.x.
- Stevens, R. D. and Tello, J. S. (2011) 'Diversity begets diversity: relative roles of structural and resource heterogeneity in determining rodent community structure', *Journal of Mammalogy*, 92(2), pp. 387–395. doi: 10.1644/10-mamm-a-117.1.
- Sturges, H. A. (1926) 'The choice of a class interval', *Journal of the American Statistical Association*, 21(153), pp. 65-66. doi: 10.1080/01621459.1926.10502161.
- Tews, J. *et al.* (2004) 'Animal species diversity driven by habitat heterogeneity/diversity: The importance of keystone structures', *Journal of Biogeography*, 31(1), pp. 79–92. doi: 10.1046/j.0305-0270.2003.00994.x.
- Velde, B., Moreau, E. and Terribile, F. (1996) 'Pore networks in an Italian vertisol: Quantitative characterisation by two dimensional image analysis', *Geoderma*, 72(3–4), pp. 271–285. doi: 10.1016/0016-7061(96)00033-X.
- Vezzani, F. M. *et al.* (2018) 'The importance of plants to development and maintenance of soil structure, microbial communities and ecosystem functions', *Soil and Tillage Research*. Elsevier, 175(March 2017), pp. 139–149. doi: 10.1016/j.still.2017.09.002.
- Wickham, H. (2016) *ggplot2: Elegant Graphics for Data Analysis*. New York: Springer-Verlag. Available at: <http://ggplot2.org>.
- Wickham, H. *et al.* (2019) 'dplyr: A Grammar of Data Manipulation'.
- Wijesinghe, D. K., John, E. A. and Hutchings, M. J. (2005) 'Does pattern of soil resource heterogeneity determine plant community structure? An experimental investigation', *Journal of Ecology*, 93(1), pp. 99–112. doi: 10.1111/j.1365-2745.2004.00934.x.

Wobbrock, J., Findlater, L., Gergle, D., Higgins, J. (2011) 'The Aligned Rank Transform for Nonparametric Factorial Analyses Using Only ANOVA Procedures.' In *Proceedings of the ACM Conference on Human Factors in Computing Systems (CHI '11)*, pp. 143-146.

Young, I. M., Crawford, J. W. and Rappoldt, C. (2001) 'New methods and models for characterising structural heterogeneity of soil', *Soil and Tillage Research*, 61(1–2), pp. 33–45. doi: 10.1016/S0167-1987(01)00188-X.

Young, I. M. and Ritz, K. (2000) 'Tillage, habitat space and function of soil microbes', *Soil and Tillage Research*, 53(3–4), pp. 201–213. doi: 10.1016/S0167-1987(99)00106-3.

Young, I. M. and Ritz, K. (2009) 'The habitat of soil microbes', in *Biological Diversity and Function in Soils*, pp. 31–43.

Zeileis, A. (2014) 'ineq: Measuring Inequality, Concentration, and Poverty.' R package version 0.2-13. <https://CRAN.R-project.org/package=ineq>

3.7. Appendices

Appendix 1. Network extraction process

For all images:

1. Convert the image to a text file containing RGB triplets
2. Identify and eliminate all non-soil pixels (set to -1)
3. Calculate mean pixel intensity at all points
4. Adjust pixel intensity to remove variations in brightness across image
5. Threshold the image to retain the darkest 30 % soil pixels
6. Carry out erosion and thinning operators
7. Clean image to produce skeletal pixels
8. Identify networks
9. Remove redundant pathways
10. Calculate distances between nodes
11. Save the network

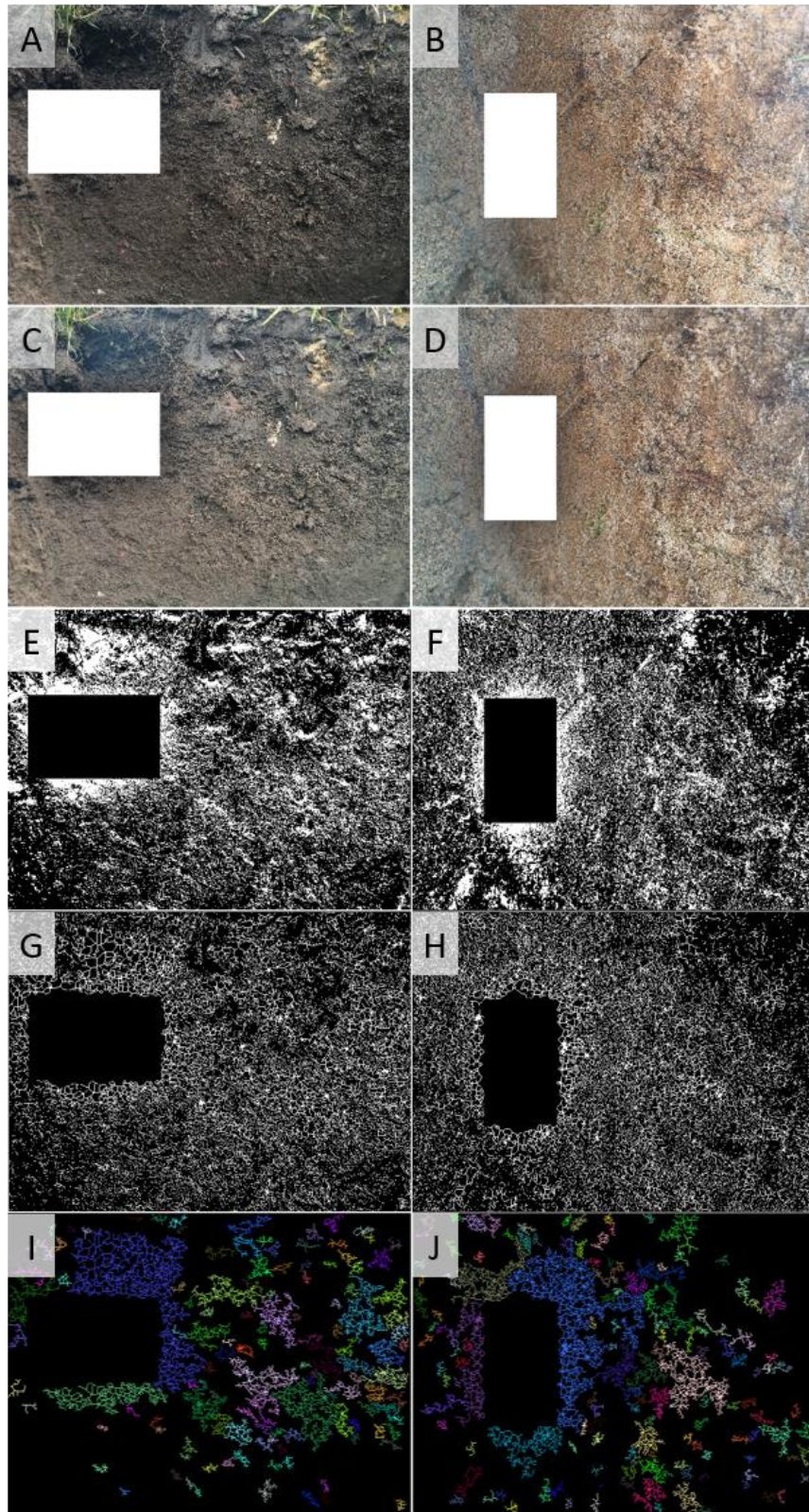


Figure A1. Soil image morphology process for a Cambisol (a) and Arenosol (b) profile image. Steps show include (c-d) colour correction, (e-f) thresholding, (g-h) erosion and thinning operations, and (i-j) subnetwork identification. White areas represent colour correction cards, which were excised.

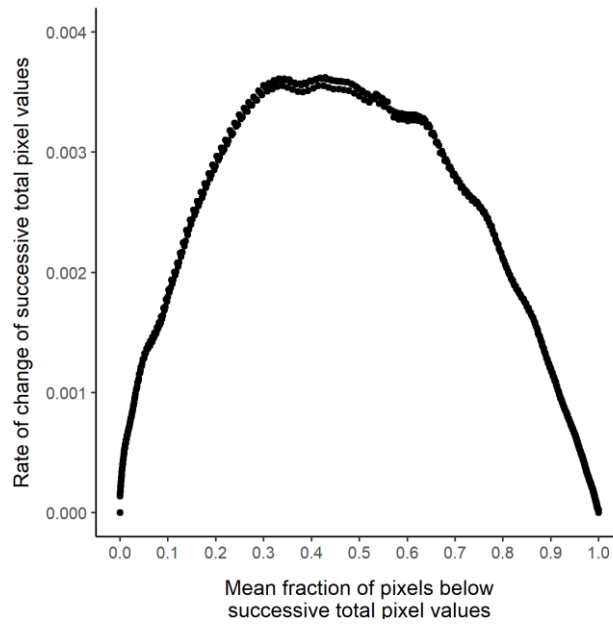


Figure A2. The rate of change of mean fraction of pixels for each mean fraction below a given threshold value. The plot starts on the left with pixel values of 0, with no pixels below this value, and ends on the right with pixel values of 755 (with correction card removed from image). The y-axis shows the rate of change of the mean fraction of pixels below each value.

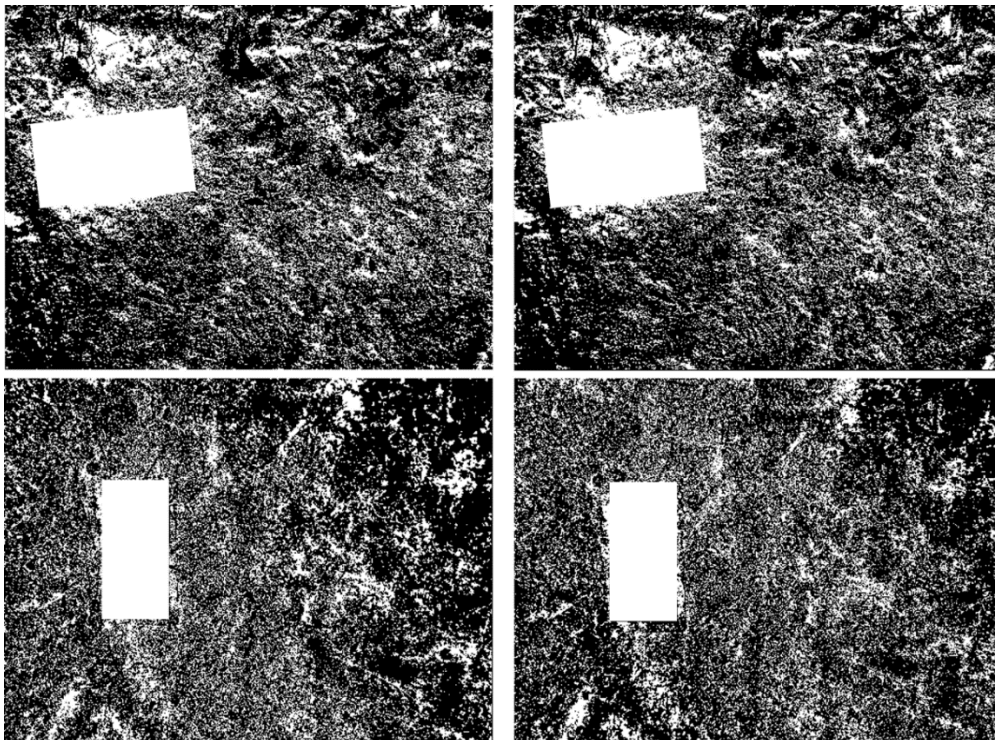


Figure A3. Comparison of different images from the same pit after thresholding. The two pairs of images from each pit are arranged horizontally. The white rectangle is the correction card. The thresholding process was the same as described in Section 2.2, where the darkest 30 % of pixels have been retained as pores, and other pixels removed.

Appendix 2. ODD design concepts, initialisation, input data, and submodels

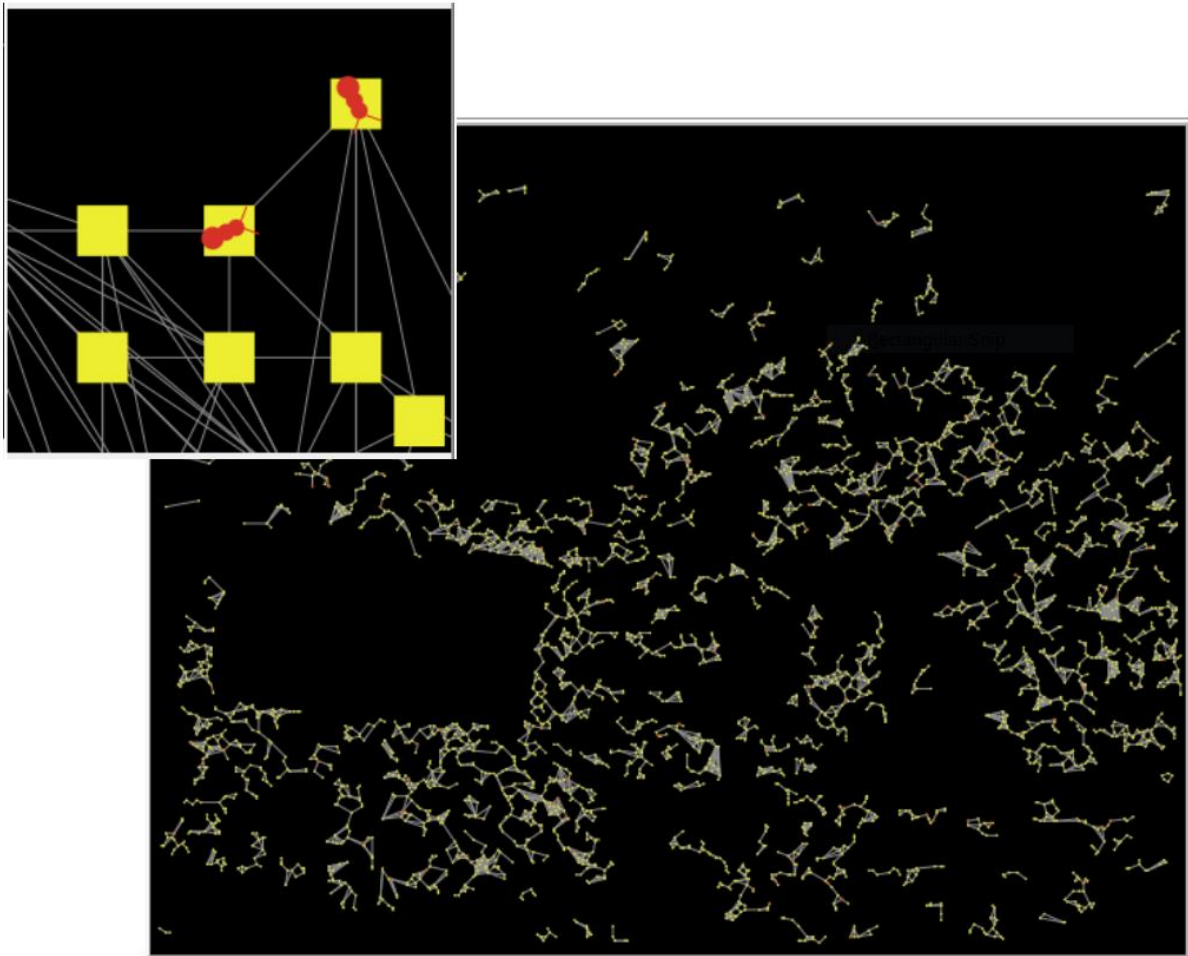


Figure A4. A screenshot of the model. The inset at the top left shows an enlarged version of some of the resource nodes (yellow squares) and agents (red ants).

IV. Model purpose

The model is designed to be an analytical tool to explore the heterogeneity in resource supply potential of a network by populating it with idealised energy-consuming agents, and to quantify the effects of consumer, resource, and network characteristics on resulting consumer population outcomes.

V. Entities, state variables, and scales

i. Consumer entities

State variables

Property	Description
Location	The resource on which the consumer is located
Target location	The resource to which the consumer will move next
Active?	Whether a consumer is active (or dead)

Parameters

Property	Description
Basal metabolism	How much resource an agent needs per day to stay alive
Active metabolism	How much resource an agent uses with each step
Resource stock	How much resource an agent has consumed but not metabolised
Consumption rate	Maximum number of resource units that an agent takes from a resource it visits, per timestep
Spawn energy	How much energy an agent requires to spawn (depletes this quantity from stocks and passed to offspring as starting quota)

ii. Resource entities

State variables

Property	Description
Current supply	The current quantity of resource at this point

Parameters

Property	Description
Resource capacity	How much energy is stored in a resource when it is full
Regrow rate	The amount the resource regrows each timestep

iii. Link entities

State variables

Property	Description
Length	The length of the link - determines energy and time required to traverse it

Scales

Property	Description
Timestep	A single unit of time in the model, defined as that which is required for consumers to move 1 pixel (approximately 0.3 – 0.5 mm), and for which they require basal-metabolism units of energy.
World size	400 x 500, determined by the size of the soil networks used as the environment.

VI. Sequence of events

1. Consumers start on random nodes around a pre-specified network, where nodes are resource patches.
2. Consumers move around the network randomly following links. If they find a resource patch, they consume as much as they can from it, and the patch depletes.
 - Consumers require basal-metabolism units of resource per timestep. If they do not consume this resource, they die.
 - Consumers can stay put on a resource and consume it (consumption-rate units consumed per timestep), but it depletes, and if there is no more resource there then they move on.
 - Consumers metabolise active-metabolism units of resource per patch of link that they cross.
 - If there is more than one agent on a resource patch, they each take consumption-rate units per timestep, or split the remainder if there is not enough resource remaining for them to each get consumption-rate units.
3. If consumers have twice as much energy as the set spawn-energy, they can spawn new consumers (who take the same amount of resource-stock from their parent that the parent started with, so now parent and offspring both have the same resource-stock).
4. Resources regrow at a constant rate (regrow-rate) per timestep, up to their maximum capacity (resource-capacity).

VII. Design concepts

a. Basic principles

- i. Consumers attempt to consume as much free energy from a resource as they are able, to maximise energy reserves for future movement, and spawning capability.
- ii. Conservation equations: energy and matter cannot be created (except at the start of the simulation) or destroyed. In spawning, this is represented by consumers transferring some of their energy to their offspring. Consumers only die when their energy reserves are completely depleted (starvation).
- iii. Entropy production: some resource energy is consumed in movement and cannot be recaptured.

b. Emergence

- i. The distribution of consumers in space around the network and the distribution of resource stocks across the consumers both emerge from the interactions in the model.

c. Objectives

- i. The consumers' objective is to consume as much resource energy as possible, allowing them to stay alive, move, and potentially reproduce.

d. Prediction

- i. Consumers do not 'predict' the results of their course of action per se, they are random walkers, but they do 'predict' that they will die if they stay in a non-resource patch, or depleted resource patch, so they keep moving.

e. Sensing

- i. Consumers can sense if they are on a resource patch or not, and if it has any resource energy in it. They also know the link-neighbours of the resource patch that they are currently on.
- f. Learning
 - i. Consumers are random walkers; they do not learn in any capacity.
- g. Adaptation
 - i. The population adapts to fill the network in a way that reflects the density of resource availability in that area, as consumers will cluster and reproduce around resources where they can consume what they need.
- h. Interaction
 - i. Consumers interact stigmergically through their consumption of resources. While they do not interact directly in any meaningful way, their consumption of resources affects the availability of resources for others to consume.
- i. Collectives
 - i. There are no collectives present.
- j. Stochastic elements
 - i. Consumers are initialised in random locations and move randomly. Additionally, resources are all initialised with random maximum capacity between 1 and `maximum-resource-capacity` and regrow rates between 1 and `maximum-regrow-rate`.
- k. Observation
 - i. Number of currently active ('alive') consumers at each timestep.
 - ii. Mean, standard deviation (SD), Gini coefficient, and entropy of the distribution of consumer resource stocks at each timestep.

- iii. The resource capacity and regrow rate of each resource at the start of the simulation.
- iv. The resource stock and location of each active consumer at 10, 100, 500, 1000, and 2000 timesteps.

VIII. Initialisation

- a. The network was supplied as two Comma-Separated Values (CSV) files: one of resource node locations and another of the connections between the resource nodes. The node locations and connections were determined during the process of extracting the soil network from a soil profile image, as described in the main text (Section 2.2). The resource and consumer types and parameters were specified in an Extended Markup Language (XML) file. The models were initialised with 500 consumers located on random resource nodes throughout the network. The consumers each began with 30 resource units in their `resource-stock`, and metabolic rates, consumption rate, and spawn energy thresholds as specified in the XML file. Resources were all initialised with random maximum capacity between 1 and `maximum-resource-capacity` and regrow rates between 1 and `maximum-regrow-rate` and began the simulation at full capacity.

IX. Input data

- a. This model has no input data.

X. Submodels

- a. Regrowth of resources: at each timestep, all resources that are less than their maximum capacity regrow by `regrow-rate` units.
- b. Consuming resources: at each timestep, all consumers currently located on a resource node check whether there is any resource available at that node. If there is enough for each consumer to take `consumption-rate` units, they do, and these are added to their `resource-supply`. If there is not enough, each

consumer receives what is at the resource, divided by the number of consumers at the resource. If there is no resource available at that node, the consumer identifies a new target-node, selecting randomly from the other resources connected to the first, and moves to the target-node.

- c. Spawning new consumers: at each timestep, consumers check whether they have twice the amount of energy specified as spawn-energy in their resource-stock. If so, they spawn a new consumer who is an exact clone of themselves. The new consumer starts with spawn-energy units as their initial resource-supply, and the parent consumer loses spawn-energy units of resource from their resource-stock.
- d. Check consumer resource stocks: at each timestep, all consumers check whether they have more than resource-requirement units, or their basal metabolism, of resource in their resource-supply. If they do, they consume resource-requirement units, removing them from their resource-supply, otherwise they die.

1.1.1. Appendix 3. Sensitivity Analysis

First, a pre-test was conducted to determine the number of time steps for which to run the simulations, and the number of replicates of each parameter set that were necessary for the outputs to reach equilibrium (ten Broeke, van Voorn and Ligtenberg, 2016). The first set of 500 runs used varied parameter values and a fixed network architecture, determined by Latin Hypercube Sampling from the range of values for global analysis (Table A1). One replicate of each parameter set was run for 3000 timesteps, and the output variables were plotted to determine whether the model reached a stable state, and if so, when. As all runs showed stability in output parameters after 500 – 1000 timesteps (Figure A5), apart from small variations due to stochasticity, the final output variable values for all future runs were calculated as the mean of the values at timesteps 500, 750, and 1000.

Table A1. Parameter ranges used for testing to determine length of simulations. Values shown are the minimum and maximum for that parameter. Latin Hypercube Sampling was used to generate the values, which were then multiplied by the range plus the minimum, to get the value for the parameter for testing.

Parameter	Value
Initial population size	50, 1000
Consumer basal metabolism	1, 3
Consumer active metabolism	1, 3
Initial consumer resource stock	20, 50
Consumer consumption rate	5, 10
Consumer spawn energy	50, 100
Maximum resource capacity	20, 50
Maximum resource regrowth rate	10, 20

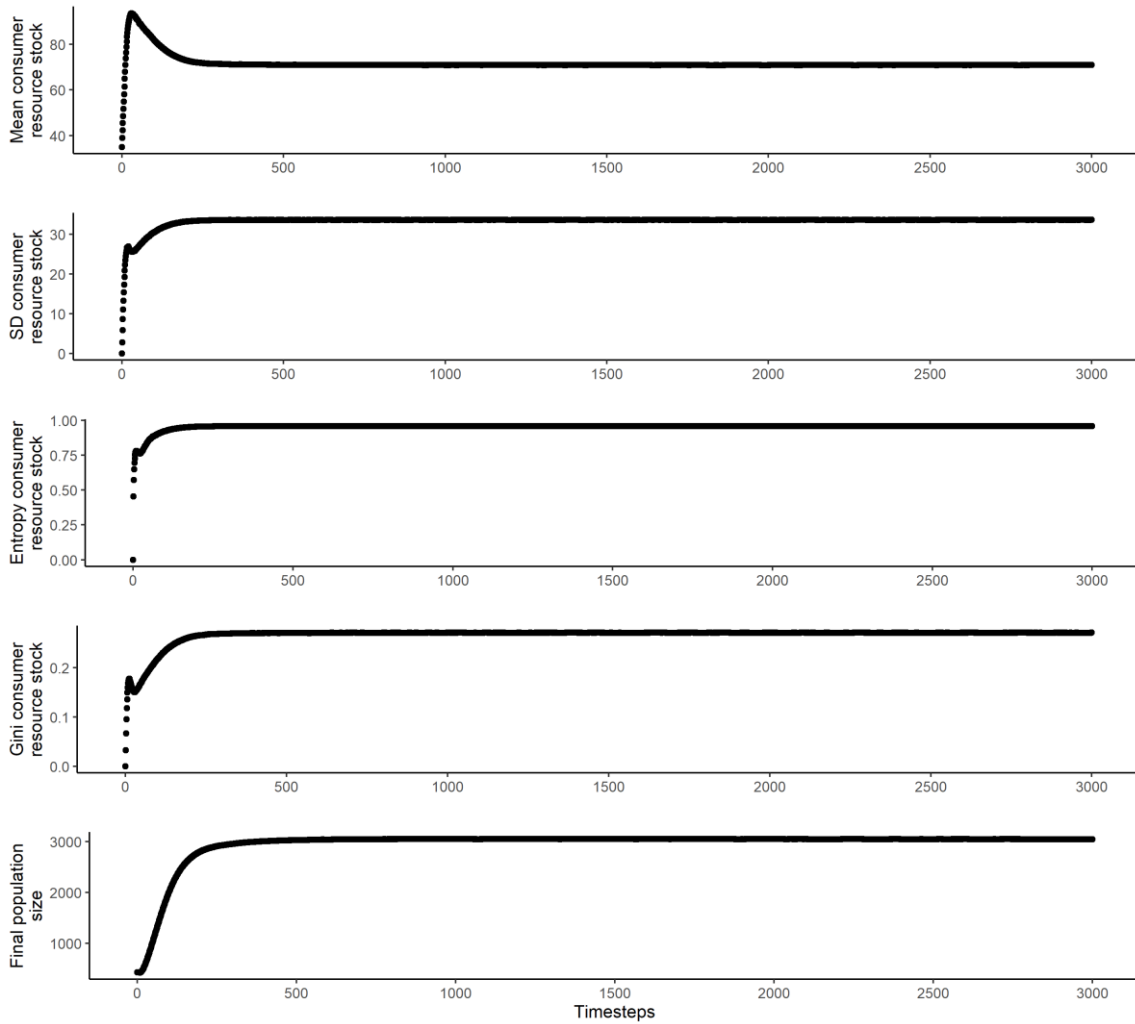


Figure A5. Stability plots from testing to determine the length of simulations. Shown are values averaged for each timestep over 500 runs.

The second set of pre-test runs used the baseline parameter values for all parameters, and a fixed network, which we repeated 100 times. We then calculated a rolling coefficient of variation for the output variables, including progressively more replicates (Figure A6). The coefficients of variation for all output variables stabilised around 10 runs. Plotting the distribution of the output variables at that point show approximate normality, such that the mean value across runs is a reasonable measure of centre. Therefore, for all future simulations, the mean of the outcome variables across 10 replicates was used to reduce the effects of stochasticity on the output. As the mean value across replicates was used, there was no effect from replication on the experimental results.

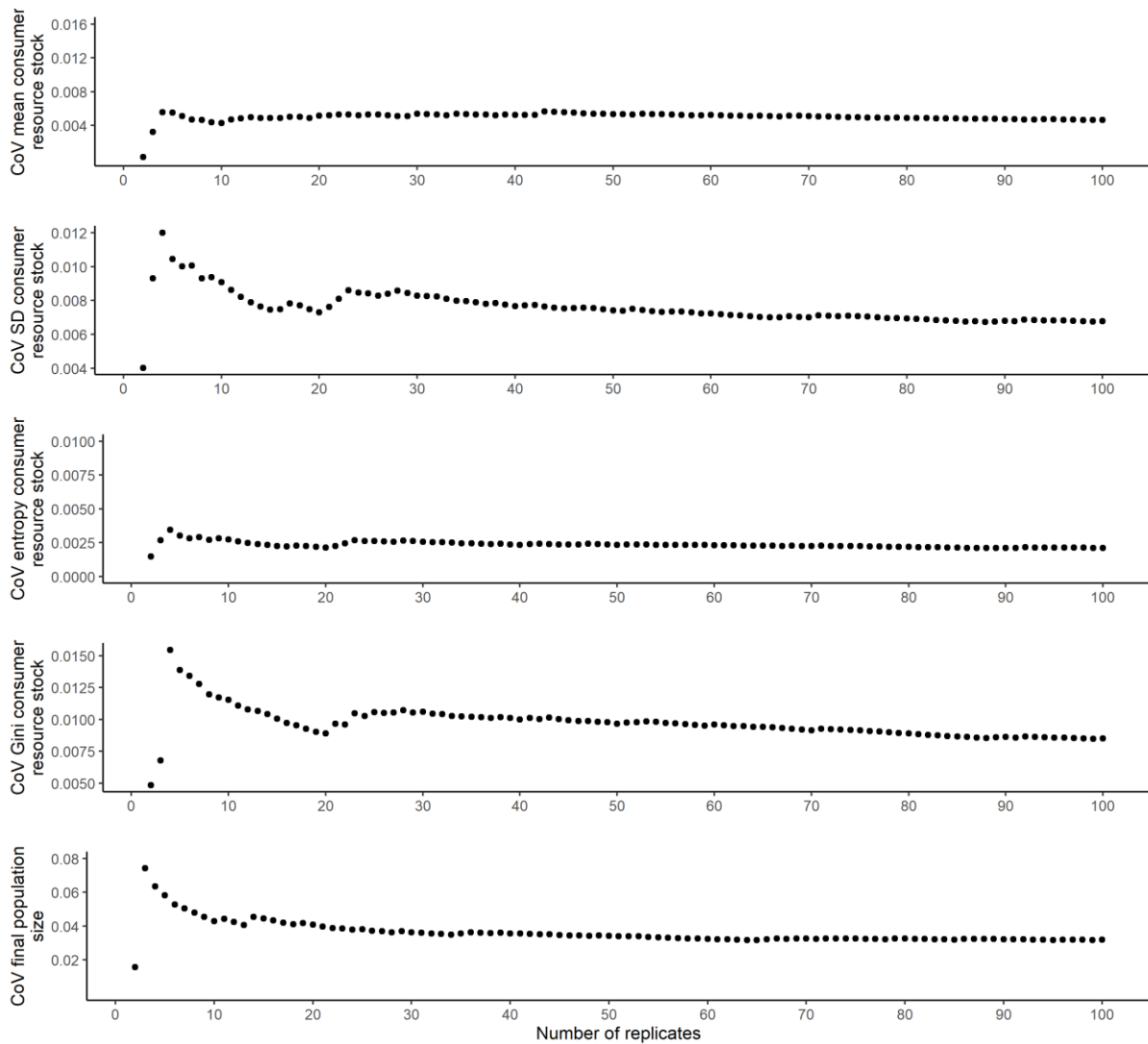


Figure A6. Plots of rolling Coefficient of Variation (CoV) for each outcome variable against the number of replicates included in its calculation. This was used to determine number of replicates needed to average across to minimise stochasticity in output variables.

After the pre-test, we used the One-Factor-at-a-Time methodology to identify which of the control variables significantly affected the output variables, and which could be held constant. For this test, the four control variables (initial consumer population, initial consumer resource stock, maximum resource regrowth rate, and maximum resource capacity) were varied across four levels each, changing one variable at a time, while holding all other variables constant at middle values for each. Both the maximum resource regrowth rate and maximum resource capacity significantly affected the output variables, while initial consumer resource stock did not (Table A2). The initial consumer population size significantly affected all but the standard deviation of consumer resource

stock (Table A2e), but as the magnitude of the effect was quite small, both the initial population size and initial consumer resource stock were held constant at middle values for the rest of the simulations.

Table A2. Regression results from One-Factor-at-a-Time analysis. This was used to identify which control parameters could be fixed, and which significantly affected the outcome variables and needed to be explored. The asterisks designate level of significance: $p < 0.1$: ·, $p < 0.05$: *, $p < 0.01$: **, $p < 0.001$: ***.

a. Mean consumer resource stock

	Estimate	Standard error	t value	p
Intercept	54.360	0.100	543.566	0.000 ***
Initial population size	0.000	0.000	-3.728	0.002 ***
Initial consumer resource stock	0.000	0.001	0.100	0.920
Maximum resource regrow rate	0.054	0.004	12.874	0.000 ***
Maximum resource capacity	0.060	0.001	41.088	0.000 ***
F(4, 251) = 467 ($p < 0.001$)		R ² = 0.88		

b. SD consumer resource stock

	Estimate	Standard error	t value	p
Intercept	27.110	0.038	711.283	0.000 ***
Initial population size	0.000	0.000	0.948	0.344
Initial consumer resource stock	0.000	0.000	0.333	0.739
Maximum resource regrow rate	0.016	0.002	10.073	0.000 ***
Maximum resource capacity	-0.010	0.000	-17.718	0.000 ***
F(4, 251) = 104.1 ($p < 0.001$)		R ² = 0.62		

c. Entropy consumer resource stock

	Estimate	Standard error	t value	p
Intercept	0.953	0.000	2288.704	0.000 ***
Initial population size	0.000	0.000	6.500	0.000 ***
Initial consumer resource stock	0.000	0.000	0.446	0.656
Maximum resource regrow rate	0.000	0.000	19.891	0.000 ***
Maximum resource capacity	0.000	0.000	2.891	0.004 **
F(4, 251) = 111.6 ($p < 0.001$)		R ² = 0.63		

(cont.)

d. Gini consumer resource stock

	Estimate	Standard error	t value	p
Intercept	0.283	0.000	431.434	0.000 ***
Initial population size	0.000	0.000	3.472	0.001 ***
Initial consumer resource stock	0.000	0.000	0.154	0.876
Maximum resource regrow rate	0.000	0.000	-2.267	0.024*
Maximum resource capacity	0.000	0.000	-38.517	0.000 ***
F(4, 251) = 375.2 ($p < 0.001$)	R ² = 0.85			

e. Final population size

	Estimate	Standard error	t value	p
Intercept	-2787.749	188.701	-14.773	0.000 ***
Initial population size	2.496	0.118	21.110	0.000 ***
Initial consumer resource stock	0.589	2.738	0.215	0.830
Maximum resource regrow rate	191.341	8.038	23.805	0.000 ***
Maximum resource capacity	61.961	2.738	22.634	0.000 ***
F(4, 251) = 381.2 ($p < 0.001$)	R ² = 0.86			

1.1.2. Appendix 4. Calculation of Entropy

The entropy of the consumer resource stocks was calculated as the Shannon index, or Shannon entropy, of the resource stocks held by consumers. As the Shannon entropy is meant to be applied to discrete data, the consumer resource stocks were discretised into a fixed number of ‘bins’ using Sturges’ formula (Sturges, 1926), and the Shannon entropy was calculated for the bins.

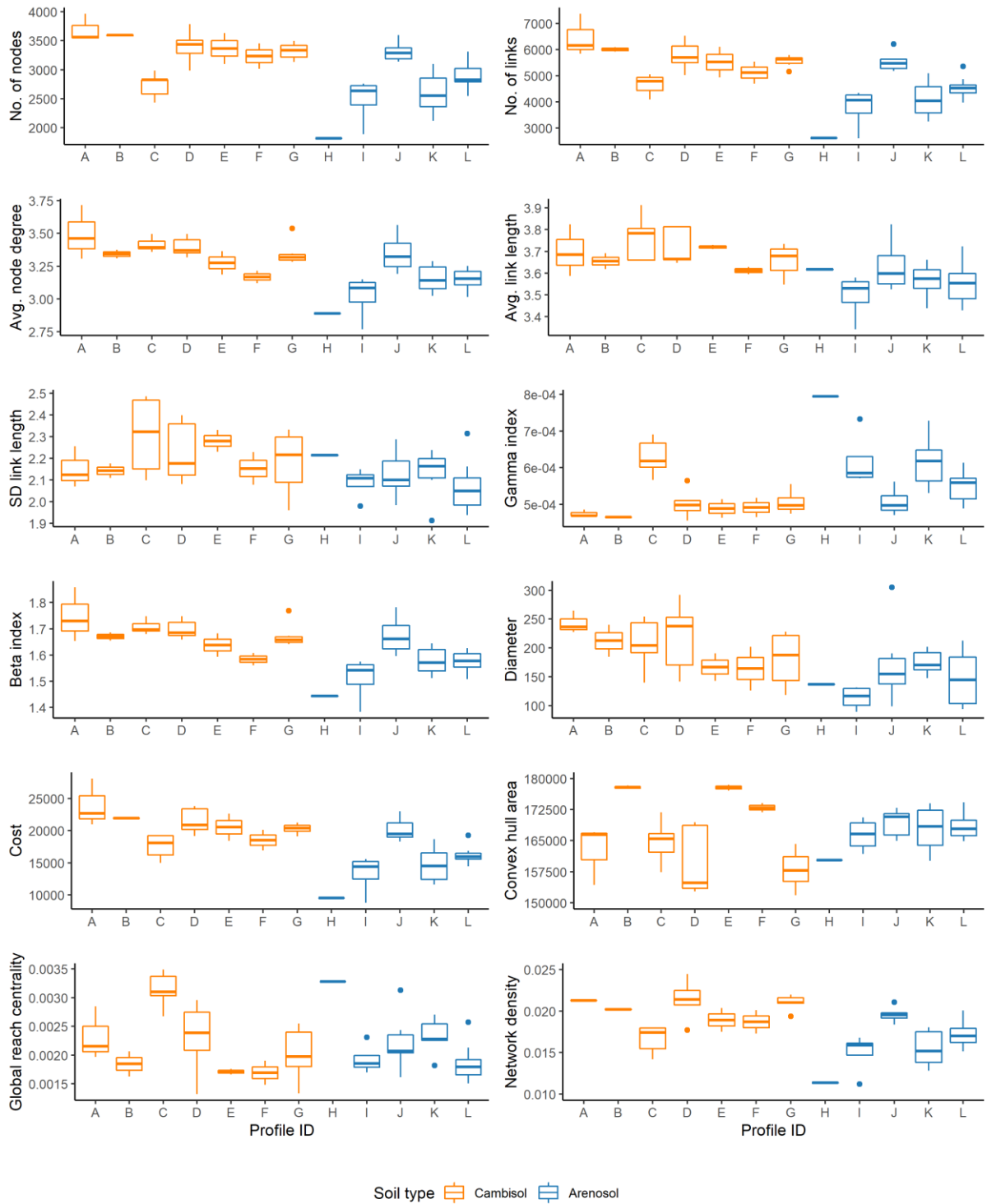
Sturges’ formula for the number of bins k for a population of size n is

$$k = \lceil \log_2 n \rceil + 1. \quad (1)$$

Using a sample of 100 runs from the stability test for run length (Section A3), the normality of the consumer resource stocks at the sampling timesteps $T = 500$, $T = 750$, and $T = 1000$ was tested. Additionally, the entropy was calculated for 5, 10, 15, 20, 25, 50, 75, and 100 bins and compared with the entropy binned using Sturges’ formula. By normalising the calculated entropy by the maximum possible entropy for that number of bins, $\log(N)$, the differences in entropy between

different numbers of bins were < 0.001 . As the data were found to be approximately normally distributed at the sampling timesteps, the assumptions for Sturges' formula was met, and it was chosen to determine the final bin width.

A



B

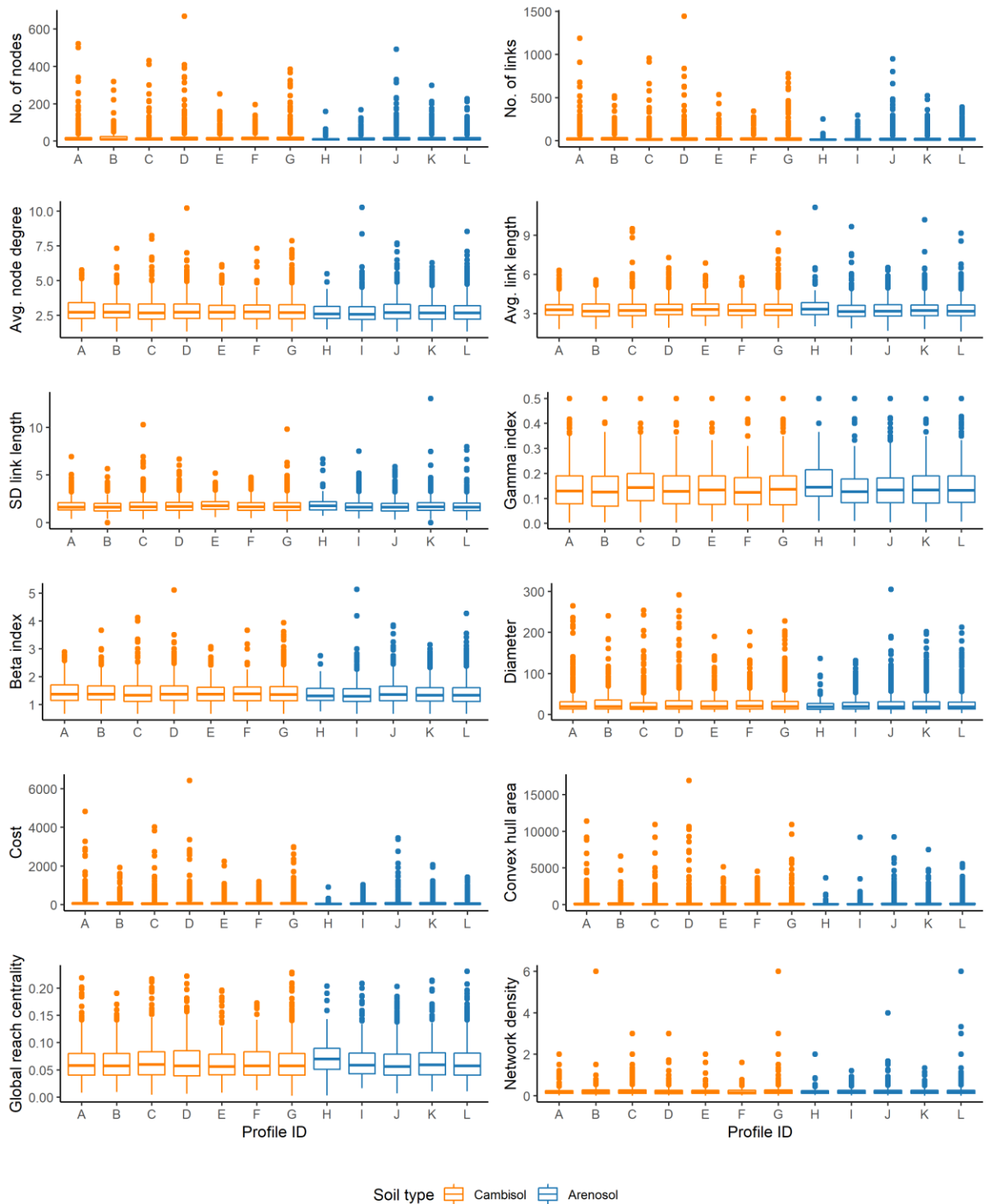


Figure A7. Boxplots showing distributions of network metrics across soil profiles for (a) main networks and (b) subnetworks. Profiles A – G correspond to Cambisol soil profiles, and profiles H – L are Arenosol soil profiles. Descriptions of network metrics are in Table 3.1.

4

The co-evolution of network structure and consumer inequality in a spatially explicit model of resource acquisition

Abstract

The inequality of resource distribution in society has been linked to significant public and individual health challenges, while in ecosystems heterogeneity is considered a driver of biodiversity and stability. Resource acquisition and distribution is mediated by complex networks that co-evolve with the system in question, to move resources from points of origin or acquisition to those of end use. Past research has focussed on effects of spatiotemporal resource heterogeneity in ecosystems, or socioeconomic drivers of inequality, but there has been less attention to the interactions between resource network structure and these population-level outcomes. Here, we investigate the relationships between landscape heterogeneity, resource network structure, and inequality between consumers. We develop a spatially-explicit, stock-flow consistent agent-based model of generic consumers building and crossing links between resources, attempting to maximise their own time-discounted consumption. We use this model to examine the co-evolution of the emergent network structure and inequality in the population across three distinct landscapes. Initially, the consumer inequality decreased during network construction, then increased rapidly as the network decayed to a more stable state. The spatial distribution of resources in each landscape constrained the structures that could emerge, and therefore the specific rates and timings of these dynamics. This work advances the understanding of possible relationships among a spatially-distributed set of resources, the network structure that connects them to a population, and inequality in that population, which can inform further work to better understand causes of inequality and heterogeneity in empirical systems.

4.1. Introduction

One of the most notable characteristics of ecological and socio-ecological systems is the difference in the quantities and types of energy sources that species and individuals consume. These inter- and intra-species differences in resource consumption are typically referred to as heterogeneity and inequality, respectively. Discussions of heterogeneity often focus on the environmental and ecological conditions governing the spatiotemporal distribution of resources, and the ways organisms move and adapt to exploit various resource niches (Tews *et al.*, 2004). In contrast, inequality is usually discussed in terms of differences between consumers – usually humans – in the quality or quantity of resources they have to meet their basic needs, and any excess (Mattison *et al.*, 2016). While the term ‘resources’ can refer to energy or water sources; habitats or housing; or the wealth, social status, skills, or ability to acquire these (Smith *et al.*, 2010), this work will focus on energy sources.

The movement of energetic resources to consumers, and vice versa, occurs through a diverse array of resource acquisition, distribution, and end-use (RADE) networks. These can take the form of flow networks, such as vascular systems or electrical grids, where the resource is transported through the network to the end consumers. Other networks are active transport networks, such as roads, railways, and foraging trails, where the consumers navigate through the network to obtain and use or relocate resources. These resources, whether naturally occurring in the landscape or artificially grown or generated, are heterogeneously located in space. The consumers are also heterogeneously located and may have a range of resource-related behaviours and preferences that determine how they construct, maintain, or interact with the RADE networks on which they rely. Therefore, the structure of the RADE networks connecting consumers and resources is rarely, if ever, uniformly distributed across the landscape. This can lead to inequality in resource access for the end consumers, either in the quantity or quality of resources they receive through the network,

or in the time and energy they spend navigating the network. In this way, the heterogeneous spatiotemporal distribution of resources in the environment is propagated through the network.

The energy required for transportation of resources, consumers, or both through RADE networks results from the frictional losses incurred by moving mass through space, in addition to the necessary losses resulting from the conversion of stored energy into these movements. All energy is contained within a mass carrier, such as the chemical bonds in food molecules, or the charged particles in electricity. Transporting this matter over space causes friction, which is also known as resistance, impedance, or drag in some systems. Overcoming friction consumes energy: this can be drained from the potential energy of the resource in flow networks, such as voltage drop in electrical grids, or taken from reserves of stored energy from previous resource flows in active transport networks, such as metabolism of previously eaten food during later foraging efforts. As both matter and energy are conserved, these frictional losses entail that the net energy that consumers gain from a resource flow is less than the energy output by that resource. When stored energy is considered, the full energy balance may have to be resolved over multiple timescales, but the reduction in energy due to frictional losses still applies. Given that these losses are proportional to the distance the resource or consumer moves, the environmental and RADE network heterogeneity described above implies that consumers experience unequal energetic costs for moving resources or themselves through the network, and therefore unequal net energy consumption.

There is an evolutionary pressure to maximise this net energy consumption, as it determines the fitness of the consumers, and the likelihood of their survival and reproduction (Lotka, 1922). This can be accomplished by minimising the energy used in transport, through reinvestment of net energy to expand and improve the RADE network. For example, widening or smoothing frequently used links in the network decreases the frictional losses incurred when moving consumers or resources through them. However, when consumers and groups direct the evolution

of the network to maximise their own consumption, the more well-endowed consumers can direct even more flow or create better access for themselves. This could lead to a self-perpetuating cycle of inequality. Many naturally-occurring and human-engineered RADE networks are in the form of hierarchical branching structures, or other minimum spanning tree networks, which are hypothesised to minimise the frictional losses of transportation when connecting heterogeneously located resources and consumers (West, Brown and Enquist, 1997; Banavar *et al.*, 2000). While this maximises the energy throughput, the highly heterogeneous network structure causes unequal resource flows and net energy consumption, especially as flows increase (Davis *et al.*, 2020).

Notably, although heterogeneity across species and inequality within species share similar origins in landscape and RADE network structural heterogeneity, the difference in possible outcomes in natural and social systems means that the former is a valued driver of biodiversity, while the latter is considered a major public health concern. Within ecological systems, the quantities, types, and accessibility of resources determines the amount and complexity of life that an area can support. While the exact shape of the ‘heterogeneity-biodiversity’ relationship posited for ecosystems is debated (*e.g.* Naeem and Colwell, 2012; Heidrich *et al.*, 2020), there is wide consensus on the presence of this relationship, and the positive outcomes for ecosystem stability (see reviews in Tews *et al.*, 2004; Stein, Gerstner and Kreft, 2014). In contrast, inequality in society has typically been studied through an economic or sociological lens (*e.g.* Stiglitz, 2012; Charlton, 1997). While financial inequality undoubtedly affects the distribution of physical resources such as food and energy, insecurity in these resources has also been implicated in increasing economic inequality and limiting the prospects of individuals to lift themselves out of poverty (see reviews in Olson, 1999; Gaye, 2007; Perez-Escamilla and de Toledo Vianna, 2012; Sovacool, 2012; Laraia, 2013; Long *et al.*, 2020).

Despite the considerable effects of inequality and heterogeneity, and the importance of RADE networks in mediating resource-consumer relationships, previous work has rarely focussed on the

inequality emerging in RADE networks or its co-evolution with network structure. Instead, RADE networks have typically been studied from the perspective of understanding or optimising some measure of efficiency, rather than equality. For example, work on the underlying physics of RADE networks has shown which network structures are optimally efficient for transporting materials under a range of cost functions (Banavar *et al.*, 2000), how varying economies of scale and network structures determine which nodes become more dominant (Han *et al.*, 2019), and trade-offs between optimising building and maintenance costs in networks with new nodes being added (Bottinelli, Louf and Gherardi, 2017). These optimal networks have been shown to emerge through local adaptation in response to changes in flow rates, and positive feedbacks leading to preferential strengthening or pruning of links (Hu and Cai, 2013; Louf, Jensen and Barthelemy, 2013; Ronellenfitsch and Katifori, 2016). The resilience of these networks has also been studied, such as by quantifying the relationship between network structures and their ability to contain perturbations in flow (Gavrilenko and Katifori, 2019). While the hierarchical branching structures introduced above have been shown to be less resilient than structures with loops or redundancy (Hu and Cai, 2013; Gavrilenko and Katifori, 2019), the efficiency of these structures means that they pervade many of the human-engineered systems such as electrical or water grids (Banavar, Maritan and Rinaldo, 1999; Jarvis, Jarvis and Hewitt, 2015), which are another frequent subject of optimisation (Miranda *et al.*, 1994; Montesinos, Garcia-Guzman and Ayuso, 1999; Mahmood and Kubba, 2009; Shrawane and Diagavane, 2013; Zischg, Rauch and Sitzenfrei, 2018; Bernstein and Dall'Anese, 2019; Karimianfard and Haghghat, 2019; Huang *et al.*, 2020).

Another frequent area of study is the emergence and dynamics of transport networks, including road networks in human society, and foraging networks of animals and plant roots. Given the considerable energetic costs associated with movement, it is hypothesised that these networks experience evolutionary pressure to optimise energy use. For foraging, the origin of this idea is often attributed to work on marginal value theorem (Charnov, 1976) and optimal giving-up time

(McNair, 1982), which have since been expanded with research on the role of cognition and memory in foragers (Trapanese, Meunier and Masi, 2019; Ranc *et al.*, 2021); chemotaxis and adaptation (Klyubin, Polani and Nehaniv, 2004; Calhoun, Chalasani and Sharpee, 2014; Lecheval *et al.*, 2021); and improved understanding of the interacting landscape and physiological factors and goals that give rise to foraging routes and behaviour (Hopkins, 2011; Wilson, Quintana and Hobson, 2012; Shepard *et al.*, 2013; Halsey, 2016; Masello *et al.*, 2017; Schlägel, Merrill and Lewis, 2017; Green, Boruff and Grueter, 2020). Similarly, the structure of human transport networks often emerges from positive reinforcement through collective action (Yerra and Levinson, 2005; Levinson and Yerra, 2006; Xie and Levinson, 2009; Strano *et al.*, 2012). Even when the network is centrally planned, the structure is similar to those that emerge through more decentralised decision-making (Chan, Donner and Lämmer, 2011).

One method that has shown considerable promise in both understanding the emergence of complex phenomena such as inequality or network structure, and allowing for spatially-explicit system representations, is simulation modelling, such as agent-based models (ABMs, also known as individual-based models in ecology). These have been widely used to study inequality, such as how it emerges among foragers searching a landscape (*e.g.* Epstein and Axtell, 1996; Little and McDonald, 2007) or moving through a fixed network (*e.g.* Davis *et al.*, 2021). In ABMs, the system-level phenomena emerge from the decentralised decisions and interactions of autonomous agents. This can be used to explore feedbacks and other complex causal structures arising from simple behavioural rules and interactions, without requiring the structure of feedbacks or other system-level dynamics to be specified in advance.

To explore the relationship between RADE network structure and consumer inequality, the work presented here develops and analyses a spatially-explicit ABM of resource acquisition that rigorously adheres to the principle of energy conservation in the simulated system. The network structure develops over time, due to consumers building and maintaining links to maximise their

resource consumption, within their currently available resource capacity. By modelling the system from the perspective of individual actors, the network structure, consumer inequality, and their co-evolution are emergent, mimicking the dynamics of empirical systems. Additionally, model outcomes and dynamics are compared across three different resource arrangements (“landscapes”), to explore how landscape heterogeneity constrains possible network structures and consumer inequality. The work focusses on two main questions: (1) What is the effect of landscape heterogeneity on network structure and consumer inequality, and (2) how do network structure and inequality co-evolve? While this model is highly stylised and theoretical, understanding of the relationship between network structure and inequality can inform further specific work to better understand causes of heterogeneity and inequality in empirical systems, and how it can be preserved or alleviated.

The paper is structured as follows: the next section presents an overview of the model, including the sequence of events and equations governing agent behaviour and model dynamics. This is followed by a Methods section outlining the technical details of the model and analysis, then presentation and discussion of results, and conclusions.

4.2. Model description

To explore the co-evolutionary relationship between network structure and inequality, any model must incorporate the laws constraining transformations of matter and energy in earth systems. Namely, the first and second laws of thermodynamics specify that energy cannot be created or destroyed, but some is released as entropy, an unusable form such as heat, with any transformation. In the context of RADE network models, energy is required to build, maintain, and use the network, and the network transports future resource flows to consumers or consumers to resource points. Therefore, energetic and physical consistency ensures that only net energy flows can be re-invested in maintaining or expanding the network, and the network structure and inequality that emerges reflects this. This constraint is similar to the stock-flow consistent methodologies such as

energy analysis, social metabolism, and input-output analysis, where the stocks and flows of energy and matter are balanced (*e.g.* Odum, 1971; Liao, Heijungs and Huppes, 2012; Haberl *et al.*, 2019). This ensures the system is represented accurately and therefore can be used to analyse and predict resource consumption.

In the model presented here, the equations governing agent decisions and describing model dynamics were based on the stock-flow consistent equations of systems dynamics models, ensuring that units were balanced, and the model maintained physical and energetic consistency as far as possible. Additionally, the model extends beyond typical stock-flow consistent analyses, by comparing resource consumption across a population, and analysing the interactions between the inequality of consumption and the emergent network structure. In the remainder of this section, the characteristics of the agents, sequence of events, and equations defining agent behavioural rules and model dynamics will be discussed. This is followed by a model description following the Overview, Design Concepts, and Details (ODD) protocol in the Methods and Appendix 1.

The model consists of agents, called consumers, who build and use links to navigate between resources (Figure 4.1). The consumers store and use energy from the resources to meet their basal metabolic requirements and build and repair more links, by investing net energy to decrease patches' roughness and make them crossable. The consumers' aim is to maximise their individual energy reserves to allow for both reproduction and future network expansion and improvement. They accomplish this maximisation by using a simple discounting model to choose between resources within their vicinity, calculating the expected time-discounted energetic costs and returns for each, and choosing the resource with the maximum return.

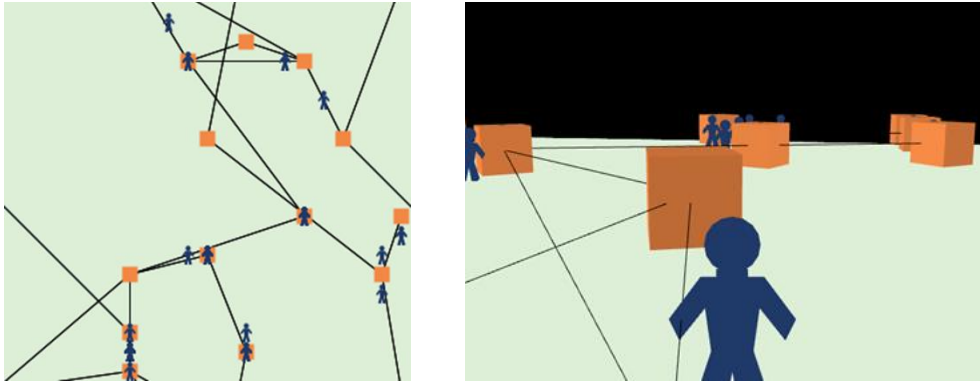


Figure 4.1. Images from the simulations. The blue figures represent the consumers, the orange boxes represent resources, and the black lines show which patches have been transformed into links.

At the start of each timestep, each consumer attempts to consume its basal metabolic requirement from its energy reserves. If the consumer does not have adequate energy to cover this, it dies. Otherwise, the consumer then updates its vision radius, which is the distance around itself in which it can scan for resources. The vision radius is calculated as

$$V_i = P_i A_i, \quad (1)$$

where V_i , P_i , and A_i are the vision radius, risk penchant, and accumulated energy reserves of consumer i , respectively. The risk penchant is a constant (in units of length per energy, or $\text{m}\cdot\text{J}^{-1}$) that determines what proportion of the energy supply the consumer is willing to risk on building, repairing, or walking along links.

After this, consumers who are not currently building or walking assess the resources within their vision radius. Based on their expected consumption from the resource they are located on, and the expected provision of the resources they can evaluate, they decide whether to stay where they are, or move to a different resource by building a new link, repairing an existing link, or walking across an existing link. Consumers who are building or repairing links walk across them simultaneously.

The consumers use a simple discounting model to choose between resources, which places a higher weight on quicker returns. Consumers each have a rate of time preference, or ρ , that they apply when discounting. They evaluate each resource in their vision radius, including their current

location, by applying a discounting function to the expected consumption gain G at each timestep t of their overall time horizon T . From this, they subtract the expected costs C of each timestep, and sum the differences to calculate a net discounted utility. The consumer then chooses the action with the maximum net discounted utility U .

$$\max U = \sum_{t=0}^{T-1} \frac{(G_t^{1-\rho} - 1)(1 + \rho^{-t})}{1 - \rho} - C_t. \quad (2)$$

Time preferences and discounting have been demonstrated across a range of species (see reviews in Hannon, 1994; Vanderveldt, Oliveira and Green, 2016; but see also Hayden, 2016) and are included in most microeconomic models since their introduction by Ramsey (1928). By discounting returns in the future, which are more uncertain given the possibility of other consumers simultaneously constructing links or consuming resources, each consumer prosecutes an energy investment strategy that attempts to minimise risk and maximise energy consumption, within the limits of the energy it can invest.

Any consumers who are not currently building, repairing, or walking links, and have at least twice their initial energy allocation, produce an offspring. The offspring inherits all traits from its parent, such as risk penchant, time preference, and basal metabolism. Moreover, offspring are also given the same initial energy reserves as their parent, with the parent transferring this amount from their own energy reserves when they reproduce. This ensures consistency of the overall energy balance of the model. Reproduction was included to reflect empirical systems where population size evolves alongside the network structure and inequality, which can allow the system to explore a range of possible dynamic equilibrium states.

Consumers who are building, repairing, or walking continue to do so, moving one patch per timestep. The patches closest to the shortest path between the consumers' initial and target resources are altered by the consumers to form links. These links can be conceptualised as stocks

of infrastructure, or energy that has been embodied into the landscape through doing work to modify it (L , in J). The rate of change of this infrastructure at each timestep is

$$\frac{dL_i}{dt} = E_{B_i} - kL_i, \quad (3)$$

where E_{B_i} is the energy invested by a consumer in that patch, and k is the rate of decay, such that the decay of a link-patch is proportional to the current level of infrastructure.

This infrastructure is in turn inversely proportional to the roughness or friction of the patch,

$$R_i = \frac{\beta_i}{L_i}, \quad (4)$$

where β_i is a conversion factor equal to the baseline roughness of the patch, with units of N·J. Each patch is assumed to have a lower bounded embodied energy of $L_i = 1$. This way, R_i has an upper bound of the baseline roughness when L_i is at its minimum, and a lower bound of 1 when L_i is at its maximum due to energy investment. As consumers cannot cross a patch that has not been built into a link, the roughness is technically infinite before energy investment. However, for the purposes of the model here, it is bounded to represent the amount of energy required to invest to make the patch crossable, and it varies by patch depending on the landscape.

Therefore, the energy spent at a given timestep to build or repair that patch, which leads to the accumulation of embodied energy L , can be conceptualised as increasing the smoothness of the patch, or $C = R^{-1}$ (in N⁻¹). In these simulations, this is simplified as

$$E_{B_i} = \eta(1 - C_i), \quad (5)$$

or the energy required to increase the patch's smoothness to the maximum ($C=1$). The parameter η (in J·m·s⁻¹) represents the energy that must be embodied in one patch per timestep to change the smoothness by 1 N⁻¹, or the roughness by 1 N. For simplicity, here we set $\eta = R$, so E_{B_i}

reduces R to the minimum as it increases C to the maximum. Although a consumer could spend a lower amount to partially improve the patch, it would then spend more energy crossing it, such that the total building and walking energy requirement would be the same. This is because the roughness of the patch determines the energy required to cross it (assuming the constant speed defined above of $S_W =$ one patch per timestep):

$$E_{W_i} = S_W R_i . \quad (6)$$

At the end of each timestep, any consumers who are located on resources consume as much as they can, up to their maximum consumption rate, or the total supply of that resource, whichever is less. If there are more consumers on a resource than it can support, the consumers split the available resource supply evenly. In this way, there is competition for resources, but it is indirect rather than more overt territoriality. Resources that are below their maximum capacity also regrow a fixed rate per timestep. While this introduces new energy into the system, it is assumed that the boundaries of the ‘world’ inhabited by the consumers includes processes such as nutrient cycling and rainfall that govern resource regrowth, which are not modelled directly for simplicity.

Therefore, the final energy balance of a consumer includes energy from consumption (gain G) minus energy spent on building or repairing links, walking links, individual maintenance (basal metabolism M , which also includes the energy required for converting resource energy into a form that can be invested in the landscape), and any energy passed on to offspring (O). The balance of these terms over time, A (from Eq 1), forms the energy reserves that are used for future metabolism and reproduction, and determine how much energy the consumer can reinvest in expanding and maintaining the network:

$$\frac{dA}{dt} = E_G - E_B - E_W - E_M - E_O . \quad (7)$$

Although the resources in the model regrow each timestep, and consumers are not territorial over their occupied resources or built links, there is clearly a zero-sum component to the model that creates the possibility for competition and inequality. Consumers eat resources that others were targeting, and they move through spaces with varying degrees of patch roughness, existing architecture, and resource availability. While consumers follow the same rules for making choices, their individual rates of time preference and horizon, risk penchant, energy reserves, and location mean that they follow divergent life histories. When enacted over the landscape, these give rise to the interconnected inequality and network structure that will be explored.

4.3. Methods

The following sections outline the ABM, following the ODD template of Grimm *et al.* (2006, 2010, 2020). Also discussed are the experimental design and analytical method. The model code is published as Davis and Polhill (2021).

4.3.1. Overview, design concepts, and details (ODD)

For simplicity, just the ‘overview’ part of the ODD description of the model is presented below. A complete ODD is included in Appendix 1. The model was developed using Netlogo 6.1.1 (Wilensky, 1999).

I. Model purpose

The purpose of the model is to explore the co-evolution of network structure and inequality that emerge from the decentralised, autonomous decisions of consumers following a simple time-discounted maximisation strategy, set within a stock-flow consistent, energy conserving framework.

II. Entities

Consumers

Property	Description	Constant for run
Initial energy reserves	The energy with which a consumer begins the simulation, and the amount that any offspring inherit. In joules (J).	X
Energy reserves	The energy available to a consumer for metabolism and movement. In J.	
Basal metabolism	The amount of energy a consumer requires per timestep to maintain basic functioning. In J timestep ⁻¹ .	X
Consumption rate	The rate at which consumers take up energy from a resource patch on which they are located. In J timestep ⁻¹ .	X
Risk penchant	The percentage of energy-reserves that a consumer is willing to spend on movement and/or link construction and improvement.	X
Vision radius	The distance to which a consumer can scan for resources – based on energy reserves as consumers cannot ‘see’ resources that they do not have enough energy to access. In generic length units.	
Time horizon	The number of timesteps over which the consumer makes predictions and decisions. In timesteps.	X
ρ	The consumer’s rate of time preference, which determines how strongly discounted future consumption is when making decisions about building, repairing, and walking links. In timestep ⁻¹ .	
Building?	Whether a consumer is currently working on a construction project.	
Repairing?	Whether a consumer is currently working on a repair project.	
Walking?	Whether a consumer is currently walking along a link.	
Current intake table	The data structure used to store predictions of intake at the consumer’s current resource.	
Expected consumption table	The data structure used to store predictions of intake at the resources within the consumer’s vision radius.	
Costs table	The data structure used to store the costs associated with each of the build, repair, and walk activities applicable to each resource within the consumer’s vision radius.	
Repairs table	The data structure used to store data about repairs that could be done on links to resources within the consumer’s vision radius.	
Location	The current resource where the consumer is located (or was located last).	
Target location	The resource toward which the consumer is building, repairing, or walking.	

Resources

Property	Description	Constant for run
Current supply	The resource flow remaining in this resource. In joules (J).	
Resource capacity	The maximum resource flow that could be in this resource, if not depleted by consumer consumption. In J.	X
Regrow rate	The rate at which the resource regrows after depletion. In J timestep ⁻¹ .	X

Links

Property	Description	Constant for run
Patches list	A list of the patches comprising the link – used to determine length, roughness.	X
Link roughness	A measure of the condition of the link, used to calculate energy required for traversal by a consumer or resource flow (higher roughness requires more energy). Stored as a list of the roughness of each patch, in newtons (N).	
Mean roughness	The mean roughness of the patches comprising the link. In N.	
Decay rate	The rate of decay of energy embodied in the patch. In timestep ⁻¹ .	X
Link crossing count	Count of consumers who have crossed the link.	
Under construction?	A flag to denote whether the link is under construction or if all patches it crosses have been built into the link	
Past lifespan?	Whether the link has decayed past its maximum decay (see global variables) and will disappear after all consumers currently crossing it complete their journeys. Prevents consumers from beginning to cross the link.	

Environment patches

Property	Description	Constant for run
Initial patch roughness	The baseline difficulty of crossing the terrain in this patch, if it has not been altered by construction or decay. In newtons (N).	X
Current patch roughness	The current difficulty of crossing this patch, potentially altered by construction or decay. In N.	
Embodied energy	The energy that has been embodied into the patch by consumers constructing or repairing a link over it. Used to determine patch roughness. In joules (J).	
Under link?	Whether the patch has been built into a link or not	
Patch crossing count	The number of times the patch has been crossed as part of a link.	

Global variables

Property	Description
Number of consumers	The initial number of consumer consumers in the simulation.
Link decay rate	The proportion of the embodied energy (energy invested in construction and maintenance) in a link-patch that decays each timestep. In timestep ⁻¹ .
Mean resource regrow rate	The mean number of units per timestep by which a resource can regrow if depleted. In joules (J) timestep ⁻¹ .
Standard deviation (SD) of resource regrow rate	The standard deviation of number of units per timestep by which a resource can regrow by if depleted. In kcal timestep ⁻¹ .
Mean resource capacity	The mean energy store that a resource can hold. In J.
SD of resource capacity	The standard deviation of energy store that a resource can hold. In J.
Mean initial energy reserves	The mean energy reserves with which consumers can be initialised. In J.
SD of initial energy reserves	The standard deviation of energy reserves with which consumers can be initialised. In J.
Minimum initial patch roughness	The minimum initial roughness of a patch (before alteration by construction). In newtons (N).
Maximum initial patch roughness	The maximum initial roughness of a patch (before alteration by construction). In N.

All global variables are constant for the duration of a run.

III. Sequence of events

1. Consumers consume basal metabolism from energy reserves and update vision radius.
2. Consumers who are not currently building, repairing, or walking a link may choose a resource to which they will build a new link or repair an existing link, or may choose not to change the architecture.
3. Consumers who do not build, repair, or walk, and who have at least twice their `initial-energy-reserves`, produce one offspring who inherits `initial-energy-reserves` and all other characteristics from its parent. The parent's energy is depleted by its original `initial-energy-reserves` to balance that which it gave to its offspring.

4. Consumers start building and repair work, walking, or continue work or walking that is already underway.
5. Consumers who are located on resources consume what is available to them based on the resource's current supply and the number of other consumers, up to each consumers' maximum consumption-rate.
6. Resources regrow, if applicable.
7. The patches comprising links decay, and the link may disintegrate. Any link that is under construction is checked to make sure construction has not been completed (*e.g.* by two consumers working from opposite ends of the link).

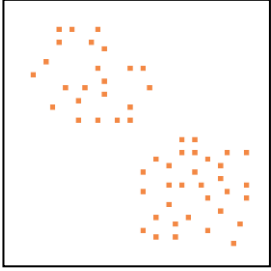
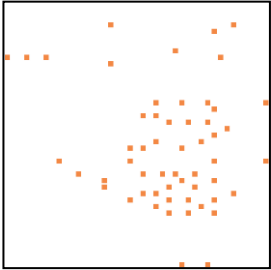
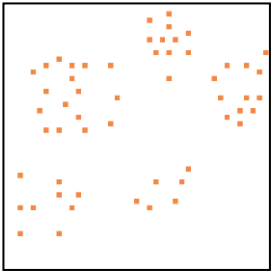
4.3.2. Generating the landscape

The landscape of the model was represented by a grid of patches on a toroid, each of which had an inherent or baseline 'roughness,' which determined the energy required to build a link across them (Eq 4 – 6). The model also required a map of resource node locations. To explore the effect of patch and resource landscape in the sensitivity analysis, qualitatively different patch grids and resource location maps were generated. Both patch and resource maps for a given landscape were fixed for all runs, rather than randomly generated for each run; for example, uniformly random patch roughness was determined only once, then this baseline roughness of each patch was used for all runs with that patch map. The full description of landscape generation is included in Appendices 1 and 2, and only the landscapes used in the final experiments are listed in Table 4.1. For the experiments explored in the remainder of the text, only 'random' patches were used, where patches had uniformly random roughness between a specified minimum and maximum.

The landscapes for the final experiments were chosen to represent three distinct combinations of denser clumps with shorter intra-group distances, and longer inter-group distances. While the names 'Cities', 'Villages' and 'Transition' were used to reflect how resources and consumers might be distributed in human settlements, comparable distributions could be easily identified in a range

of ecosystems. For the model exploration here, a uniform distribution was not explored, as those are rarely, if ever, seen in empirical systems.

Table 4.1. Descriptions and diagrams of resource maps used in final experiments. The resources are shown as orange squares.

Resource map name	Description	Illustration
Cities	Resources are grouped into two larger 'cities.' Mean (standard deviation, SD) of distance between resources: 2.81 (0.60) Min. distance: 2 Max. distance: 3.61	
Transition	Resources are grouped into one larger 'city' with some spread outward into the surrounding area. Mean (SD) of distance between resources: 3.88 (2.09) Min. distance: 1 Max. distance: 7.21	
Villages	Resources are grouped into 5 smaller 'villages.' Mean (SD) of distance between resources: 3.42 (1.03) Min. distance: 2 Max. distance: 5	

4.3.3. Final experiments

Before the final experiments were run, a sensitivity analysis was performed (details in Appendix 1). In summary, the distributions of outcome variables at differing run lengths (in timesteps) and number of replicates were compared for high, medium, and low input parameter levels, and a range of possible landscape types. The outcome variable distributions stabilised at 25 replicates and 3000 timesteps, so these were chosen for the model exploration runs.

For the model exploration, a 2^K factorial approach was adopted (Lorscheid, Heine and Meyer, 2012), which explored every possible combination of high and low values for input parameters,

across each of the final landscapes (Table 4.1). This experimental design was chosen to elucidate the dynamics across the parameter space, and to highlight individual and combined variables with particularly strong effects to explore in future work.

While insightful, the full model exploration did not allow for the in-depth analysis of network and inequality co-evolution, so only a subset of the runs is presented here for clarity. The full model exploration is included in Appendix 3. Final values for each parameter of the runs presented in the main text, hereon called the final experiments, are given in Table 4.2.

Table 4.2. The values for each parameter in the final experiments.

Parameter	Value
Number of consumers	500
Maximum patch roughness	6 N
Minimum patch roughness	2 N
Link decay rate	0.1 J timestep ⁻¹
Mean resource capacity	45 J
Standard deviation (SD) of resource capacity	2 J
Mean resource regrowth rate	9 J timestep ⁻¹
SD of resource regrowth rate	1 J timestep ⁻¹
Mean time horizon	18 timesteps
SD of time horizon	4 timesteps
Mean initial energy reserves	70 J
SD of initial energy reserves	15 J
Mean basal metabolism	3 J timestep ⁻¹
SD of basal metabolism	0.5 J timestep ⁻¹
Mean consumption rate	5 J timestep ⁻¹
SD of consumption rate	1 J timestep ⁻¹
Mean rho	1 timestep ⁻¹
SD of rho	0.025 timestep ⁻¹
Mean risk penchant	72 %
SD of risk penchant	4 %

4.3.4. Analytical method

After each run, simulation-level output variables were calculated using the consumer state variables and the currently constructed links. These covered a range of consumer population metrics, such

as the population size and inequality of energy reserves, measured by the standard deviation (SD), as well as metrics for network size and connectivity. The high-level variables and analyses chosen here were used to reflect the population-level statistics typically applied to measure heterogeneity or inequality in socio-ecological systems. They also allowed for quantification of the large, complex networks that emerged, from both link- and node-level perspectives, to compare with the overall population dynamics. These analyses helped demonstrate the overall behaviour of the model and general trends that emerged, which will help guide any future, more individually-focussed analyses. The reported outcome variables are shown in Table 4.3.

Table 4.3. Outcome variables calculated for each simulation run.

Variable name	Description
Population size	The number of consumer agents currently active in the simulation
Mean energy reserves	The mean of consumer energy reserves
Standard deviation (SD) of energy reserves	The standard deviation of consumer energy reserves
Number of links	The number of links (bi-directional) in the network
Number of (included) resource nodes	The number of resource nodes included in the network
Total link length	The total link length around the network
Mean link length	The mean link length
SD of link length	The standard deviation of link length
Mean node degree	The mean number of links attached to each included resource node

The analytical approach focussed on identifying the inequality and network structure that emerged in each run, and the dynamics of their co-evolution. First, Kruskal-Wallis tests were used to compare values of the outcome variables (Table 4.3) across landscapes, at fixed time points. This captured the role of landscape heterogeneity in the network and consumer outcomes. Non-parametric tests were used as the data did not consistently meet the normality assumptions of ANOVA.

Next, the evolution of the networks that emerged in each run was visualised, by plotting the links that occurred between resources, coloured by the number of times they were crossed. This

highlighted the links that were used most frequently, as opposed to those that were built and used only a few times but were maintained through the maintenance of intersecting links. Three networks that showed diverse evolutionary trajectories were then selected from each of the three landscapes, and the evolution of their structures and values of outcome variables were compared, to note any differences that the distinct structural features they displayed had on the measured outcomes.

Finally, population size, mean and SD of consumer energy reserves, and total link length were plotted over time together, both with means across all replicates of a given landscape, and individually for each run. Total link length was chosen to represent network size, as it was a proxy for total energy investment in the network. This identified major shifts in the dynamics of the simulation, which could be observed from the averaged plots as changes in the slope (breakpoints) of the outcome variables over time. Visual estimates for the breakpoints were quantified for both averaged and individual plots with piecewise regressions, taking the identified slope before each breakpoint as the slope for that segment of the time series. The adjusted R^2 was calculated for each piecewise regression model, and all were found to be over 0.9. The breakpoints were linked back to the events in the simulation by recording and watching animations of the simulations for the nine example networks selected previously.

All analyses and visualisations were done in R version 4.0.3 (R Core Team, 2020), using the *igraph* (Csardi and Nepusz, 2006), *segmented* (Muggeo, 2008), and *ggplot2* libraries (Wickham, 2016).

4.4. Results

Overall, the networks explored showed similar trends of consumer inequality and network structure evolution across the three landscapes. Consumer inequality, measured by SD of energy reserves, increased considerably before stabilising, and network size and connectivity first increased during an initial building phase, then decayed back to a dynamic equilibrium. This section

first explores the network structures and consumer inequality that emerged in the three landscapes overall, and within specific example runs showing distinct patterns of evolution. It then describes the co-evolutionary dynamics of network structure and inequality, starting with the overall trend, then comparing it across the three landscapes.

4.4.1. Network structure and consumer inequality

4.4.1.1. Comparison among landscapes

All simulations reached their dynamic equilibrium state at around 500 timesteps for each of the metrics calculated. While the inequality was quite similar across the three landscapes once the simulations had stabilised, it reached its highest point in the Cities networks (Figure 4.2). The inequality was only found to be significantly different between landscapes at timesteps 20 – 110; time periods before and after this were not significant (Appendix 5). In contrast, the network metrics were all significantly different across landscapes for all timesteps (Appendix 5), with the Transition networks showing the highest peaks for total and standard deviation (SD) of link length, and mean node degree (Figure 4.2).

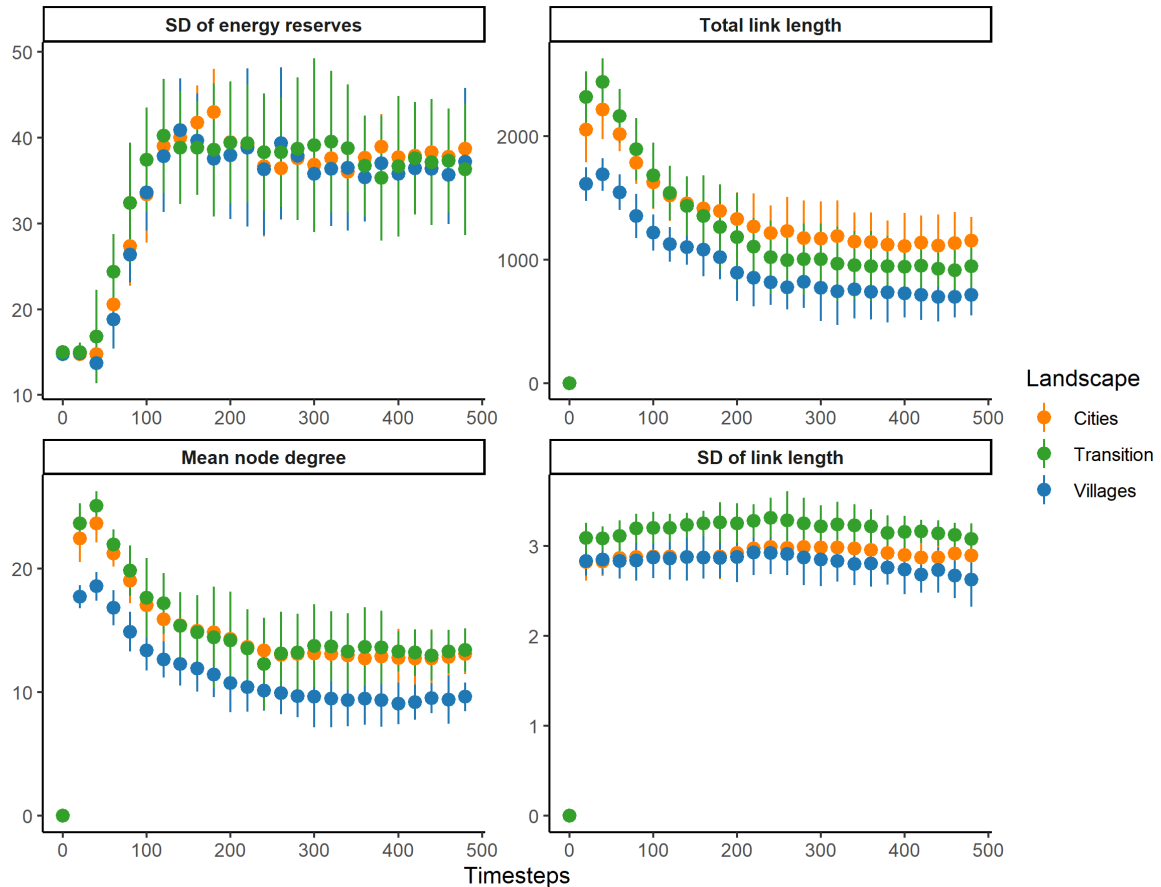


Figure 4.2. Standard deviation (SD) of consumer energy reserves, total link length, mean node degree, and SD of link length over time, for Cities, Transition, and Villages landscapes. Point and error bars show median and interquartile range (IQR) respectively, over 25 replicates per landscape. The values at timestep 500 can be taken as indicative of the dynamic equilibrium state for that metric over the remainder of the simulation.

The overall network development and link use is shown in Figure 4.3. Across all runs for each landscape, a similar pattern emerges of initially high network density and more uniform use of links, coupled with increasing skewness of energy reserves across the population. This is followed by a pruning phase in which the less frequently crossed links decay away, and both network structure and the distribution of energy reserves stabilise. This stability is marked by considerably higher consumer inequality than at initialisation (Figure 4.2), but the distribution of energy reserves is approximately normal. Additionally, the most used links in the networks (Figure 4.3), denoted by darker lines, are often quite short. While longer links do occur, especially during initial construction, the shorter links dominate throughout and are the ones most used and maintained in later timesteps.

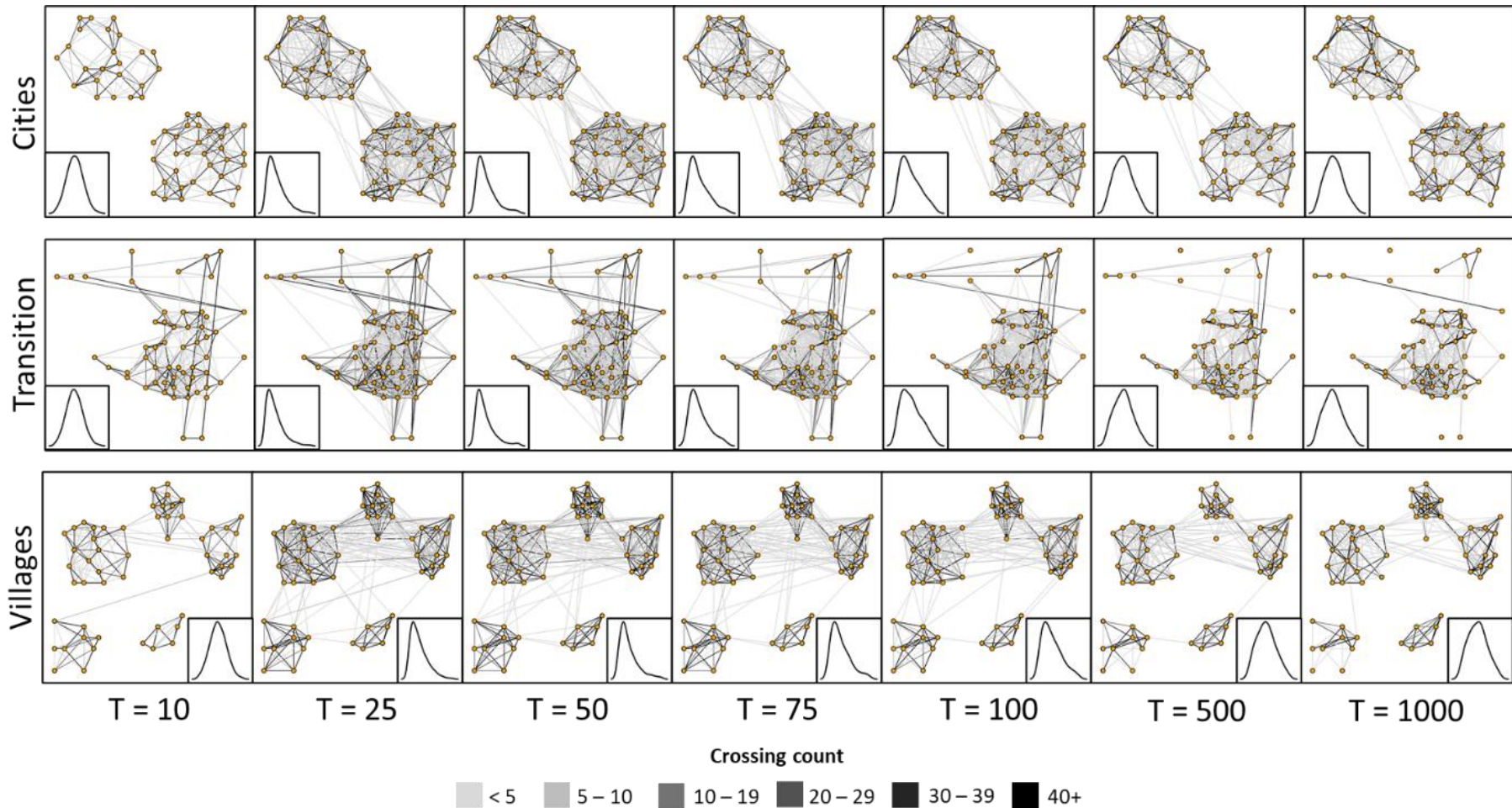


Figure 4.3. The overall network development and consumer energy reserves distributions, for Cities, Transition, and Villages networks, by timestep (T). The lines show the links that were present at each timestep shown, across the 25 replicates per landscape. The line shading represents the total number of times the link was crossed up to that timestep, also across the 25 replicates. The density plot in the inset shows the distribution of consumer energy reserves. As the landscapes were on a torus (see Methods), some of the longer links shown in the Transition and Villages networks wrap around the ‘back’ of the world.

4.4.1.2. Example networks

Within each of the landscapes, three example networks with diverse development trajectories were chosen for further exploration. Their consumer inequality and key network metrics are shown in Figure 4.4, and maps for each example network are shown in Figure 4.5. As with the overall trends (Figure 4.2), Cities and Transition networks showed the highest values for metrics measuring network size, connectivity, and heterogeneity. Villages-1 and Villages-2 showed higher peaks for the consumer inequality metrics, while Villages-3 had consistently lower inequality and network metrics than other examples. The mean node degree is relatively consistent within landscapes, although Transition-3 had a peak in both total link length and connectivity between timesteps 200 – 300. The SD of link length is quite consistent across the example networks.

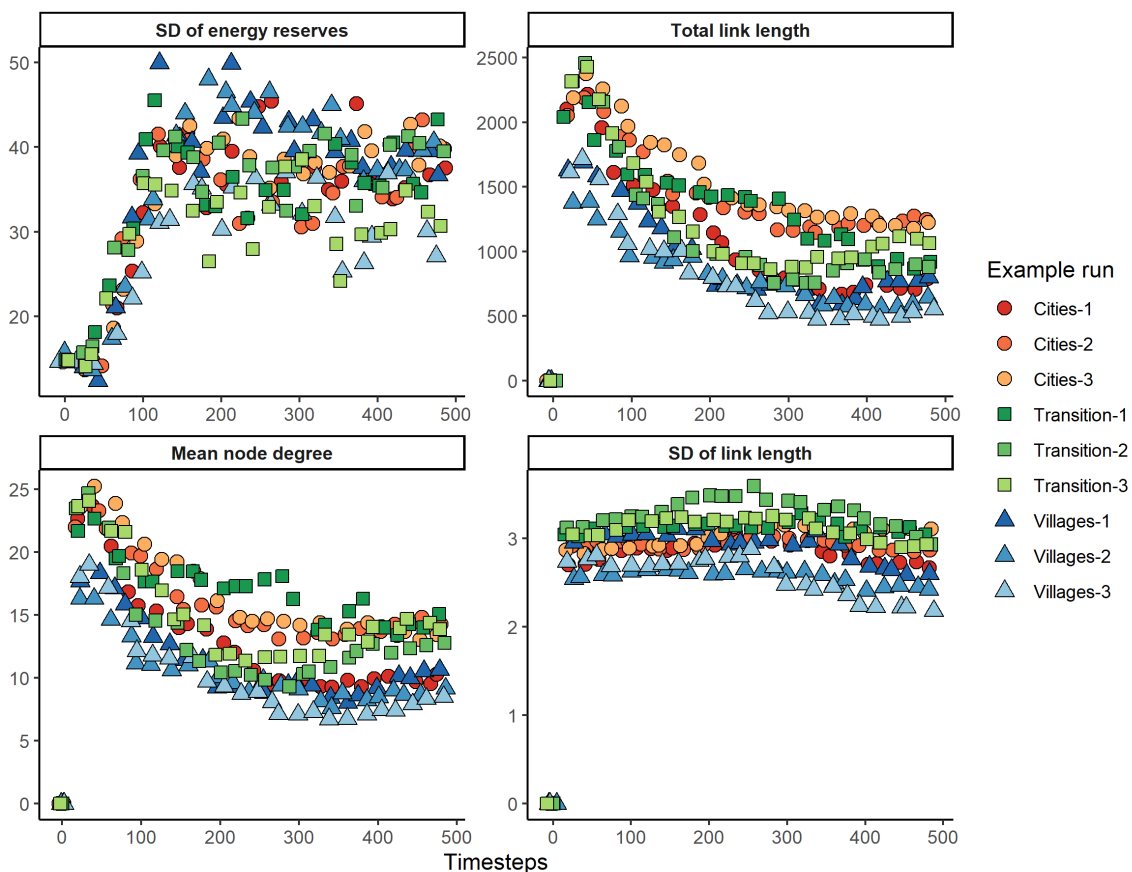
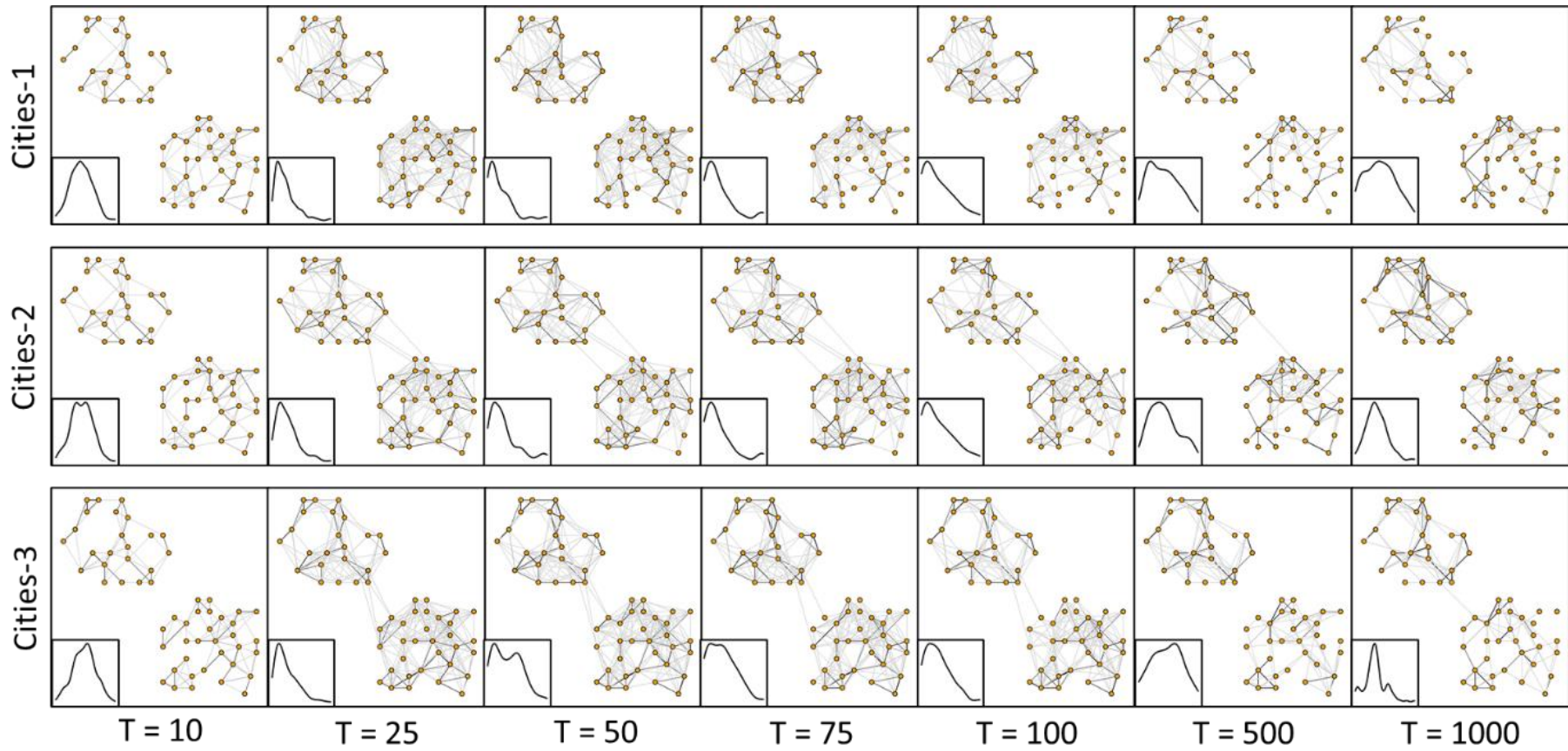
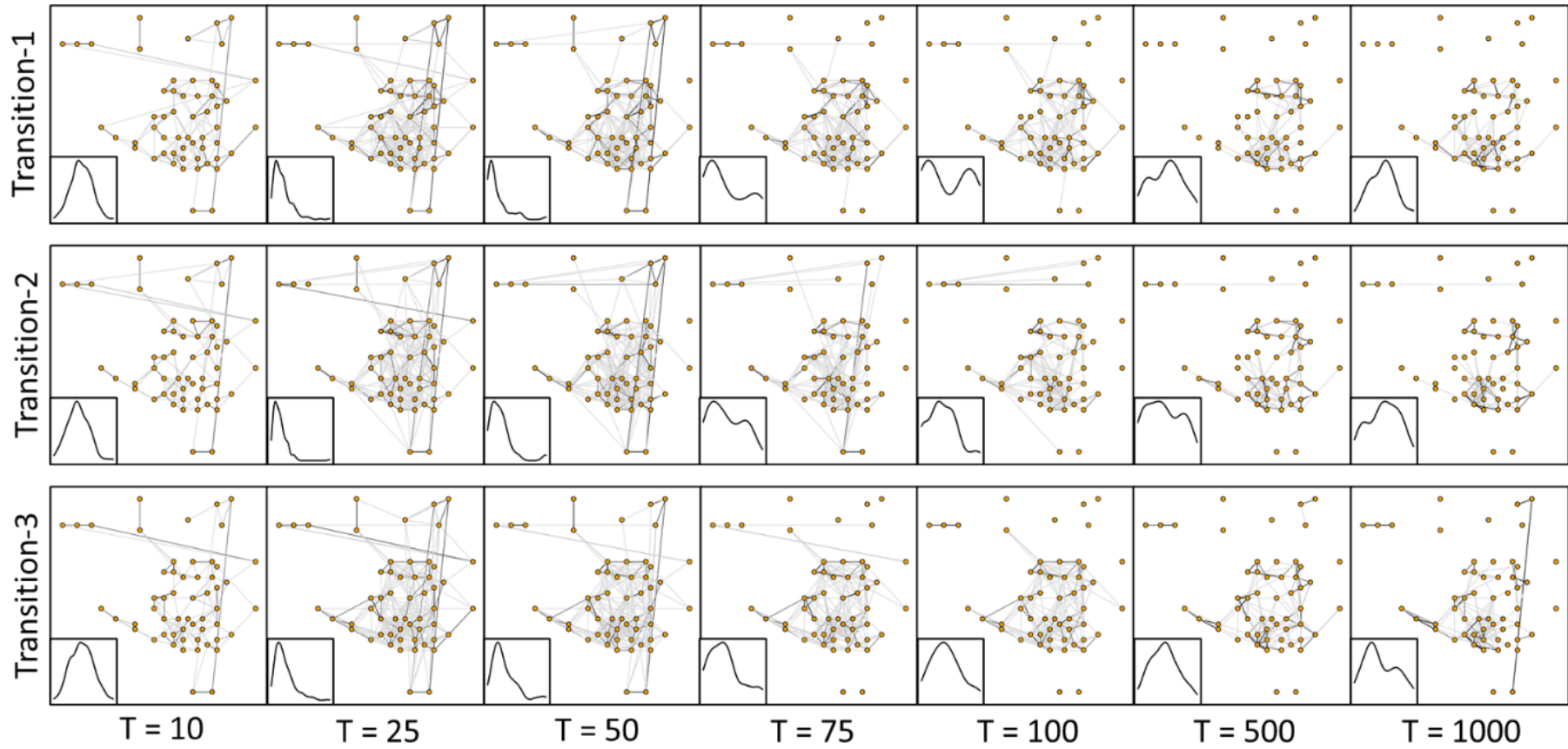


Figure 4.4. Standard deviation (SD) of consumer energy reserves, total link length, mean node degree, and SD of link length over time, for three example networks of each Cities, Transition, and Villages landscapes. Only the first 500 timesteps are shown as runs stabilise after this point. Points are jittered slightly to reduce overlap if possible.





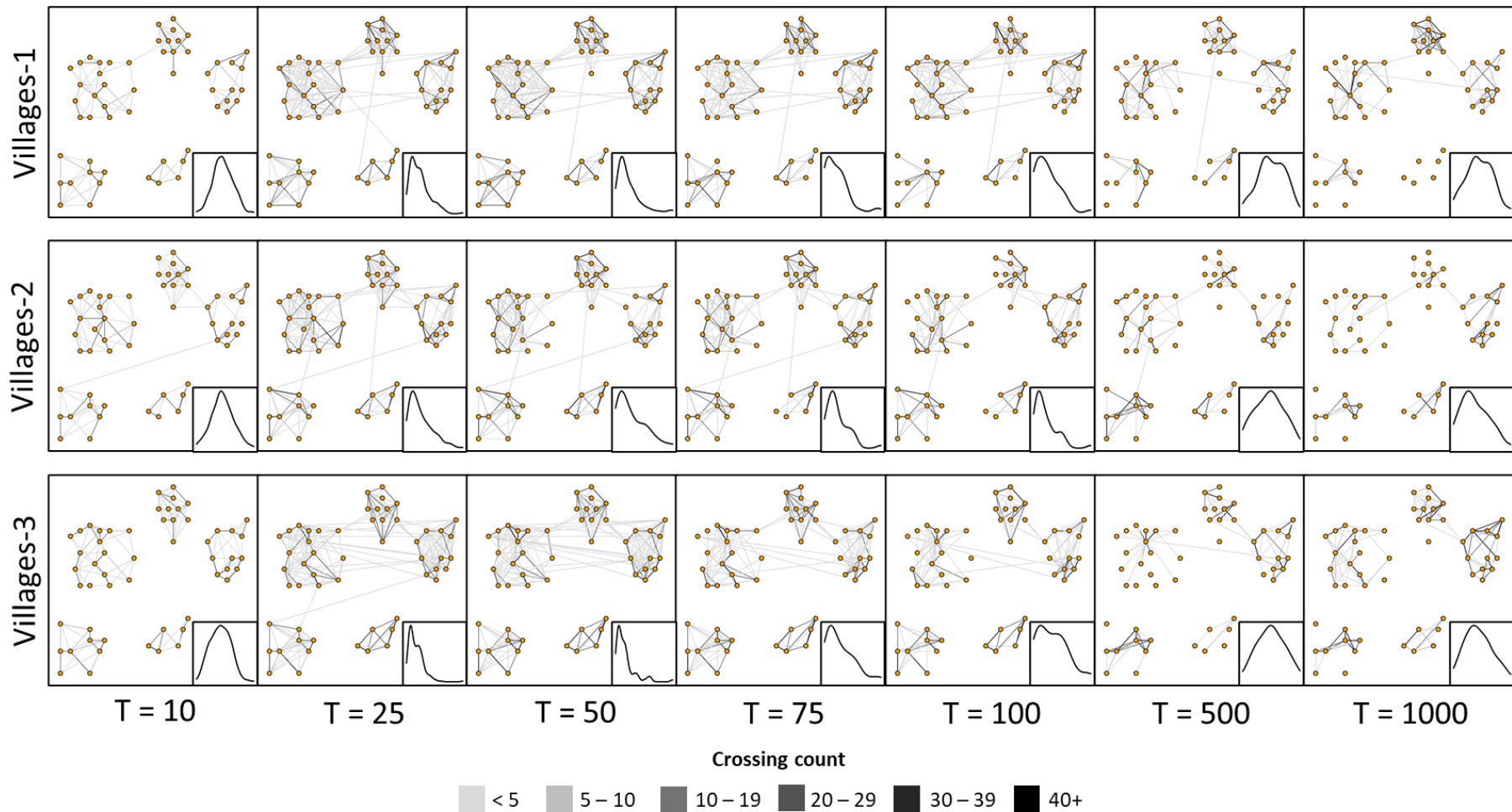


Figure 4.5. The network development and consumer energy reserves distributions, for three examples of each (a) Cities, (b) Transition, and (c) Villages networks, by timestep (T). The lines show the links that were present at each timestep shown. The line shading represents the total number of times the link was crossed up to that timestep. The density plot in the inset shows the distribution of consumer energy reserves. As the landscapes were on a torus (see Methods), some of the longer links shown in the Transition and Villages networks wrap around the ‘back’ of the world.

In the Cities example networks (Figure 4.5a), as with the overall Cities network (Figure 4.3), there is an initial construction phase in the first 100 timesteps before pruning. Cities-2 and Cities-3 retain more links after pruning, and a resulting higher total link length and connectivity (Figure 4.4). There is typically a denser spatial distribution of links at the bottom of the upper cluster of resources, or ‘city,’ and the top of the lower city, which is likely driven by denser clustering of resources in those areas. The distributions of energy reserves also all followed similar patterns of becoming heavily skewed, then shifting back to a more normal distribution. Cities-1 showed higher spikes in SD of consumer energy reserves (Figure 4.4), and the distributions around timesteps 25 – 75 suggest the presence of high outliers. In contrast, Cities-2 had consistently lower inequality, and a less sharply skewed distribution at the compared timesteps. Cities-3 did not maintain a highly skewed distribution for as long as the other two Cities examples; it shifted toward a more bimodal distribution by timestep 50. It also had a consistently higher total link length and connectivity (Figure 4.4).

The Transition networks also went through an initial construction phase, followed by pruning, with the latter resulting in many of the more distant or ‘rural’ resources becoming disconnected from the main ‘city’ centre. In Transition-1, there are no links to or between any of the furthest rural resources; the disconnecting of these more distant areas from the main network is contemporary with a bimodal distribution of consumer energy reserves, which returns to a more normal distribution as the intra-connection among rural resources also disappears. Transition-2 and Transition-3 show similar bimodality in energy reserves distribution in the timesteps when the rural resources have disconnected from the main network but remain intra-connected.

As with the Transition networks, the Villages networks showed a high degree of pruning of longer, inter-village links, with the shorter, intra-village links being retained and much more frequently used. Notably, Villages-1 and Villages-2 had the highest peak across all example networks in SD of consumer energy reserves (Figure 4.3), especially between timesteps 100 and 500. This

corresponds to considerable pruning of both short intra-village links and longer inter-village links. In contrast, Villages-3 had a consistently low SD of consumer energy reserves (Figure 4.4), especially in timesteps before 200, which corresponds to the even spatial distribution and more frequent use of intra-village links, as compared with the other Villages examples.

4.4.2. Co-evolution of network structure and inequality

4.4.2.1. Overall dynamics

Figure 4.6 shows the overall dynamics of the population size, mean and SD of energy reserves, and total link length, for the Cities landscape. As the general pattern is quite similar across the three landscapes, and individual simulations, this is used as an example to illustrate the general dynamics before comparing specific landscapes and runs.

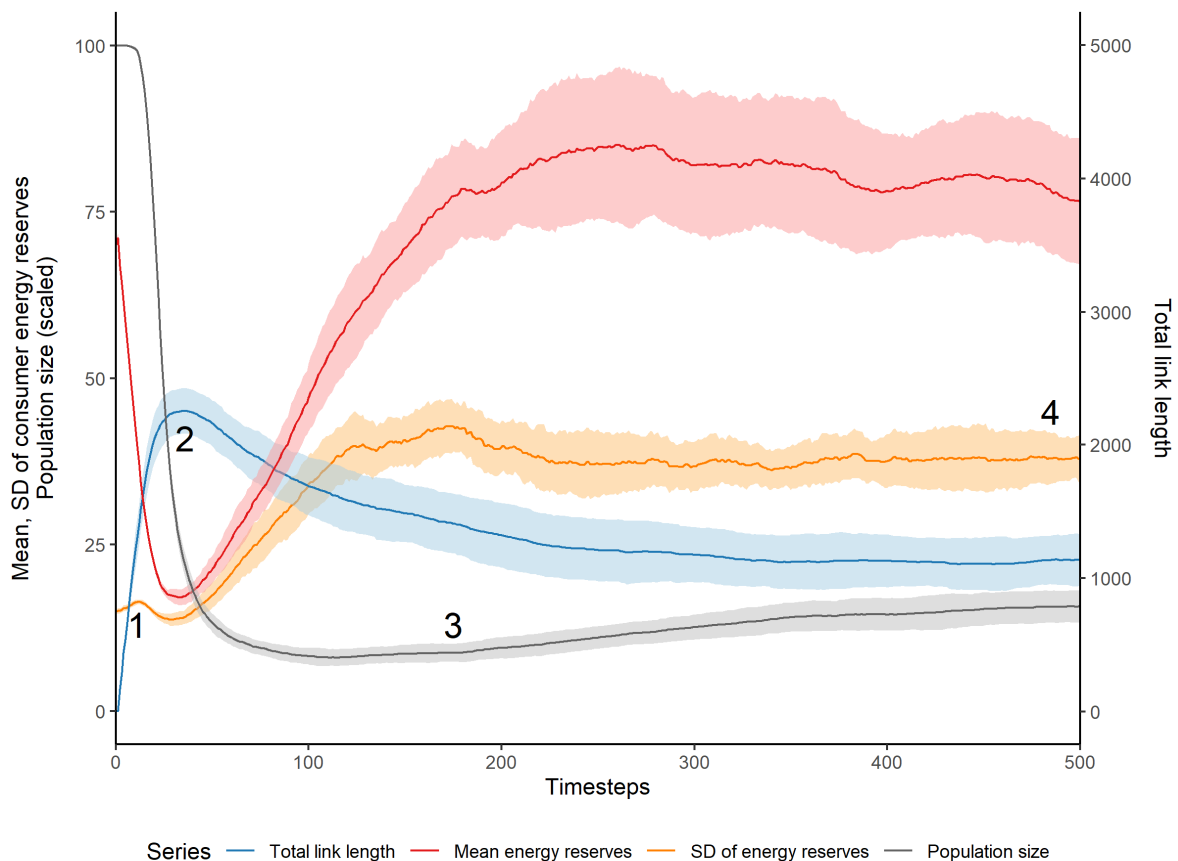


Figure 4.6. Time series showing evolution of total link length, mean and standard deviation of consumer energy reserves, and population size for Cities networks, with labels showing main simulation events. The population size is scaled by a factor of 0.2. The lines represent means across 25 replicates, and the shading shows standard deviations. The labelled events are described in the text.

The major events, labelled on Figure 4.6 as 1-4, are as follows:

1. Consumers begin constructing links and moving through the network. The total link length increases rapidly with the new links, and the mean energy decreases. As many consumers do not survive the first round of building, the population decreases sharply, as do the mean energy reserves. The SD of energy reserves increases briefly before decreasing slightly.

2. The network reaches its maximum size. The mean and SD of energy reserves are both quite low. Notably, this means that the coefficient of variation is at its highest; this is a more relative measure of inequality that is reflected in the highly skewed energy reserves distribution between timesteps 25 – 75 (Figures 4.3, 4.5). Consumer energy reserves, and inequality between them, begin to increase rapidly. Other links that are not maintained start to decay away slowly, giving rise to the more pruned architectures in later timesteps (Figures 4.3, 4.5).

3. After their energy reserves reach the threshold for reproduction, consumers start producing offspring. The population increases in size again, and mean energy reserves and inequality stabilise.

4. The network size and consumer inequality reach a stable equilibrium where almost all remaining links are frequently used and maintained (Figure 4.5), as consumers go back and forth between nodes that provide the optimal balance of resource capacity and proximity to other resources. While consumers cannot plan multiple trips in advance, the resulting network structure shows that links are well-maintained between denser resource patches as consumers frequently commute between these nodes (Figures 4.3, 4.5).

4.4.2.2. Comparison among landscapes

The overall dynamics illustrated in Figure 4.6 are shown for each landscape in Figure 4.7. While the specifics differ across networks, such as the maximum mean and SD of energy reserves or total link length reached, the major dynamics highlighted above occur at similar times in each landscape,

and each simulation (Table A7). Given the distinctions between the three landscapes, the similarity highlights the dominance of the consumer characteristics and decision-making in determining the dynamics. However, the differences in the rates of those dynamics and timings of shifts shows the role of landscape in mediating consumer and resource interactions through the possible network architectures.

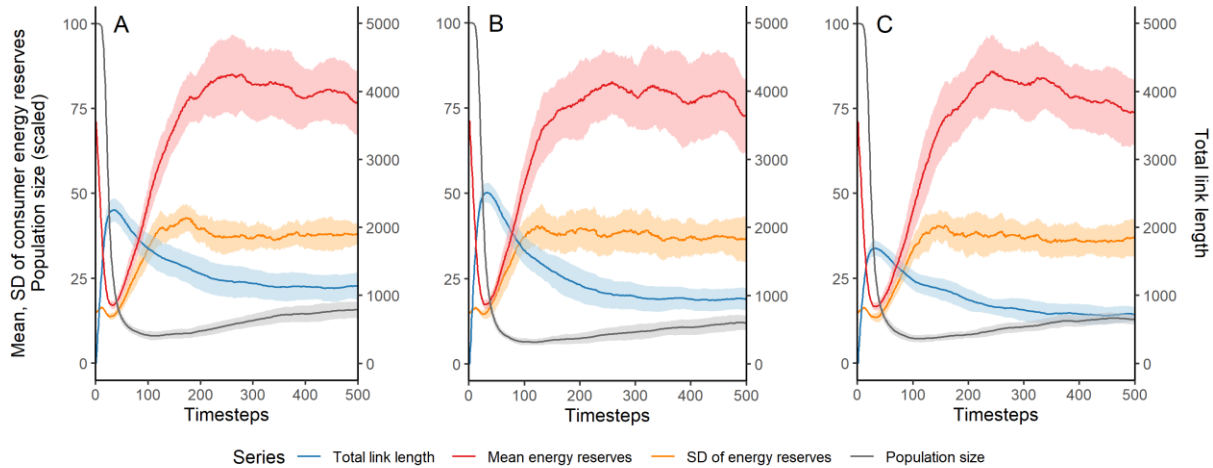


Figure 4.7. Time series showing evolution of total link length, mean and standard deviation (SD) of consumer energy reserves, and population size for (a) Cities, (b) Transition, and (c) Villages networks. The population size is scaled by a factor of 0.2. The lines represent means across 25 replicates, and the shading shows standard deviations.

As observed in the metrics calculated for the example networks (Figure 4.4), the Villages and Cities networks show the highest peak in SD of consumer energy reserves, around timestep 100 (Figure 4.7). The Cities networks show a larger decrease after the initial peak, however, while the SD of consumer energy reserves in Transition and Villages networks quickly stabilise. While the Cities and Transition networks have similar final total link lengths, the Transition network total link length has a higher peak during its initial construction phase. This is concurrent with the presence of longer ‘city-to-rural’ links in the evolution of the overall network and example networks (Figures 4.3, 4.5).

The breakpoints and slopes in the grouped time series plots (Figure 4.7), identified by the piecewise regression, are shown in Table 4.4. These were close to the mean breakpoint and slope for the

regressions calculated over the individual runs (Table A7). Overall, the breakpoints and slopes were similar across the three landscapes. Cities and Villages runs were more similar in their later dynamics, though, such as second and third slopes and breakpoints, while Transition runs were closer to those of the other landscapes in dynamics at the beginning of the runs, but then diverged. All runs showed little to no change once they reached their dynamic equilibrium point, shown by the final slope.

Table 4.4. The breakpoints and slopes identified by piecewise regression, showing the time points of major state changes in the simulations, and the rate of change of measured variables before and after these changes. The estimates for the slopes are accompanied by their standard error (SE). Shown are the breakpoints and slopes for the three landscapes, with the mean of each outcome variable taken over the replicates at each timestep before calculating the breakpoints.

Mean energy reserves

Landscape	Slope 1 (SE)	Breakpoint 1	Slope 2 (SE)	Breakpoint 2	Final slope (SE)
Cities	-0.58 (0.05)	26.58	0.49 (0.00)	163.63	0.00 (0.00)
Transition	-0.53 (0.03)	27.29	0.57 (0.01)	136.43	0.00 (0.00)
Villages	-0.53 (0.02)	27.55	0.51 (0.01)	159.44	0.00 (0.00)

SD of energy reserves

Landscape	Slope 1 (SE)	Breakpoint 1	Slope 2 (SE)	Breakpoint 2	Slope 3 (SE)	Breakpoint 3	Final slope (SE)
Cities	0.14 (0.01)	11.82	-0.21 (0.01)	26.45	0.31 (0.01)	116.25	0.00 (0.00)
Transition	0.14 (0.01)	11.51	-0.15 (0.01)	26.70	0.34 (0.00)	104.69	0.00 (0.00)
Villages	0.12 (0.01)	12.30	-0.23 (0.01)	25.68	0.31 (0.00)	123.41	0.00 (0.00)

Total link length

Landscape	Slope 1 (SE)	Breakpoint 1	Slope 2 (SE)	Breakpoint 2	Final slope (SE)
Cities	20.32 (0.98)	28.03	-9.80 (0.00)	98.49	-0.07 (0.00)
Transition	17.34 (1.15)	28.38	-14.31 (0.11)	98.50	-0.08 (0.00)
Villages	12.53 (0.96)	27.39	-7.70 (0.06)	100.47	-0.04 (0.00)

The Cities runs showed a slightly faster decrease in mean energy reserves before the first breakpoint, and slower increase after, as well as an earlier first breakpoint and later second breakpoint, corresponding to the shift to a more stable state. The Transition runs had a much faster increase in mean energy reserves after the first breakpoint, and earlier stabilisation. The

Villages runs had a similar rate of mean energy reserves decrease before the first breakpoint to Transition, and mean energy reserves increase after the first breakpoint to Cities.

For SD of energy reserves, the runs across the landscapes showed similar initial increases, with Villages runs increasing slightly slower and having a slightly later breakpoint. The Transition runs had a much slower decrease in SD of energy reserves after the first breakpoint, and faster increase after the second. This increase in SD of energy reserves was contemporary with a faster decrease in total link length after the second breakpoint, during the decay of longer ‘city-to-rural’ links (Figures 4.3, 4.5b). Cities runs had the fastest initial total link length increase and earliest first breakpoint, concurrent with a high density of links constructed rapidly (Figures 4.3, 4.5a). In contrast, Villages runs had the slowest increase and latest first breakpoint, as the longer inter-village links took longer to emerge (Figures 4.3, 4.5c). Cities and Villages were more similar in the rate of total link length decrease after the first breakpoint and the timing of the second breakpoint to the stable state.

4.5. Discussion

This analysis explored the effects of landscape heterogeneity on network structure and consumer inequality, and how that structure and inequality co-evolved, in a simple model of resource acquisition. In the following sections, the findings will be discussed, along with limitations and areas of future work.

4.5.1. Effect of landscape heterogeneity on network structure and consumer inequality

In the model presented here, landscape heterogeneity referred to the spatial variability of resources in the landscape, both within and across resource patches. In any system, the landscape constrains the network structures that can emerge to connect resources, but the networks themselves are a co-creation of landscape and consumer behaviour. For example, despite the distinct arrangement of resources in each landscape, the total and standard deviation (SD) of link length of the networks

presented here were quite similar across landscapes (Figure 4.2). The main difference in outcomes between the landscapes was instead the rates and times of network structure and population dynamics (Table 4.4). Network growth depended somewhat on the location of consumers and resources with high energy reserves and capacities, respectively. Given the low SD of resource capacity (see Table 4.2), though, most resources were quite similar. Consumers' decisions would consequently be more influenced by the distance between themselves and a potential target resource, the presence of an existing link, and the resulting cost of moving to it. Therefore, the rate of total link length increase, and the similar mean link lengths in all landscapes, resulted from a combination of the consumers' discounting causing them to prefer to build and maintain shorter links, and the density and spatial distribution of resources constraining what was available to them.

For example, in the runs in the densely patchy Cities landscape, consumers could easily find resources within a range they could build to, and the total link length increased quickly (Table 4.4c, Figure 4.7a). In the smaller and more distant patches of the Villages landscape (Figure 4.7c), total link length increased more slowly, as there were fewer possibilities for short intra-Village links, and longer inter-Village links took more time to build (Table 4.4c). Additionally, the Transition and Cities landscapes had the highest peak network link lengths (Figure 4.2), due to a combination of many links within the dense 'city' sections in each, and the possibility of longer 'city-to-rural' and 'inter-city' links, respectively. These two landscapes also showed the most rapid decay in total link length, after networks reached their maximum size, likely due to the loss of these longer links (Figures 4.3, 4.7a and 4.7b). These links would require a considerable amount of energy to maintain or cross, and therefore were often abandoned, shortening the total link length considerably. The similar dynamics of the network size of Cities and Transition networks suggests that the 'city' section of resources in the Transition landscape had a more dominant effect on network dynamics than the spread of 'rural' resources. This is possibly due in part to the likelihood of links being retained in the network, as links between close 'city' resources were more likely to be maintained,

and the overlapping links in these densely resourced areas meant that maintaining the link-patches of one link effectively maintained the intersecting links as well.

As with the network metrics, consumer inequality, measured by the SD of energy reserves, was similar across the three landscapes (Figures 4.2, 4.7), with differences in maximum inequality and rates of change. Some of this inequality can be attributed to the heterogeneous spatial distribution and capacity of the resources. Even in a theoretical perfectly uniform landscape, however, slight differences between consumers in time preference or willingness to spend energy on movement could lead to distinct experiences of the same space. As these would cause consumers to have unique decision-making, energy consumption, and interaction trajectories, this ‘experienced heterogeneity’ could have a similar effect to physical heterogeneity in accelerating consumer inequality. It could also feed into network structure to create physical heterogeneity, making it difficult to separate the effects of physical and experienced heterogeneity on consumer inequality over time. The combination of physical and experienced heterogeneity is similar to the theory of energy landscapes in behavioural ecology, which posits that forager behaviour is a response to the unique environmental and physiological conditions they experience (see review in Halsey, 2016). Experienced heterogeneity even in the absence of physical heterogeneity has also been discussed in relation to food acquisition by human consumers (Caspi *et al.*, 2012).

In the model explored here, the random order of consumer decision-making and movement in each timestep meant that consumers also experienced varying degrees of influence from each other’s decisions and actions. This suggests that it is not solely the spatiotemporal heterogeneity of resources that drives network structural heterogeneity and consumer inequality, but rather a combination of environmental heterogeneity, differences among consumers and among resources (however minor), and the level of interaction and interference consumers experience, which propagate through the network architecture to create markedly different outcomes for individual consumers. Exploring the individual and joint effects of physical resource heterogeneity and

experienced heterogeneity on consumer outcomes would be a potentially fruitful area of future work.

4.5.2. Co-evolution of network structure and consumer inequality

Across all three landscapes, the network structure and consumer inequality followed a similar pattern of co-evolution. Initially, consumer inequality increased with total link length (Figures 4.6, 4.7), as consumers made different decisions and experienced a range of energetic costs and consumption possibilities while building. After this initial increase in inequality, construction continued, but inequality decreased as consumers with the lowest energy reserves died; this truncated the distribution of energy reserves in the population by removing consumers from the low end. This phenomenon is illustrated by the contemporary decrease in inequality and population size in Figures 4.6 and 4.7. After this point, the dynamics change to a negative feedback between consumer inequality and network growth, with inequality increasing faster in networks where the total link length decreases faster (Table 4.4), and more pruning occurring in networks with higher inequality.

Specifically, in networks that had a larger decrease in population, such as the Transition networks where there were more isolated resources for consumers to become trapped (Figure 4.7b), there were fewer consumers to maintain and use the links built during the initial construction phase. Consequently, more links decayed, and more rapidly (Table 4.4). The links that were maintained allowed some consumers to navigate between resources while consuming less energy: Consumers in well-connected areas or who moved toward these could minimise construction costs by walking across and maintaining existing links, which required less energy than building new links. Similarly, consumers who were in more dense resource patches could spend less energy to move to another resource if their current resource were drained. Less well-positioned consumers had to spend more energy to rebuild links to denser or better-connected areas, or they became trapped in less energy-rich parts of the network where they could not build up enough reserves to reconnect to the better

developed sections. This contrast was likely the cause of the bimodal distribution of consumer energy reserves in the Transition networks, when there were links between the distant ‘rural’ resources and the denser ‘city’ resources, but few, if any, links connecting these areas (Figure 4.5b). Similar effects could emerge in the disconnected Villages networks (Figure 4.5c), and in distant parts of the Cities networks (Figure 4.5a). Each of these networks created distinct trajectories for these sub-populations who have different amounts of resources and links available to them, which caused inequality to increase rapidly.

The increase in inequality eventually stopped, as consumers with adequate energy reserves started to reproduce, shortening the upper tail of the distribution of energy reserves across the population. As described in the Methods, consumers who were not currently building or moving would produce an offspring after they reached at least twice their initial energy reserves, transferring an amount equal to their initial energy reserves to their new offspring. Reproduction thus limited inequality by preventing consumers from accumulating too much energy: they had to keep investing energy in the network, or in offspring. This is shown in Figures 4.6 and 4.7 where the mean and SD of energy reserves stabilise concurrently with an increase in population size, with the mean energy reserves close to the mean at initialisation.

Given the multiple interactions between population and network outcomes, it is difficult to determine the exact causes of inequality due to different individual trajectories. Even the high-level analyses presented here, however, show that the dynamics and feedbacks that emerge between population size, inequality, and network structure are broadly similar across landscapes, but the density and location of resources in each landscape constrain the possible networks that can emerge, and therefore regulate the extent of and rates at which these dynamics occur. Consumers are constrained in their decisions and ability to reproduce by their energy reserves, which are determined by the resources and links available to them. In turn, however, their decisions shape the network structure for themselves, their contemporaries, and future generations.

4.5.3. Maximum power, entropy production, and inequality

While understanding the specifics of the role played by these time-discounted, net consumption-maximising consumer decisions would require further exploration of the discounting parameters and algorithm, two important points can be inferred: the range of time preference in the population would have allowed for a range of target resources at different distances from the consumers to be chosen, and the drive to maximise consumption kept consumers from remaining on resources that met their basal metabolic needs but were not the best within their reach. As discussed in Sections 4.1 and 4.2, both discounting and maximisation have been observed in or theoretically demonstrated for a range of species, including humans, due to the evolutionary pressure to increase fitness in a highly uncertain world. This individual-level competition and attempted maximisation in ecological and socio-ecological systems results in the emergence of system-level evolutionary trajectories, such as maximum power and entropy production (Vallino, 2010; also see reviews in *e.g.* Martyushev and Seleznev, 2006; Kleidon, Malhi and Cox, 2010; Kleidon, 2016). The appearance of a dynamically stable state in the model presented here, driven by the maximising decisions of each consumer, could suggest that the system has reached some sort of maximum operating state, governed by the capacity of the resources and the energy requirements of consumers for basal metabolism, movement, and reproduction.

Notably, this dynamic equilibrium state is not characterised by a highly skewed or power-law distribution of energy reserves (Figures 4.3, 4.5), as might be expected of a system operating at a maximum (Banerjee and Yakovenko, 2010; Tao *et al.*, 2019). This may be due in part to the theoretically unlimited reproduction of the consumers, which keep any one consumer from accumulating too much. However, depending on the structure of the network, maximum power and entropy production does not have to be associated with consumer inequality (Davis *et al.*, 2020), and the non-hierarchical connectivity of the networks here (Figures 4.3, 4.5) likely have contributed to a more normal distribution of energy reserves when the system stabilised. While

our previous work focussing on this theme used networks with fixed consumers and flowing resources, the model presented here suggests that systems operating at a state driven by the maximising decisions of constituents can exhibit patterns of inequality resembling the spread of a more normal distribution. This would suggest that power-law and other fat-tailed distributions are not the exclusive signature of maximisation, depending on other dynamics and constraints within the system.

4.5.4. Limitations and future work

Although the possibilities for expanding any given model are effectively endless, three main limitations of the current model are arguably the most important for improving in future work. These include expanding the spatial, temporal, and interactional domains of consumers' decision-making processes; varying more consumer parameters and resource dynamics, and levels within the parameters explored here; and more comparison between the model and empirical systems. These are each explored in more detail below.

In this model, the consumers constructing and using the network only thought one action ahead at a time: they did not consider the proximity of a resource to other resources or links when making their decisions to build, improve, or walk a link. They also did not know about resource regrowth rates, apart from their current resource, and even this information could be obscured by the presence of other consumers on that node with them. This design choice was made to limit the number of free parameters, such as decision weightings, and to limit the consumers' knowledge to local levels, both temporally and spatially. However, if the model were adapted to focus on decision-making processes in humans, or another species known for sophisticated cognition or perception, it would be relevant to include more elements of foresight.

Relatedly, the consumers had little knowledge of or interaction with one another during the simulation. Consumers could tell if links were currently under construction and could 'help' by building or maintaining it simultaneously with other consumers. By building and modifying links

that other consumers could use, and consuming resources from shared nodes, consumers also affected one another indirectly through stigmergy (*e.g.* Klyubin, Polani and Nehaniv, 2004; Lecheval *et al.*, 2021). However, there was no explicit consideration of other consumers or discussions involved in decision-making, such as resource sharing to build longer or better links. As with expanding the consumers' spatial and temporal considerations in decisions, including elements of cooperation or even competition could provide insight on how social dynamics affect the emergence of inequality.

Further exploration of consumer parameters and resource dynamics, such as pulsing or finite resources, a combination of fixed and flowing resources of multiple types, or more exploration of different landscapes, could also provide insight into other key variables for model behaviour. Different resource dynamics were not the focus of the work presented here, and so were fixed to limit the scope of the analysis. As the results indicate that the landscape is a key factor in determining rates and time spans of consumer and network outcomes, exploring spatiotemporal resource distribution further could also provide insight into how known empirical resource changes, such as seasonality and droughts, could affect resource distribution and consumer populations. Similarly, more exploration of levels of different parameters may highlight tipping points, especially around population-level events such as extinction or stabilisation.

Lastly, while the model is quite theoretical and stylised, the outcomes presented show clear parallels to empirical systems, which would be important to explore further. For example, the indirect relationship between landscape heterogeneity and consumer inequality, through the development of the RADE network connecting them, is similar to the heterogeneity-diversity relationships observed in ecological systems (see Section 4.1), and the adaptation and speciation that can occur in geographically isolated groups. Less attention has been given to the role of RADE networks in previous work on heterogeneity-diversity relationships, but the results here suggest that it may play a significant role in mediating them. Similarly, links between lack of transport connectivity and

poverty have been observed in cities (Brelsford *et al.*, 2018), which is comparable to the model showing the possibility of different trajectories experienced by consumers, depending on the connectivity of their area of the network. Models such as the one presented here could be used with more system-specific parameterisation to explore the emergence of relationships between landscape heterogeneity, network structure, and consumer inequality, and how this relationship is affected by external forces such as landscape and environmental change in ecological systems or increasing the connectivity of transport and other RADE networks in cities.

4.6. Conclusion

In the work presented here, a simple model was developed of consumers building, maintaining, and using a network to move between resources, trying to maximise their time-discounted consumption. The emergent network structure was quantified using metrics such as total, mean, and standard deviation (SD) of link length, and related to the inequality that emerged between consumers, as measured with the SD of their energy reserves. The structure, inequality, and their co-evolution was analysed over time and compared across three distinct landscapes: A Cities landscape, with two distinct patches of resources; a Transition landscape, with a single patch of resources and other resources scattered more distantly around it; and a Villages landscape, with five smaller patches of resources.

Overall, the results showed broadly similar dynamics and outcomes across the landscapes, with differences in the size of the network or degree of consumer inequality at their maximum, and the rate at which inequality increased and the network size decreased during pruning of less-used links. During the initial build-up phase of the network, consumers experienced different conditions, causing inequality to increase. This was then offset by the energy consumption of all consumers during link building efforts, and the subsequent death of consumers with lower energy reserves. As the network was then maintained by and for consumers with high enough energy reserves to be able to do so, inequality increased considerably. At its stable state, the final structure acted to

‘fix’ the level of inequality in the population, by allowing consumers in more densely linked areas to move between resources without needing to rebuild links, while other consumers had to spend more energy, if they could, building links to access these areas. Additionally, reproduction meant that consumers could not go on accumulating energy reserves indefinitely, and therefore limited the extent of inequality.

This work provides a simple but coherent picture of how network structure and inequality can emerge and co-evolve, and how each are related to other dynamics within the population. While highly theoretical, this could be compared with the network structures and inequality that emerge in a range of social species, including humans. Beyond expanding the exploration of the model here, such as increasing the realism of the consumer decision-making process, future work could use the model to examine this network and inequality co-evolution in empirical systems to identify their relationship and any mechanisms controlling inequality. This would provide insight into how beneficial ecological heterogeneity could be maintained, and how the harmful effects of socio-ecological inequality could be mitigated.

4.7. References

- Banavar, J. R. *et al.* (2000) ‘Topology of the fittest transportation networks’, *Physical Review Letters*, 84(20), pp. 4745–4748. doi: 10.1103/PhysRevLett.84.4745.
- Banavar, J. R., Maritan, A. and Rinaldo, A. (1999) ‘Size and form in efficient transportation networks’, *Nature*, 399(6732), pp. 130–132. doi: 10.1038/20144.
- Banerjee, A. and Yakovenko, V. M. (2010) ‘Universal patterns of inequality’, *New Journal of Physics*, 12, pp. 1–25. doi: 10.1088/1367-2630/12/7/075032.
- Bernstein, A. and Dall’Anese, E. (2019) ‘Real-Time Feedback-Based Optimization of Distribution Grids: A Unified Approach’, *IEEE Transactions on Control of Network Systems*, 6(3), pp. 1197–1209. doi: 10.1109/TCNS.2019.2929648.
- Bottinelli, A., Louf, R. and Gherardi, M. (2017) ‘Balancing building and maintenance costs in growing transport networks’, *Physical Review E*, 96(3). doi: 10.1103/PhysRevE.96.032316.
- Brelsford, C. *et al.* (2018) ‘Toward cities without slums: Topology and the spatial evolution of neighborhoods’, *Science Advances*, 4(8), pp. 1–9. doi: 10.1126/sciadv.aar4644.
- Calhoun, A. J., Chalasani, S. H. and Sharpee, T. O. (2014) ‘Maximally informative foraging by *Caenorhabditis elegans*’, *eLife*, 3(3), pp. 1–13. doi: 10.7554/eLife.04220.001.
- Caspi, C. E. *et al.* (2012) ‘The relationship between diet and perceived and objective access to supermarkets among low-income housing residents’, *Social Science and Medicine*, 75(7), pp. 1254–1262. doi: 10.1016/j.socscimed.2012.05.014.
- Chan, S. H. Y., Donner, R. V. and Lämmer, S. (2011) ‘Urban road networks — spatial networks with universal geometric features?’, *The European Physical Journal B*, 84(4), pp. 563–577. doi: 10.1140/epjb/e2011-10889-3.
- Charlton, B. G. (1997) ‘The Inequity of Inequality’, *Journal of Health Psychology*, 2(3), pp. 413–425. doi: 10.1177/135910539700200309.
- Charnov, E. L. (1976) ‘Optimal foraging, the marginal value theorem’, *Theoretical Population Biology*, 9, pp. 129–136.

Csardi, G. and Nepusz, T. (2006) ‘The igraph software package for complex network research’, *InterJournal*, *Complex Sy*, p. 1695.

Davis, N. *et al.* (2020) ‘Trajectories toward maximum power and inequality in resource distribution networks’, *PLOS ONE*. Edited by R. Muneeppeerakul, pp. 1–19. doi: 10.1371/journal.pone.0229956.

Davis, N. *et al.* (2021) ‘Measuring heterogeneity in soil networks: a network analysis and simulation-based approach’, *Ecological Modelling*, 439. doi: 10.1016/j.ecolmodel.2020.109308.

Davis, N. and Polhill, J. G. (2021) *Network Development ABM*. Available at: 10.5281/zenodo.4911978.

Epstein, J. M. and Axtell, R. (1996) *Growing artificial societies: social science from the bottom up*. Brookings Institution Press.

F. P. Ramsey (1928) ‘A mathematical theory of saving’, *The Economic Journal*, 38(152), pp. 543–559.

Gavrilchenko, T. and Katifori, E. (2019) ‘Resilience in hierarchical fluid flow networks’, *Physical Review E*, 99(1). doi: 10.1103/PhysRevE.99.012321.

Gaye, A. (2007) ‘Access to Energy and Human Development’, *United Nations Development Programme*, (25), p. 21.

Green, S. J., Boruff, B. J. and Grueter, C. C. (2020) ‘From ridge tops to ravines: landscape drivers of chimpanzee ranging patterns’, *Animal Behaviour*, 163, pp. 51–60. doi: 10.1016/j.anbehav.2020.02.016.

Grimm, V. *et al.* (2006) ‘A standard protocol for describing individual-based and agent-based models’, *Ecological Modelling*, 198(1–2), pp. 115–126. doi: 10.1016/j.ecolmodel.2006.04.023.

Grimm, V. *et al.* (2010) ‘The ODD protocol: A review and first update’, *Ecological Modelling*, 221(23), pp. 2760–2768.

Grimm, V. *et al.* (2020) ‘The ODD Protocol for Describing Agent-Based and Other Simulation Models: A Second Update to Improve Clarity, Replication, and Structural Realism’, *Journal of Artificial Societies and Social Simulation*, 23(2), p. 7. doi: 10.18564/jasss.4259.

- Haberl, H. *et al.* (2019) ‘Contributions of sociometabolic research to sustainability science’, *Nature Sustainability*, 2(3), pp. 173–184. doi: 10.1038/s41893-019-0225-2.
- Halsey, L. G. (2016) ‘Terrestrial movement energetics: current knowledge and its application to the optimising animal’, *Journal of Experimental Biology*, 219(10), pp. 1424–1431. doi: 10.1242/jeb.133256.
- Han, C. *et al.* (2019) ‘The winner takes it all—Competitiveness of single nodes in globalized supply networks’, *PLOS ONE*, 14(11), p. e0225346. doi: 10.1371/journal.pone.0225346.
- Hannon, B. (1994) ‘Sense of place: geographic discounting by people, animals and plants’, *Ecological Economics*, 10(2), pp. 157–174. doi: 10.1016/0921-8009(94)90006-X.
- Hayden, B. Y. (2016) ‘Time discounting and time preference in animals: A critical review’, *Psychonomic Bulletin and Review*, 23(1), pp. 39–53. doi: 10.3758/s13423-015-0879-3.
- Heidrich, L. *et al.* (2020) ‘Heterogeneity–diversity relationships differ between and within trophic levels in temperate forests’, *Nature Ecology and Evolution*. doi: 10.1038/s41559-020-1245-z.
- Hopkins, M. E. (2011) ‘Mantled Howler (*Alouatta palliata*) Arboreal Pathway Networks: Relative Impacts of Resource Availability and Forest Structure’, *International Journal of Primatology*, 32(1), pp. 238–258. doi: 10.1007/s10764-010-9464-9.
- Hu, D. and Cai, D. (2013) ‘Adaptation and optimization of biological transport networks’, *Physical Review Letters*, 111(13), pp. 1–5. doi: 10.1103/PhysRevLett.111.138701.
- Huang, Y. *et al.* (2020) ‘Multi-Objective Optimal Design of Water Distribution Networks Accounting for Transient Impacts’, *Water Resources Management*, 34(4), pp. 1517–1534. doi: 10.1007/s11269-020-02517-4.
- Jarvis, A. J., Jarvis, S. J. and Hewitt, C. N. (2015) ‘Resource acquisition, distribution and end-use efficiencies and the growth of industrial society’, *Earth System Dynamics*, 6(2), pp. 689–702. doi: 10.5194/esd-6-689-2015.
- Karimianfard, H. and Haghghat, H. (2019) ‘Generic Resource Allocation in Distribution Grid’, *IEEE Transactions on Power Systems*, 34(1), pp. 810–813. doi: 10.1109/TPWRS.2018.2867170.
- Kleidon, A. (2016) *Thermodynamic Foundations of the Earth System*. First. Cambridge, UK: Cambridge University Press.

- Kleidon, A., Malhi, Y. and Cox, P. M. (2010) 'Maximum entropy production in environmental and ecological systems', *Philosophical Transactions of the Royal Society B: Biological Sciences*, 365(1545), pp. 1297–1302. doi: 10.1098/rstb.2010.0018.
- Klyubin, A. S., Polani, D. and Nehaniv, C. L. (2004) 'Tracking information flow through the environment: Simple cases of stigmergy', *Proceedings of the Ninth International Conference on the Simulation and Synthesis of Living Systems (ALIFE '04)*, pp. 563–568.
- Laraia, B. A. (2013) 'Food Insecurity and Chronic Disease', *Advances in Nutrition*, 4(2), pp. 203–212. doi: 10.3945/an.112.003277.
- Lecheval, V. *et al.* (2021) 'From foraging trails to transport networks: how the quality-distance trade-off shapes network structure', *Proceedings of the Royal Society B: Biological Sciences*, 288(1949), p. 20210430. doi: 10.1098/rspb.2021.0430.
- Levinson, D. and Yerra, B. (2006) 'Self-Organization of Surface Transportation Networks', *Transportation Science*, 40(2), pp. 179–188. doi: 10.1287/trsc.1050.0132.
- Liao, W., Heijungs, R. and Huppes, G. (2012) 'Thermodynamic analysis of human-environment systems: A review focused on industrial ecology', *Ecological Modelling*, 228, pp. 76–88. doi: 10.1016/j.ecolmodel.2012.01.004.
- Little, L. R. and McDonald, A. D. (2007) 'Simulations of agents in social networks harvesting a resource', *Ecological Modelling*, 204(3–4), pp. 379–386. doi: 10.1016/j.ecolmodel.2007.01.013.
- Long, M. A. *et al.* (2020) 'Food Insecurity in Advanced Capitalist Nations: A Review', *Sustainability*, 12(9). doi: 10.3390/su12093654.
- Lorscheid, I., Heine, B.-O. and Meyer, M. (2012) 'Opening the 'black box' of simulations: increased transparency and effective communication through the systematic design of experiments', *Computational and Mathematical Organization Theory*, 18(1), pp. 22–62. doi: 10.1007/s10588-011-9097-3.
- Lotka, A. J. (1922) 'Contribution to the Energetics of Evolution', *Proceedings of the National Academy of Sciences*, 8(6), pp. 147–151. doi: 10.1073/pnas.8.6.147.

- Louf, R., Jensen, P. and Barthelemy, M. (2013) 'Emergence of hierarchy in cost driven growth of spatial networks', *Proceedings of the National Academy of Sciences*, 110(22), pp. 8824–8829. doi: 10.1073/pnas.1222441110.
- Mahmood, S. S. and Kubba, H. A. (2009) 'Genetic algorithm based load flow solution problem in electrical power systems', *Journal of Engineering*, 15(4), pp. 4142–4162.
- Martyushev, L. M. and Seleznev, V. D. (2006) 'Maximum entropy production principle in physics, chemistry and biology', *Physics Reports*, 426(1), pp. 1–45. doi: 10.1016/j.physrep.2005.12.001.
- Masello, J. F. *et al.* (2017) 'How animals distribute themselves in space: variable energy landscapes', *Frontiers in Zoology*, 14(1), p. 33. doi: 10.1186/s12983-017-0219-8.
- Mattison, S. M. *et al.* (2016) 'The evolution of inequality', *Evolutionary Anthropology: Issues, News, and Reviews*, 25(4), pp. 184–199. doi: 10.1002/evan.21491.
- McNair, J. N. (1982) 'Optimal giving-up times and the Marginal Value Theorem.', *American Naturalist*, 119(4), pp. 511–529. doi: 10.1086/283929.
- Miranda, V. *et al.* (1994) 'Genetic algorithms in optimal multistage distribution network planning', *IEEE Transactions on Power Systems*, 9(4), pp. 1927–1933. doi: 10.1109/59.331452.
- Montesinos, P., Garcia-Guzman, A. and Ayuso, J. L. (1999) 'Water distribution network optimization using a modified genetic algorithm', *Water Resources Research*, 35(11), pp. 3467–3473. doi: 10.1029/1999WR900167.
- Muggeo, V. M. R. (2008) 'segmented: an R Package to Fit Regression Models with Broken-Line Relationships.', *R News*, 8(1), pp. 20–25.
- Naeem, S. and Colwell, R. K. (2012) 'Ecological Consequences of Heterogeneity of Consumable Resources', in Kolasa, J. and Pickett, S. T. A. (eds) *Ecological Heterogeneity*. Springer Science & Business Media (Ecological Studies).
- Odum, H. T. (1971) *Environment, Power and Society*. New York: Wiley.
- Olson, C. M. (1999) 'Nutrition and Health Outcomes Associated with Food Insecurity and Hunger', *The Journal of Nutrition*, 129(2), pp. 521S-524S. doi: 10.1093/jn/129.2.521S.

Perez-Escamilla, F. and de Toledo Vianna, R. P. (2012) 'Food Insecurity and the Behavioral and Intellectual Development of Children: A Review of the Evidence.', *Journal of Applied Research on Children*, 3(1), p. 9.

R Core Team (2020) *R: A Language and Environment for Statistical Computing*, R Foundation for Statistical Computing, Vienna, Austria. Available at: <http://www.r-project.org>.

Ranc, N. *et al.* (2021) 'Experimental evidence of memory-based foraging decisions in a large wild mammal', *Proceedings of the National Academy of Sciences*, 118(15), p. e2014856118. doi: 10.1073/pnas.2014856118.

Ronellenfitsch, H. and Katifori, E. (2016) 'Global Optimization, Local Adaptation, and the Role of Growth in Distribution Networks', *Physical Review Letters*, 117(13), pp. 1–5. doi: 10.1103/PhysRevLett.117.138301.

Schlägel, U. E., Merrill, E. H. and Lewis, M. A. (2017) 'Territory surveillance and prey management: Wolves keep track of space and time', *Ecology and Evolution*, 7(20), pp. 8388–8405. doi: 10.1002/ece3.3176.

Shepard, E. L. C. *et al.* (2013) 'Energy Landscapes Shape Animal Movement Ecology.', *The American Naturalist*, 182(3), pp. 298–312. doi: 10.1086/671257.

Shrawane, S. S. and Diagavane, M. (2013) 'Application of Genetic Algorithm for Power Flow Analysis', *International Journal of Engineering Research & Technology*, 2(9), pp. 453–456.

Smith, E. A. *et al.* (2010) 'Wealth transmission and inequality among hunter-gatherers', *Current Anthropology*, 51(1), pp. 19–34. doi: 10.1086/648530.

Sovacool, B. K. (2012) 'The political economy of energy poverty: A review of key challenges', *Energy for Sustainable Development*, 16(3), pp. 272–282. doi: 10.1016/j.esd.2012.05.006.

Stein, A., Gerstner, K. and Kreft, H. (2014) 'Environmental heterogeneity as a universal driver of species richness across taxa, biomes and spatial scales', *Ecology Letters*, 17(7), pp. 866–880. doi: 10.1111/ele.12277.

Stiglitz, J. E. (2012) *The price of inequality: How today's divided society endangers our future*. WW Norton & Company.

- Strano, E. *et al.* (2012) ‘Elementary processes governing the evolution of road networks’, *Scientific Reports*, 2(1), p. 296. doi: 10.1038/srep00296.
- Tao, Y. *et al.* (2019) ‘Exponential structure of income inequality: evidence from 67 countries’, *Journal of Economic Interaction and Coordination*, 14(2), pp. 345–376. doi: 10.1007/s11403-017-0211-6.
- Tews, J. *et al.* (2004) ‘Animal species diversity driven by habitat heterogeneity/diversity: The importance of keystone structures’, *Journal of Biogeography*, 31(1), pp. 79–92. doi: 10.1046/j.0305-0270.2003.00994.x.
- Trapanese, C., Meunier, H. and Masi, S. (2019) ‘What, where and when: spatial foraging decisions in primates’, *Biological Reviews*, 94(2), pp. 483–502. doi: 10.1111/brv.12462.
- Vallino, J. J. (2010) ‘Ecosystem biogeochemistry considered as a distributed metabolic network ordered by maximum entropy production’, *Philosophical Transactions of the Royal Society B: Biological Sciences*, 365, pp. 1417–1427. doi: 10.1098/rstb.2009.0272.
- Vanderveldt, A., Oliveira, L. and Green, L. (2016) ‘Delay discounting: Pigeon, rat, human—does it matter?’, *Journal of Experimental Psychology: Animal Learning and Cognition*, 42(2), pp. 141–162. doi: 10.1037/xan0000097.
- West, G. B., Brown, J. H. and Enquist, B. J. (1997) ‘A General Model for the Origin of Allometric Scaling Laws in Biology’, *Science*, 276, pp. 122–126. doi: 10.1126/science.276.5309.122.
- Wickham, H. (2016) *ggplot2: Elegant Graphics for Data Analysis*. New York: Springer-Verlag. Available at: <http://ggplot2.org>.
- Wilensky, U. (1999) *NetLogo*. Evanston, IL: Center for Connected Learning and Computer-Based Modeling, Northwestern University. Available at: <http://ccl.northwestern.edu/netlogo/>.
- Wilson, R. P., Quintana, F. and Hobson, V. J. (2012) ‘Construction of energy landscapes can clarify the movement and distribution of foraging animals’, *Proceedings of the Royal Society B: Biological Sciences*, 279(1730), pp. 975–980. doi: 10.1098/rspb.2011.1544.
- Xie, F. and Levinson, D. (2009) ‘Modeling the growth of transportation networks: A comprehensive review’, *Networks and Spatial Economics*, 9(3), pp. 291–307. doi: 10.1007/s11067-007-9037-4.

Yerra, B. M. and Levinson, D. M. (2005) 'The emergence of hierarchy in transportation networks', *Annals of Regional Science*, 39(3), pp. 541–553. doi: 10.1007/s00168-005-0230-4.

Zischg, J., Rauch, W. and Sitzenfrei, R. (2018) 'Morphogenesis of Urban Water Distribution Networks: A Spatiotemporal Planning Approach for Cost-Efficient and Reliable Supply', *Entropy*, 20(9). doi: 10.3390/e20090708.

4.8. Appendices

Appendix 1. Model Description (ODD)

Overview, design concepts, and details (ODD)

Following the template of Grimm et al. (2006, 2010, 2020), the overview, design concepts, and details (ODD) of the model are presented below.

Model purpose

The purpose of the model is to explore the co-evolution of network structure and inequality that emerge from the decentralised, autonomous decisions of consumers following a simple time-discounted maximisation strategy, set within a stock-flow consistent, energy conserving framework.

Entities

Consumers

Property	Description	Constant for run
Initial energy reserves	The energy with which a consumer begins the simulation, and the amount that any offspring inherit. In joules (J).	X
Energy reserves	The energy available to a consumer for metabolism and movement. In J.	
Basal metabolism	The amount of energy a consumer requires per timestep to maintain basic functioning. In J timestep ⁻¹ .	X
Consumption rate	The rate at which consumers take up energy from a resource patch on which they are located. In J timestep ⁻¹ .	X
Risk penchant	The percentage of energy-reserves that a consumer is willing to spend on movement and/or link construction and improvement.	X
Vision radius	The distance to which a consumer can scan for resources – based on energy reserves as consumers cannot ‘see’ resources that they do not have enough energy to access. In generic length units.	
Time horizon	The number of timesteps over which the consumer makes predictions and decisions. In timesteps.	X
ρ	The consumer’s rate of time preference, which determines how strongly discounted future consumption is when making decisions about building, repairing, and walking links. In timestep ⁻¹ .	
Building?	Whether a consumer is currently working on a construction project.	
Repairing?	Whether a consumer is currently working on a repair project.	
Walking?	Whether a consumer is currently walking along a link.	

Current intake table	The data structure used to store predictions of intake at the consumer's current resource.
Expected consumption table	The data structure used to store predictions of intake at the resources within the consumer's vision radius.
Costs table	The data structure used to store the costs associated with each of the build, repair, and walk activities applicable to each resource within the consumer's vision radius.
Repairs table	The data structure used to store data about repairs that could be done on links to resources within the consumer's vision radius.
Location	The current resource where the consumer is located (or was located last).
Target location	The resource toward which the consumer is building, repairing, or walking.

Resources

Property	Description	Constant for run
Current supply	The resource flow remaining in this resource. In joules (J).	
Resource capacity	The maximum resource flow that could be in this resource, if not depleted by consumer consumption. In J.	X
Regrow rate	The rate at which the resource regrows after depletion. In J timestep ⁻¹ .	X

Links

Property	Description	Constant for run
Patches list	A list of the patches comprising the link – used to determine length, roughness.	X
Link roughness	A measure of the condition of the link, used to calculate energy required for traversal by a consumer or resource flow (higher roughness requires more energy). Stored as a list of the roughness of each patch, in newtons (N).	
Mean roughness	The mean roughness of the patches comprising the link. In N.	
Decay rate	The rate of decay of energy embodied in the patch. In timestep ⁻¹ .	X
Link crossing count	Count of consumers who have crossed the link.	
Under construction?	A flag to denote whether the link is under construction or if all patches it crosses have been built into the link	
Past lifespan?	Whether the link has decayed past its maximum decay (see global variables) and will disappear after all consumers currently crossing it complete their journeys. Prevents consumers from beginning to cross the link.	

Environment patches

Property	Description	Constant for run
Initial patch roughness	The baseline difficulty of crossing the terrain in this patch, if it has not been altered by construction or decay. In newtons (N).	X
Current patch roughness	The current difficulty of crossing this patch, potentially altered by construction or decay. In N.	
Embodied energy	The energy that has been embodied into the patch by consumers constructing or repairing a link over it. Used to determine patch roughness. In joules (J).	
Under link?	Whether the patch has been built into a link or not	
Patch crossing count	The number of times the patch has been crossed as part of a link.	

Global variables

Property	Description
Number of consumers	The initial number of consumer consumers in the simulation.
Link decay rate	The proportion of the embodied energy (energy invested in construction and maintenance) in a link-patch that decays each timestep. In timestep ⁻¹ .
Mean resource regrow rate	The mean number of units per timestep by which a resource can regrow if depleted. In joules (J) timestep ⁻¹ .
Standard deviation (SD) of resource regrow rate	The standard deviation of number of units per timestep by which a resource can regrow by if depleted. In kcal timestep ⁻¹ .
Mean resource capacity	The mean energy store that a resource can hold. In J.
SD of resource capacity	The standard deviation of energy store that a resource can hold. In J.
Mean initial energy reserves	The mean energy reserves with which consumers can be initialised. In J.
SD of initial energy reserves	The standard deviation of energy reserves with which consumers can be initialised. In J.
Minimum initial patch roughness	The minimum initial roughness of a patch (before alteration by construction). In newtons (N).
Maximum initial patch roughness	The maximum initial roughness of a patch (before alteration by construction). In N.

All global variables are constant for the duration of a run.

Sequence of events

1. Consumers consume basal metabolism from energy reserves and update vision radius.
2. Consumers who are not currently building, repairing, or walking a link may choose a resource to which they will build a new link or repair an existing link, or may choose not to change the architecture.
3. Consumers who do not build, repair, or walk, and who have at least twice their `initial-energy-reserves`, produce one offspring who inherits `initial-energy-reserves` and all other characteristics from its parent. The parent's energy is depleted by its original `initial-energy-reserves` to balance that which it gave to its offspring.
4. Consumers start building and repair work, walking, or continue work or walking that is already underway.
5. Consumers who are located on resources consume what is available to them based on the resource's current supply and the number of other consumers, up to each consumers' `maximum consumption-rate`.
6. Resources regrow, if applicable.
7. The patches comprising links decay, and the link may disintegrate. Any link that is under construction is checked to make sure construction has not been completed (*e.g.* by two consumers working from opposite ends of the link).

Design concepts

1. Basic principles

The basic principle at the core of this model is the maximum power principle, which states that systems self-organise to maximise their rate of free energy capture and consumption, or power.

To do this, consumers should attempt to minimise energy consumed in transport, by making their networks as efficient as possible. Additionally, this model relies on the principle of time discounting, which has been shown in humans and other species to influence decision making through discounting a reward (such as resource consumed) by the amount of time in the future that it will occur.

2. Emergence

The network structure emerges throughout the simulation from consumers' decisions and the resulting free energy they have available to invest in network expansion and improvement. While some base level of inequality among consumers is specified at initialisation, the final level of inequality is also emergent.

3. Adaptation

The consumers adapt to their environment by building a network that allows them to attempt to maximise their own consumption within that environment: at each timestep, each consumer decides what resource within their vision radius will yield the most returns, based on their personal time discounting rate, then builds, repairs, or walks the link to move to that resource. The population also adapts over time, as consumers who are successful enough to accumulate energy reserves adequate to reproduce pass on their traits (parameter values) to their offspring.

4. Objectives

The consumers' objectives are to survive, and to maximise their consumption of free energy, which in turn allows them to maximise their output in improving the network or reproducing. The consumers survive by maintaining a minimum level of energy reserves to support basic operation, i.e. basal metabolism.

5. Learning

Consumers can learn as they consume more resources and gain a larger field of vision (from higher energy stores), which allows them to survey further across their environment. Although they can

potentially include more resources in their vision radius if they move to more central locations, they do not ‘remember’ previously surveyed resources that are no longer in view.

6. Prediction

Consumers predict which resources within their field of vision will provide the highest energetic returns, based on the current energy supply of each resource, and their personal time discounting rate. They can then preferentially build and improve links to those resources.

7. Sensing

All consumers have a field of vision proportional to their energy reserves, that they use to survey their surroundings and choose which resource(s) to which they build or improve links. As their energy reserves fluctuate, and they move, which resources that are included within their field of vision may change.

8. Interaction

Consumers do not interact directly, but they can use and repair one another’s links between resources, and indirectly collaborate by contributing to building a link that is already under construction. They therefore interact stigmergically through the network they construct, what they reinforce or allow to decay, and the resources they consume.

9. Stochasticity

Consumers are initialised with state variable values (e.g. initial energy reserves, risk penchant, ρ) from a normal distribution with a set mean and standard deviation and are placed on random resources across the network. Resource capacity and regrowth rate are also initialised with a normally-distributed level of energy reserves (see ‘Initialisation’).

10. Collectives

There are no collectives explicitly specified within the model, but consumers could aggregate into informal collectives who utilise the same resource(s) and links in a specific area of the network.

11. Observation

At each timestep, the state variable values for consumers, patches, and links will be recorded. Additionally, the locations and state variable values for resources are recorded at the start of each run.

Initialisation

The resource, consumer, and link parameters are specified in an Extended Markup Language (XML) file. The landscape is specified in Comma-Separated-Values (CSV) files that store the `initial-patch-resistance` for each patch in the environment, and the location for each resource in the environment.

The models were initialised with a population of consumers randomly located on resource nodes throughout the space. The consumers began with normally-distributed resource units their energy-reserves. The distributions from which the values were drawn were all truncated such that the lower bound was 1 (energy reserves, consumption rate, time horizon) or 0.01 (basal metabolism, risk penchant, rho).

Resources were all initialised with normally-distributed resource capacity and resource regrow rate values, with the distributions of each truncated such that the minimum of each was 1. Resources all began the simulation at full capacity.

Input data

This model has no input data.

Submodels

1. Vision radius update

At the start of each timestep, each consumer consumes its basal metabolic requirement from its reserves (see below) and updates its vision radius to the product of its risk penchant and energy reserves,

$$V_i = P_i A_i, \quad (8)$$

where V_i , P_i , and A_i are the vision radius, risk penchant, and energy reserves of consumer i , respectively. The risk penchant is a fixed constant that determines what proportion of the energy supply the consumer is willing to risk on building, repairing, or walking along links.

If the consumer does not have adequate energy to cover its basal metabolic requirement, it dies.

2. Target resource selection

At each timestep, consumers who are not currently building or walking assess the resources within their vision radius. Based on their expected consumption from the resource they are located on, and the expected provision of the resources they can evaluate, they decide whether to stay where they are, or move to a different resource by building a new link, repairing an existing link, or walking an existing link. The consumers use a simple discounting model to incorporate a rate of time preference into their decisions, which places a higher weight on quicker returns.

Utility function

Consumers each have a rate of time preference, or ρ , that they apply when discounting. To determine the action they will take, consumers apply a discounting function to the expected consumption gain G at each timestep t of their overall time horizon T . From this, they subtract the expected costs C of each timestep, and sum the differences to calculate a net discounted utility. The consumer then chooses the action with the maximum net discounted utility.

$$\max U = \sum_{t=0}^{T-1} \frac{(G_t^{1-\rho} - 1)(1 + \rho^{-t})}{1 - \rho} - C_t. \quad (9a)$$

When $\rho = 1$, this simplifies to

$$\max U = \sum_{t=0}^{T-1} \log G_t + \log G_t^{-t} - C_t. \quad (10b)$$

3. Link construction, maintenance, and decay

The links between resources can be conceptualised as stocks of infrastructure, or embodied energy (L , in J), comprised of the patches along the shortest path between two resources. At each timestep, the change of this infrastructure is

$$\frac{dL_i}{dt} = E_{B_i} - kL_i, \quad (11)$$

where E_{B_i} is the energy invested by a consumer in that patch, and k is the rate of decay, such that the decay of a link-patch is proportional to the current level of infrastructure. This infrastructure is in turn inversely proportional to the roughness or friction of the patch, such that

$$R_i = \frac{\beta_i}{L_i}, \quad (12)$$

where β_i is a conversion factor equal to the baseline roughness of the patch, with units of N·J. This way, R has a lower bound of 1 and an upper bound of the baseline roughness of that patch (*i.e.* natural state), since L has a lower bound of 1 and an upper bound of the baseline roughness of the patch.

Therefore, the energy spent at a given timestep to build or repair that patch, which leads to the accumulation of embodied energy L , can be conceptualised as increasing the smoothness of the patch, or $C = R^{-1}$ (in N⁻¹). In these simulations, this is simplified as

$$E_{B_i} = \eta(1 - C_i), \quad (13)$$

or the energy required to increase the patch's smoothness to the maximum ($C = 1$). η (in J·m·s⁻¹) represents the energy that must be embodied in one patch per timestep to change the smoothness by 1 N⁻¹, or the roughness by 1 N.[†] Although a consumer could spend a lower amount to improve

[†]For simplicity, here we set $\eta = R$, such that $\eta(1 - C) = R - 1$, so E_{B_i} reduces R to the minimum as it increases C to the maximum.

the patch, it would then spend a higher amount to cross it following construction or repair, such that the total building and walking energy requirement would be the same. This is because the roughness of the patch determines the energy required to cross it (assuming a constant speed S_W = one patch per timestep):

$$E_{W_i} = S_W R_i . \quad (14)$$

4. Energy balance, resource consumption and basal metabolism

The final energy balance of a consumer includes energy from consumption (gain G) minus energy spent on building or repairing links, walking links, individual maintenance (basal metabolism M), and any energy passed on to offspring (O):

$$\frac{dA}{dt} = E_G - E_B - E_W - E_M - E_O . \quad (15)$$

Resource and patch maps

Patch grid generation and evaluation

For the sensitivity analysis, three layouts of patch resistance were explored: banded, where five bands of higher-resistance patches crossed the otherwise uniform landscape; random, where patch resistances were chosen from a uniform distribution between the minimum and maximum patch resistance; and uniform, where all patches had the same resistance. The random and banded maps were compared by calculating the spatial autocorrelation of patch resistances, to confirm that the replicates of each layout were similar to one another, but different from those of the other layouts. Overall, the spatial autocorrelation was significant for all banded resource maps (Moran's I 0.20 – 0.78, $p < 0.05$) and not significant for all random resource maps (Moran's I -0.05 – 0.03, $p > 0.05$). Spatial autocorrelation could not be calculated for uniform maps, since all patches have the same resistance, so it is considered a maximum.

Resource map generation and evaluation

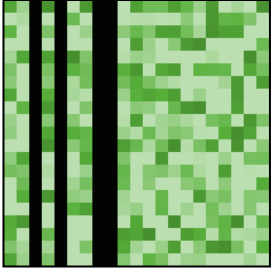
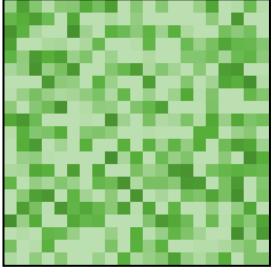
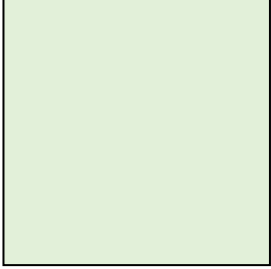
Additionally, three resource location maps were used: patchy, where resources were grouped in patches centred around three random points in the space; random, where resources were located uniformly across the space; and patchy-random, where most resources were clumped as in the patchy maps, but 15% of them were located randomly between patches. Ten of each resource map were generated for each world size, each with a resource density of 3.3 %. As the presence or absence of resources at each point was binary, the resource location maps were compared within and across qualitative types using resource accumulation curves, based on the idea of species accumulation curves (Ugland, Gray and Ellingsen, 2003). These were generated by a simple Netlogo model of a random walker, who recorded the cumulative number of resources it encountered on a random walk through the space, with the walk length proportional to the size of the space (Appendix 2).

The resource accumulation curves showed distinct patterns for each of the three resource maps (full results in Appendix 2). For the patchy resource maps, the curves had a large range of means, and very high standard deviations (SDs) across the repeated trials for each map. The random resource maps had smaller ranges of means and lower SDs, and the patchy-random resource maps were between random and patchy for the range of means and the size of the SDs.

For the full model exploration, nine stylised landscapes were created using three resource maps (shown in main text), each with three patch maps (Table A1). The resource maps were styled to represent urban centres, urban to rural transition areas, and smaller villages. The urban centres and urban-to-rural transition resource maps were paired with uniform, random, and banded patches, with bands falling approximately between or around the resource clusters. The village resource maps were paired with random patches and two maps each of banded patches. These allowed for comparison of runs across a more limited range of landscapes, such that different arrangements of resources and patches were included, but clearer causal links between landscape features and

model dynamics and outcomes could be drawn. For the final experiments presented in the main text, only random patches were used.

Table A1. Descriptions and diagrams of patch maps used in full model exploration. The patch maps are shown with each patch coloured to represent the roughness, with lighter colour representing lower roughness.

Patch map name	Description	Illustration
Banded	Patches have uniformly random roughness between a specified minimum and maximum, with bands of maximum roughness, located at random.	
Random	Patches have uniformly random roughness between a specified minimum and maximum.	
Uniform	Patches have uniform roughness (equal to the maximum roughness used in other patch maps).	

Sensitivity analysis

As each simulation run contains stochastic elements in the initialisation and among resource and patch landscapes of the same qualitative type, replicates of each simulation run were performed. This minimised noise and ensured full coverage of the possible outcome variable distributions. As a stable value for each outcome variable was less of interest than the possible range of network structures and consumer outcomes, the distribution of each outcome variable rather than the final value was taken as the point of comparison between runs.

To determine the number of replicates needed per simulation run, a pre-test was conducted following Lorscheid *et al.* (2012). The high, middle, and low values for each parameter, combined with all possible combinations of resource and patch landscape, were run over 50 replicates. The distributions of outcome variables were compared, using the Kolmogorov-Smirnov test, between runs of the same parameter set, world size, and landscape for 3000 and 5000 timesteps, 25 and 50 replicates, and 3000 timesteps/25 replicates and 5000 timesteps/50 replicates, as well as across landscapes and world sizes.

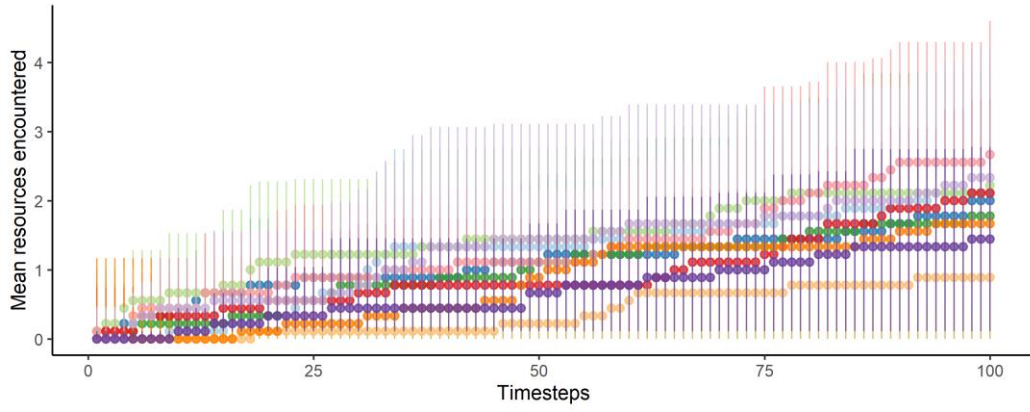
Overall, the distributions were not significantly different for most outcome variables at different timesteps and replicates, except for variables measuring cumulative totals, which were more varied for longer runs. Comparisons between world sizes, resource maps, and patch maps were significant. The final simulations for the full model exploration were therefore performed over a smaller range of resource and patch maps, for 3000 timesteps and 25 replicates of each run.

Appendix 2. Random walker model

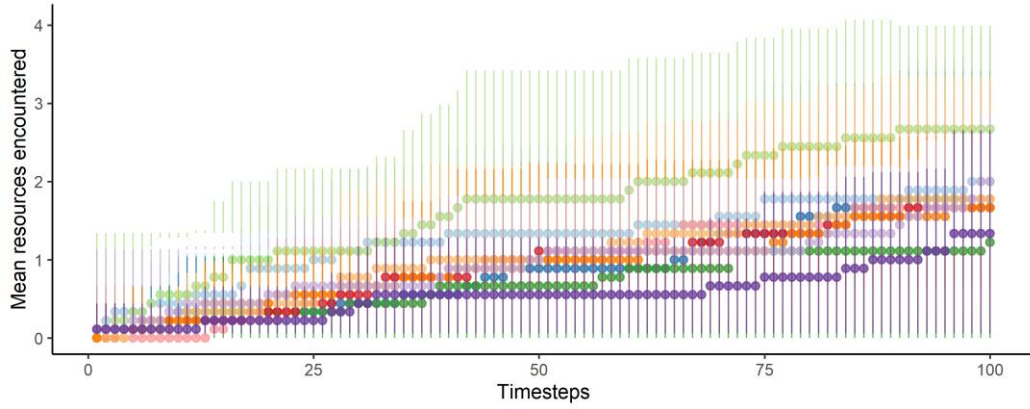
To ensure that the landscapes generated for the sensitivity analysis were different enough to test model dynamics, they were each tested with a random walker model to generate the resource accumulation curve. For each timestep of the model, the random walker moved to one of the six neighbouring patches of its own patch, checked if there were any resources there that it had not yet encountered, and if so, added them to the list of resources it had encountered. This continued for a duration proportional to the size of the landscape and was repeated ten times for each landscape. The number of unique identified resources was plotted over time for each repetition to generate the resource accumulation curve. The mean and standard deviation were then compared for each landscape.

The resource accumulation curves for each landscape are shown below. Overall, the patchy resource landscapes had quite high standard deviations and a large range of means, while the random resource landscapes had lower standard deviations and more similar means across replicates. The patchy-random resource landscapes had a range of means and standard deviations in between those of the patchy and random resource landscapes, as would be expected. This suggests that consumers could be expected to have qualitatively different outcomes given the resource landscape in which they are placed, when their specific behavioural rules are not directly considered.

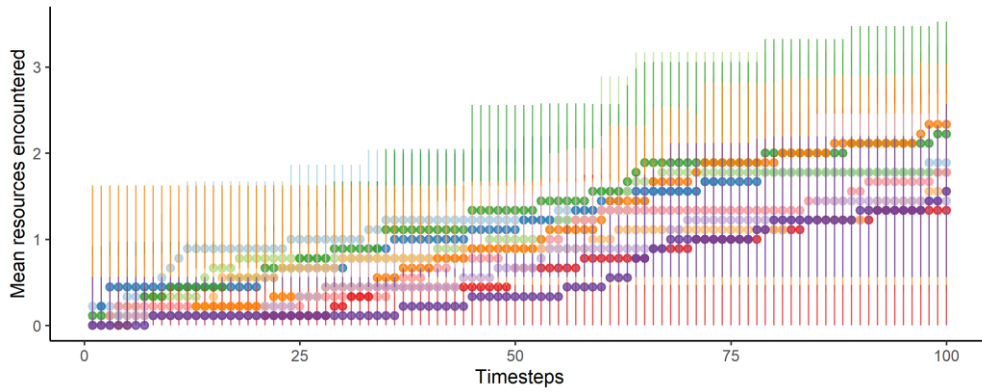
Structure, flow, and inequality



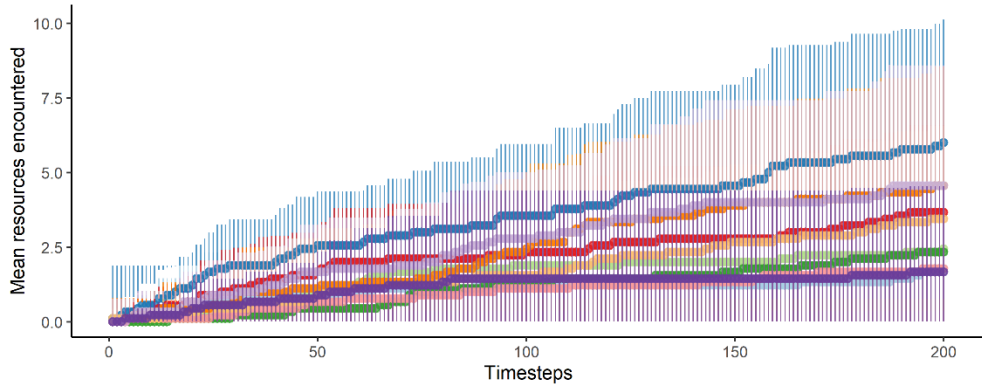
a.



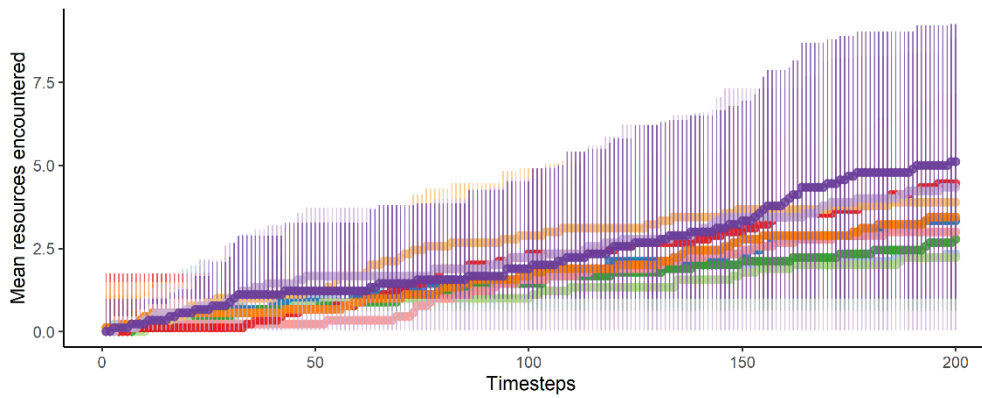
b.



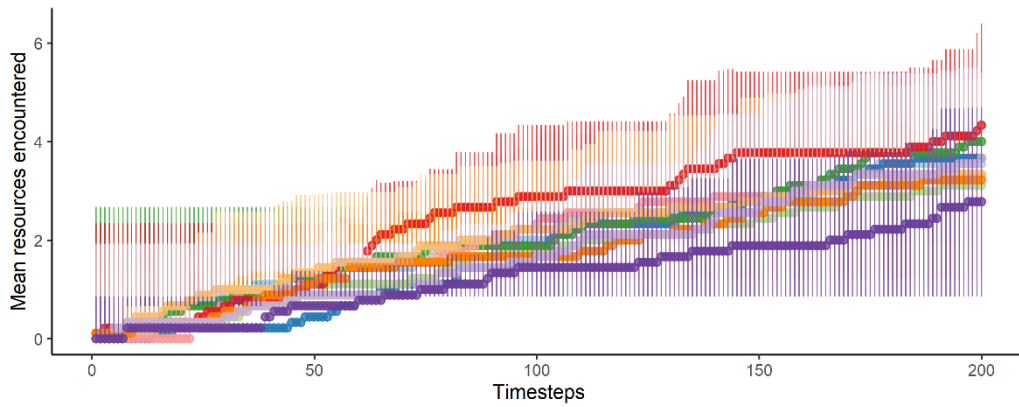
c.



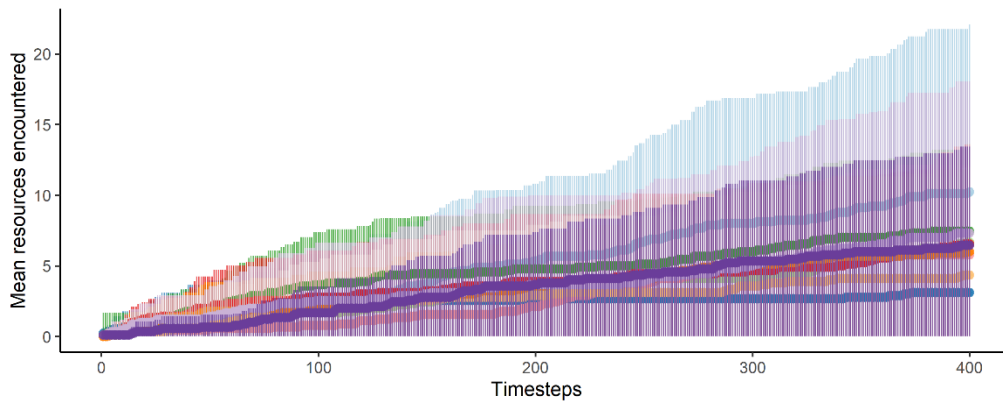
d.



e.



f.



g.

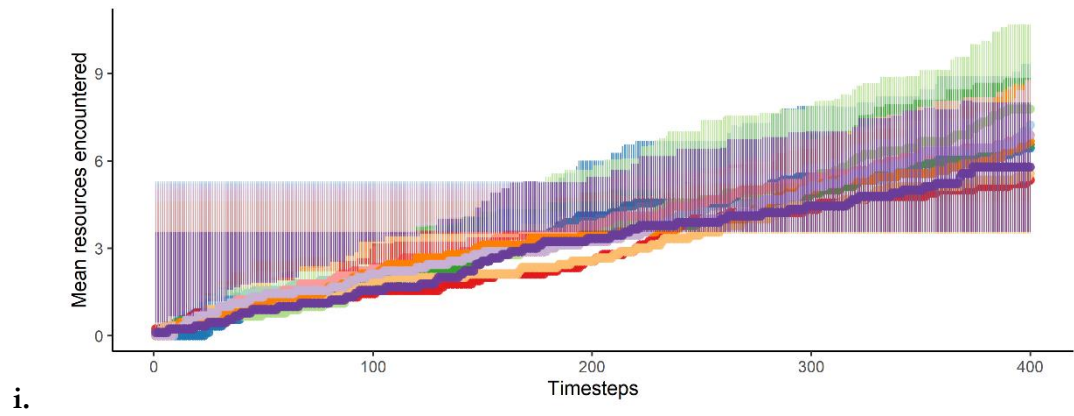
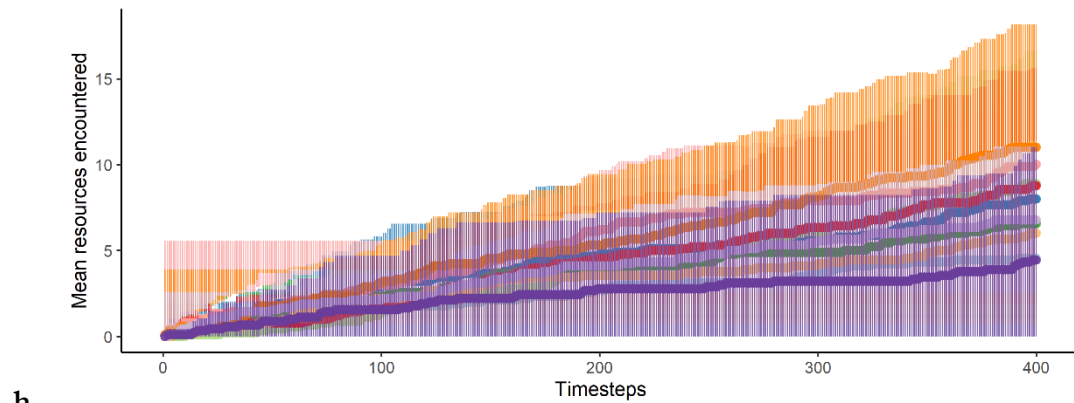


Figure A1. Resource accumulation curves for 10x10 (a) patchy, (b) patchy-random, (c) random; 20x20 (d) patchy, (e) patchy-random, (f) random; and 40x40 (g) patchy, (h) patchy-random, and (i) random landscapes. The points represent means for that timestep, and the bars represent standard deviations. Each colour series is one replicate.

Appendix 3. Full model exploration

Table A2. The (a) low and high values for each explored variable, and (b) fixed value for each control variable, used to parameterise the final experiments.

a.

Explored parameter	Low value	High value
Number of consumers	25	500
Maximum patch roughness	6 N	10 N
Minimum patch roughness	2 N	6 N
Link decay rate	0.1 J timestep ⁻¹	0.5 J timestep ⁻¹
Mean resource capacity	25 kcal	45 kcal
Standard deviation (SD) of resource capacity	2 kcal	7 kcal
Mean resource regrowth rate	9 kcal timestep ⁻¹	15 kcal timestep ⁻¹
SD of resource regrowth rate	1 kcal timestep ⁻¹	3 kcal timestep ⁻¹

b.

Control parameter	Fixed value
Mean time horizon	18 timesteps
SD of time horizon	4 timesteps
Mean initial energy reserves	70 kcal
SD of initial energy reserves	15 kcal
Mean basal metabolism	3 kcal timestep ⁻¹
SD of basal metabolism	0.5 kcal timestep ⁻¹
Mean consumption rate	5 kcal timestep ⁻¹
SD of consumption rate	1 kcal timestep ⁻¹
Mean rho	1
SD of rho	0.025
Mean risk penchant	72 %
SD of risk penchant	4 %

Table A3. Outcome variables calculated for each simulation run.

Variable name	Description
Population size	The number of consumer agents currently active in the simulation
Mean energy reserves	The mean of consumer energy reserves
Standard deviation (SD) of energy reserves	The standard deviation of consumer energy reserves
Gini energy reserves	The Gini coefficient of consumer energy reserves
Theil energy reserves	The Theil coefficient of consumer energy reserves
Mean offspring produced	The mean number of offspring produced
SD of offspring produced	The standard deviation of offspring produced
Gini offspring produced	The Gini coefficient of offspring produced
Number of links	The number of links (bi-directional) in the network
Number of (included) resource nodes	The number of resource nodes included in the network
Total link length	The total link length around the network
Diameter	The distance between the two furthest resource nodes included in the network
Mean link length	The mean link length
SD of link length	The standard deviation of link length
Gamma index	The ratio of possible links to observed links
Beta index	The ratio of links to total resource nodes in the landscape
Mean node degree	The mean number of links attached to each included resource node
Percentage of resource nodes included	The percentage of total resource nodes in the landscape that are included in the network

Analytical approach

The analytical approach emphasised visualisation and identification of visible and practical differences, rather than frequentist statistics. The latter are often overly sensitive in cases with large numbers of samples (here, replicates), making them likely to identify most differences as statistically significant (White et al., 2010).

To identify the relationships among outcome variables, however, traditional correlations and regressions were used. For the correlations, a random sample of 500 parameterisations was selected for each world size, and the Spearman's rank correlation coefficient was calculated for each set of replicates at 1000, 2000, and 3000 timesteps. Spearman's rank was chosen as not all relationships were approximately linear. Additionally, linear regressions were performed at 1000, 2000, and 3000 timesteps. The linear models were fit by selecting a sample of 100 parameterisations, fitting a

regression to model each outcome variable with all other outcome variables for each set of replicates, and testing the residuals for normality and heteroskedasticity. This was repeated for each world size. Models with normal residuals were kept, and the significant coefficients were identified. These were further compared across time steps.

All analyses and visualisations were done in R version 4.0.3 (R Core Team, 2020), using the *ineq* (Zeileis, 2014), *igraph* (Csardi and Nepusz, 2006), and *ggplot2* libraries (Wickham, 2016).

Results

Across a range of analyses, the input parameters of link decay rate, initial population size, and mean resource capacity were the most important, both individually and combined, in determining both consumer outcomes and network size and structure. In contrast, the standard deviations of resource capacity and regrow rate had little to no noticeable effect on the outcome variables.

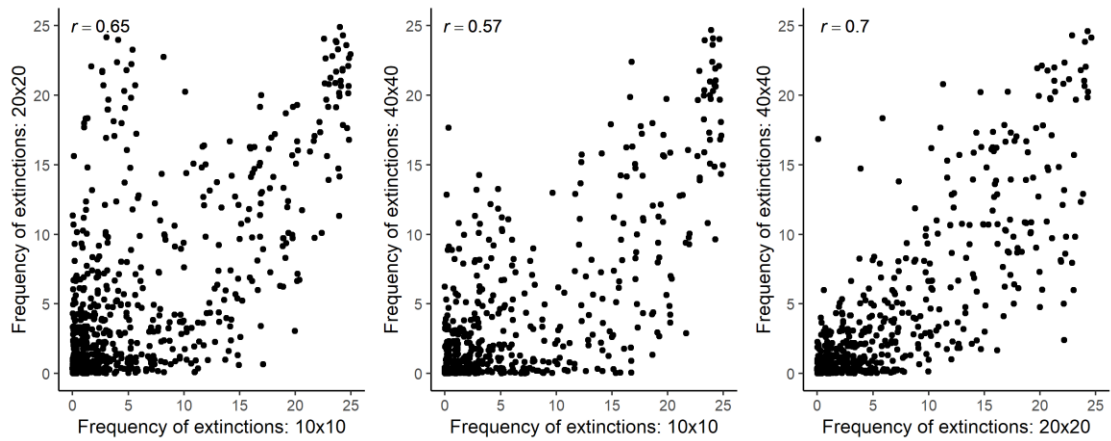
The results identified in the following sections were broadly stable across time and world size, with the range of the outcome variables sometimes increasing in larger world sizes, but the qualitative relationships remaining the same. In the next sections, the following will be explored: first, broad patterns of outcomes such as runs where the population went extinct or did not construct any links, followed by analyses relating both the outcome variable values with input parameters, and with one another.

Extinctions

In some runs, the population went extinct before the simulation completed. The frequency of these extinctions was compared across world sizes, landscapes, and input parameter values. For all pairs of world sizes, the frequency of extinctions was significantly correlated (Figure A4), and the pattern of extinctions by landscape and input parameters were similar, suggesting that world size did not strongly influence whether a population would survive in a run with a given landscape and starting parameterisation. Extinctions predominantly occurred in random cities and random

villages, with some occurring in uniform cities (10x10) and banded cities (20x20) (Figure A5). The frequency of extinctions was related to link decay rate, resource capacity and regrow rate, and population size, with most extinctions occurring in runs with high link decay rate, high mean resource capacity, and low initial population size (Figure A5).

A



B

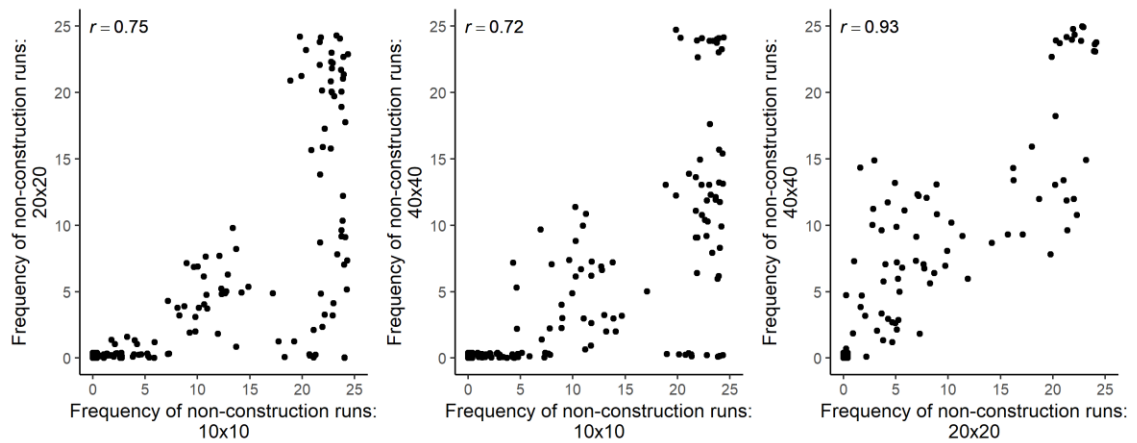
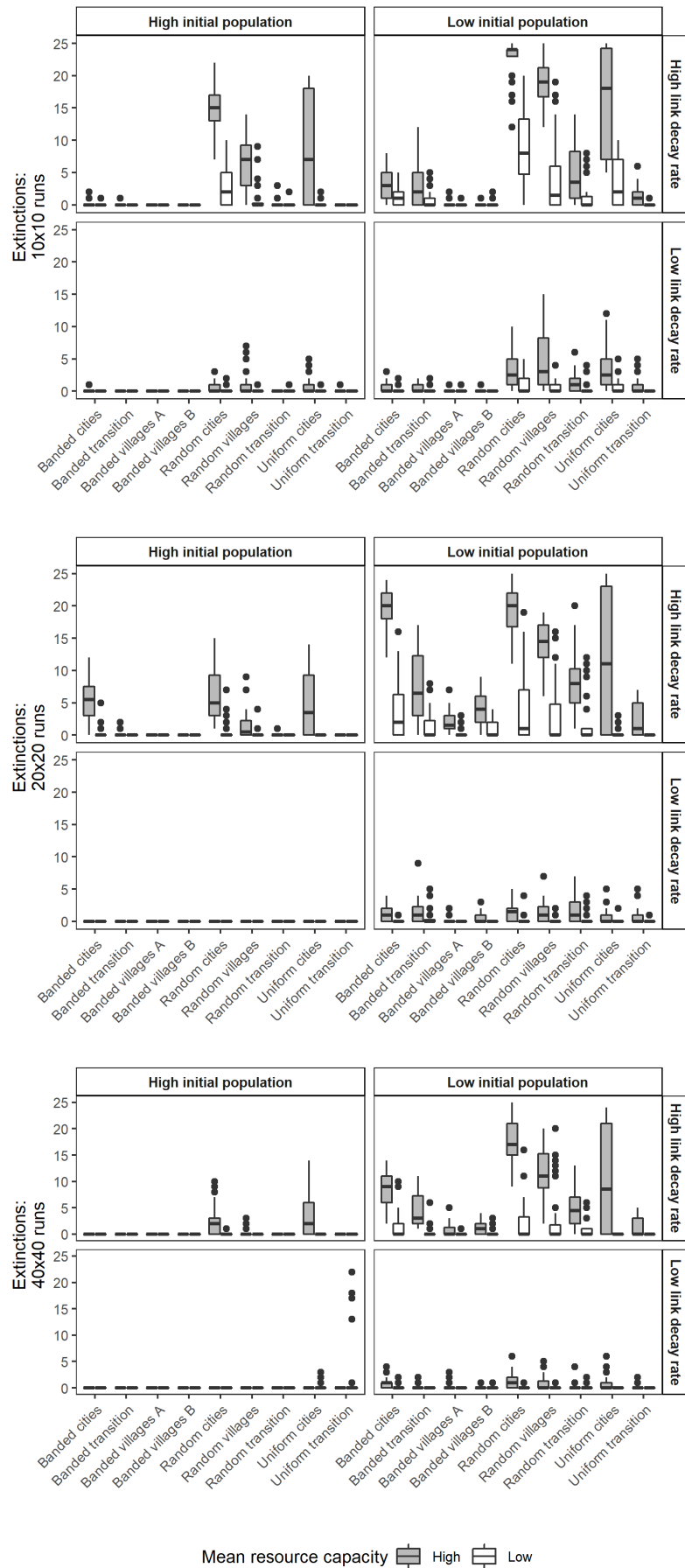


Figure A4. Correlations of the frequency of (a) extinction events and (b) non-construction runs between world sizes, for each parameterisation (replicate). Shown in the top left corner is the Spearman's correlation coefficient for the correlation between events in the two world sizes. All correlations were significant ($p < 0.001$, $N = 2304$ pairs).

A



B

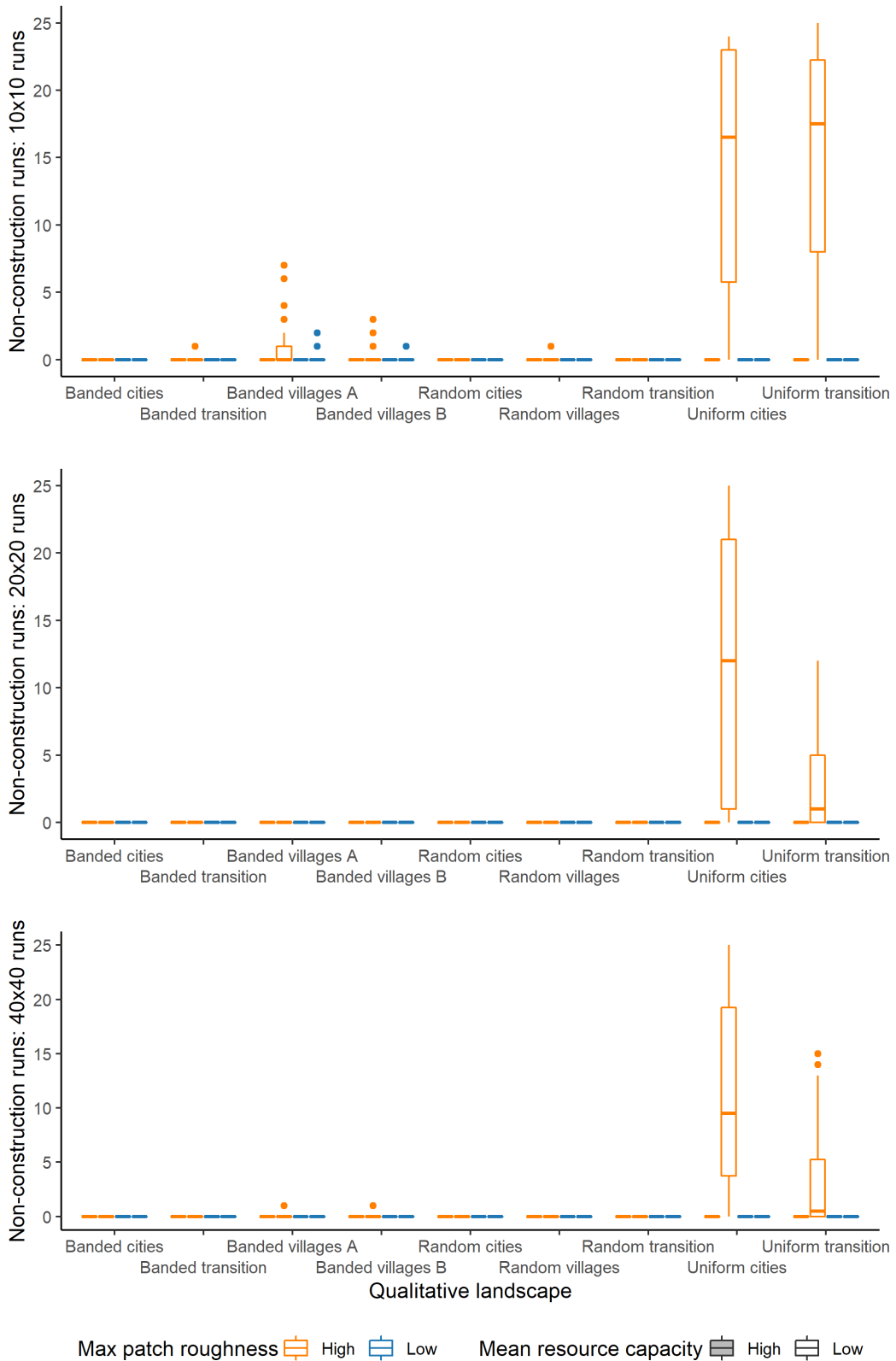


Figure A5. Number of runs by landscape where the population (a) went extinct and (b) did not construct a network. The rows and columns in (a) are link decay rate and initial population size, respectively, and the outline and fill colour of both plots represent the maximum patch roughness and mean resource capacity, respectively.

Non-construction runs

There were also runs where the consumers did not build or maintain links between resources, and instead remained in their starting positions throughout the simulation. While these populations sometimes went extinct, in other runs they survived the duration of the simulation, albeit with typically low population sizes. As with the extinctions, the frequency of non-construction runs was significantly correlated and similar in pattern of occurrence across world sizes (Figure A5). These runs occurred almost exclusively in uniformly high-roughness landscapes with low mean resource capacity.

Correlations

After determining the parameterisations related to extinctions and non-construction events, the relationships between outcome variables were explored. The correlations for each pair of outcome variables were calculated for a sample of runs in each world size (see Methods) and the distribution of correlation coefficients was plotted (Appendix 4). The distributions of correlation coefficients for each pair of outcome variables were quite similar across timesteps, world sizes, and landscapes. Moreover, several outcome variables were consistently strongly positively correlated, such that these were grouped for later analyses with one variable used as the representative of the grouping (Appendix 4).

The identified groupings were consumer inequality, offspring produced, total network size, and network connectivity. In the first grouping, the Gini, Theil, and standard deviation of consumer energy reserves all consistently positively correlated, so the standard deviation (SD) of consumer energy reserves was used to represent consumer inequality in later analyses. For offspring production, mean and SD of offspring produced were quite strongly correlated, so the SD of offspring produced is used to represent offspring production across the population. For total network size, counts of links and included nodes, total link length, diameter, gamma index, beta index, and percentage of nodes used were all strongly positively correlated, with link length used to represent this grouping. Finally, the average node degree, gamma index, beta index, and

percentage of nodes used were highly or perfectly correlated, so average node degree was used to represent network connectivity in future analyses.

Apart from the grouped variables of the same type, there were few meaningful correlations between outcome variables of different types (Table A4). One exception was the current population size, which was consistently positively correlated with total link length and mean node degree. Population size was slightly positively correlated with mean link length in most landscapes (Table A4, Appendix 4), though this was diminished in landscapes with less total construction, such as banded villages, and frequent non-construction events, such as uniform cities and uniform transition. Mean and SD of energy reserves were not notably correlated with link outcome variables but mean and SD of offspring produced were slightly negatively correlated with total link length.

Table A4. Mean and standard deviation of correlation coefficients for relationships between representative outcome variables. The standard deviations for the correlations reflect the sample of 500 replicates from each world size used for calculations (see Methods of this section). For simplicity, only the correlations for the 40x40 world size at timestep 3000 are shown here, as all world sizes and timesteps followed the same pattern of relationships (Appendix 4).

	Mean energy reserves	SD of energy reserves	SD of offspring produced	Total link length	Mean link length	SD of link length	Mean node degree
Population size	0.037 (0.319)	0.123 (0.34)	0.089 (0.321)	0.483 (0.322)	0.257 (0.295)	0.093 (0.313)	0.374 (0.302)
Mean energy reserves		0.448 (0.227)	-0.019 (0.312)	0.052 (0.234)	0.041 (0.226)	0.004 (0.217)	0.039 (0.233)
SD of energy reserves			0.084 (0.31)	0.019 (0.249)	0.033 (0.234)	-0.015 (0.234)	0.014 (0.247)
SD of offspring produced				-0.055 (0.257)	-0.024 (0.238)	-0.019 (0.221)	-0.022 (0.247)
Total link length					0.776 (0.215)	0.277 (0.49)	0.856 (0.15)
Mean link length						0.467 (0.558)	0.739 (0.254)
SD of link length							0.226 (0.482)

Faceting

In addition to identifying relationships among outcome variables, the distributions of outcome variables by initial parameterisation were visualised. These plots were generated for the data at 1000, 2000, and 3000 timesteps, and all world sizes, although as with the other analyses, the distributions did not show much difference over time or world size.

Overall, the distributions showed that larger, more heterogeneous networks, as measured by the total and SD of link length, occurred in runs with low patch roughness, low link decay rate, and a high initial population size (Figure A6), though the latter levelled off some over time (Figure A7). Both the largest and most connected networks, as measured by mean node degree, occurred in banded and random cities and transition landscapes (Figure A6).

Structure, flow, and inequality

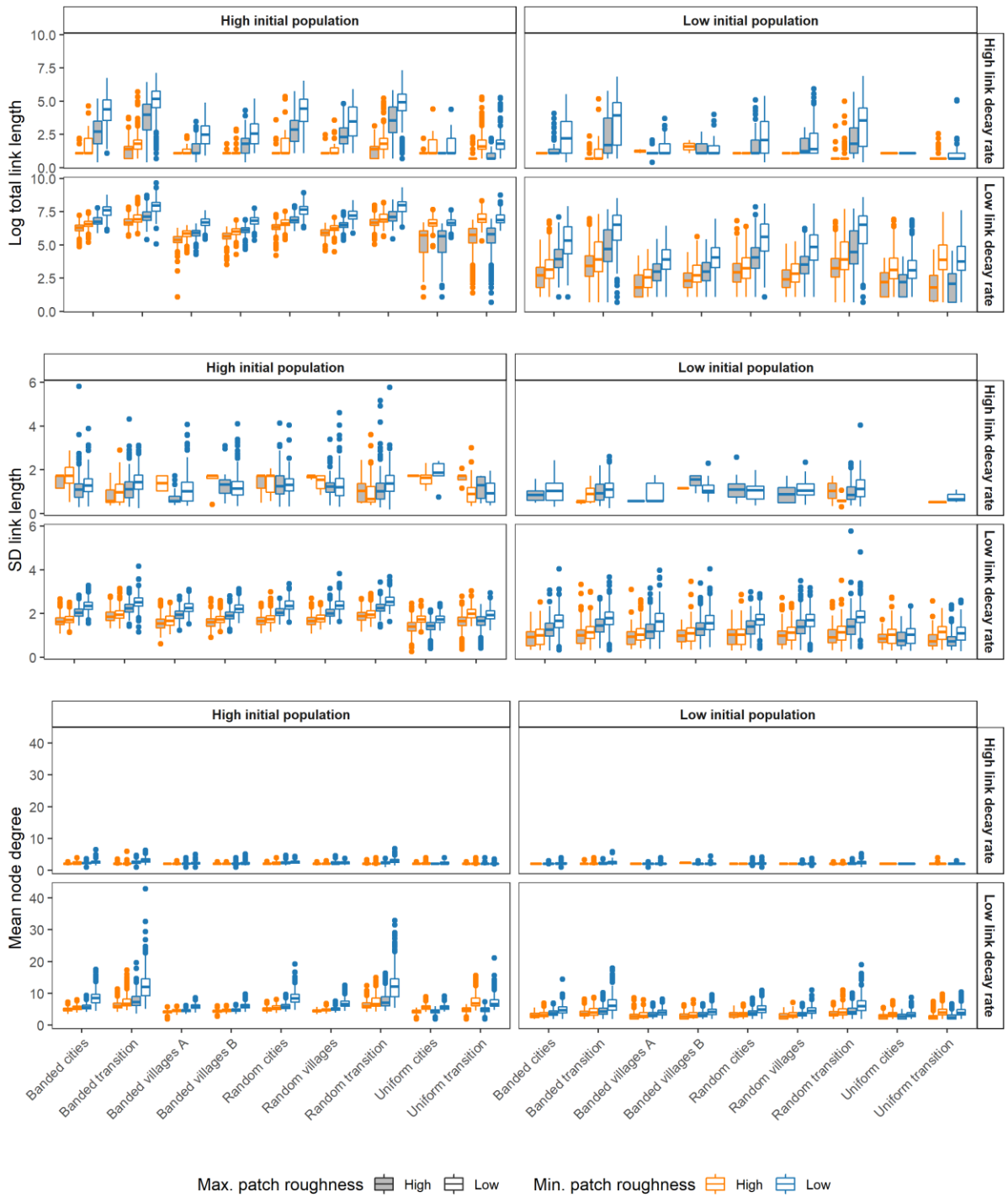
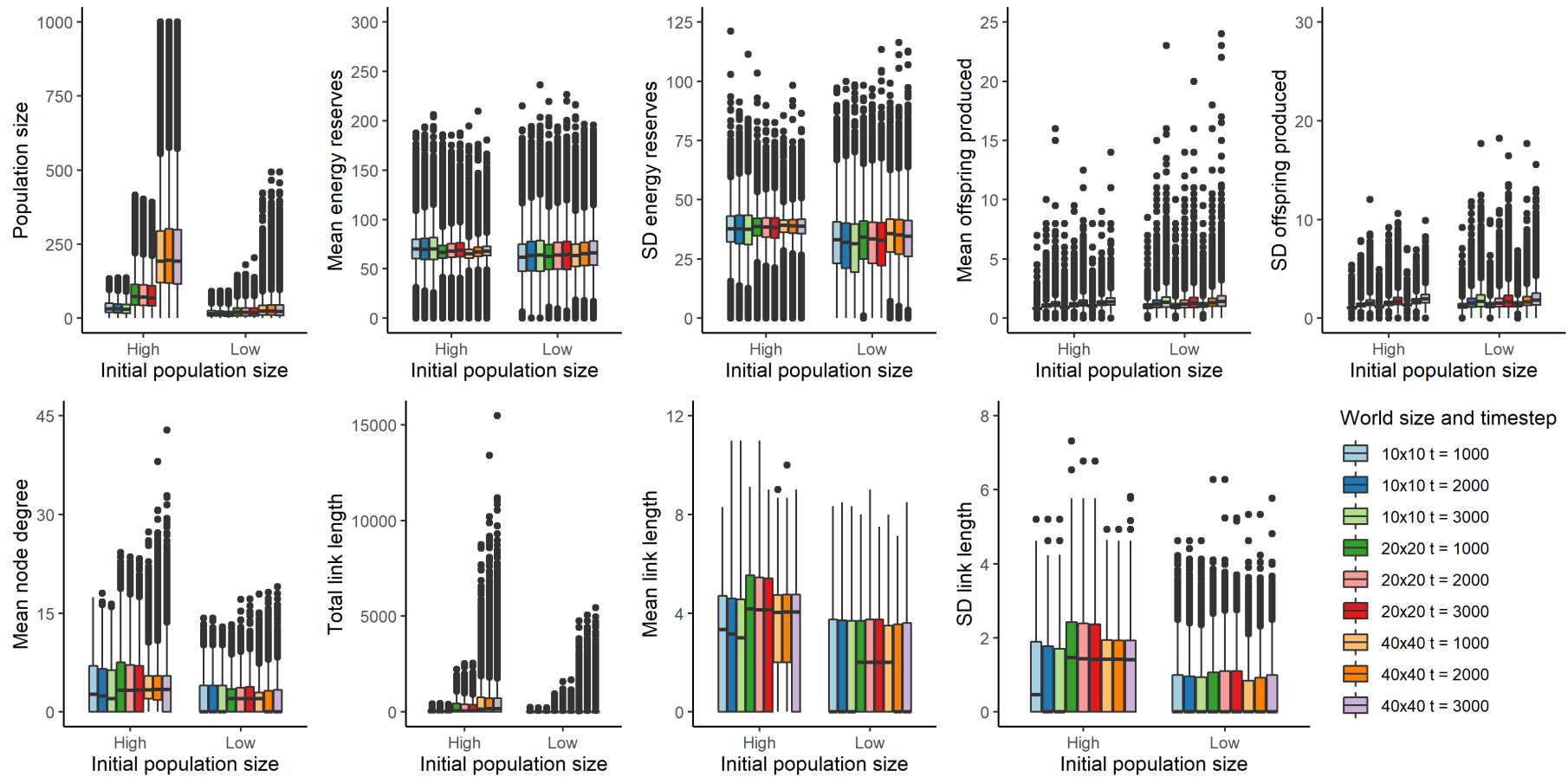
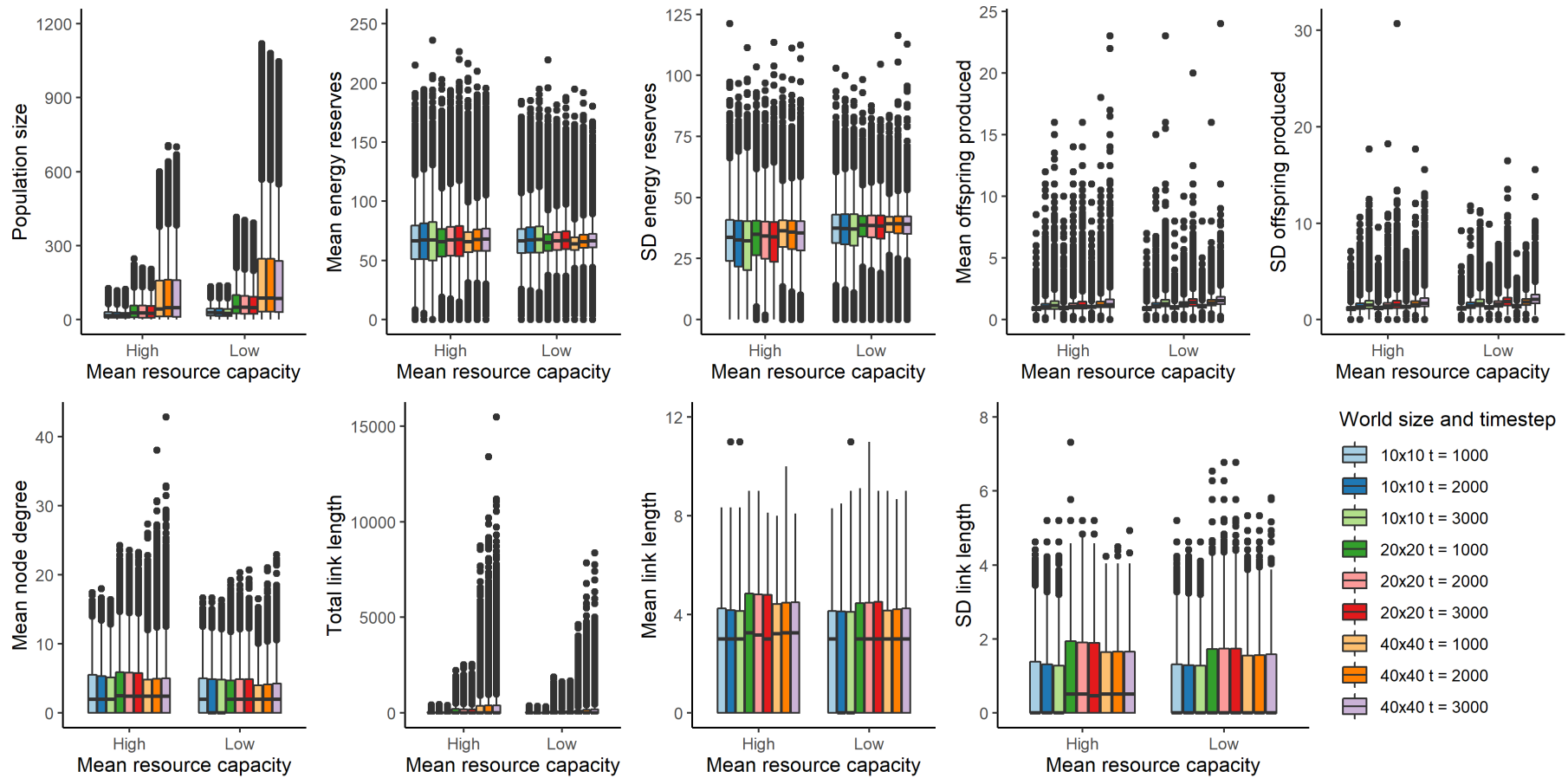


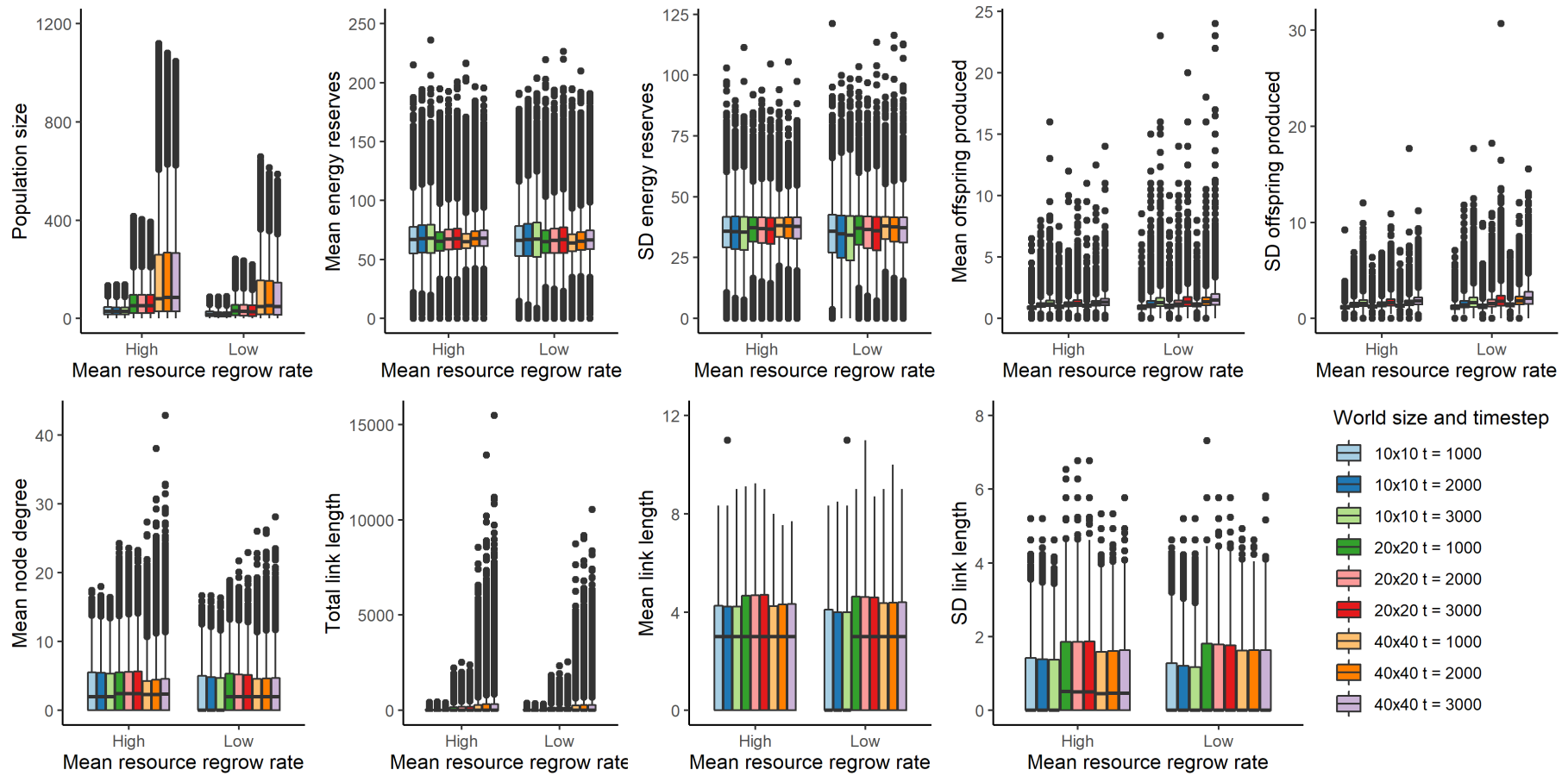
Figure A6. The distribution of total network link length, SD of link length, and mean node degree, by landscape, maximum and minimum patch roughness. The total link length has been logged for clarity, and total and SD of link length are in generic length units. The rows and columns are link decay rate and initial population size, respectively.



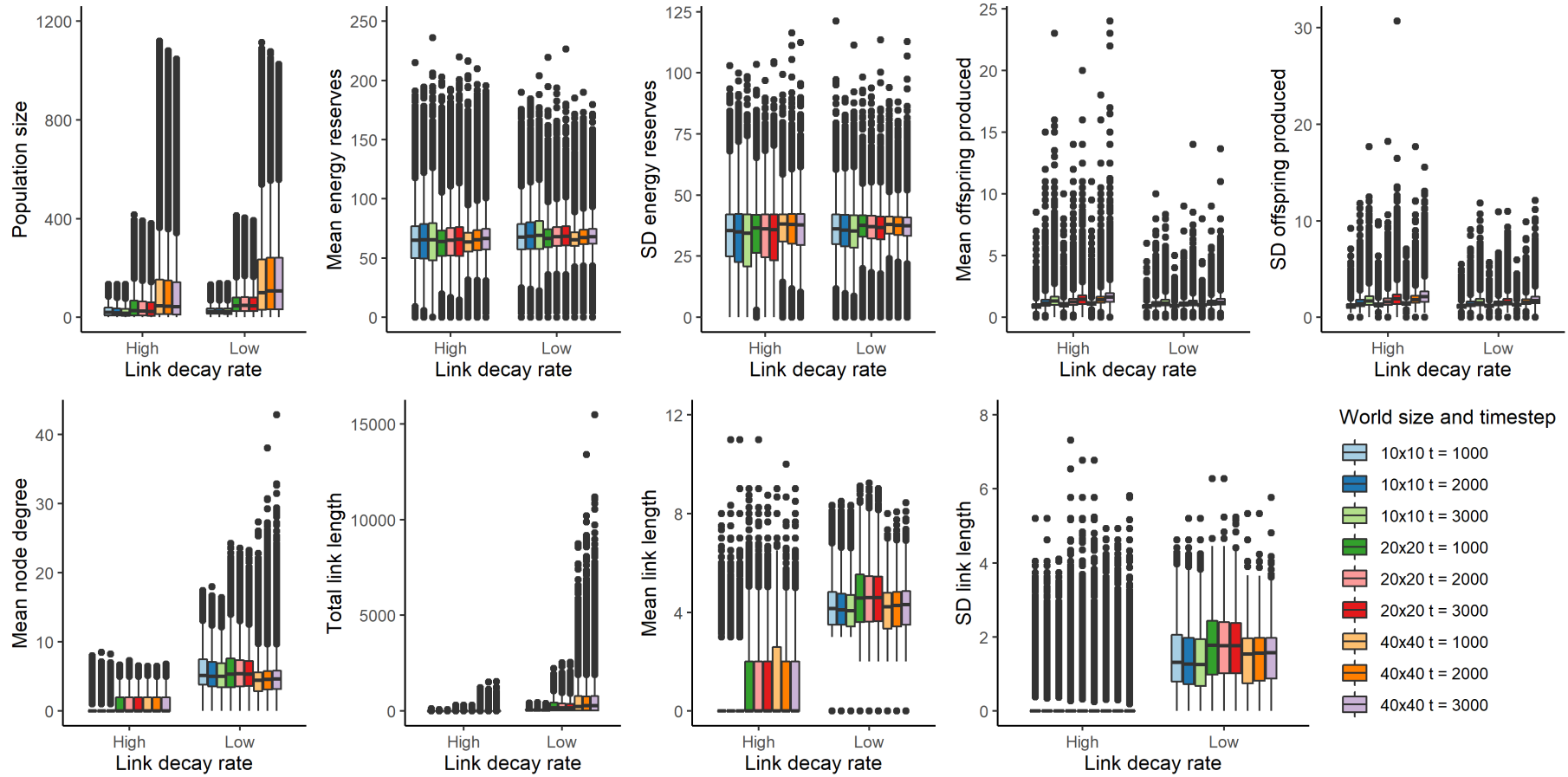
Structure, flow, and inequality



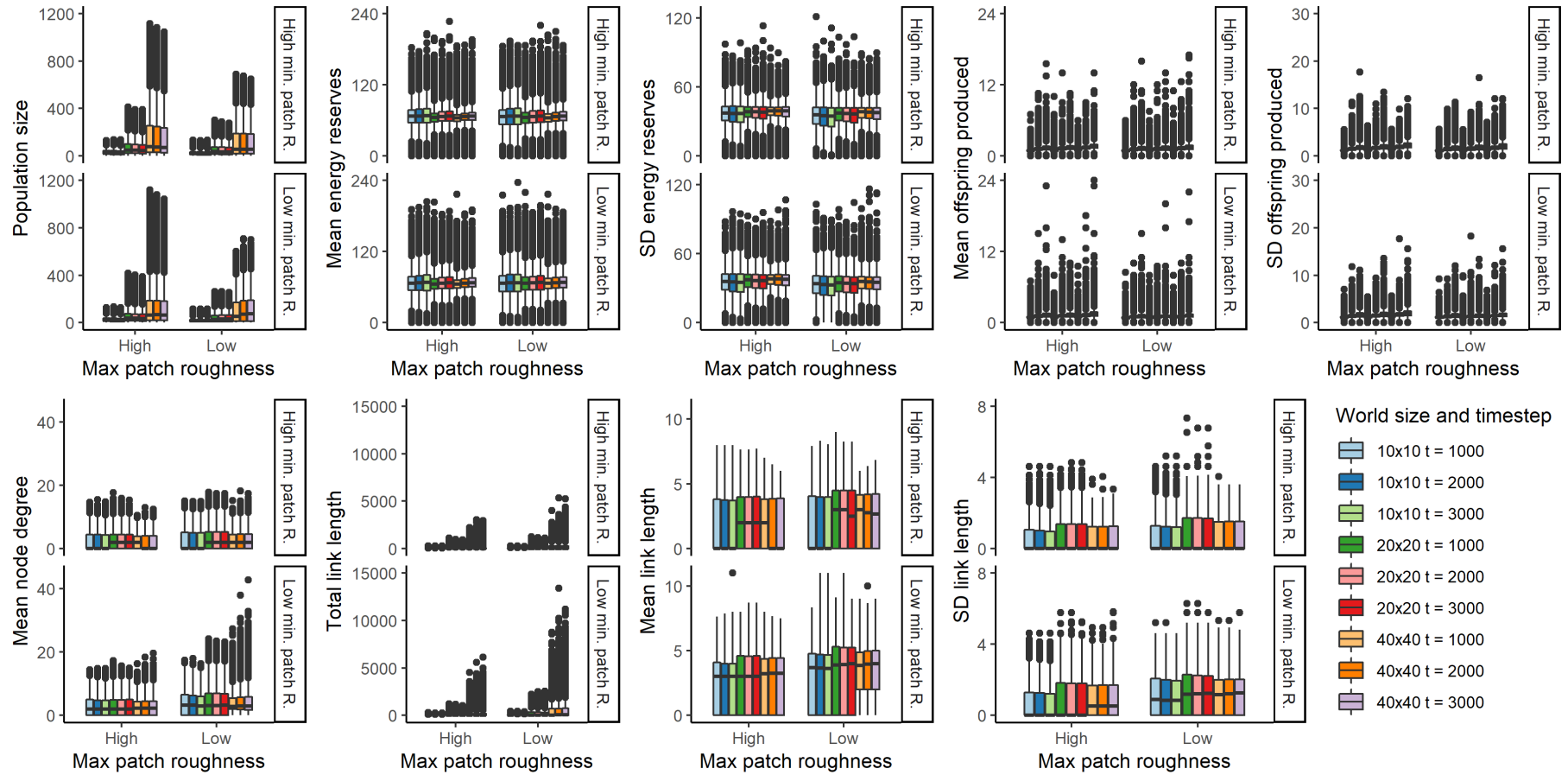
Chapter 4: Co-evolution of network structure and consumer inequality



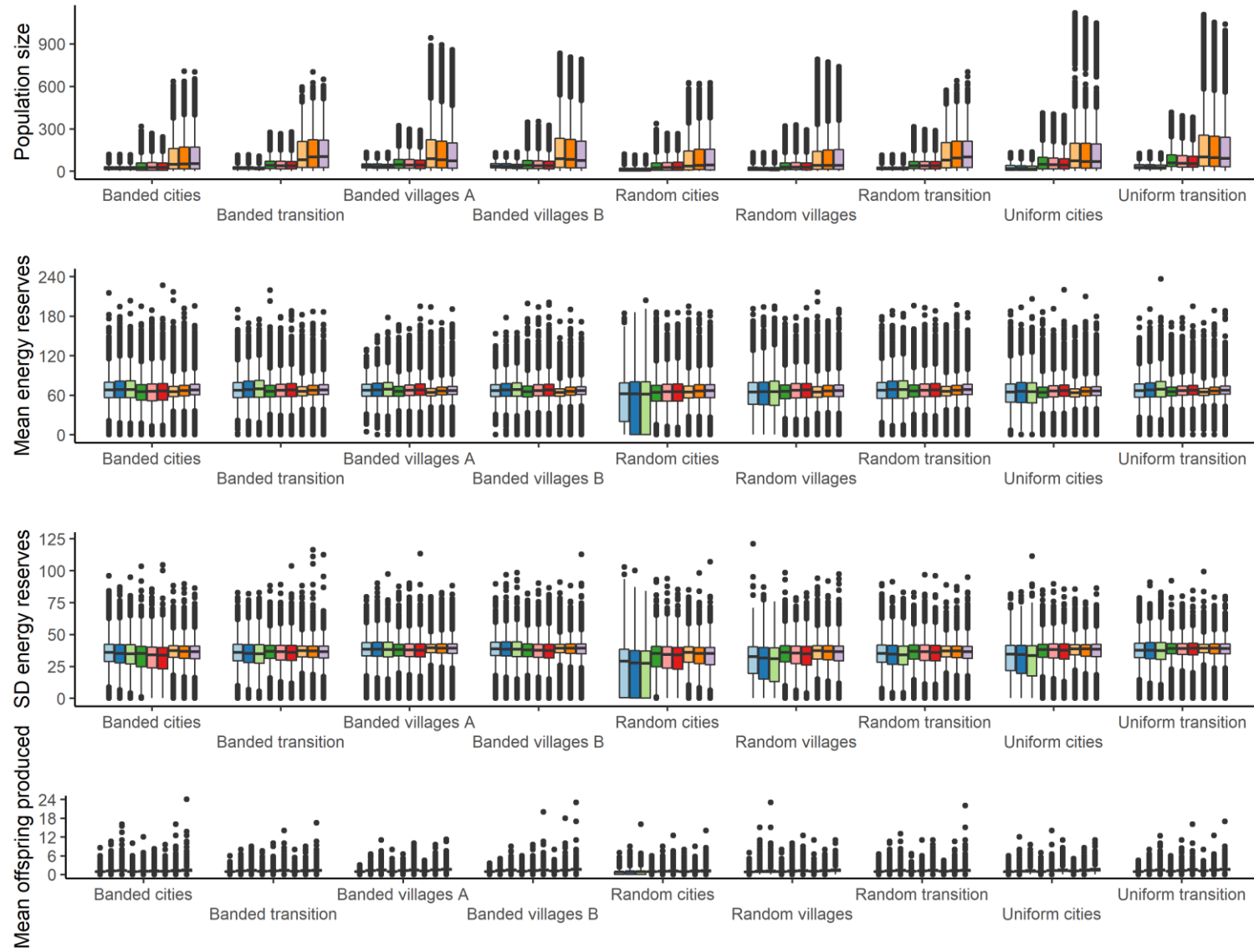
Structure, flow, and inequality



Chapter 4: Co-evolution of network structure and consumer inequality



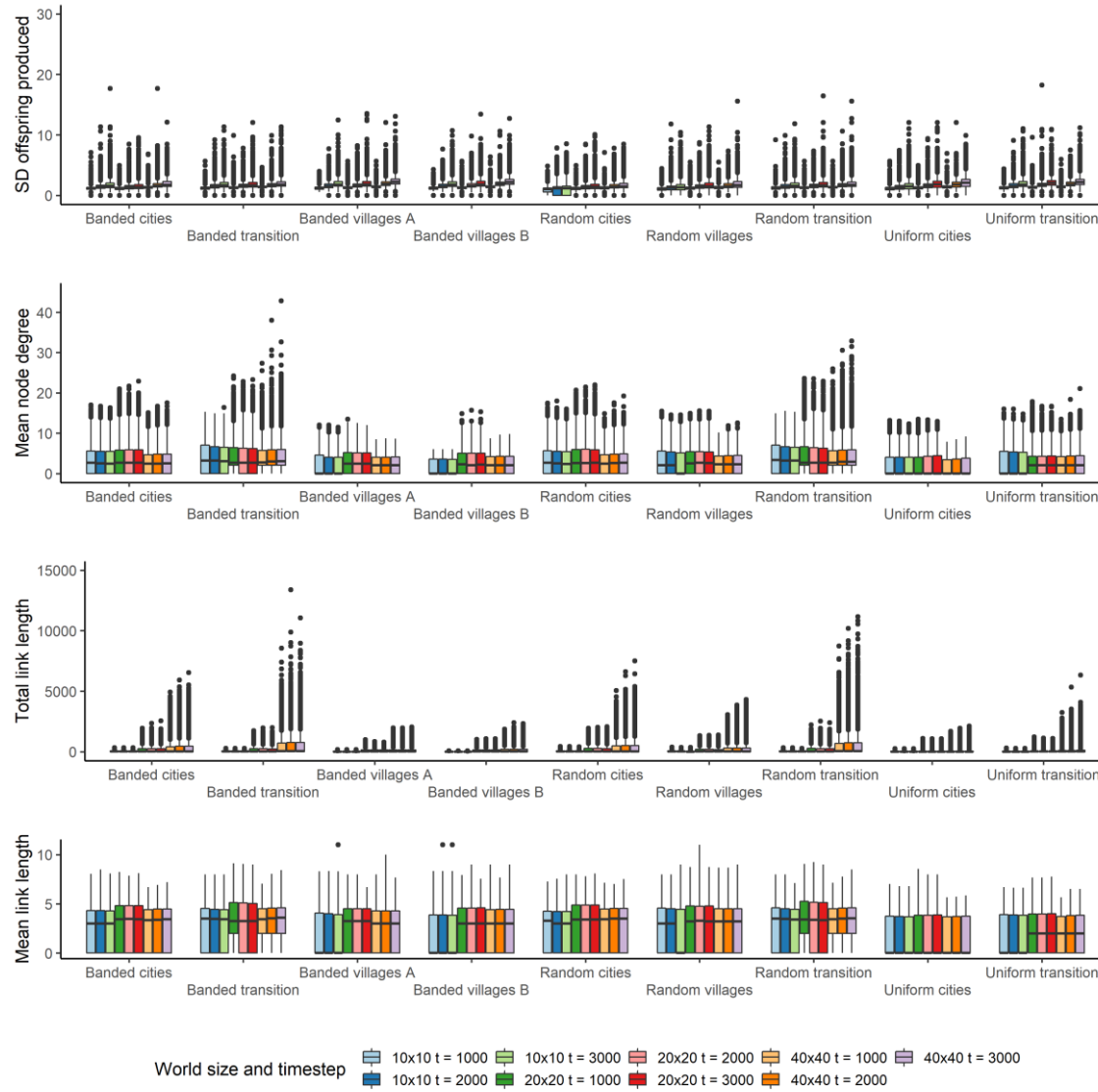
Structure, flow, and inequality



World size and timestep

10x10 t = 1000	10x10 t = 3000	20x20 t = 2000	40x40 t = 1000	40x40 t = 3000
10x10 t = 2000	20x20 t = 1000	20x20 t = 3000	40x40 t = 2000	

Chapter 4: Co-evolution of network structure and consumer inequality



Structure, flow, and inequality

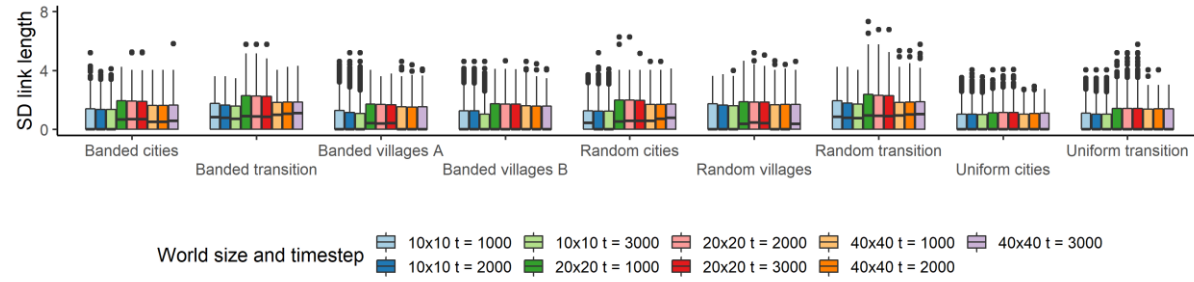


Figure A7. Distributions of outcome variables by parameter levels.

Network heterogeneity and connectivity were also typically higher in runs with high initial population size, low link decay rate, and high mean resource capacity (Figure A6). Distributions of both variables also showed more high outliers in runs with low patch roughness and high mean resource regrow rate (Figure A7).

Similarly, consumer inequality was affected by initial population size and mean resource capacity, with lower inequality related to each low initial population size, high mean resource capacity, and to a lesser extent, low patch roughness (Figures A6, A7). Link decay rate also appears to have affected consumer inequality, as SD of energy reserves had a slightly lower median and first quartile when link decay rate was high (Figure A7). There was also much less construction in these runs, however, and more extinctions associated with this parameterisation. The distribution of consumer outcome variables was quite similar across landscapes, except for random cities and villages, where there were more frequent extinction events.

As discussed previously, the mean and standard deviation of offspring produced were closely correlated, as generally very few offspring were produced in most runs. Both variables showed higher medians and distributions in runs with low initial population size and high link decay rate, and more high values in runs with high mean resource capacity and low mean resource regrow rate (Figure A7).

Most notably of the consumer-related variable outcomes, the distribution of mean energy reserves for any given input parameter value or landscape was quite small, with a median close to 70, which was the value used as the mean of the distribution of initial energy reserves of the population (Figure A7). However, the SD of energy reserves increased from 15 at initialisation to a distribution with a median close to 38 (Figure A7). Put another way, the variance of energy reserves increased considerably in most runs, but the mean stayed close to the original value.

Ergodicity and stationarity

Before any timeseries analyses could be run, the stationarity and ergodicity of the outcome variables was tested for each outcome variable in each run or set of replicates, following the method of Grazzini (2012). No outcome variables were consistently both stationary and ergodic, and the parameterisations associated with ergodicity and stationarity in link variables, and ergodicity in consumer variables, were the opposite of those associated with stationarity in consumer outcome variables.

Specifically, stationarity in consumer outcome variables was associated with parameterisations that produced little to no network construction (Figure A8), such as high link decay rate, low resource capacity, and low initial population size. The opposite was true for both stationarity in link-related outcome variables, and ergodicity of all variable types: here, they were associated with parameterisation that produced larger, more interconnected networks and more inequality among consumers (Figure A8), such as low link decay rate, high resource capacity, and high initial population size.

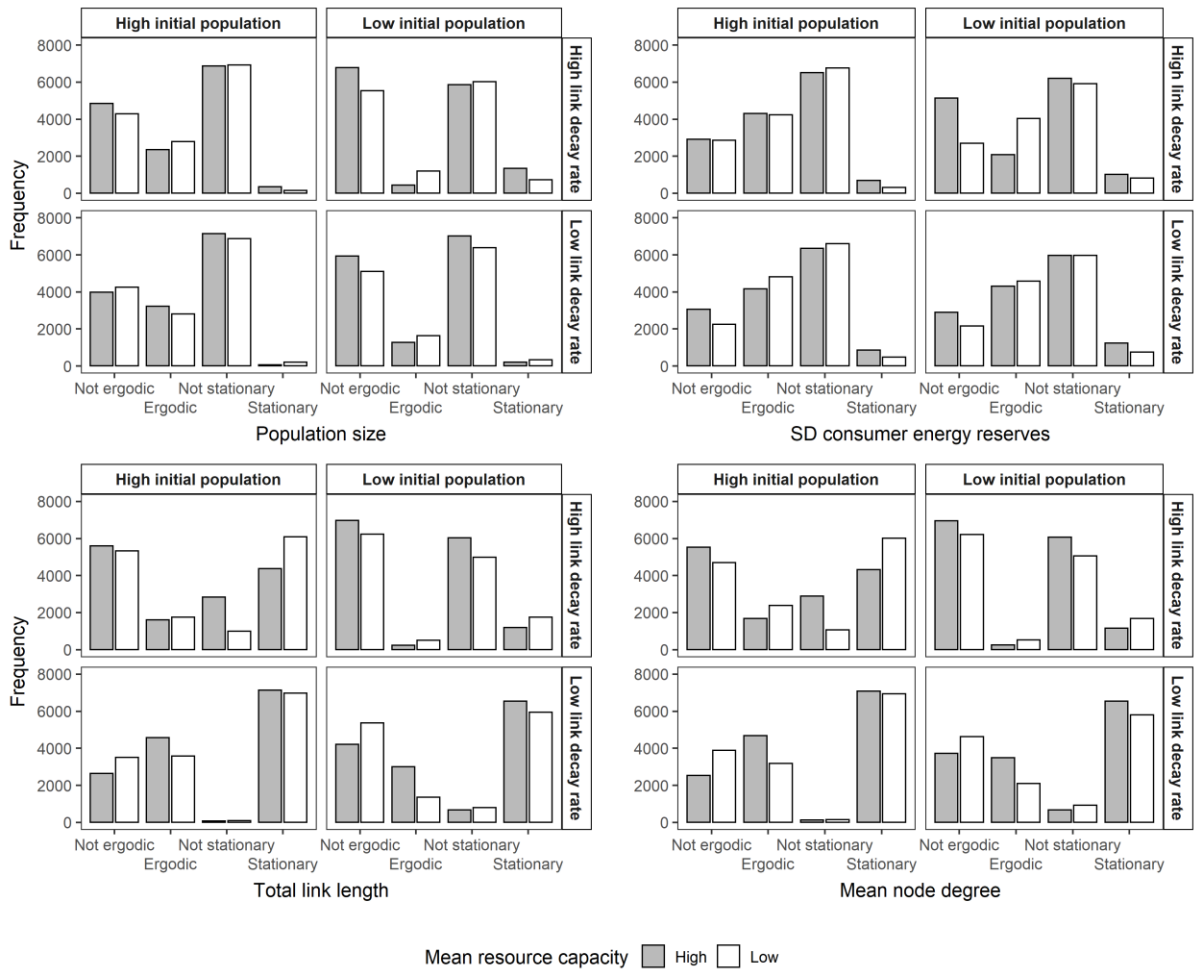


Figure A8. The frequency of ergodicity and stationarity for population size, SD of consumer energy reserves, total link length, and mean node degree. For simplicity, only 40x40 world size is shown, as all world sizes followed the same pattern. Rows are link decay rate and columns are initial population size.

Regressions

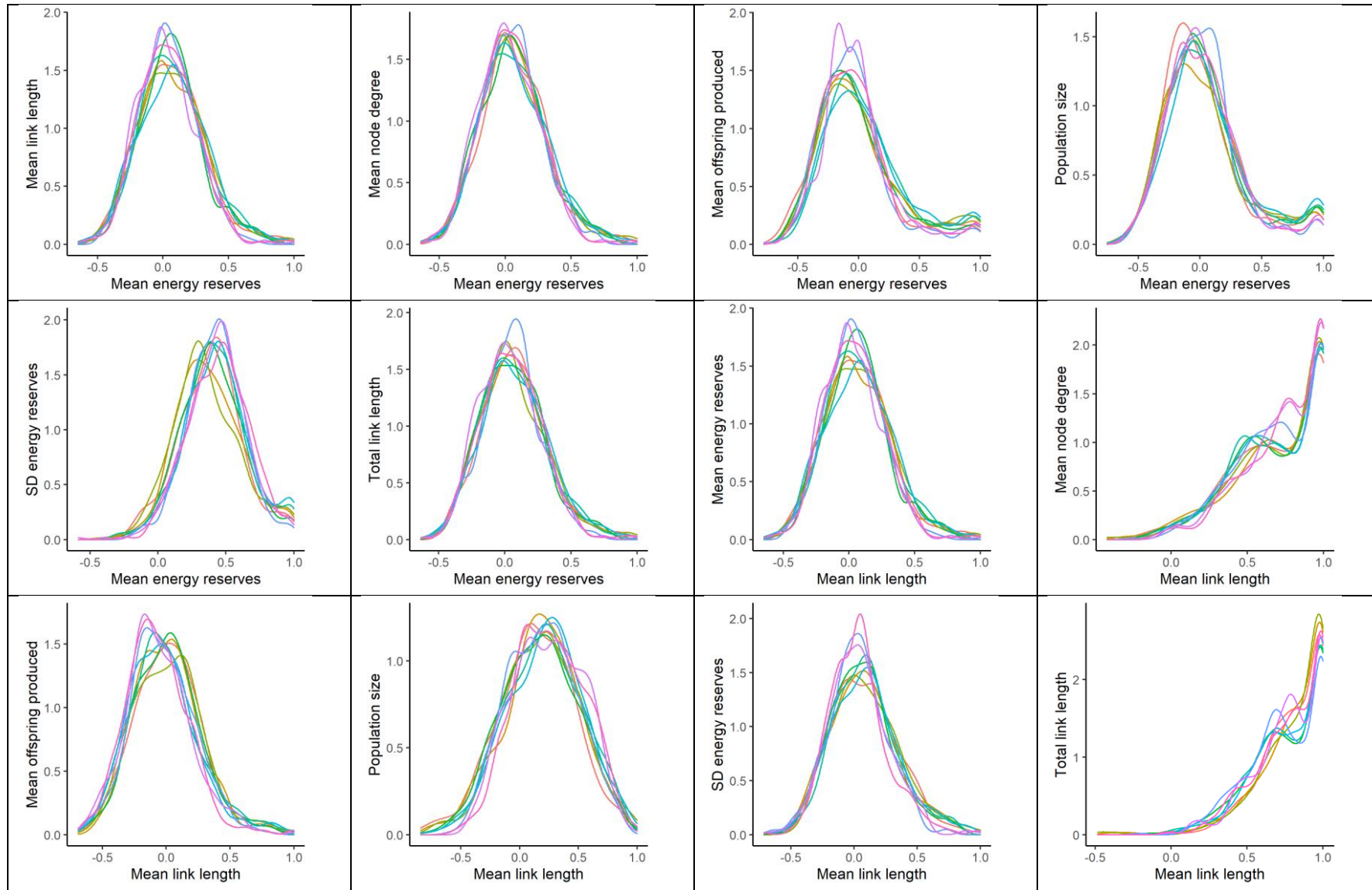
As most of the outcome variables were only rarely both ergodic and stationary, as required by traditional time series analyses, linear regressions at 1000, 2000, and 3000 timesteps were used to examine the relationships among outcome variables. No clear, consistent relationships were present, once models with non-normal residuals and relationships that occurred during only one or two of the tested time points were removed (see Methods in this appendix). The number of consumers occasionally showed both positive (10x10, 40x40) and negative (10x10, 20x20) effects on the mean link length, though there were not clear patterns of other outcome variable relationships or input parameters that determined this directionality.

Appendix 4. Correlations

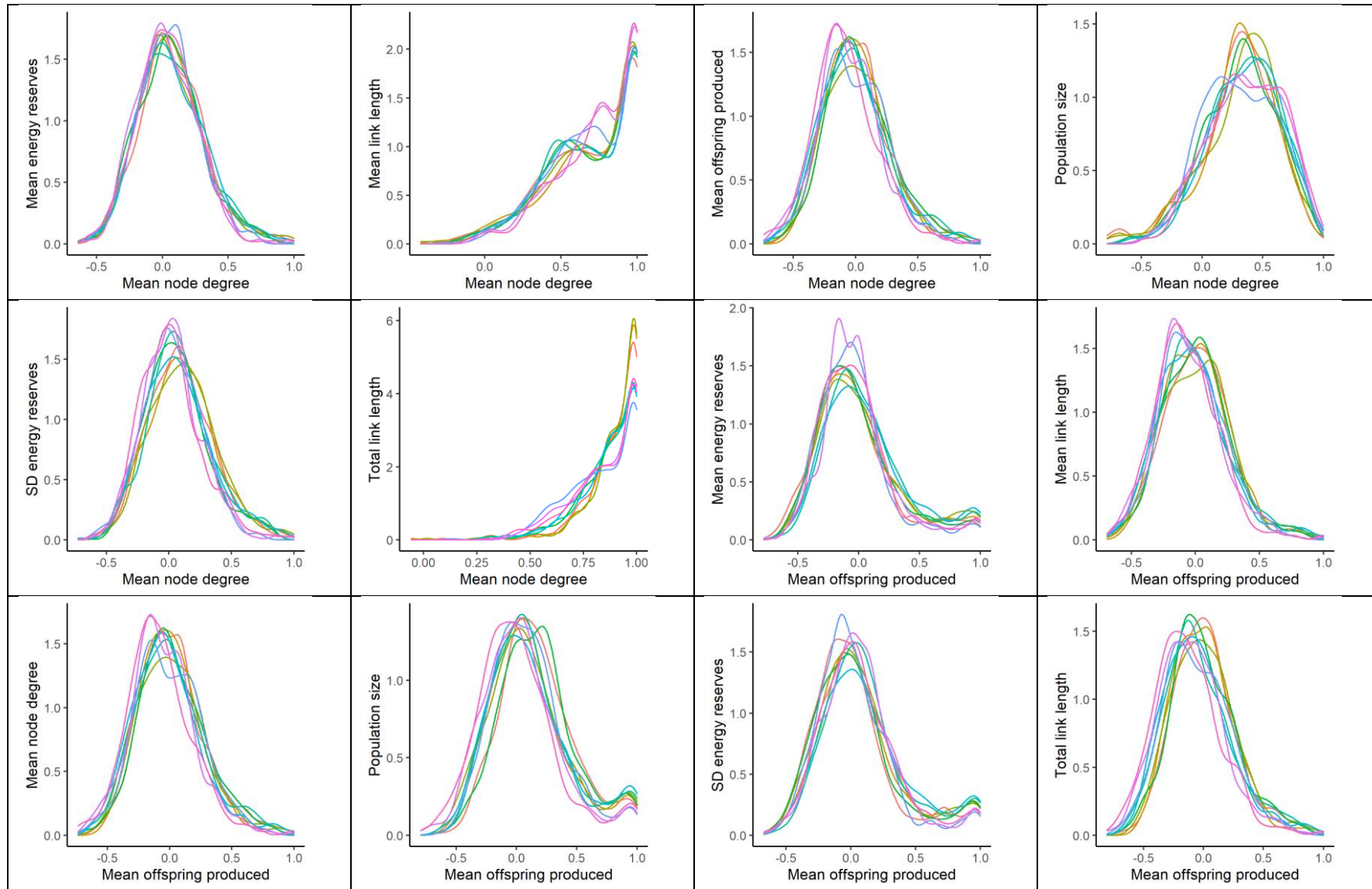
Table A5. Mean and standard deviation of correlation coefficients for relationships between related outcome variables (all types). The standard deviations for the correlations reflect the sample of 500 replicates from each world size used for calculations (see Methods). For simplicity, only the correlations for the 40x40 world size are shown here, as all world sizes followed the same pattern of relationships (see Figure A4).

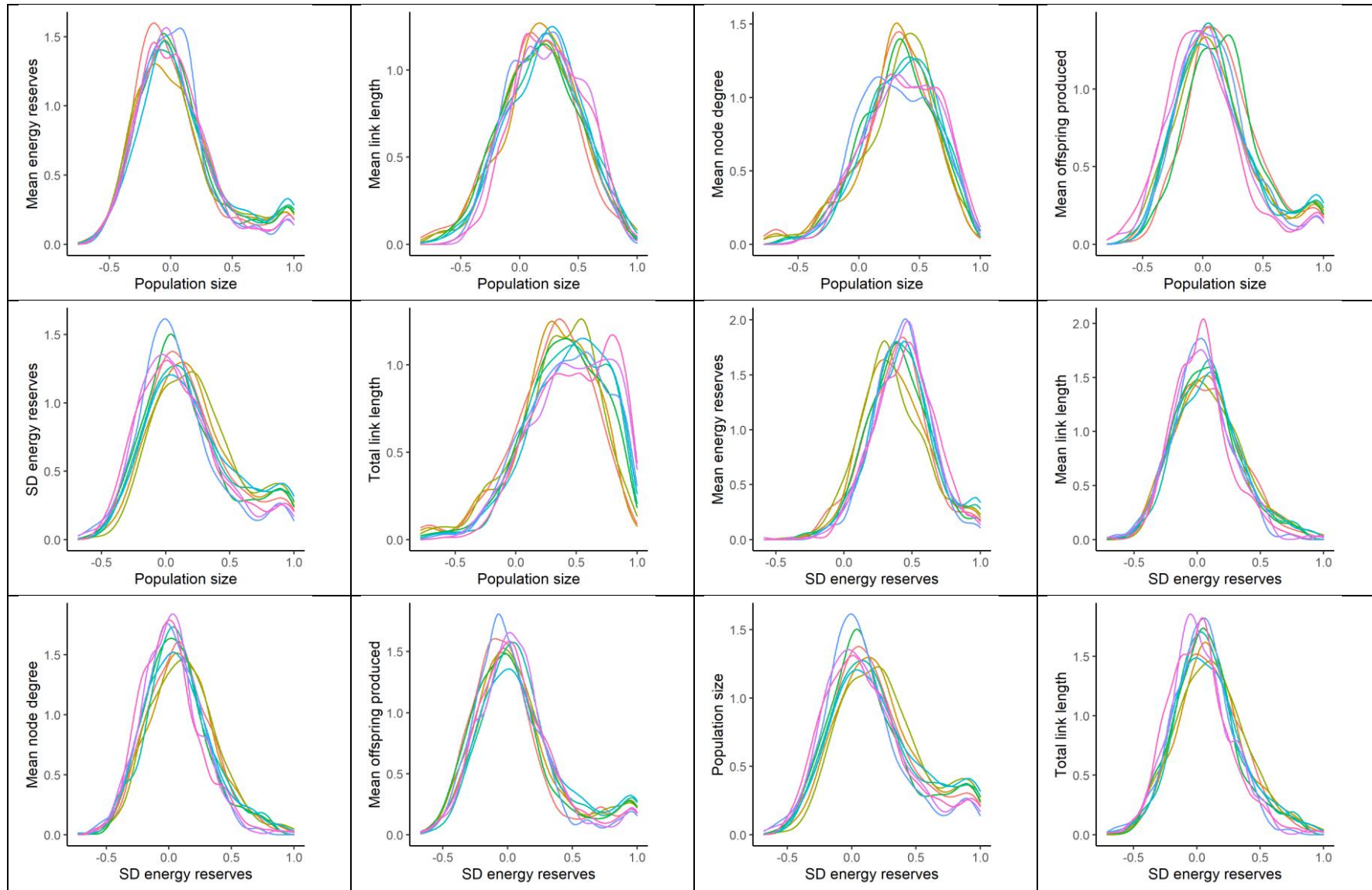
	Gini energy reserves	Theil energy reserves	Mean offspring produced	SD of offspring produced	No. of links	No. of included nodes	% of total resources included	Cost	Diameter	Gamma index	Beta index
SD of energy reserves	0.576 (0.206)	0.579 (0.207)	0.066 (0.311)	0.084 (0.310)	0.016 (0.252)	0.020 (0.255)	0.020 (0.255)	0.019 (0.249)	0.032 (0.238)	0.047 (0.230)	0.014 (0.247)
Gini energy reserves		0.977 (0.027)	0.144 (0.294)	0.160 (0.296)	0.036 (0.273)	0.034 (0.272)	0.034 (0.272)	0.039 (0.273)	0.044 (0.257)	0.062 (0.243)	0.043 (0.261)
Theil energy reserves			0.144 (0.296)	0.159 (0.297)	0.017 (0.269)	0.015 (0.268)	0.015 (0.268)	0.020 (0.269)	0.027 (0.254)	0.060 (0.240)	0.026 (0.258)
Mean offspring produced				0.823 (0.094)	-0.138 (0.28)	-0.146 (0.281)	-0.146 (0.281)	-0.136 (0.277)	-0.094 (0.259)	0.068 (0.268)	-0.079 (0.26)
SD of offspring produced					-0.056 (0.26)	-0.062 (0.264)	-0.062 (0.264)	-0.055 (0.257)	-0.035 (0.251)	0.05 (0.24)	-0.022 (0.247)
No of links						0.948 (0.088)	0.948 (0.088)	0.987 (0.016)	0.724 (0.348)	0.085 (0.712)	0.846 (0.16)
No of included nodes							1.000 (0.000)	0.930 (0.102)	0.708 (0.338)	-0.038 (0.762)	0.708 (0.279)
Percentage of total nodes included								0.930 (0.102)	0.708 (0.338)	-0.038 (0.762)	0.708 (0.279)
Cost									0.740 (0.349)	0.104 (0.700)	0.856 (0.150)
Diameter										0.150 (0.613)	0.680 (0.374)
Gamma index											0.389 (0.516)

Chapter 4: Co-evolution of network structure and consumer inequality



Structure, flow, and inequality





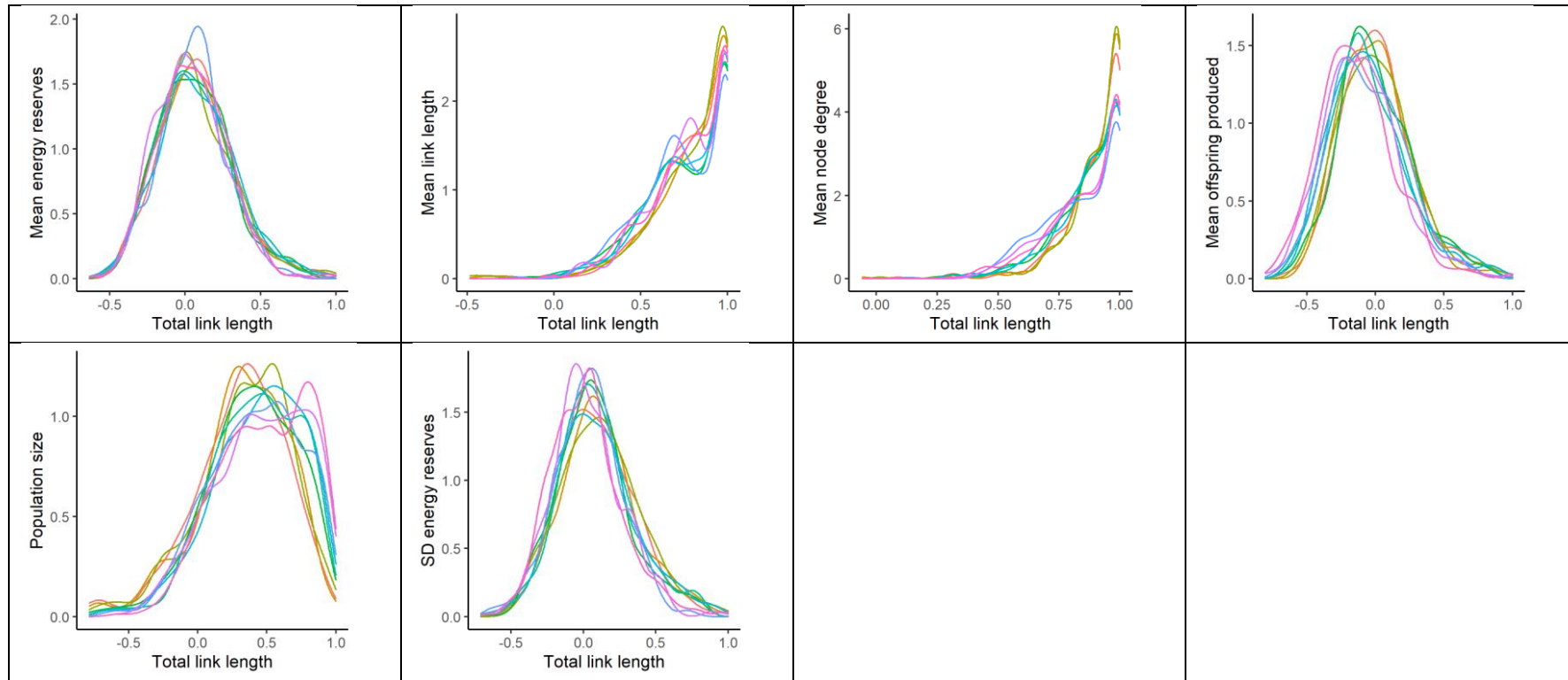


Figure A9. Density plots of correlation coefficients for all pairs of unrelated outcome variables. Each colour series represents one world size/timestep combination. Shown are data for all world sizes (10x10, 20x20, 40x40) at timesteps 1000, 2000, and 3000.

Appendix 5. Kruskal-Wallis tests and piecewise regression tables

Table A6. Kruskal-Wallis tests comparing consumer inequality and network metrics across the three simulated landscapes at distinct points in time. Consumer inequality is calculated as the standard deviation (SD) of consumer energy reserves. Timesteps after those chosen followed the same pattern of significance for network metrics, but not for inequality. Degrees of freedom for the Chi-squared statistic is always 2.

Timestep	5		10		25		50		100		500	
	χ^2	Sig.	χ^2	Sig.	χ^2	Sig.	χ^2	Sig.	χ^2	Sig.	χ^2	Sig.
SD of energy reserves	0.11	0.95	1.38	0.50	8.61	0.01	18.23	0.00	10.93	0.00	1.04	0.59
Total link length	39.81	0.00	52.50	0.00	58.81	0.00	55.71	0.00	41.33	0.00	41.85	0.00
Mean node degree	39.40	0.00	53.50	0.00	57.00	0.00	54.24	0.00	43.19	0.00	42.62	0.00
Mean link length	49.31	0.00	45.86	0.00	50.20	0.00	52.89	0.00	48.43	0.00	35.43	0.00
SD of link length	46.57	0.00	42.48	0.00	35.85	0.00	36.62	0.00	43.29	0.00	39.89	0.00

Table A7. The breakpoints and slopes identified by piecewise regression, showing the time points of major state changes in simulations and the speed of increase or decrease of measured variables on either side. Energy reserves is abbreviated ER. Shown is the mean and standard deviation for the breakpoints and slopes for the three landscapes individually, where breakpoints and slopes were calculated for each replicate then averaged.

Landscape	Mean ER slope 1 (SE)	Mean ER breakpoint 1 (SD)	Mean ER slope 2 (SE)	Mean ER breakpoint 2 (SD)	Mean ER slope final (SE)
Cities	-0.63 (0.13)	27.76 (3.34)	0.49 (0.01)	171.60 (26.69)	0.00 (0.00)
Transition	-0.57 (0.09)	28.52 (3.72)	0.54 (0.01)	161.02 (43.87)	0.00 (0.00)
Villages	-0.55 (0.08)	28.39 (2.85)	0.51 (0.01)	171.44 (32.38)	0.00 (0.00)

Landscape	SD of ER slope 1 (SE)	SD of ER breakpoint 1 (SD)	SD of ER slope 2 (SE)	SD of ER breakpoint 2 (SD)	SD of ER slope 3 (SE)	SD of ER breakpoint 3 (SD)	SD of ER slope final (SE)
Cities	0.14 (0.02)	11.83 (1.00)	-0.23 (0.03)	27.02 (3.68)	0.32 (0.01)	116.91 (27.69)	0.00 (0.00)
Transition	0.14 (0.02)	11.72 (1.86)	-0.16 (0.03)	27.33 (3.05)	0.38 (0.02)	101.90 (19.11)	0.00 (0.00)
Villages	0.13 (0.02)	12.28 (1.03)	-0.21 (0.02)	27.14 (2.87)	0.31 (0.00)	130.20 (19.91)	0.00 (0.00)

Landscape	Total link length slope 1 (SE)	Total link length breakpoint 1 (SD)	Total link length slope 2 (SE)	Total link length breakpoint 2 (SD)	Total link length slope 3 (SE)
Cities	24.93 (2.40)	27.49 (2.10)	-11.34 (0.31)	103.63 (26.73)	-0.07 (0.00)
Transition	18.88 (1.68)	28.48 (2.43)	-15.28 (0.38)	103.18 (24.06)	-0.08 (0.00)
Villages	13.79 (1.90)	27.72 (2.88)	-9.00 (0.28)	101.07 (26.93)	-0.04 (0.00)

Appendix 6. Appendix references

Csardi, G. and Nepusz, T. (2006) ‘The igraph software package for complex network research’, *InterJournal*, Complex Sy, p. 1695.

Grazzini, J. (2012) ‘Analysis of the Emergent Properties: Stationarity and Ergodicity’, *Journal of Artificial Societies and Social Simulation*, 15(2), pp. 1–15.

Lorscheid, I., Heine, B.-O. and Meyer, M. (2012) ‘Opening the ‘black box’ of simulations: increased transparency and effective communication through the systematic design of experiments’, *Computational and Mathematical Organization Theory*, 18(1), pp. 22–62. doi: 10.1007/s10588-011-9097-3.

R Core Team (2020) *R: A Language and Environment for Statistical Computing*, R Foundation for Statistical Computing. Vienna, Austria. Available at: <http://www.r-project.org>.

Ugland, K. I., Gray, J. S. and Ellingsen, K. E. (2003) ‘The species-accumulation curve and estimation of species richness’, *Journal of Animal Ecology*, 72(5), pp. 888–897. doi: 10.1046/j.1365-2656.2003.00748.x.

Wickham, H. (2016) *ggplot2: Elegant Graphics for Data Analysis*. New York: Springer-Verlag. Available at: <http://ggplot2.org>.

Zeileis, A. (2014) *ineq: Measuring Inequality, Concentration, and Poverty*. Available at: <https://CRAN.R-project.org/package=ineq>.

5

Discussion

To ensure long-term flourishing of ecological and socio-ecological systems, the respective heterogeneity and equality of resource distribution is crucial. This distribution takes place through interconnected resource acquisition, distribution, and end-use (RADE) networks, such that any attempt to manage or change heterogeneity or inequality must involve a clear understanding of the relationships among RADE network structure, resource flows, and consumer outcomes. The work presented here aimed to deepen that understanding, by using simulation modelling of stylised networks to elucidate general patterns in RADE network development and its interactions with consumer inequality.

Overall, these chapters demonstrate that heterogeneity and inequality are fundamental aspects of ecological and socio-ecological systems, due to the heterogeneous structures of RADE networks and the spatial distribution of resources across the landscape. As shown in Chapter 2, increasing flows through heterogeneously structured networks, or increasing the hierarchical structure of the networks, leads to rapid increases in inequality between end consumers. As these changes also facilitate higher system-level power consumption, thus entropy production, they are seen across all earth systems evolving toward these thermodynamic extrema. In Chapter 3, this heterogeneity of network structure was shown to lead to greater consumer heterogeneity, which could result in speciation and biodiversity, but only if the heterogeneity occurred at a biologically relevant spatiotemporal scale for the consumers to experience. Lastly, Chapter 4 showed how inequality and network structure co-evolved, and how both were influenced by the spatial distribution of resources and the population size and biology of the consumers. Together, these findings highlight

the ubiquity of heterogeneity and inequality due to the structure and dynamics of the networks facilitating resource consumption, and how both can be increased by the development trajectory of the overarching system, and feedbacks between network structure and consumer state.

This chapter discusses the main findings presented in the thesis, considering the questions and proposed work outlined in the introductory chapter, and describes areas of future work. In the first section, the findings of each chapter are summarised and discussed, focussing on how they connect with each other and the overall context of the thesis. The second section then reviews common themes across the chapters, which are picked up in the programme of research outlined in the closing section.

5.1. Discussion of findings

5.1.1. Chapter 2

In Chapter 2, a simple model of resource distribution was developed based on an electrical analogue, which modelled consumers' resource intake as power consumption. Simulations were used to quantify individual and total network power consumption as the flows through the network increased. The increased flows drove the total power consumption of the network to a maximum, before decreasing again due to frictional losses. In networks with heterogeneous connectivity or link lengths, however, the outcomes of individual consumers diverged with increasing flow; power consumption of the most distant consumers decreased even as the total network power consumption approached its maximum. The inequality in consumption was found to be proportional to the effective resistance, a metric defined to include both link length and upstream connectivity.

The work presented in Chapter 2 bridges the considerable literature on maximum power and entropy production in natural and socio-ecological systems (*e.g.* Odum and Pinkerton, 1955; Martyushev and Seleznev, 2006; Kleidon, Malhi and Cox, 2010) with that discussing resource

distribution network structure (*e.g.* West, Brown and Enquist, 1997; Banavar *et al.*, 2010; Jarvis, Jarvis and Hewitt, 2015). The results show that networks develop along trajectories toward maximum power by increasing flows, becoming more hierarchical in structure, or both. As both the consumers and resources which these networks connect are distributed throughout space, the optimal, space-filling network structure to maximise resource throughput is a hierarchical branching structure. However, increasing flows across a heterogeneously structured network, especially a hierarchical structure, leads to a rapid increase in the inequality among end consumers. By connecting the established trajectory of systems to evolve toward maximum power and entropy production, and the optimality of heterogeneously structured networks in facilitating this, the chapter provides a possible explanation for the seemingly ubiquitous emergence of both beneficial heterogeneity in natural systems and damaging inequality in socio-ecological systems.

For example, in ecological systems, the heterogeneity of resource distribution creates environmental niches and increases biodiversity (see reviews in Tews *et al.*, 2004; Stein, Gerstner and Kreft, 2014). The networks in Chapter 2 could represent rivers, soil macropore networks, mycelia, or foraging trails, all of which move nutrients to points of consumption, such as individual organisms, groups, or areas. As shown, this relocation replicates or even increases the heterogeneity of the original spatial and temporal distribution of resources, especially as nutrient flows or cycling increases. A variety of types and quantities of resources in an area leads to diverse populations of primary producers, which in turn creates a range of resources for consumers in higher trophic levels. This increases the transformations the energy flows undergo, and the overall power and entropy production of the system. In this way, biodiversity across and within trophic levels is also part of this trajectory toward maximum power and entropy production (Vallino, 2010). This biodiversity is linked to greater stability and resilience of ecosystems (Wang *et al.*, 2019), so they can more consistently take advantage of the resources available to them, and are less vulnerable to collapse due to extinction of any given species (Ulanowicz *et al.*, 2009). Therefore, in

natural systems, the larger trajectory toward maximum power and entropy production is associated with biodiversity and the healthy functioning of the biosphere.

In human-engineered systems, the RADE networks relocating resources from farms, oil rigs, solar fields, and other production points, and the control of these networks by powerful individuals and groups, creates opportunities for natural heterogeneity to be exacerbated or replicated through the network. In modern society, however, heterogeneity of natural resources is not the sole contributor to inequality, at least at the timescale of individual lives. Instead, it is a combination of heterogeneity in socioeconomic resources such as wealth and influence causing unequal access to physical resources like food and fuel, and unequal access to physical resources diminishing prospects for socioeconomic stability. As Chapter 2 demonstrates, highly structurally heterogeneous network architectures are the most energetically efficient for connecting the spatially distributed consumers. This in turn, especially when combined with powerful actors who can shape the network to their own benefit, causes heterogeneity of distribution.

Chapter 2 also demonstrates the insufficiency of focussing only on the economic status of individuals when trying to understand and reduce inequality. Alleviating economic poverty, such as through direct cash payments for environmental services, may help reduce inequality temporarily (*e.g.* Pagiola, Arcenas and Platais, 2005; Edward, 2006). If there is a positive feedback between inequality in resource distribution and socioeconomic inequality, as described above, then it will also take restructuring the physical or economic architecture of RADE networks distributing those resources to disrupt this cycle. In society, when financial and network restructuring alleviation efforts are not coupled, increasing socioeconomic resources may actually cause environmental damage, as there is more money for extractive resource consumption, but no access to more sustainably sourced resources available through larger markets (Alix-Garcia *et al.*, 2013). In short, if resources are not distributed to an area, then money will be useless unless it is enough to restructure resource distribution or allow people to move to better-resourced areas.

Overall, given that all earth systems tend toward maximum power and entropy production, and heterogeneous network structures have the highest maximum power throughput, the work presented in Chapter 2 would suggest that RADE network structure is a key factor in the ubiquity and persistence of inequality and heterogeneity. While the latter is beneficial in ecosystems, inequality in society has been linked with a range of individual- and societal-level health and social challenges, demanding restructuring efforts to address its emergence and increase. The results from this chapter show that the structurally symmetrical radial burst networks, with a central resource equally and directly linked to each consumer, had equal distribution for any amount of resource flow. However, restructuring all RADE networks to this level of equality is unlikely to be possible. Furthermore, the trajectory for networks to shift out of this state and into one with a higher power and entropy production, such as hierarchical branching, suggests that restructuring will need to occur on many interconnected social, political, economic, and physical levels, to limit the emergence and increase of inequality in a system.

5.1.2. Chapter 3

Chapter 3 also developed and used a model of RADE networks to understand relationships between structure and consumer heterogeneity, but instead focussed on understanding heterogeneity in soil ecosystems. Soil macropore networks were extracted from profile images, analysed with network science and transport geography metrics, and used as the environment in an agent-based model (ABM) of generic consumers foraging for resources. The larger, more connected, and more structurally heterogeneous networks, as measured by the network metrics, led to larger, more heterogeneous consumer populations in the simulations. This was also influenced by resource and consumer characteristics, however. For example, consumer populations with low metabolism, consumption rate, and energy threshold for spawning had a lower mean resource stock for any given resource base, while interaction between soil type and

resource type strongly influenced mean consumer resource stocks and final population size across all simulations.

Overall, this chapter contributed insights into the relationship between resource heterogeneity and consumer diversity, by highlighting the role that RADE networks play in mediating consumer-resource relationships. Here, the networks allowed consumers to move between resources, determining energy consumption in foraging and which resources a consumer could access. As the consumers here could not modify the network, the resource heterogeneity to which they were exposed was at the scale of the subnetwork in which they were located. Therefore, as they did not experience the level of heterogeneity as was measured here in the overall network, the relationship that emerged between heterogeneity and diversity was limited, though noticeable. The effect of scale on heterogeneity-diversity relationships has been discussed (Gazol *et al.*, 2013; but see also Seiferling, Proulx and Wirth, 2014), but this work expands on that by connecting scale effects explicitly to the access that the RADE network provides.

This chapter also contributes a new methodology for studying heterogeneity-diversity relationships, both with and without explicit RADE networks. Here, empirical data about an area, including imagery, is coupled with traditional and simulation-based analysis and modelling to explore possible dynamics in that area. By incorporating more empirical data in models, simulations can be used to test more realistic hypotheses about causal mechanisms and to observe effects of environmental change or population composition change, without modifying real systems. This can then generate and improve ideas for future empirical work. Similar methods have applied image analysis to measuring environmental complexity (Parrott, 2010) and identifying inaccessible and under-serviced parts of a city (Brelsford *et al.*, 2018), but to our knowledge, this is the first coupled image analysis and simulation modelling paper.

Although not as frequently discussed, this chapter and related work on environmental heterogeneity and biodiversity could be applied to understanding more generally how complex life

emerges and is sustained. Previous work on heterogeneity-diversity relationships has been mostly limited to identifying descriptive relationships between resources and species currently present in an ecosystem. Future applications could expand this to more predictive work, to see if the relationships observed in empirical systems could estimate the quantity and complexity of life that would emerge in a novel system. This could take the form of a heavily altered earth system, such as one impacted by environmental change, human activity, or invasive species, or even environments on other planets. As discussed in Chapters 1 and 2, there is a trajectory for systems to evolve toward maximum power and entropy production that is accelerated by heterogeneously structured networks, along with the heterogeneity in resources and habitats these networks create, and the resulting biodiversity. While the role of life in sustaining entropy production has been posited (Vallino, 2010), the tipping points or thresholds at which complex life could emerge, and their relationship with the RADE network structures present, have not yet been explored.

Specifically, any such threshold must be related to the location of resources and resulting structure and dynamics of the RADE networks present in the system, such as those constructed by simpler life forms or gradient-based flows. In any system, the RADE networks that emerge to connect resources and consumers necessarily co-evolve with them, such that the quantity and complexity of life that emerges would both predict and be predicted by the size and complexity of the RADE networks which they construct and use. This is demonstrated in Chapter 3 by the larger and more heterogeneous populations that emerge in the larger and more heterogeneous networks. While consumers could not modify the network in the modelled system here, in observed soil ecosystems, larger consumers, plant roots, water, and geological processes all adapt the network further. As soil networks are used as both foraging networks for animals and plant roots, and facilitate the diffusion of nutrients through groundwater seepage, there is likely a positive feedback between increasingly complex network structures, and the biodiversity of both above- and below-ground ecosystems. Understanding the specifics of this feedback, and its relationship to other

characteristics of the systems in question, could provide insight into how it might emerge in novel systems.

In novel or existing systems, however, the importance of soil biodiversity for ecosystem health, and the role of RADE networks in mediating heterogeneity-diversity relationships, must be considered in discussions of land management practices. As discussed in Chapter 3, the preservation of soil network structural heterogeneity can take the form of preserving wild spaces across a range of biomes, minimising or eliminating tilling, planting cover crops, and coincident planting of species with distinct root structures and foraging patterns. These management practices, and the resulting maintenance and increase of soil structural heterogeneity, allow for a diverse and healthy soil biota, which provides the foundation for stable and productive ecosystems.

5.1.3. Chapter 4

The fourth chapter focussed on the relationships between landscape heterogeneity, network structure, and consumer inequality. It developed and analysed a simple model of consumers building and using a network to move between resources, maximising their time-discounted consumption. The dynamics and outcomes were then compared across three distinct spatial distributions of resources, or landscapes. The consumer inequality, measured as the standard deviation of consumer energy reserves; the network size and connectivity, measured as the total link length and mean node degree; and the rates of change of each were widely similar in values and dynamics across the three landscapes studied. However, the networks in the ‘Cities’ and ‘Transition’ landscapes were slightly larger and more connected, and the Cities networks showed the highest peak of consumer inequality. This suggests that characteristics shared across simulations, such as the discounting mechanism, reproduction threshold, metabolic rate, and consumption rate of consumers; and the regrowth rate and capacity of resources; drove the overall dynamics of the systems. The spatial distribution of the resources, and therefore the characteristic network link lengths associated with each landscape and the popularity of certain links, constrained

the rate of those dynamics and the times at which dynamics shifted. For example, the networks in the Transition landscape, which included many short links between nearby resources in the denser central area, and longer links to more distant resources, showed a much more rapid decay of total link length after initial construction, and more rapid contemporary increase in consumer inequality.

This contemporary increase and decrease of consumer inequality and network size, respectively, was part of the distinctive co-evolutionary pattern between the two. Network size first increased rapidly, before decaying back to a more stable state as preferred links were more frequently used and maintained. Consumer inequality decreased during the initial construction phase, then increased rapidly as the network decayed back to a more stable state. This increased inequality is due to consumers having different access to established links in the smaller, stable network, and therefore using different amounts of energy to navigate between resources. As maps of the networks over time showed that consumers used and maintained links predominantly between local resources, the consumers with the highest energy reserves were those who could access many resources in a small area without building new links. The other consumers were often trapped in less well-resourced parts of the network and had to use more energy to move between resources or build links back to denser areas. Therefore, the consumers with the highest energy reserves were not necessarily those who could build links for their own benefit, but those who were positioned in space and time in such a way that they could take advantage of links built by others, thereby minimising the energy they spent traversing the network.

This mechanism of inequality and structure co-evolution is comparable to consumers in preferential positions in flow networks, who can then reinvest energy in bringing more resources through the network toward themselves. While the consumers in the Chapter 4 model actively moved through the network, the pattern of preferentially maintaining links between some resources – such as those with the highest capacity, regrowth rate, or proximity to other resources – allowed nearby consumers to increase their own intake. The relationship between the energy

reserves of a given consumer, and the position and actions of other consumers building and maintaining links in the network, is similar to the models in Chapters 2 and 3, where consumers interact indirectly through their actions and resource consumption. In those models, however, consumers could not alter the network, and in Chapter 2, they also could not move. The emergence of inequality in each model, albeit with a range of distributions from heavily skewed to nearly normal, suggests that inequality is a robust outcome of consumers relying on heterogeneous spatial networks for resource acquisition. This thinking will be expanded in Section 5.2.2.

The relationship between consumer state and indirect interactions with other consumers adds complexity to unravelling the specific causes and feedbacks around inequality and connecting individual-level interactions to system-level observations. While time series methods such as panel analysis could allow simultaneous visualisation and quantification of multiple individual consumers' trajectories, many such methods impose stringent requirements such as stationarity. This highlights the need for new methods to analyse data produced by empirical and model complex systems, which include both individual-level interactions and systems-level emergence, and which may not meet the assumptions of traditional time series analysis methods. These new methods would likely take the form of analysing the life history or trajectory of individual actors, including location and decisions, and aligning that with simultaneous or preceding events in the system. This would incorporate the path dependency of individual actions with the evolution of the system. In the context of Chapter 4, this could show how some consumers navigated to better-resourced parts of the network and rapidly increased their consumption, while others remained in less accessible or resourced areas.

This path dependence of consumer state, and feedback between consumer inequality and network structure, also provides further evidence for the importance of explicit structuring and governance of networks, if reducing or eliminating inequality is a goal. This is not necessarily the case for all systems that the model in Chapter 4 could represent, but it is a named objective in many modern

societies. As the consumers in the model made decisions to maximise their own consumption, the network emerged to favour those who could maintain it to their own benefit, and the network structure in turn helped maintain the status of those consumers. Unlike the naturally-occurring networks such as those discussed in Chapter 3, where heterogeneity and the resulting biodiversity are important to the sustained health and functioning of the system, most modern human societies claim equality in consumption and access as an ideal. Proponents of modern economic systems would likely argue that increasing flows through current resource networks would increase the standard of living for those relying on them, following a pro-growth logic championed by Kuznets (1955) and similar (though see references and discussion in Edward, 2006). According to this logic, allowing the networks to develop along maximally efficient routes would be of most benefit to all. The results of Chapters 2 and 4 demonstrate that a ‘free market’ approach to network construction, with the most well-endowed consumers making choices to benefit themselves, will inevitably interact with the natural heterogeneity of resources in the landscape and any starting level of inequality to increase the divergence of consumer outcomes over time.

When eliminating inequality by explicitly structuring the network in a spatially homogenous way is not possible, due to factors such as heterogeneity of resource and consumer spatial distribution, increasing connectivity of the network can also reduce inequality between consumers. This was shown by the lower inequality in the higher connectivity networks in Chapter 2, and during the dense initial phases of network construction in Chapter 4. However, this introduction of potential redundancy goes against the tendency for these networks to evolve toward maximum power and entropy production, with maximally efficient, albeit less resilient, architectures. Therefore, to bring about distributional equity, it may be necessary to also restructure how society governs and relies on its resource networks, to overcome the heterogeneity that their physical structures tend toward. This will be discussed more in the following sections.

5.2. Common themes

Beyond the main findings discussed in the sections above, several common themes emerged across the chapters of the thesis, including agency, comparability between networks, contrasting ecological heterogeneity with socio-ecological inequality, and different uses of systems-level and individual-level modelling and analysis. These are discussed in the following sections, and feed into the future work proposed in the closing section.

5.2.1. Agency

Any discussion of how to restructure RADE networks to become more equitable assumes that the actors operating on the network, whether they are the same as the end consumers or at a higher organizational level, hold some amount of individual- and group-level agency. Agency is typically described as the ability to act, which is understood to occur within social, cultural, and linguistic boundaries (Ahearn, 1999). Although less discussed, it is relevant here to acknowledge the resource-related constraints on agency as well: An actor of any species is only able to act insofar as it has the energetic capacity to do so. Additionally, the question of free will becomes relevant: Can actors use that energy in a manner of their own choice, or are they constrained by larger systemic trajectories? Within the context of the work presented here, agency and free will are relevant in discussions of whether network restructuring is possible, especially in the face of thermodynamic extremization principles, and the combination of individual- and group-level decisions and governance structures that would be required.

The work presented in Chapters 2 and 4 highlights the need for explicit effort of the actors within a system to restructure the networks if equality is their goal, as is stated in many modern and historical human societies. As all actors are limited by their resources, restructuring necessitates action especially by the better-positioned and endowed actors, with net excess resources to reinvest in shaping the networks. In Chapter 4, consumers built the network from decentralised decisions to maximise their own consumption, which resulted in increased inequality over the course of the

simulation. As discussed, this has parallels with consumers shaping flow networks to preferentially increase their own intake. To successfully bring about restructuring and equality in networks shaped by agents working toward their own interests, system actors must all believe that changing the system toward equality is of benefit to themselves, even if it results in a reduction of their possible net resource flow.

Notably, the consumers in Chapter 4 were not aware of the inequality emerging in the system, beyond the effect it had on the network structure. The level of other-, group-, and self-awareness that an actor possesses can considerably modify their actions, and the resulting inequality that emerges in a system. For example, actors who become aware of others with less resources may choose to share theirs, if they consider it to be the most beneficial action – either to the other actor, the group, themselves, or some combination thereof. If the consumers of Chapter 4 had shared resources to collaborate on building and repairing links, they may have been able to maintain a larger, more connected network, and supported a more equal population. In contrast, actors may become more territorial or competitive, observing the advantage provided by being more affluent in an unequal society, and actively working to maintain or improve their holdings. It would be considerably more difficult to engage in restructuring networks in the latter system, where powerful actors are prosecuting a self-preservation strategy that contributes to inequality.

Although humans have shown a considerable capacity for altruism, especially toward their perceived ‘in-group’ (*e.g.* Kurzban, Burton-Chellew and West, 2015), RADE network restructuring to create equity in society would require a much broader, even global, conceptualisation of in-group. It would also require acknowledgement that increasing the current flows in a heterogeneous network will increase inequality, and that systemic effects from network structure can cause reduced resource access and limited or no net excess. This physically prevents individuals from changing their own circumstances. While this shift in attitudes would be beneficial to restructuring efforts, if inequality has emerged or increased over the course of the system’s development, then

the entire trajectory of how that system develops must also be shifted. Otherwise, any enacted change would only be temporary, as further development would move the system back toward inequality and undo any changes.

Given the thermodynamically-driven trajectory of the overall earth system to evolve toward maximum power and entropy production; the facilitation of this through maximally efficient, highly heterogeneous branching networks; and humanity's position as a part of this evolving earth system, there seems little that can be done to change the trajectory of network development and the resulting inequality: Our agency and free will do not extend so far as to counteract physics. Perhaps then it would be more realistic to acknowledge this trajectory, and instead attempt to adapt our societies to become more equitable by changing how we rely on and interact with RADE networks. This will be discussed further in Section 5.2.3.

5.2.2. Comparability of networks

Importantly, the precise shape of any relationship between network heterogeneity and consumer inequality is likely determined by the attributes of the network, consumers, and resources in question. Therefore, any implications of the findings presented in these chapters must be understood within the context of the specifications of the models that generated them. The defining characteristics of the environment, resources, and consumers for each model are summarised in Table 5.1.

Table 5.1 Characteristics of environment, network, resources, and consumers in the models presented in Chapters 2-4.

	Environment and network	Resources	Consumers
Chapter 2	Uniform roughness, pre-specified network structure, no decay.	Point resources with linear, infinite flows. One resource type.	Fixed consumers, no ability to change network or interact. No starting resource allocation.
Chapter 3	Uniform roughness, pre-specified network structure, no decay.	Point resources, depletable but regrowing at a constant rate. One resource type.	Mobile consumers, no ability to change network or interact, random search strategy. Identical starting resource allocations.
Chapter 4	Varying roughness, no initial network structure, links decay.	Point resources, depletable but regrowing at a constant rate. One resource type.	Mobile consumers, can modify network but not directly interact, decisions based on limited information. Varying starting resource allocations.

While the models in each chapter share some similarities, there are also clearly considerable differences in consumer behaviour and level of agency, environment heterogeneity, and resource dynamics. The most significant involves the consumers' ability to relocate within or modify the network: in Chapter 2, consumers and links were fixed; in Chapter 3, consumers could move, albeit randomly; and in Chapter 4, consumers employed a more sophisticated algorithm to weigh options, and could build and maintain links. While any inequality that emerged in the models was a result of network structure and the location and consumption of other consumers, only in Chapter 4 could the consumers modify the network, within the bounds of the spatial configuration of the resources. With each layer of possible consumer actions and interactions in the models, understanding the exact causes of inequality among consumers becomes more difficult. Given the incredible level of complexity and interaction in empirical systems, this becomes even more relevant for understanding and addressing inequality and heterogeneity in them, and for generalising model outcomes to real-world scenarios.

Rather than attempt to capture this level of complexity, the models presented in this thesis were explicitly designed to incorporate the minimum requirements of resource distribution: consumers and resources, spatially explicit networks, and physical and thermodynamic consistency. The inequality that emerged and persisted or increased during the simulations showed that the starting conditions of each model, and these minimum requirements, were enough to generate at least qualitatively similar patterns of inequality and heterogeneity to those observed in empirical systems. Future work increasing the complexity of the models, as discussed in each chapter, may make them more specifically accurate. This could also identify additional features that empirical RADE networks incorporate to cause any divergence from the qualitative similarities present in the current results.

For example, distinct types of resources are likely to have different energetic cost functions associated with their transportation (Banavar *et al.*, 2000; Bohn and Magnasco, 2007; Han *et al.*, 2019). While one resource may have a linearly or exponentially increasing energetic cost associated with a higher flow rate, another may have an economy of scale. This may be further influenced by the materials forming the network architecture, whether pavement, wires, paths, or veins. In the models developed for this thesis, only one cost function for resource or consumer movement was explored in each. Therefore, more exploration of parameter spaces and design choices would be required to connect different cost functions with the emergence and increase of consumer inequality, and map this back to empirical systems.

This exploration would also be necessary to clarify the implications and reasonable level of generalisation of findings from any specific RADE network model. For example, as covered in Chapters 1 and 2, many RADE networks share a similar hierarchical branching architecture, or more generally, minimum spanning tree architecture, despite their diverse contexts. This architecture is an optimal space-filling structure (*e.g.* West, Brown and Enquist, 1997) under certain conditions, such as when the incremental increase of cost for transporting more materials

decreases with the amount of material transported (Banavar *et al.*, 2000; Bohn and Magnasco, 2007). However, under other cost functions or constraints, redundancy and loops are more optimal, and more resilient (Banavar *et al.*, 2000; Gavrilchenko and Katifori, 2019). The frequency with which branching architectures are observed in empirical systems suggests that the conditions for their optimality are widely experienced across systems, but perhaps not universally.

Similarly, inequality emerges in many systems, including those with hierarchical branching or other spanning tree architectures. While inequality was not ubiquitous in the networks studied here, and emerged at different rates or extents, it emerges in all but explicitly equally structured RADE networks. Given the diversity of the contexts of these networks, the phenomenon of inequality is perhaps best described as a specific case that can arise from different initial conditions and evolutionary trajectories; this is known as equifinality. In the context of RADE networks, equifinality in consumer outcomes such as inequality means that it can be difficult to determine causality of inequality observed in one system, based on its causes in another system where it emerged, unless clear proofs for its emergence can be provided and compared. This is especially true for complex systems, where outcomes and drivers can co-evolve through feedbacks, as shown in Chapter 4. Therefore, further explorations could help identify the extent to which certain network structures, inequality, or both emerge, and how much and when structure and inequality are causally linked.

For the purposes of the discussion of the chapters here, it is worth noting that the diverse range of contexts and characteristics of RADE networks clearly impacted the specific findings of each chapter, such as the precise values of consumer inequality, relationship between resource flows and inequality, and rates of population dynamics. Moreover, the highly stylised, theoretical nature of the models limits the extent to which these findings can be taken as predictive of specific dynamics or outcomes in empirical systems. For example, while increasing flows through heterogeneous network structures will necessarily drive the system toward increased inequality, the

specific rate of its emergence and increase may be different with nonlinear flows or multiple resource points. Similarly, larger, more heterogeneous soil macropore network structures will support larger, more heterogeneous populations of soil biota, *ceteris paribus*, but the emergence of population heterogeneity could be increased by consumers pursuing more sophisticated search strategies or modifying the network. Given these caveats, the findings presented in these chapters must be interpreted and applied with care, though they remain useful, informative, and qualitatively comparable with empirical systems.

5.2.3. Heterogeneity and inequality

Despite the similar drivers of heterogeneity and inequality in naturally-occurring and human-engineered systems, each has a very distinct conceptualisation and set of norms for understanding it. As discussed throughout this thesis, ecological, environmental, and biological heterogeneity is considered natural and vital to healthy system functioning (Tews *et al.*, 2004; Tylianakis *et al.*, 2008; Stein, Gerstner and Kreft, 2014). Even inequality between consumers within the same non-human species is usually regarded as normal and a driver of adaptation and evolution (Lotka, 1922), rather than a moral wrong. In contrast, inequality of basic resources in modern human society is often conceptualised as a moral wrong enacted on individuals by the socio-political and socio-economic systems and those with power in them, although it is sometimes still framed as being the fault of the individual – they were lazy or had some other character flaw (Furnham and Gunter, 1984; Franks, 2020). Notably, this conceptualisation only became relevant as humans began settling in larger groups; the smaller family groups and tribes associated with many indigenous societies were often highly egalitarian, which is usually ascribed to a combination of pragmatism regarding possessions in a mobile group, and enforcing egalitarian behaviour to maintain social cohesion (Smith *et al.*, 2010; Mattison *et al.*, 2016).

There are at least two possible drivers for the transition in socio-political discourse and political and ethical norms in larger, modern societies, from the ‘survival of the fittest’ mentality popularised

by social Darwinists (*e.g.* Spencer, 1860), to repudiating inequality and attempting to limit it in the face of a highly heterogeneous world. First, it could have been driven by awareness of the deleterious impacts on individual and public health and wellbeing resulting from inequality, as discussed in Chapter 1. It is also possible that empathy and consciences have shifted over time, especially through globalisation, to become more widely aware of the inherent equality of all people and therefore the injustice of inequality, beyond one's family group or tribe (Sheehy-Skeffington and Thomsen, 2019). It is likely some combination of these two possibilities that has led to the emphasis on and broadening understanding of equality and justice in economic and political systems, and the different conceptualisations of inequality in society and heterogeneity in ecological systems. Importantly, the inequality emerging in Chapter 4 would suggest that the complex interactions of individual maximising choices in a heterogeneous landscape can lead to inequality, even in systems with agents who are nearly identical, and use the same mechanisms for decision-making. This suggests the blame for inequality may also lie with the emergent system arising from these interactions, rather than only one of the more visible top-down political and economic systems, or the choices and work ethic of individuals.

Regardless of the cause for shifting attitudes and norms, in many modern societies there are attempts to limit or eliminate poverty, provide food and energy more widely, and distribute other services publicly, such as healthcare and education (United Nations, 2015). Various levelling mechanisms may have also been common in egalitarian pre-modern societies (Mattison *et al.*, 2016). These groups also frequently moved or adapted their behaviour and technology to match available resources (*e.g.* Dyson-Hudson and Smith, 1978; Mattison *et al.*, 2016), which limited within-group inequality and led to different resource specialisms across groups. Suggesting that people continue to respond to resource differentials through adaptation, migration, or speciation would be viewed as unethical and reprehensible. However, the reality of the over 66 million migrants, many fleeing food and water shortages and resource-related conflict, shows that

considerable migration still occurs (World Food Programme, 2017), and food insecurity is a problem for all nations (International Food Policy Research Institute, 2015). Clearly, there is much more that needs to be done for our ideals of equality and justice, if only of the most basic resources, to be matched by the outcomes of our systems. Incorporating a deeper understanding of the role of RADE networks in creating and reinforcing this inequality is crucial.

While prescription was not the aim of the chapters presented here, given the very theoretical nature of the models, their findings suggest a few options for conserving heterogeneity in natural systems and reducing inequality in society. First, ecological heterogeneity can be maintained or encouraged by focussing on the diversity of habitats and resources at lower trophic levels, including below-ground ecosystems. Ensuring a healthy, heterogeneous soil matrix will create habitat for diverse soil organisms and plants, which will carry up the trophic levels to higher-level consumers (Baer *et al.*, 2005; García-Palacios, Maestre and Gallardo, 2011; Hutchings, John and Wijesinghe, 2011; Vezzani *et al.*, 2018). Additionally, keeping corridors open for animals to hunt, forage, migrate, or maintain larger territories makes it less likely for species to be trapped in unsuitable or overcrowded habitats (Ziv and Davidowitz, 2019). In short, conserving wild spaces that cover connected, diverse areas, and promoting biodiversity through rewilding, cover-cropping, and similar efforts, will help maintain the heterogeneity needed for healthy ecosystem functioning.

In human society, inequality could be addressed through restructuring RADE networks where possible, through decentralising, localising, and increasing connectivity. For example, decentralised energy systems, such as renewables, hold considerable promise for providing equitable energy access, if the needs of the population are truly prioritised (Fathoni, Setyowati and Prest, 2021). Localising food systems can also increase access to healthy, seasonal, sustainable food (Martinez, 2010). In effect, these restructuring efforts would attempt to create RADE networks with a more structurally equal, centralised topology, such as the radial burst networks shown in Chapter 2 to have equal distribution. Where more physical resource distribution restructuring is not possible,

economic governance structures and social networks could be used to increase redistribution and offset the heterogeneity of the network architecture. This could include systems such as food sharing, which has been practiced in many pre-modern and contemporary societies (*e.g.* Ahedo *et al.*, 2019). Similarly, systems such as universal basic income or energy provision, tiered to increase payments or provision to more vulnerable individuals and communities, could help increase access to resources.

As this thesis focussed on inequality of necessary, basic, energy-related resources such as food or fuel, the findings and implications may not necessarily extend to inequality in higher-level societal resources. The connections between energy poverty, poor nutrition, and other individual outcomes such as educational attainment (see Chapter 1, Section 1.2) suggest that this inequality in access and inequality in opportunity are not separate issues. However, a discussion of the philosophical, moral, and political dimensions of the extent to which absolute equality should be pursued are beyond the scope of the work presented here.

5.2.4. Systems-level and individual-level analysis

To further study and implement these solutions, there also needs to be more standardised, widely used analytical methods for complex systems. For example, in addition to the ethical and moral considerations detailed above, another plausible reason for the different treatment of heterogeneity and inequality is the distinct data sources and analyses used for each. Systems with more granular data – individual or household – are often represented and studied at a more individual level, while systems with only estimates for individuals but more data on larger scales – populations, ecosystems, geographic regions – are approached from a more system-wide level. Much of the work to date done on system trajectories, such as maximum power and entropy production, has focussed on ecological, environmental, or large-scale socio-ecological systems (see reviews in Odum, 1971; Martyushev and Seleznev, 2006; Kleidon, Malhi and Cox, 2010). Any inequality among consumers has therefore largely been missed, or in analyses covering multiple species, is

considered beneficial heterogeneity. Analyses of inequality in society, however, have focussed more on deleterious effects on individuals and communities of resource-related inequality (for example, see reviews for outcomes linked to energy poverty in Gaye, 2007; Sovacool, 2012; and food insecurity in Laraia, 2013; Long *et al.*, 2020) and how socioeconomic inequality is related to top-down forces like policy and economic growth (Edward, 2006; Hoy, 2015). There is considerably less focus on the interactions between individual and system level, and how those can give rise to inequality and heterogeneity.

As discussed with regards to Chapter 4, there are no widely used methods yet for quantifying and capturing these conditions and interactions at the individual level that translate to inequality and heterogeneity at the system level. Both system-level and individual-level analyses can provide useful insights, but with contrasting conceptualisations of the system under study: System-level models, such as systems dynamics models or the network model in Chapter 2, treat the individual state as predominantly emerging from the system state, while the reverse is true for individual-level models such as the ABMs in Chapters 3 and 4.

However, system state is rarely, if ever, entirely driven by top-down dynamics or bottom-up emergence. In the case of inequality, natural heterogeneity of resources and the energy they provide constrain the system, but the decisions made by and interactions between individuals also determine the inequality that emerges, as shown in Chapter 4. This becomes increasingly complex with higher levels of consumer agency, as feedbacks between consumer state and environmental dynamics can also emerge, causing shifts in what may have previously been considered a driving or constraining force. Anthropogenic climate change is a clear example of this. In the preceding chapters, the first two models focussed on top-down effects of the RADE network on inequality, while the model in Chapter 4 demonstrated the emergence of inequality and network structure from individual decisions. This was still bounded by the energy supplied by the resources, and beyond building and maintaining the network, the consumers had no effect on the larger

environment. This limits the feedbacks to occurring only between network structure and consumer inequality, rather than incorporating any effect of consumers on resource dynamics. This could have increased the rate or quantity of inequality emerging in the system if network construction or maintenance somehow decreased resource capacity or regrowth, and consumers with more energy reserves or a better location could use these as temporary leverages against environmental changes.

Interestingly, both the systems-level and individual-level conceptualisations and analyses in the literature focus little attention on the RADE networks connecting resources and consumers. These networks are the physical connection mapping the individual decisions and interactions and the constraints of the system level, showing how the outcomes at each level interact and mediate one another. For example, the networks modelled in this thesis can transfer the natural heterogeneity of the simulated landscape into inequality between consumers. In empirical systems, anthropogenic RADE networks also allow humans to act on the environment, by moving people and raw materials, all forms of embodied energy, across the landscape. Over the timescales for which we now have data, we can observe how resource extraction and anthropogenic changes to natural systems cause and accelerate environmental change, which in turn can impact the ability of communities around the world to grow food for themselves. Given the importance of understanding these feedbacks, and regulating the heterogeneity and inequality observed in natural and social systems, there should be a continued focus on how RADE networks translate resource heterogeneity to consumer heterogeneity, and how the latter feeds back into the networks and encompassing systems. This will necessarily be accompanied by new analytical methods for connecting the dynamics at individual and systemic levels through the network.

5.3. Future work

As each chapter contained a discussion of limitations and possible extensions, the future work associated with each is only briefly summarised below. After these, a programme of research is

laid out, which includes expansion of the models presented in the chapters here, as well as questions raised by the proceeding discussion of common themes in the work.

5.3.1. Summary of future work from each chapter

To continue the work of Chapter 2, the model presented could be expanded considerably, such as including multiple types of resources and resource flow dynamics, as well as non-linear flows. For example, the emergence of consumer inequality and maximum power in networks with two or three types of resources, or with pulsing as opposed to constant resources, could be explored. Additionally, the results could be compared with data from empirical networks, such as rivers and roads. This could determine how their materials, flow dynamics, and governance structures cause any divergence between their actual outcomes and those presented here.

For Chapter 3, both the network extraction and analysis methodology and the agent-based model (ABM) could be improved and expanded. The chapter lists several improvements to the network extraction methodology, including retention of more detailed soil structure than straight-line distances between pores, and quantifying edge effects around colour correction cards and image borders. The network metrics calculated for each soil type could also be compared with traditional measures of soil structure, and across more soil types, to understand the range and interpretation of each metric. This would be an important next step to expanding the analysis methodology to wider field use, as is intended. Furthermore, the model could be made more biologically realistic and specific, by including predation, explicit speciation or multiple starting species, consumers who could expand or change the network, and more refined resource search strategies and energy accounting. This would allow for a greater degree of comparability between the model and empirical soil ecosystems, and therefore exploration of more detailed hypotheses around population responses to different network structures and soil conditions.

The model in Chapter 4 could also be analysed further and expanded. Specifically, common network structures or motifs could be identified by cluster analysis of networks with similar values

for the calculated network metrics, as well as new metrics measuring frequency or probability of link construction and use between given nodes. These would likely take the form of information-related measures such as Shannon entropy. The structural groupings could also be identified by comparing networks to known structures, such as small-world and scale-free networks, using the ranges of metrics values such as node degree and link length distribution. The identified structure for a given network could then be compared across time and related to consumer inequality. Furthermore, if the exact capacity and regrowth rate of each resource were fixed, rather than drawn from a distribution, the network structures that emerged across runs would likely be quite similar and could provide useful insights into the trajectories of consumers who started on one resource as opposed to another. This could allow for more individually-focussed analyses, such as examining the decisions and energy reserves of individual consumers over time.

5.3.2. Programme of research

Considering the areas of future work highlighted from each chapter, and the common themes discussed, the following programme of research could be undertaken.

As the models in the chapters presented here have already generated a considerable database of results and could easily be explored further, expanding the model design and results analysis as discussed in the sections above would be a useful starting point. In particular, the ABMs in Chapters 3 and 4 could be easily expanded, to further the biological realism of the model in Chapter 3, and to incorporate more consumer interaction and foresight, and different resource dynamics into the model in Chapter 4. These expansions would provide a better understanding of how and when certain network structures and inequality emerge, and how they co-evolve under different conditions and levels of consumer agency. As discussed previously, this would clarify how results from the models could be interpreted and mapped to empirical systems.

Alongside this, work should be undertaken to improve and develop new analysis methods. These could incorporate some elements of the network extraction method in Chapter 3, such as

identifying and extracting networks in maps, images, and other visual data, and connecting that with modelling and analysis of the consumers constructing and using the network. For some networks, this could be combined with associated empirical resource flow data, such as rates of blood or phloem flow, traffic, amps, or shipments, or with data measuring inequality in resource consumption. Even if these data were not available, the network structures could be used as the basis for models, as done in Chapter 3, to explore possible dynamics and development trajectories. These models could also be used to estimate measures of inequality within and across groups of consumers to compare to the empirical data for that system. This would create a database of empirical networks, coupled with empirical or model-generated estimates of resource flows and inequality, to better relate network structures, flows, and outcomes. As discussed, while there has been some connection between extrapolated network structure of roads and inequality in urban areas (Brelsford *et al.*, 2018), this is an underexplored area, especially in ecological and environmental systems.

Future work could also expand methods for bottom-up analysis of models, especially ABMs, and how that could be connected to existing top-down analysis methods. Top-down analysis focusses on quantifying some aspect of the entire population, such as size or Gini coefficient, or looks at time series data for these population-level measures. In the chapters presented here, the measurements of population size and heterogeneity, and the network-level metrics, were all top-down analyses. These provided a useful representation of the entire system state and the emergence of inequality across the population. In contrast, bottom-up analyses could take the form of analysing decision trees showing the decisions consumers made and different conditions surrounding each, panel analysis of time series data for individuals, or clustering of consumer states. Although to our knowledge these methods have not yet been tested, they could more clearly identify when and how inequality and heterogeneity emerge, persist, and increase, and the effects of any measures taken to alleviate or conserve it.

The increased understanding of the relationships among RADE network structure, development, and inequality, as presented in this thesis, is necessary to inform appropriate and useful controlling or intervening actions: we cannot fix that which we do not understand. Additionally, the work presented here highlights the possible limitations to our agency to modify RADE networks and their development trajectories, which is an important consideration when identifying strategies for inequality mitigation and heterogeneity conservation. Using the understanding generated by this thesis, and the future work proposed here, governance structures and interventions could be explored to reduce inequality and preserve heterogeneity. Models such as those presented here could be used to test some of the proposed heterogeneity preservation and inequality alleviation measures in previous sections. For example, what happens when we give people food or energy directly, such as through assistance programmes or installing solar panels on their homes? What about when we practice no-till agriculture, or build new roads, wildlife corridors, or railway lines? Identifying and simulating a range of possibilities within our agency to enact could identify effective strategies and unexpected externalities, as well as long-term outcomes beyond our agency to address. By increasing the theoretical knowledge base to support this work, the thesis presented here helps provide a basis to understand, modify, and adapt to RADE networks, and transition toward a more just, sustainable future.

5.4. References

- Ahearn, L. M. (1999) ‘Agency’, *Journal of Linguistic Anthropology*, 9(1/2), pp. 12–15.
- Ahedo, V. *et al.* (2019) ‘Quantifying the relationship between food sharing practices and socio-ecological variables in small-scale societies: A cross-cultural multi-methodological approach’, *PLOS ONE*, 14(5), pp. 1–31. doi: 10.1371/journal.pone.0216302.
- Alix-Garcia, J. *et al.* (2013) ‘The Ecological Footprint of Poverty Alleviation: Evidence from Mexico’s Oportunidades Program’, *The Review of Economics and Statistics*, 95(2), pp. 417–435. doi: 10.1162/REST_a_00349.
- Baer, S. G. *et al.* (2005) ‘Soil Heterogeneity Effects on Tallgrass Prairie Community Heterogeneity: An Application of Ecological Theory to Restoration Ecology’, *Restoration Ecology*, 13(2), pp. 413–424. doi: 10.1111/j.1526-100x.2005.00051.x.
- Banavar, J. R. *et al.* (2000) ‘Topology of the fittest transportation networks’, *Physical Review Letters*, 84(20), pp. 4745–4748. doi: 10.1103/PhysRevLett.84.4745.
- Banavar, J. R. *et al.* (2010) ‘A general basis for quarter-power scaling in animals’, *Proceedings of the National Academy of Sciences*, 107(36), pp. 15816–15820. doi: 10.1073/pnas.1009974107.
- Bohn, S. and Magnasco, M. O. (2007) ‘Structure, scaling, and phase transition in the optimal transport network’, *Physical Review Letters*, 98(8), pp. 3–6. doi: 10.1103/PhysRevLett.98.088702.
- Brelsford, C. *et al.* (2018) ‘Toward cities without slums: Topology and the spatial evolution of neighborhoods’, *Science Advances*, 4(8), pp. 1–9. doi: 10.1126/sciadv.aar4644.
- Dyson-Hudson, R. and Smith, E. A. (1978) ‘Human Territoriality: An Ecological Reassessment’, *American Anthropologist*, 80(1), pp. 21–41. doi: 10.1525/aa.1978.80.1.02a00020.
- Edward, P. (2006) ‘Examining Inequality: Who Really Benefits from Global Growth?’, *World Development*, 34(10), pp. 1667–1695. doi: 10.1016/j.worlddev.2006.02.006.
- Fathoni, H. S., Setyowati, A. B. and Prest, J. (2021) ‘Is community renewable energy always just? Examining energy injustices and inequalities in rural Indonesia’, *Energy Research and Social Science*, 71(October 2020), p. 101825. doi: 10.1016/j.erss.2020.101825.

- Franks, A. S. (2020) 'Economic Issues Are Moral Issues 2: Attributing Blame for Inequality Occurring in the United States versus Foreign Countries', *Analyses of Social Issues and Public Policy*, 20(1), pp. 7–25. doi: <https://doi.org/10.1111/asap.12190>.
- Furnham, A. and Gunter, B. (1984) 'Just world beliefs and attitudes towards the poor', *British Journal of Social Psychology*, 23, pp. 265–269. doi: <https://doi.org/10.1111/j.2044-8309.1984.tb00637.x>.
- García-Palacios, P., Maestre, F. T. and Gallardo, A. (2011) 'Soil nutrient heterogeneity modulates ecosystem responses to changes in the identity and richness of plant functional groups', *Journal of Ecology*, 99(2), pp. 551–562. doi: [10.1111/j.1365-2745.2010.01765.x](https://doi.org/10.1111/j.1365-2745.2010.01765.x).
- Gavrilenko, T. and Katifori, E. (2019) 'Resilience in hierarchical fluid flow networks', *Physical Review E*, 99(1). doi: [10.1103/PhysRevE.99.012321](https://doi.org/10.1103/PhysRevE.99.012321).
- Gaye, A. (2007) 'Access to Energy and Human Development', *United Nations Development Programme*, (25), p. 21.
- Gazol, A. *et al.* (2013) 'A negative heterogeneity-diversity relationship found in experimental grassland communities', *Oecologia*, 173(2), pp. 545–555. doi: [10.1007/s00442-013-2623-x](https://doi.org/10.1007/s00442-013-2623-x).
- Han, C. *et al.* (2019) 'The winner takes it all—Competitiveness of single nodes in globalized supply networks', *PLOS ONE*, 14(11), p. e0225346. doi: [10.1371/journal.pone.0225346](https://doi.org/10.1371/journal.pone.0225346).
- Hoy, C. (2015) *Leaving no one behind: the impact of pro-poor growth*. October. London: Overseas Development Institute, p. 27. Available at: <http://www.odi.org/sites/odi.org.uk/files/odi-assets/publications-opinion-files/9996.pdf>.
- Hutchings, M. J., John, E. A. and Wijesinghe, D. K. (2011) 'Toward Understanding the Consequences of Soil Heterogeneity for Plant Populations and Communities', *America*, 84(9), pp. 2322–2334.
- International Food Policy Research Institute (2015) *Global Nutrition Report 2015: Actions and accountability to advance nutrition and sustainable development*. Washington, D.C.
- Jarvis, A. J., Jarvis, S. J. and Hewitt, C. N. (2015) 'Resource acquisition, distribution and end-use efficiencies and the growth of industrial society', *Earth System Dynamics*, 6(2), pp. 689–702. doi: [10.5194/esd-6-689-2015](https://doi.org/10.5194/esd-6-689-2015).

- Kleidon, A., Malhi, Y. and Cox, P. M. (2010) 'Maximum entropy production in environmental and ecological systems', *Philosophical Transactions of the Royal Society B: Biological Sciences*, 365(1545), pp. 1297–1302. doi: 10.1098/rstb.2010.0018.
- Kurzban, R., Burton-Chellew, M. N. and West, S. A. (2015) 'The Evolution of Altruism in Humans', *Annual Review of Psychology*, 66(1), pp. 575–599. doi: 10.1146/annurev-psych-010814-015355.
- Kuznets, S. (1955) 'Economic growth and income inequality', *The American Economic Review*, 90(4), pp. 393–413.
- Laraia, B. A. (2013) 'Food Insecurity and Chronic Disease', *Advances in Nutrition*, 4(2), pp. 203–212. doi: 10.3945/an.112.003277.
- Long, M. A. *et al.* (2020) 'Food Insecurity in Advanced Capitalist Nations: A Review', *Sustainability*, 12(9). doi: 10.3390/su12093654.
- Lotka, A. J. (1922) 'Contribution to the Energetics of Evolution', *Proceedings of the National Academy of Sciences*, 8(6), pp. 147–151. doi: 10.1073/pnas.8.6.147.
- Martinez, S. (2010) *Local Food Systems: Concepts, Impacts, and Issues*. Darby, Pennsylvania: DIANE Publishing.
- Martyushev, L. M. and Seleznev, V. D. (2006) 'Maximum entropy production principle in physics, chemistry and biology', *Physics Reports*, 426(1), pp. 1–45. doi: 10.1016/j.physrep.2005.12.001.
- Mattison, S. M. *et al.* (2016) 'The evolution of inequality', *Evolutionary Anthropology: Issues, News, and Reviews*, 25(4), pp. 184–199. doi: 10.1002/evan.21491.
- Odum, H. T. (1971) *Environment, Power and Society*. New York: Wiley.
- Odum, H. T. and Pinkerton, R. C. (1955) 'Time's speed regulator: The optimum efficiency for maximum power output in physical and biological systems', *American Scientist*, 43(2), pp. 331–343.
- Pagiola, S., Arcenas, A. and Platais, G. (2005) 'Can Payments for Environmental Services Help Reduce Poverty? An Exploration of the Issues and the Evidence to Date from Latin America', *World Development*, 33(2), pp. 237–253. doi: <https://doi.org/10.1016/j.worlddev.2004.07.011>.

- Parrott, L. (2010) 'Measuring ecological complexity', *Ecological Indicators*, 10(6), pp. 1069–1076. doi: 10.1016/j.ecolind.2010.03.014.
- Seiferling, I., Proulx, R. and Wirth, C. (2014) 'Disentangling the environmental-heterogeneity–species-diversity relationship along a gradient of human footprint', *Ecology*, 95(8), pp. 2084–2095. doi: 10.1890/13-1344.1.
- Sheehy-Skeffington, J. and Thomsen, L. (2019) 'Egalitarianism: Psychological and socio-ecological foundations', *Current Opinion in Psychology*, 32, pp. 146–152. doi: 10.1016/j.copsyc.2019.08.014.
- Smith, E. A. *et al.* (2010) 'Wealth transmission and inequality among hunter-gatherers', *Current Anthropology*, 51(1), pp. 19–34. doi: 10.1086/648530.
- Sovacool, B. K. (2012) 'The political economy of energy poverty: A review of key challenges', *Energy for Sustainable Development*, 16(3), pp. 272–282. doi: 10.1016/j.esd.2012.05.006.
- Spencer, H. (1860) 'The social organism', *Westminster Review*, 73(143), pp. 90–121.
- Stein, A., Gerstner, K. and Kreft, H. (2014) 'Environmental heterogeneity as a universal driver of species richness across taxa, biomes and spatial scales', *Ecology Letters*, 17(7), pp. 866–880. doi: 10.1111/ele.12277.
- Tews, J. *et al.* (2004) 'Animal species diversity driven by habitat heterogeneity/diversity: The importance of keystone structures', *Journal of Biogeography*, 31(1), pp. 79–92. doi: 10.1046/j.0305-0270.2003.00994.x.
- Tylianakis, J. M. *et al.* (2008) 'Resource heterogeneity moderates the biodiversity-function relationship in real world ecosystems', *PLoS Biology*, 6(5), pp. 0947–0956. doi: 10.1371/journal.pbio.0060122.
- Ulanowicz, R. E. *et al.* (2009) 'Quantifying sustainability: Resilience, efficiency and the return of information theory', *Ecological Complexity*, 6(1), pp. 27–36. doi: 10.1016/j.ecocom.2008.10.005.
- United Nations (2015) *Transforming our World: The 2030 Agenda for Sustainable Development*. United Nations. Available at: <https://sdgs.un.org/publications/transforming-our-world-2030-agenda-sustainable-development-17981>.

Vallino, J. J. (2010) 'Ecosystem biogeochemistry considered as a distributed metabolic network ordered by maximum entropy production', *Philosophical Transactions of the Royal Society B: Biological Sciences*, 365, pp. 1417–1427. doi: 10.1098/rstb.2009.0272.

Vezzani, F. M. *et al.* (2018) 'The importance of plants to development and maintenance of soil structure, microbial communities and ecosystem functions', *Soil and Tillage Research*, 175(March 2017), pp. 139–149. doi: 10.1016/j.still.2017.09.002.

Wang, Y. *et al.* (2019) 'Global evidence of positive biodiversity effects on spatial ecosystem stability in natural grasslands', *Nature Communications*, 10(1), pp. 1–9. doi: 10.1038/s41467-019-11191-z.

West, G. B., Brown, J. H. and Enquist, B. J. (1997) 'A General Model for the Origin of Allometric Scaling Laws in Biology', *Science*, 276, pp. 122–126. doi: 10.1126/science.276.5309.122.

World Food Programme (2017) *At the root of exodus: food insecurity, conflict, and international migration*. Available at: https://docs.wfp.org/api/documents/WFP-0000015358/download/?_ga=2.152370107.30142471.1586690135-125583866.1584463855.

Ziv, Y. and Davidowitz, G. (2019) 'When landscape ecology meets physiology: Effects of habitat fragmentation on resource allocation trade-offs', *Frontiers in Ecology and Evolution*, 7(APR), pp. 1–8. doi: 10.3389/fevo.2019.00137.